EXPLORING PHYSIOLOGY OF AN EXOPOLYSACCHARIDE (EPS) PRODUCING FACULTATIVELY OLIGOTROPHIC BACTERIUM *KLEBSIELLA PNEUMONIAE* PB12 WITH SPECIAL EMPHASIS ON STRUCTURE-FUNCTION ANALYSIS OF EPS

A THESIS SUBMITTED TO THE UNIVERSITY OF NORTH BENGAL

FOR THE AWARD OF
DOCTOR OF PHILOSOPHY
IN
BIOTECHNOLOGY

BY

Amit Kumar Mandal

Under the supervision of
Dr. Ranadhir Chakraborty

DEPARTMENT OF BIOTECHNOLOGY
UNIVERSITY OF NORTH BENGAL
DARJEELING- 734013
WEST BENGAL, INDIA

Oct-2015

"It's not in the open we feel comforted but in the shadows. ... We can't feel at home with the infinite sky above and around us. Space must be cut off, shaped, defined, for us to inhabit. From cradle to coffin, it's enclosure that defines us." —Robert Morgan

"Dedicated to my beloved parents"

DECLARATION

I hereby declare that the research work embodied in this thesis has been carried out by me in the Department of Biotechnology, University of North Bengal, Darjeeling-734 013, West Bengal, India, under the supervision of Dr. Ranadhir Chakraborty. I also affirm that this work is original and has not been submitted partially or in full for any other degree or diploma to this or any other University or Institution.

Amit Kr. Mandal

(Amit Kumar Mandal)
Department of Biotechnology
University of North Bengal

UNIVERSITY OF NORTH BENGAL

DEPARTMENT OF BIOTECHNOLOGY

DARJEELING-734 013, WEST BENGAL, INDIA

Dr. Ranadhir Chakraborty

Associate Professor

CERTIFICATE

The research work presented in this thesis entitled "**Exploring physiology of an exopolysaccharide (EPS) producing facultatively oligotrophic bacterium *Klebsiella pneumoniae* PB12 with special emphasis on structure-function analysis of EPS**" has been carried out under my supervision and a bonafide research work of **Mr. Amit Kumar Mandal**. This work is original and has not been submitted for any degree or diploma to this or any other University or Institution.

Date: 05.10.2015

(Ranadhir Chakraborty)

Supervisor and Head

DR. R. Chakraborty
Deptt. of Biotechnology
NBU

ACKNOWLEDGEMENTS

I would like to express my sincere respect and heartfelt gratitude to my supervisor Dr. Ranadhir Chakraborty, Associate Professor, Department of Biotechnology, University of North Bengal, Darjeeling-734 013, West Bengal, India, for his excellent guidance, constant encouragement and valuable suggestions throughout the course of my research work. His perpetual inspiration and philosophy give me an enjoyable experience not only in journey of research but it will also be memorable in future. He was the one, who gave me the strength to fight in every harsh situation that often created hindrances throughout the journey of my life…

I express my sincere thanks to the Hon'ble Vice-Chancellor and Registrar, North Bengal University, for granting me the privilege to carry out my research work in my beloved University.

I express my warm regards and deepest gratitude to all the faculty members of our Department, Dr. Dipanwita Saha, Dr. Shilpi Ghosh, Dr. Anoop Kumar for their constant motivation during my research work.

I am thankful to all the non-teaching staff members of this Department for their co-operation and support especially Dipak Da, Raja Da, Biswajit Kaku and Papai Da.

I record my special thanks to all my seniors' research scholars and friends of my laboratory: Dr. Shriparna Mukherjee, Dr. Suparna Saha Bhowal, Dr. Arvind Kumar, Dr. Krishna Kant Yadav, Mr. Bipransh Kumar Tiwary, Mr. Subhonil Chakraborty, and Mr. Vivek Kumar for their kind help and co-operation.

I am also thankful to Mr. Ipsita Kumar Sen, Dr. Soumyananda Chakraborti, Ms. Shamila Sarwar and Mr. Dilip Kumar Manna, for their active co-operation during the research work.

It's a great pleasure to express my sincere thanks to Prof. Syed Sirajul Islam, Department of Chemistry and Chemical Technology, Vidyasagar University, Midnapore-721 102, Prof. Pinak Chakrabarti, Professor, Department of Biochemistry, Bose Institute, Kolkata-700 054, West Bengal, India and Dr. Pradipta Saha,

Department of Microbiology, Burdwan University for their co-operation and helpful suggestions.

I am extremely thankful to Mr. Barun Majumder, Bose Institute, Kolkata-700 054, West Bengal, India, for preparing NMR spectra.

I express my profound regards to my beloved parents (Shri Deepak Kumar Mandal and Smt. Rekha Mandal), my brother (Samit Kumar Mandal), and my best friend (Srijana Darnal), for their inspiration and encouragement throughout the whole course of my work. It is very difficult to mention every individual name and his/her contribution in my life. I thank all of them.

I greatly acknowledge the University of North Bengal for providing financial assistance.

Amit Kr. Mandal ,

(Amit Kumar Mandal)
Department of Biotechnology,
University of North Bengal-734 013,
Darjeeling, West Bengal, India.

Abstract

An oligotrophic bacterium, growing in nutrient-poor condition, is very likely to have a strategy to concentrate nutrient molecules from highly diluted solution to its own survival advantage. In this study a facultative oligotrophic strain isolated from the water sample of River Mahananda, Siliguri India was selected for its property to produce exopolysaccharide (EPS) in nutrient-poor (oligotrophic) medium. Based on phenotypic and phylogenetic analyses, the strain PB12 was identified as *Klebsiella pneumoniae*. Viability assay of the strain was performed in sterile liquid LB, R2A, river water and diluted (10^{-3} or 0.001x) LB at 30 °C and pH 7 to understand oligotrophy. PB12 cells were able to grow in 0.001x LB broth as well as sterile river water without supplementation of any carbon or nitrogen source or growth factors. An increment of nearly 13 times the initial cell number was noted in a span of 3 days in 0.001x LB. The ability of PB12 to survive without any reduction in viable cell number from the input cells explains the oligotrophic nature. A decrease in approximately 31% of EPS during further incubation beyond 48 h (from 48 h to 72 h) in the same batch culture was associated with two times increment in viable cell number. Colony diameter (*d*) of PB12 grown on LB agar after 24 h was found to be 1.5 mm, whereas, colony diameter of PB12 on 0.01x LB after 24 h of incubation was 0.5 mm. After assessing the number of cells presents in this colony it was noted that colonies obtained on LB agar (*d*=1.5 mm) there are 1.8×10^8 cells present. Interestingly, 5.4×10^8 number of cells was obtained from the colony grown on diluted LB agar plates. Scanning electron micrograph of PB12 cells grown on LB or 0.01X LB was found to be 1.55 ± 0.15 µm or 0.787 ± 0.18 µm respectively, which supports the

earlier observations. Flow cytometric analysis revealed that PB12 cells population grown in LB was skewed to the right on the *x* axis (forward- scattered light), indicating that the cells were possibly larger than PB12 cells grown in 0.01x LB (which as skewed to the left on the *x* axis). While observing the intracellular ROS it was noted that intracellular ROS production is more in the LB grown PB12 cells compared to the cells when allowed to grow in diluted LB. It is well-known that NO exerts both pro-oxidant and antioxidant effects, depending on the ambient redox status, the presence of other reactants, and the nature of the reaction. It was found that the PB12 cells grown in LB exhibited higher NO production than the cells grown in 0.01x LB. It now seems clear that starvation adaptation is important for cells to initiate long-term survival via developing resistance to oxidative stress. Clearly, oxidative stress is a condition likely to be professed by many bacteria, for example, in the form of reactive oxygen species. As SOD functions to detoxify superoxide, we sought to determination of Cu, ZnSOD activity in *Klebsiella pneumoniae* PB12 grown in LB and 0.01x LB. Our present result exhibited that Cu,ZnSOD activity has increased significantly ($P< 0.05$) in 0.01x LB grown PB 12 cells compared to LB grown PB 12 cells. Moreover, cells grown in diluted LB were found to be much more resistant towards potent ROS generator ZnO-PEI nanoparticles (NPs). It was noted that LD_{50} dosage of ZnO-PEI NPs cause only 35% reduction in bacterial growth of 0.01x LB grown cells whereas, approximately 50% reduction in bacterial growth was noted when LB grown cells were treated with same dosage of NPs. Moreover, Raman spectroscopy was used to obtain more insight. Results showed differences in the spectra of LB grown cells compared to 0.01x LB grown cells treated with same concentration of ZnO-PEI NPs. *Klebsiella pneumoniae* PB12 spectra showed distinctive absorption bands between

600 and 1800 cm^{-1}, that includes peak for proteins, lipids, carbohydrates and nucleic acids and these spectra are in good agreement with the previously published spectra. The main Raman peaks of PB12 cells showing bands around 853, 1005, 1252 and 1665 cm^{-1} were assigned to proteins; bands around 726, 783, 936, 1101, 1340 and 1577 cm^{-1} were assigned to nucleic acids; bands around 977 and 1453 cm^{-1} were assigned to lipids; and those around 1035 cm^{-1} was assigned to carbohydrates. An exopolysaccharide (KNPS) of an average molecular weight $\sim 1.8 \times 10^5$ Da was isolated from the culture medium of *Klebsiella pneumoniae* PB12. Structural characterization of KNPS was carried out using sugar and methylation analysis, Smith degradation and 1D/2D NMR experiments. Sugar analysis showed that the KNPS composed of arabinose, galactose, 3-O-methyl-galctose and glucose in a molar ratioof nearly 4:3:1:1. The proposed repeating unit of the KNPS has a backbone chain consisting of two (1 → 6)-galactopyranosyl residues, two (1 → 5)-arabinofuranosyl residues, one (1 → 6)-glucopyranosylresidue and one (1 → 3)-arabinopyranosyl residue, out of which one (1 → 6)-galactopyranosyl residuewas branched at O-2 position with a (1 → 2)-linked-galactopyranosyl residue terminated with non reduc-ing arabinofuranosyl residue and one (1 → 5)-arabinofuranosyl residue branched at O-3 position with nonreducing end 3-O-Me-galactopyranosyl residue. KNPS was found non-toxic toward human lymphocyte up to the dosage of 100 µg/ml. KNPS enhanced malondialdehyde (MDA), reactive oxygen species (ROS), and have the potential to alter the ratio of oxidized glutathione (GSSG) and reduced glutathione (GSH) levels in the cellular system. Fourier transform infrared (FT-IR) spectroscopy indicated the presence of hydroxyl, carboxylic and methoxyl functional groups. The optimal dosages for flocculation of activated carbon suspension were 17 mg/l EPS and 4 mM

$CaCl_2$. EPS showed flocculating rate of above 80% over a wide range of pH (pH 3-10) whereas, more than 90% rate was noted in the temperature range (10-50°C) tested in presence of $CaCl_2$. Moreover, EPS showed characteristic emulsifying activity with toluene (66.6%), n-hexadecane (65%), olive oil (63.3%) and kerosene (50%). The physiological studies of the facultatively oligotrophic bacterium, *K. pneumoniae* PB12, along with the structure-function analysis of its EPS have not only contributed to the knowledge domain of the oligotrophic bacteria but have also pointed out the promise of biotechnological application of PB12 EPS.

PREFACE

The knowledge of physiology and metabolism of prokaryotes underpins our understanding of the roles and activities of these organisms in the environment, including pathogenic and symbiotic relationships, as well as their exploitation in biotechnology. Prokaryotic organisms especially bacteria, although remaining relatively small and simple in structure throughout their evolutionary history, exhibit incredible diversity regarding their metabolism and physiology. Such metabolic diversity is reflective of the wide range of habitats where they can thrive and in many cases dominate the biota, and is a distinguishing contrast with eukaryotes that exhibit a more restricted metabolic versatility. Thus, prokaryotes can be found almost everywhere under a wide range of physical and chemical conditions, including aerobic to anaerobic, light and dark, low to high pressure, low to high salt concentrations, extremes of acidity and alkalinity, and extremes of nutrient availability like oligotrophic (nutrient-poor) conditions. The field of microbial physiology has expanded at an incredibly rapid pace. However, knowledge about the physiology of bacteria thriving under oligotrophic conditions is scanty in terms of quality as well as quantity. The objective of the work that has been presented in this thesis was to explore partially the lifestyle of a facultatively oligotrophic bacterium, *Klebsiella pneumoniae* PB12. Since production of exo-polysaccharide was an event triggered in nutrient-deficient condition, the title of the thesis took the form as- "*Exploring physiology of an exopolysaccharide (EPS) producing facultatively oligotrophic bacterium Klebsiella pneumoniae PB12 with special emphasis on structure-function analysis of EPS*". The thesis is divided into four chapters. The first chapter dealt with the screening and identification of EPS-producing bacteria from river water samples. The second chapter revealed the basic growth physiology of *K. pneumoniae* strain PB12. Determination of structure and immunological function of the exopolysaccharide synthesized by *K. pneumoniae* PB12 was elaborately described in the third chapter. The fourth chapter dealt with the biotechnological prospect of exopolysaccharide produced by *K. pneumoniae* PB12 by studying in details the flocculation properties of the EPS. The

overall findings shall definitely enrich the science of oligotrophy and extend the premise of biotechnology application using EPS in bio-remediation.

ABBREVIATIONS

Ac	Acetyl
Ac_2O	Acetic anhydride
AcOH	Acetic acid
Ara	Arabinose
BSTFA	N,O-bis (trimethylsilyl) trifluoro acetamide
C	Carbon
CAT	Catalase
CF_3COOH	Trifluoro acetic acid
CFU	Colony-forming unit
$CHCl_3$	Chloroform
CH_3I	Methyl iodide
CH_3OH	Methanol
cm	Centimetre
d	diameter
$DCFH_2$-DA	2', 7'-dichlorodihydrofluoroscein diacetate
1D	1-Dimensional
2D	2-Dimensional
Da	Dalton
DEPT	Distortionless enhancement by polarization transfer
DMSO	Dimethyl sulfoxide
DQF-COSY	Double-quantum filtered correlation spectroscopy
DSC	Differential Scanning Calorimetry
eDNA	Extracellular DNA
EDS	Energy dispersive X-ray study
EPS	Exopolysaccharide
EPSs	Exopolymeric substances
f	Furanose
FACS	Fluorescence assisted cell sorting

FITC	Fluorescein isothiocyanate
FSC	Forward scattering
FT-IR	Fourier transform infrared spectroscopy
g	Gram
Gal	Galactose
GC	Gas chromatography
GC-MS	Gas chromatography mass spectrometry
Glc	Glucose
GPC	Gel permeation chromatography
GSH	Reduced glutathione
GSSG	oxidized glutathione level
h	Hour(s)
HMB	Heteronuclear multiple bond correlation
HOD	Deuterated water
HSQC	Heteronuclear single quantum coherence
Hz	Hertz
IFN	Interferon
IL	Interleukin
J	Coupling constants
Kg	Kilogram
KNPS	*Klebsiella pneumoniae* polysaccharide
l	Liter
LD	Lethal dose
LPS	Lipopolysaccharide
M	Molar
MDA	Malondialdehyde
Me	Methyl
mg	Milligram
MHz	Mega hertz
min	Minute(s)

ml	Mililiter
mm	Millimeter
mM	Millimolar
$NaBH_4$	Sodium borohydride
NaOH	Sodium hydroxide
NMR	Nuclear magnetic resonance
NO	Nitrous oxide
NOE	Nuclear overhauser effect
NOSs	Nitric-oxide synthases
NOESY	Nuclear overhauser enhancement spectroscopy
NPs	Nanoparticles
p	Pyranose
PBMCs	Peripheral blood mononuclear cells
PBS	Phosphate buffered saline
PE	Phycoerythrin
PMAA	Partially methylated alditol acetate
ppm	Parts per million
PS	Polysaccharide
ROS	Reactive oxygen species
rpm	Rotation per minute
RPMI	Roswell Park Memorial Institute
SEM	Scanning electron microscope
SOD	Superoxide dismutase
SRB	Sulforhodamine B assay
SSC	Side scattering
TGA	Thermo gravimetric analysis
TNF-α	Tumor necrosis factor-α
TOCSY	Total correlation spectroscopy
UV	Ultraviolet
vis	Visible

v/v	Volume by volume ratio
ZnO-PEI NPs	Polyethylenimine capped zinc oxide nanoparticles
µm	Micrometer
µg	Microgram
µl	Microliter
µM	Micromolar
°C	Degree Celsius

CONTENTS

List of tables and figures

Table captions

Figure captions

GENERAL INTRODUCTION

General Introduction

I. Historical perspectives

The formation of exopolymeric substances enables single-cell organism to live an impermanent multicellular lifestyle, in which "collective behavior" facilitates survival in adverse environments. The switching from planktonic growth to biofilm occurs in response to external stimuli that involves various regulatory networks (O'Toole et al., 2000; Monds & O'Toole 2009). This cellular reprogramming equips bacteria with a weapon that enables their survival in unfavorable conditions (Whiteley et al., 2001; Vuong et al., 2004). Microbial biofilm formation is known to be a sequential bacterial development process (O'Toole et al., 2000) and is regulated by a series of genetic and phenotypic determinants (O'Toole et al., 2000). Bacteria take shelter in an extracellular matrix (self-produced) inside biofilm, accounting ~90% of the biomass (Flemming & Wingender, 2010). The matrix is composed of extracellular polymeric substances that along with carbohydrate-binding proteins (Branda et al., 2006), pili, flagella, other adhesive fibers (Cegelski et al., 2009), and extracellular DNA (eDNA) (Qin et al., 2007), act as a scaffold for the three dimensional biofilm structure. There was a period (1978-1990) when biofilms were considered as unstructured accretions of bacterial cells, surrounded by the exopolysaccharide (EPS) matrices. Inside the matrix, nutrients are trapped for metabolic utilizations by the resident bacteria and through H-bond interactions with hydrophilic polysaccharides; water is efficiently retained (Flemming &

Wingender, 2010). There are speculations that production of exopolymeric substances (EPSs) by bacteria growing under extremely nutrient-poor conditions (where these nutrients are available at levels below threshold concentrations) might aid in concentrating the nutrient for sustenance (Pahm & Alexander, 1993). Enzymes secreted by the bacteria modify EPS composition in response to changes in nutrient availability (Sauer et al., 2004). Hence, the structural components of the matrix provides a highly hydrated, robust structure which keeps bacteria in close proximity, enabling intimate cell-to-cell interactions and DNA exchange (Flemming & Wingender, 2010). Moreover, it protects the biomass from desiccation, predation, oxidizing molecules, radiation, and other detrimental agents (Flemming & Wingender, 2010). The matrix, more particularly EPS, protects biofilm bacteria from exposure to innate immune defenses (such as opsonization and phagocytosis) inside the host, and against various antibiotics (Walters et al., 2003; Cerca et al., 2006). Inter bacterial interactions within the matrix can promote the spread of drug resistance markers and other virulence factors (Vuong et al., 2004). As a result, biofilm-forming pathogens (*Pseudomonas aeruginosa*) establish chronic and recalcitrant infections like upper respiratory infections (Govan & Deretic, 1996), urinary tract infections (UTIs) caused by uropathogenic *Escherichia coli* [UPEC] and *Klebsiella pneumoniae* (Foxman, 2010), periodontitis (Kuramitsu & Wang, 2011), catheter-induced and other device-associated infections (Venditti et al., 1993). In immuno-compromised patients, the symptom of infections by opportunistic biofilm-forming or EPS forming pathogens can be shocking, leading to harsh symptoms and, in many cases, death. Formation of biofilm or colony by bacteria is a behavior that allows prompt utilization of the substrate. The combined exo-enzymatic action of growing colony provides benefits to

the individual cells when growing in nutrient rich (copiotrophic) condition. Alternatively, an oligotrophic bacterium growing slowly in nutrient-poor condition may have a life strategy in which dispersal is promoted to optimize cell access to substrates. In the latter scenario colony formation is possibly not adaptive. While aquatic ecologists have had an interest in oligotrophic bacteria (Costerton et al., 1981; Yokoi et al., 1995), these organisms are still relatively unknown to many microbiologists, especially clinical microbiologists. Growth and continued existence of bacteria are often influenced by EPS produced by them.

II. Oligotrophic style of growth

Oligotrophic environments usually deficient in exogenous supply of nutrients and are defined by a low nutrient flux, <1 mg carbon per litre per day (Schut et al., 1993) as well as by low absolute concentrations of nutrients (Morita, 1997). The aquatic environment is the largest habitat on Earth, accounting for >90% of the biosphere by volume and harbouring microorganisms responsible for ~50% of total global primary production. Despite of highest cellular production rate of any ecosystem on the planet, aquatic environments has vast oligotrophic (e.g., nutrient-limited open ocean water) situation. As a result, the aquatic environment is often considered a marine desert. Oceanic ecosystems are far more productive than terrestrial ecosystems in terms of per unit of biomass, and as a result, the turnover rate of nutrients per unit of biomass is several hundred times higher. But, due to limited nutrient availability and low population densities, the effective overall turnover rate is still so low (Munster, 1993) that the ocean classifies as oligotrophic with organic carbon fluxes of a milligram of carbon l^{-1} d^{-1} as

well as by low ambient concentrations of nutrient (Poindexter, 1981). However, high productivity is predominantly due to the phototrophic prokaryotic primary-producers, and the heterotrophic prokaryotes caused nutrient alteration and remineralisation. The carbon, nitrogen and phosphorus fixation by these bacteria and their subsequent conversion into particulate matter are critically important processes in aquatic environments. Heterotrophic bacteria are major contributors to oceanic and terrestrial biogeochemical cycles (Whitman et al., 1998). As reservoirs of nutrients in oligotrophic marine ecosystems, these ultramicrobacteria exhibited impacts on the productivity of all marine life by means of interacting with all trophic levels and control the nutrient fluxes via mineralisation. With predictions of increasing ocean oligotrophy as an outcome of global warming (Matear & Hirst, 1999) without any doubt it is vital to know the physiology of this class of bacteria in order to determine their impact on primary production in aquatic ecosystem. A major portion of terrestrial and marine environments are oligotrophic (nutrient poor) and thus, the routine situation for almost all bacteria is that they are in inadequate supply of one or more vital nutrients. In spite of low levels of nutrients the pelagic marine environment is dominated, in terms of biomass and activity, by small bacteria, variously referred to as ultramicrobacteria, microcells, nanoplankton or picoplankton depending on the terminology adopted by microbial ecologists and physiologists (Table I).

Table I. Description of terms relating to the small size of bacteria.

Ultramicrobacteria	**Microorganism with a cell volume of <0.1 μm^3 that maintains its size with only minor changes, irrespective of growth conditions. Observed by light microscopy.**
Ultramicrocells	Smaller forms (usually starved) of microorganisms that are larger when actively growing. Usually associated with reductive cell division during starvation. Observed by light microscopy.
Nan(n)obacteria	Possible synonym for UMB. In the literature usually associated with structures in geological samples with sizes ranging from 0.01 – 0.1 μm. Usually associated with uncultured and unsubstantiated descriptions of microorganisms. Observed by electron microscopy.
Femtoplankton	Marine microorganisms 0.02-0.2 μm
Picoplankton	Marine microorganisms 0.2-2.0 μm
Nanoplankton	Marine microorganisms 2.0-20 μm
Microplankton	Marine microorganisms 20-200 μm

Other allied terms	Dwarf cells/bacteria, lilliputian cells, femtobacterioplankton, miniature cells/bacteria, nanocells, nanosized, nanobe, nanoorganisms

Local variations in nutrient content can occur because of physical processes, including upwelling of nutrient rich deep waters or aeolian and riverine deposition, or biological processes such as phytoplankton blooms or aggregation of particulate organic matter. In addition, heterogeneity in ocean waters is not limited to gross differences in nutrient concentrations, but extends to microscale patchiness that occurs throughout the continuum of ocean nutrient concentrations (Azam & Malfatti, 2007). Bacteria, in ecological terms, are generally defined as r-strategists, having a small body, short generation time, and highly dispersible offspring that continuously challenged by conditions of nutrient limitation and starvation in natural environment (Morita, 1997). As bacteria cannot escape the environment they undergo both phenotypic and genetic changes in order to face that adverse situation. Bacteria have evolved a wide range of growth and survival strategies to maximize reproductive success. In particular, nutrient type and availability have provided strong selective pressure for defining lifestyle strategies among marine bacteria. However, although a large number of copiotrophic marine organisms (and fewer oligotrophs) have been cultured, the study of trophic strategy has been impaired by a lack of understanding of the molecular basis of adaptation. Nevertheless, oligotrophs are omnipresent in the environment and have been isolated from soil (Hattori, 1984), rivers (Yanagita et al., 1978), lakes (Lango, 1988), oceans (Deming, 1986), and tap water lacking organic substances (Jaeggi & Schmidt-

Lorenz, 1990). Some oligotrophic isolates can even grow in distilled water (Favero et al., 1971). Two different types of oligotrophs can be distinguished. Those oligotrophs that can grow on only a low concentration of carbon are called obligate oligotrophs (Fry, 1990). Those that are able to grow at both low and high concentrations of organic substances are called facultative oligotrophs (Ishida et al., 1982). There is a confusing variety of definitions for oligotrophic bacteria (Table II). Some researchers define oligotrophs as organisms able to grow at nutrient concentrations of 5 mg C 1^{-1} but not at concentrations of 7.5 g C 1^{-1} (Yanagita et al., 1978). Others define oligotrophs as those bacteria that are able to grow on media with 1 to 15 mg C 1^{-1} as well as on media with a higher nutrient content (Kuznetsov et al., 1979). Ishida et al. (1982) call such organisms facultative oligotrophs, as opposed to obligate oligotrophs (Yanagita et al., 1978) that cannot grow at substrate concentrations >0.3 g C 1^{-l}. Horowitz et al. (1983) postulated the term euryheterotroph for facultative oligotrophic bacteria and Baxter & Sieburth (1984) replaced 'facultative oligotroph' by 'eurytroph'. The confusion on the proper definition is strengthened by the fact that some researchers use the term oligotroph only for those organisms that are restricted to growth on low nutrient media, while others employ the term to broadly speak about both the obligate and facultative oligotrophs. A general characteristic of oligotrophs, and one that is currently used in all definitions, is the ability to grow in low nutrient media (0.2 to 16.8 mg C 1^{-l}). But is this truly such a remarkable characteristic? In the ocean's euphotic zone, food often comes in waves (Mopper & Lindroth, 1982) and the availability is short lasting.

Table II. Definition used to characterize oligotrophic bacteria.

Definition	Source
"Oligotrophic bacteria are heterotrophic bacteria capable of growth in the presence of organic nutrients equivalent to 16.8 mg C l^{-1}".	Akagi et al., (1977)
"Bacteria capable of growth on unamended BWA (agar-solidified Chesapeake Bay water)".	Mallory et al., (1977)
"Oligotrophic bacteria are capable to grow on media containing only minerals, and they meet their carbon and energy requirements from trace amounts of organic substances [. . .] found in the air".	Moaledj, (1978)
"A trophic group of bacteria that can grow only in the presence of a minor amount of nutrients and not in the presence of a large amount".	Yanagita et al., (1978)
"Those [bacteria] that develop at the first cultivation on media with the minimal content of organic matter of about 1-15 mg C $l^{-1}$and that grow on such media at subsequent recultivation though they can grow on richer media".	Kuznetsov et al., (1979)
"Organisms that grow in media containing organic matter at a concentration of 1 mg C per litre. [. . .] . Obligate oligotrophs may decrease in number or disappear with the onset of man-made eutrophication, facultative oligotrophs can tolerate or rapidly adapt to the higher concentrations of organic substances".	Ishida & Kadota, (1981)

"Oligotrophic bacteria can [. . .] be conceived of as those whose survival in nature depends on their ability to rnultiply in habitats of low nutrient fluxes (approaching zero to a fraction of a mg C/litre/day)"	Poindexter, (1981)
"Bacteria which grow at substrate concentrations < 1 mg C 1^{-l}".	Ishida et al., (1982)
"Bacteria that can be isolated on a low-nutrient medium (unsupplemented Bushnell Haas agar) and that are restricted to growth at low nutrient concentrations".	Horowitz et al., (1983)
"Oligotrophs are defined as those organisms known to be able not only to survive but particularly to multiply under conditions of extremely low and often discontinuous supply of nutrients. In other words, organisms adapted to low and irregular fluxes of substrates".	Van Gemerden & Kuenen, (1984)
"Among oligotrophs we tentatively define the obligate oligotroph as an organism which does not grow in rich (200 mg C l^{-1}) media, and the facultative oligotroph as an organism which grows in not only poor (0.2 mg C l^{-1}) but also rich media".	Ishida et al., (1989)
"Oligotrophic bacteria can broadly be defined as organisms that grow on low concentrations of organic substrates". Obligate oligotrophs cannot grow at substrate concentrations above 6 g C 1^{-1}".	Fry, (1990)
"…oligotrophic microorganisms are prokaryotic and eukaryotic organisms that are evolutionarily adapted to exploit ecological niches characterised by low substrate concentrations and low energy fluxes.	Semenov, (1991)

Oligotrophs, [. . .] may develop in rich as well as in poor environments [. . .]."

In river-outflow regions, or during senescence of massive phytoplankton spring blooms, conditions may actually be eutrophic. By definition such regions are characterised by a more than 50-fold higher nutrient flux than that in oligotrophic regions (Poindexter, 1981). Yet, rapid growth of bacteria and consumption of substrates will again result in low steady state substrate concentrations and growth limitation. Therefore, eutrophic environments select temporarily for K-strategists when nutrients become depleted (Andrews & Harris, 1986). The fluctuations in nutrient availability in the ocean and the presence of microniches result in the coexistence of copiotrophic and oligotrophic bacteria in an oligotrophic environment. Therefore, the r/K-selection concept is not completely synonymous with the copiotrophic/oligotrophic concept (Andrews & Harris, 1986), and this is probably the reason why the r/K-strategy concept has not been broadly adopted in marine microbiology. Total prokaryote numbers in the ocean are estimated at 10^{29} (Whitman et al., 1998), as a result, marine microorganisms contribute a large proportion of the world's biosphere in terms of carbon, nitrogen and phosphorus. Furthermore, of the three largest microbial habitats (seawater, soil and sediment/soil subsurface), the rates of cellular activity and turnover are highest in the open ocean (Whitman et al., 1998). By virtue of their abundance and biomass heterotrophic prokaryotes in the ocean play an essential role in nutrient transformation and remineralisation. In addition, picophytoplankton (phototrophic prokaryotes and

eukaryotes), contribute significantly to global primary production (Campbell et al., 1994), with estimates as high as 50% of global carbon fixation attributed to this size class (Partensky et al., 1999). Thus, together the smallest heterotrophic and phototrophic cells play an essential role in regulating the accumulation, export, re-mineralisation and transformation of the world's largest pool of organic carbon (Cole et al., 1988) resulting in an ecosystem composed primarily of a microbial food web where prokaryotes and picoeukaryotes represent the most important biological component.

III. An overview of the marine microbial community

When observed directly, indigenous bacterial communities are rich in carbon and nitrogen and exhibit a low protein and DNA content, they display typical cell volumes in the range from 0.02-0.12 μm^3, around an order of magnitude smaller than commonly studied bacteria such as *Escherichia coli* (Fuhrman, 1981; Strehl et al., 1999; Button & Robertson, 2000). Initial attempts to isolate marine bacteria on nutrient rich agar plates revealed a discrepancy of up to three orders of magnitude between plate counts and the observed total number of cells in marine samples (Ferguson et al., 1984). Taken together with the observation that a high proportion of early ocean isolates were typically larger (0.34-6.4 μm^3) and undergo starvation induced miniaturisation processes (Schut et al., 1993), it was believed that indigenous microcells represent starved and dormant forms of isolates that could not form colonies on agar plates. It was therefore assumed that in the environment starvation was the natural state of microorganisms. This assertion, however, does not account for a number of observed phenomena listed here. (i) On a per unit volume basis, oceanic microcells exhibit higher activity than the atypically large cells

(Ouverney & Fuhrman, 1999). (ii) More than 90% of the productivity in pelagic regions is due to free-living, rather than substrate-attached, cells (Cho & Azam, 1988). (iii) Bacteria that remain small when actively growing have been observed and isolated (Schut et al., 1993). (iv) The global significance and activity of ultramicrobacterial phototrophic cyanobacteria is well established (Partensky et al., 1999), and (v) Starved, or dormant, bacteria may not become predominant in the ocean while in the non-growing state. More recently molecular techniques suggest low *in situ* abundance of typically isolated bacteria (Eilers et al., 2000). Developments with molecular methods enabled the relative abundance of specific prokaryotic taxa to be determined without the need to cultivate microorganisms. Initial studies based on SSU rRNA sequence libraries found that the most abundant rDNA sequences obtained did not correspond to cultured species and were distantly related to other rDNA sequences in databases (Giovannoni & Rappe, 2000). These results clearly demonstrated that natural bacterial communities were composed of unknown species that were incapable of forming colonies on commonly used microbiological media.

IV. Predicated properties of oligotrophs

According to the fundamental roles of nutrient uptake and utilisation a list of predicted properties were advanced for a model oligotroph at the Dalhelm Conference (Hirsch et al., 1979). The proposed characteristics include: (i) the high surface per volume ratio (cells are expected to be small), (ii) favoured usage of metabolic energy for nutrient uptake especially during periods of non-growth, (iii) constitutive nutrient uptake ability, (iv) having high affinity, low-specificity transport systems for simultaneous

uptake of mixed substrates, and (iv) the organization of nutrient reserves following nutrient uptake. The small size of cells would provide a distinct advantage in terms of grazer avoidance and increased efficiency of nutrient uptake, while nutrient uptake mechanisms were expected to have a broad specificity, be inducible and subject to a minimal amount of catabolite repression in order to ensure simultaneous utilisation of the broadest range of substrates (Poindexter, 1979). Oligotrophs were also expected to regulate their biosynthetic rate in line with nutrient uptake rates (Poindexter, 1979). Finally, oligotrophs were predicted to have the ability to store diverse nutrients in reserves (Hirsch et al., 1979). Since the proposal of these characteristics was advanced a range of physiological studies have been conducted to test their validity (Schut et al., 1997). Unfortunately very few of these studies were conducted with oligotrophs, highlighting the need to obtain relevant oligotrophic isolates for laboratory studies.

V. Bioflocculation as a microbial response to substrate limitations

Bacteria have extraordinary capability for survival in the presence of extremely reduced amount of energy and nutrient sources. In the year 1995, Tada et al. isolated and identified 66 strains of facultative oligotrophs from the clinical samples out of which 27 strains were *Klebsiella pneumoniae*, 18 strains were *Pseudomonas aeruginosa*, 10 strains were *Enterobacter aerogenes*, 6 strains were *Serratia marcescens*, and 2 strains were *Klebsiella oxytoca*. *K. pneumoniae* and *P. aeruginosa* made up the majority of the bacteria identified (70%). Oligotrophic strain like *K. pneumoniae* strain MB45 was isolated from river water on diluted Luria agar (Kumar et al., 2011). In a separate study from India eight oligotrophic isolates, MB19, MB26, MB29, MB42, MB45, MB49,

MB51 and MB72 were recognized as the member of genus *Klebsiella* (Chakraborty et al., 2013). The attachment of microorganisms to the surfaces and other microorganisms is ubiquitous. Microbes preferentially grown on the surface and attached microorganisms are frequently dominant compared to freely suspended cells ranging from human digestive system to natural streams (Costerton et al., 1978). Gravitational settling, centrifugation, and filtration are enhanced if larger, faster settling aggregates. While biological and inorganic particles can be aggregated by addition of chemical coagulants, the ability of organisms to self associate or bioflocculate. Why microorganisms bioflocculate? Understanding this phenomenon is important for operating suspended growth in the biological reactors. From colloidal properties of inorganic particles, the chemical control of particle aggregation is well established (O'Melia, 1972). Various mechanisms for microbial aggregation were reported which includes polymeric materials, cell appendages like pili, fimbriae, cilia, filaments, fuzz and hairs. Phenomena of attachment involve combination of hydrogen and ionic bonds along with dipolar and hydrophobic interactions (Calleja, 1984). Finally growth within an aggregate may increase nutrient uptake compared to freely dispersed cells. For a pure culture of a bacterium to bioflocculate when substrate is nearly depleted implies that cell association may confer some advantage over freely dispersed cells. A common feature shared by *K. pneumoniae* is the ability to form biofilms, a major virulence factor contributing towards disease of the host (NIH, 2002). Some species of the genus *Klebsiella* were reported to produce exopolysaccharides in the culture medium (Baldi et al., 2009). Gallo et al. (2012) showed that *Klebsiella oxytoca* BAS-10 producing a biotechnologically relevant exopolysaccharide during Fe(III)-citrate fermentation. A strain of *Klebsiella oxytoca* was

isolated from acid pyrite-mine drainage, typically produces a ferric hydrogel, comprising of branched heptasaccharide repeating units; xopolysaccharide, which consists of 4 rhamnose (Rha), 2 glucuronic acids (GlcA) and 1 galactose (Gal) (Arcon et al., 2012). Dlamini et al., 2007, reported that the major monosaccharide constituents of the polysaccharide produced by whey utilizing bacteria *Klebsiella oxytoca,* were rhamnose (37%, w/w) and glucose (34%, w/w) along with the residues of cellobiose suggesting that the polysaccharide had a cellulose backbone. Fucogel, a polysaccharide produced by *Klebsiella pneumoniae* I-1507 was found to compose of galactose, 4-*O*-acetyl-galacturonic acid and fucose (Guetta et al., 2003). Rättö et al. (2001), isolated EPS from two similar *K. pneumoniae* strains and found that each contained approximately mannose, galactose, and GalA in a ratio of almost 3:1:1. In a different study, *K. pneumoniae* EPS isolated from ESKAPE organisms comprised of 1.3% glucose, 49.4% mannose, and 5.0% GlcA (Bales et al., 2013).

VI. Description of the bacterium *Klebsiella pneumoniae*

The genus *Klebsiella* was named after the German bacteriologist Edwin Klebs (1834–1913). *Klebsiella pneumoniae* is a gram negative, nonmotile, encapsulated, lactose-fermenting, facultative anaerobic, rod shaped bacterium. Although found in the normal flora of the mouth, skin, and intestines (Ryan & Ray, 2004), it can cause destructive changes to human lungs if aspirated, specifically to the alveoli resulting in bloody sputum. In the clinical setting, it is the most significant member of the *Klebsiella* genus of Enterobacteriaceae. *K oxytoca* and *K rhinoscleromatis* have also been demonstrated in human clinical specimens.

VII. Clinical Significance of *K. pneumoniae*

K. pneumoniae can cause destructive changes to human lungs via inflammation and hemorrhage with cell death (necrosis) that sometimes produces a thick, bloody, mucoid sputum (currant jelly sputum). These bacteria gain access typically after a person aspirates colonizing oropharyngeal microbes into the lower respiratory tract. As a general rule, *Klebsiella* infections are seen mostly in people with a weakened immune system. Most often, illness affects middle-aged and older men with debilitating diseases. This patient population is believed to have impaired respiratory host defenses, including persons with diabetes, alcoholism, malignancy, liver disease, chronic obstructive pulmonary diseases (COPD), glucocorticoid therapy, renal failure, and certain occupational exposures (such as paper mill workers). Many of these infections are obtained when a person is in the hospital for some other reason (a nosocomial infection). Feces are the most significant source of patient infection, followed by contact with contaminated instruments.

The common condition caused by *Klebsiella* bacteria is pneumonia, typically in the form of bronchopneumonia and also bronchitis. These patients possess an increased tendency to develop lung abscess, cavitation, empyema, and pleural adhesions. It shows high death rate of about 50%, even when antimicrobial therapy is used. The mortality rate can be nearly 100% for people with alcoholism and bacteremia (Forner et al., 2006). In addition to pneumonia, *Klebsiella* can also cause infections in the urinary tract, lower biliary tract, and surgical wound sites. The range of clinical diseases includes pneumonia, thrombophlebitis, urinary tract infection, cholecystitis, diarrhea,

upper respiratory tract infection, wound infection, osteomyelitis, meningitis, and bacteremia and septicemia. For patients with an invasive device in their bodies, contamination of the device becomes a risk; for example, respiratory support equipment and urinary catheters put patients at increased risk. Also, the use of antibiotics can be a factor that increases the risk of nosocomial infection with *Klebsiella* bacteria (Podschun & Ullmann, 1998). Sepsis and septic shock can follow entry of the bacteria into the blood. Two unusual infections of note from *Klebsiella* are rhinoscleroma and ozena. Rhinoscleroma is a chronic inflammatory process involving the nasopharynx. Ozena is a chronicatrophic rhinitis that produces necrosis of nasal mucosa and mucopurulent nasal discharge. Research conducted at King's College, London has implicated molecular mimicry between HLA-B27 and two Klebsiella surface molecules as the cause of ankylosing spondylitis (Rashid & Ebringer, 2007). *Klebsiella* ranks second to *E. coli* for urinary tract infections in older people. It is also an opportunistic pathogen for patients with chronic pulmonary disease, enteric pathogenicity, nasal mucosa atrophy, and rhinoscleroma.

VIII. Biotechnological applications of exopolysaccharides

Polysaccharides are polymers of carbohydrates with huge structural diversity, from long linear repetition of the same monomer to highly branched structures of different sugars. This high structural diversity reflects the functional diversity of these molecules. There are two types of polysaccharides, storage polysaccharides (i.e. glycogen) and structural polysaccharides, which are normally secreted by the cell and form different cell structures (i.e. cellulose, chitin). Extracellular polysaccharides or

exopolysaccharides belong to this last group. EPS are produced not only by microorganisms, but also by algae, plants and animals (Sutherland, 2005). Bacterial exopolysaccharides are a major component of the EPSs or matrix of biofilms, and mediate most of the cell-to-cell and cell-to-surface interactions required for biofilm formation and stabilization (Flemming & Wingender, 2010). The matrices of biofilms from natural environments, such as marine and fresh water, soil, or chronic infections, contain a ubiquitous composition of polysaccharides. More than 30 different matrix polysaccharides have been characterized so far. Several are homopolysaccharides (i.e. glucans, fructans, cellulose), but most of these are heteropolysaccharides consisting on a mixture of sugar residues. Exopolysaccharides can even differ between strains of single species, as exemplified by strains of *Pseudomonas aeruginosa*, which can produce one, two or three different exopolysaccharides (alginate, Pel and Psl) (Ryder et al., 2007). Since most mutants deficient in the synthesis of exopolysaccharides are impaired for biofilm formation it was assumed that bacterial exopolysaccharides play only a structural role in biofilms. However, in recent years an unexpected function for these molecules as inhibitors of biofilm formation has been described. This new function was meticulously reviewed by Rendueles et al. (2012). Oligosaccharides with the ability to inhibit and/or destabilize biofilm formation are referred to as antibiofilm polysaccharides, and their production appears to be a well-conserved ability among living organisms. Interestingly, antibiofilm polysaccharides do not have biocidal activity, a property that could increase the technological applications of these molecules as antibiofilm agents in industry and medicine by diminishing the emergence of resistance by natural selection. EPS occur in two basic forms: as a capsule, where the polymer is closely associated with the cell

surface, and as slime loosely associated with the cell surface. Their composition and structure vary greatly: they can be either homo- or heteropolysaccharides and may also contain a number of different organic and inorganic substituents. Most homopolysaccharides are neutral glucans, whilst the majority of heteropolysaccharides are polyanionic due to the presence of uronic acids. Furthermore, charge can be conferred by the presence of sulphate and phosphate groups, pyruvate ketals or succinyl hemiesters (Sutherland, 1990a; Freitas et al., 2011). EPS production involves a significant expenditure of carbon and energy by microorganisms, an expenditure which must afford them some benefits. EPS act as an adhesin and favour interactions and cellular associations amongst microorganisms, creating micro-environments within which the transfer of genes and metabolites is very common. Moreover, the production of EPS provides a way for microorganisms to ensure their survival in nutrient-starved environments (Sutherland, 1990b; Wolfaardt et al., 1999). They have aroused great interest among biotechnologists because of their wide range of potential applications in such fields as pharmacy, foodstuffs, cosmetics and the petroleum industry, in which emulsifying, viscosifying, suspending and chelating agents are required (Freitas et al., 2011). During the past 50 years a considerable number of bacterial EPS have been described but, with the exception of xanthan produced by *Xanthomonas campestris* and gellan produced by *Sphigomonas paucimobilis*, few have achieved great commercial success due either to their being unable to offer better properties than those already on the market or to difficulties in finding new applications (Sutherland, 2002). Purified *Vibrio* sp. A101 polysaccharide showed decrease in the minimum biofilm eradication concentration (MBEC) of amikacin, tobramycin and gentamicin against *P. aeruginosa*

biofilms (Jiang et al., 2011), suggested potential applications of antibiofilm polysaccharides or oligosaccharides as adjuvants in traditional antibiotic treatment.

The present study dealt with the following objectives:

IX. Objectives of the study

1. To screen and identify EPS-producing bacteria from river water samples.
2. To select an EPS-producing facultative oligotrophic strain from the pool of EPS-producing bacteria for further studies.
3. To reveal basic physiology of the selected strain.
4. To standardize extraction and purification of EPS from the batch culture and quantify EPS yield by the test strain at different phases of growth.
5. To determine the composition of EPS followed by an attempt to reveal the biological properties.
6. To determine the Flocculating and Emulsifying activity of the purified EPS.
7. To optimize EPS dosage, temperature, pH and metal cations on flocculating rate for biotechnology applications.

CHAPTER 1

Chapter 1

Screening and Identification of EPS-producing Bacteria from River Water Samples

1.1. Introduction

Microorganisms (like bacteria, phytoplankton and flagellates) during their life-cycle may produce hydrated polymer of high molecular weight compounds called exopolysaccharides (EPS) (Ducklow & Mitchell, 1979). Literature reveals that EPS may exist as capsules, sheaths, slimes (loosely attached to the cell wall), apical pads or mesh-like fibrils in the natural environment (Beveridge & Graham, 1991; Takeda et al., 1998). Capsules by means of non-covalent linkages are tightly bound to the cell wall where as sheaths are linear EPS-containing structures surrounding chain of cells. It was reported earlier that slime layer is a less organized form of capsule or sheath that diffuses into the surrounding environment (Wingender et al., 1999). To execute diverse functions, microorganisms produce various forms of EPS. Although not an essential feature, EPS does provide structural and functional stability to microbial assemblages in the natural environment (Decho, 2000). Most microorganisms produce EPS either for attachment to substratum (adhesion), formation of micro-consortium/biofilms or binding to other particulate matter (cohesion or aggregation). EPS produced for attachment by microorganisms may influence biofouling by conditioning the substratum (Characklis & Escher, 1988). Other functions like protection against osmotic shock, predation, gliding motility, desiccation and detoxification of toxic compounds, nutrient sequestering, chelation of metals, horizontal transfer etc. have also been accredited to microbial EPS

(Decho, 1990; Hoagland et al., 1993). In the natural environment EPS is generally heteropolymeric (made of different monomeric units) (Decho, 1990). EPS contain non-sugar components like uronic acid, methyl esters, sulphates, pyruvates, proteins, nucleic acids and lipids (Corpe, 1980; Hoagland et al., 1993). Divalent metal cations which are generally adsorbed on the EPS may act as ionic bridges linking adjacent polysaccharide chains (Fletcher, 1980). The presence of side-linkages and organic molecules influence the overall charge, stability, binding capacity, rheology and solubility of the polymer (Hoagland et al., 1993). Many bacterial cultures produce different types of EPS during its life-cycle. For example, most bacteria produce capsular form of EPS during the exponential growth phase and slime type EPS during the stationary growth phase (Decho, 1990). Similarly, the chemical characteristics of EPS changes with the age of the culture (Gloaguen et al., 1995), nutrient levels (De Philippis et al., 1991) and growth conditions (Underwood & Smith, 1998). Heissenberger and Herndl (1994) have shown that metabolically active bacteria produce EPS throughout their living period and may contribute to the EPS concentrations in marine waters, especially in oligotrophic growth conditions. Based upon the information available on the ubiquitous distribution of bacterial EPS in the oceans and its contribution to the organic carbon pool (Stoderegger & Herndl, 1999), its clear that bacterial EPS might play an important role in regulating various marine processes and fuelling the marine food-web (Decho, 1990). However, most of the laboratory and in situ studies on the factors regulating important marine processes like aggregation, flux and trophic web have focused on the role of phytoplankton and its extracellular polymers (Decho, 1990).

Thus, very little is known about the behavior of bacterial EPS in the marine environment despite its wide distribution and high abundance. Some forms of EPS showed good correlation with bacterial production suggesting its utility as a possible organic carbon source. Keeping in mind the ecological significance of the EPS in general and the limited information available on the role of bacterial EPS in marine processes, a study was carried out on screening and identification of river bacteria. Furthermore, experiments were also carried out to assess the effect of bacterial growth conditions on EPS production.

1.2. Materials and methods

1.2.1. Screening of the test strain

Composite water samples were collected using standard methodology (APHA, 1989) from a single sampling station on River Mahananda underneath the Mahananda Bridge, Siliguri, India. Serial dilutions of water samples were made in filtered (water passed through 0.2 mm filter, Millipore, Sydney, Australia) and autoclaved river water and plated on diluted (10^{-3} or 0.001x) Luria Bertani (LB) agar plates (HiMedia M575, India) (nutrient poor). After incubation at 30 °C for 72 h, culturable oligotrophic bacterial colony-forming units (CFU) were obtained. Purification of single colonies was done by dilution streaking on 0.001x LB agar plates. Single colony cultures were maintained on R2A agar (HiMedia M1687) which is a standard environmental cultivation medium. Master plate made up of R2A agar was constructed with purified single colonies. Each master plate was replicated separately in triplicate on LB, 0.001x LB, and R2A agar plate. Colonies that had grown on 0.001x LB agars but not on LB agar were termed as obligate oligotrophs, whereas colonies that were able to grow on all the three different

plates were termed as facultative oligotrophs (Kumar et al., 2010). Bacterial colonies with mucoidal appearance or colonies that had a sticky surface were picked up and purified by repeated streaking on R2A agar plates. On an average 5 to 7 colonies were randomly selected from each plate during every sampling for further study. The purified cultures were then transferred to R2A slants and stored at 4 °C. Pure colonies of each facultative oligotrophic isolates were then inoculated into 50 ml of screening medium (R2A) in 250 ml Erlenmeyer flask, incubated at 30 °C in a rotary shaker at 160 rpm for 48 h. Flocculating properties of culture broth from different isolates were examined using two different suspensions (kaolin and activated carbon) following standard method (Kurane et al., 1994; Suh et al., 1997). High concentration of Ca^{2+} (50 mM) was required for flocculation of kaolin suspension, whereas only 4 mM Ca^{2+} was required for flocculation of activated carbon. Hence, one isolate, named PB12, with high flocculating rate for activated carbon suspension was selected as test strain for further study. Viability of the test strain in different media was also performed at 30 °C to examine the nature of oligotrophic growth. Briefly, inoculum was prepared by transferring a single colony of 24 h old culture of PB12 into 10 ml sterile R2A (pH 7) in 100 ml Erlenmeyer flask. The inoculated medium was incubated at 30 °C for 12 h with agitation (160 rpm). The culture was harvested by centrifuging at 9587.5 x *g* for 5 min at 4 °C and washed twice with sterile saline (0.85% NaCl) water to remove traces of media. The washed pellet was finally suspended in 3 ml sterile saline water. Aliquot of 1.0 ml of concentrated ($1x10^7$ CFU ml^{-1}) cell suspension(s) was added to 25 ml of sterile LB or R2A or river water or 0.001x LB in 250 ml Erlenmeyer flask. The flasks were kept at 30 °C (with shaking; 160 rpm) throughout the period of investigation. Survivability of PB12 cells in each tested

medium was assessed through dilution-plating at different time intervals on fresh LB agar plates.

1.2.2. Identification of the test strain

The selected EPS producing bacterium was identified using both conventional physiological and biochemical tests followed by the molecular identification method based on 16S-rRNA sequencing.

a) *Conventional identification methods*- The bacterial isolate was studied for morphological, physiological and biochemical characteristics (like catalase, oxidase, caseinase, gelatinase, urease, amylase, indole, citrate, MR, VP, nitrate reduction, lipase, and carbohydrate fermentations) following standard methods described earlier (Gerhardt et al., 1981). The culture characteristics and biochemical characteristics were compared with those given in Bergey's Manual of Systematic Microbiology. Using these methods, the culture could be identified up to its family.

b) For further identification, phylogenetic method (16S-rRNA gene sequencing procedure) was used. It was done in three major steps: i) extraction of the chromosomal DNA; ii) gene amplification by polymerase chain reaction (PCR) followed by sequencing of the cloned amplicon; (iii) construction of phylogenetic tree to ascertain the position of the isolate.

i) *Chromosomal DNA extraction*

The chromosomal DNA was extracted by repeated freezing (-80 °C) and heating (at 95 °C) of the bacterial cells for 30 min each in Tris buffer at pH 8. The cells were centrifuged at 9587.5 x *g* for 10 min at 4 °C to separate the cells. To the supernatant, few microlitres of proteinase K, DNAase free RNAase and SDS were added and incubated at

37 °C for half an hour. Further extraction and precipitation was done as mentioned earlier (Sambrook et al., 1989).

ii) The amplification of 16S rRNA gene sequence, purification of PCR product and cloning were done as described earlier (Kumar et al., 2010). Briefly, 1504 bp-segment of the 16S-rRNA gene was amplified by primers 27F (5´-AGAGTTTGATCCTGGCTCAG3´) and 1492R (5´-TACGGTTACCTTGTTACGACTT3´) using BDT v3.1 cycle sequencing kit on ABI 3730x1 Genetic Analyzer following the manufacturer's recommendations. The PCR cycle involved denaturing of the strand at 95 °C for 5 min followed by 30 cycles of annealing (for 1 min at 40 °C), extension (for 3 min at 72°C) and denaturing at 95 °C (for 1 min). A final extension for 10 min at 72 °C was carried out before the amplified sequences were loaded on 0.8% agarose gel and separated by gel electrophoresis. The gel was then immersed in ethidium bromide for 2 h. and the products were detected using a transilluminator. The PCR products were then purified using QIAquick Purification Kit (Qiagen, USA). 16S rRNA gene sequence was used to carry out BLAST with the database of National Center for Biotechnology Information (NCBI, http://blast.ncbi.nlm.nih.gov/ Blast.cgi).

1.2.2.1. Sequence analyses

An almost complete continuous stretch of sequence represented by 1504 nucleotides of 16S rRNA gene from the strain PB12 was used for sequence analyses. The sequence was subjected to analyses at EzTaxon server (Chun et al., 2007), RDP (Cole et al., 2014) and BLAST (Altschul et al., 1990). RDP has several online tools for sequence analyses. For present study two among these were used. This includes CLASSIFIER and

SEQMATCH. The former gives a specific conclusion as to what hierarchal level the query sequence (from a prokaryotic isolate) belongs with percent value, indicative of confidence limit. While the latter gives idea of near relatives that are stored in RDP database. BLAST is the most common search tool available in the web. However, there are some strong demerits as far as results of BLAST are concerned, especially with reference to 16S rRNA gene based taxonomic analysis. Sometimes, the closest relative is missed out. Moreover, the results are not always with respect to type strains. The worker has to carry out additional search. Analyses carried out at EzTaxon displays results with respect to near types strain relative representing the closest spp. Moreover the database displays extent of sequence identity, strain and sequence information as well as link for visualizing pair wise alignment. This server has become an invaluable tool for taxonomists over past few years. Due to several advantages, this server has become an ultimate choice for taxonomic 16S rRNA gene based sequence analyses.

1.2.2.2. Phylogenetic tree construction

In order to construct phylogenetic tree, first of all 16S rRNA gene sequences, representing type strains of all near relatives of the strain in the question were retrieved following searching and retrieving using EzTaxon server, RDP and BLAST search aligned with CLUSTAL_X (Thompson et al., 1997) and edited manually. The edited sequences were then saved in PHYLIP interleaved format. This file was then use as input for construction of distance based neighbour-joining (NJ) trees; trees were also constructed by TREECON software (Van de Peer & De Wachter, 1997) using 100 replications and by using both Kimura's (Kimura, 1980) correction.

1.2.3. Production of EPS

Time course of EPS production was performed in 500 ml flasks containing 100 ml of R2A (pH 7.0) with 160 rpm agitation at 30 °C. Samples were taken every 12 h to measure growth (O.D. at 600 nm), and EPS yield (determined as dry weight of EPS). Isolation of EPS was done after incubating the test strain at 30 °C for 48 h followed by centrifugation of the culture broth, precipitation of supernatant in double volume of cold 95% ethanol followed by dialysis in a dialysis tubing cellulose membrane (D9652, Sigma-Aldrich, retaining MW >12,400 Da) against distilled water for 24 h. The dialyzed material was again centrifuged at 9587.5 × g for 40 min at 4 °C and the supernatant was freeze-dried to obtain EPS.

To study the effect of various carbon sources on EPS production, R2A medium was supplemented singly with glucose, lactose, sucrose, mannose and arabinose (1% w/v). R2A medium without any supplementation was taken as control. Stock solutions of different carbon sources were filter-sterilized and aseptically added to the sterile medium before inoculation.

1.2.4. Effect of pH and temperature on EPS production

The effect of different pH on EPS production was investigated by growing PB12 in R2A medium adjusted to different pH (within the range of 4-9) using buffer systems. Temperature was kept constant at 30 ºC. To investigate the effect of temperature, PB12 was grown in R2A broth at 20 °C, 30 °C, 37 °C and 42 °C with its optimum pH. After an optimum period of incubation (time for maximum EPS production), both growth (measured as absorbance at 600 nm) and EPS yield was determined.

1.3. Results

1.3.1. Characterization of the test strain, PB12

The strain PB12 showed highest flocculating rate (98%) amongst one fifty exopolysaccharide producing isolates. Hence, the test strain used in this study was PB12. The optimum temperature and pH of the test strain was found to be 30 °C ± 2 °C and 7.0 ± 0.1 respectively .The results of biochemical tests have been shown in Table 1.1. It was straight rod 1-2 µm (when grown in LB and observed under light microscope), gram-negative, non-motile, facultative anaerobic belonging to class γ-Proteobacteria of family Enterobacteriaceae. Colonies were circular, convex, translucent, mucoid, sticky and offwhite in color with diameters of 2.0-3.0 mm after 3 days at 30 °C on R2A agar.

>gi|523328777|gb|KF192506.1| *Klebsiella pneumoniae* strain PB12 16S rRNA gene, partial sequence

AGAGTTTGATCCTGGCTCAGATTGAACGCTGGCGGCAGGCCTAACACATGCAAGTCGAGCGGTAG
CACAGAGAGCTTGCTCTCGGGTGACGAGCGGCGGACGGGTGAGTAATGTCTGGGAAACTGCCTGA
TGGAGGGGGATAACTACTGGAAACGGTAGCTAATACCGCATAACGTCGCAAGACCAAAGTGGGGG
ACCTTCGGGCCTCATGCCATCAGATGTGCCCAGATGGGATTAGCTAGTAGGTGGGGTAACGGCTC
ACCTAGGCGACGATCCCTAGCTGGTCTGAGAGGATGACCAGCCACACTGGAACTGAGACACGGTC
CAGACTCCTACGGGAGGCAGCAGTGGGGAATATTGCACAATGGGCGCAAGCCTGATGCAGCCATG
CCGCGTGTGTGAAGAAGGCCTTCGGGTTGTAAAGCACTTTCAGCGGGGAGGAAGGCGATAAGGTT
AATAACCTTGTCGATTGACGTTACCCGCAGAAGAAGCACCGGCTAACTCCGTGCCAGCAGCCGCG
GTAATACGGAGGGTGCAAGCGTTAATCGGAATTACTGGGCGTAAAGCGCACGCAGGCGGTCTGTC
AAGTCGGATGTGAAATCCCCGGGCTCAACCTGGGAACTGCATTCGAAACTGGCAGGCTAGAGTCT
TGTAGAGGGGGGTAGAATTCCAGGTGTAGCGGTGAAATGCGTAGAGATCTGGAGGAATACCGGTG
GCGAAGGCGGCCCCCTGGACAAAGACTGACGCTCAGGTGCGAAAGCGTGGGGAGCAAACAGGATT
AGATACCCTGGTAGTCCACGCCGTAAACGATGTCGATTTGGAGGTTGTGCCCTTGAGGCGTGGCT
TCCGGAGCTAACGCGTTAAATCGACCGCCTGGGGAGTACGGCCGCAAGGTTAAAACTCAAATGAA
TTGACGGGGGCCCGCACAAGCGGTGGAGCATGTGGTTTAATTCGATGCAACGCGAAGAACCTTAC
CTGGTCTTGACATCCACAGAACTTAGCAGAGATGCTTTGGTGCCTTCGGGAACTGTGAGACAGGT
GCTGCATGGCTGTCGTCAGCTCGTGTTGTGAAATGTTGGGTTAAGTCCCGCAACGAGCGCAACCC
TTATCCTTTGTTGCCAGCGGTTGGGCCGGGAACTCAAAGGAGACTGCCAGTGATAAACTGGAGGA
AGGTGGGGATGACGTCAAGTCATCATGGCCCTTACGACCAGGGCTACACACGTGCTACAATGGCA
TATACAAAGAGAAGCGACCTCGCGAGAGCAAGCGGACCTCATAAAGTATGTCGTAGTCCGGATTG

GAGTCTGCAACTCGACTCCATGAAGTCGGAATCGCTAGTAATCGTAGATCAGAATGCTACGGTGA
ATACGTTCCCGGGCCTTGTACACACCGCCCGTCACACCATGGGAGTGGGTTGCAAAAGAAGTAGG
TAGCTTAACCTTCGGGAGGGCGCTTACCACTTTGTGATTCATGACTGGGGTGAAGTCGTAACAAG
GTAACCGTA

Fig. 1.1. Partial 16S rRNA gene sequence of the isolate PB12 (Accession no. KF192506)

Table 1.1. Biochemical characteristics and carbon source utilization of the test strain *Klebsiella pneumoniae* PB12.

+, positive; -, negative; A, acid; G, gas

S. No.	Recipe	Observations
1.	Gram's reaction	'-ve' rod
2.	Oxidase test	-
3.	Catalase test	+
4.	Indole test	-
5.	MR test	-
6.	VP test	+
7.	Citrate	+
8.	Urease	+
9.	Nitrate reduction	+
10.	Starch hydrolysis	-
11.	Glucose	AG
12.	Lactose	AG
13.	Sucrose	AG
14.	Mannitol	AG

When the16S rRNA gene sequence (1504 nucleotides; Fig. 1.1) of PB12 was used to search for similar sequences in the GenBank database, it showed closest sequence similarity (100%) with an uncultured bacterial clone SJTU_D_02_05, a representative sequence from 16SrRNA library of "human fecal sample from subject GGM"(http://www.ncbi.nlm.nih.gov/nucleotide/126111133?report=genbank&log$=nucl align&blast_rank=2&RID=VPKCM0KZ01R). Among the type strains, it showed closest sequence similarity (99.87%) with *Klebsiella pneumoniae* subsp. *rhinoscleromatis* ATCC13884^{T} (ACZD01000038), followed by *K. quasipneumoniae* subsp. *similipneumoniae* 07A044^{T} (HG933295) (99.86%), *K. quasipneumoniae* subsp. *quasipneumoniae* 01A030^{T}(HG933296) (99.86%), *K. pneumoniae* subsp. *ozaenae* ATCC 11296^{T} (Y17654) (99.5%), *K. pneumoniae* subsp. *pneumoniae* DSM 30104^{T} (AJJI01000018) (99.3%) and *Klebsiella variicola* F2R9^{T} (AJ783916) (99.2%). Such high extent of sequence identity is a strong indication that the strain PB12 is a strain within *K. pneumoniae* species. In the phylogenetic tree (Fig. 1.2), strain PB12 forms a clade along with the uncultured bacterial clone, showing very high bootstrap value of confidence. It may therefore be inferred that the isolate PB12 belongs to the *Klebsiella pneumoniae* subsp. *pneumoniae* cluster.

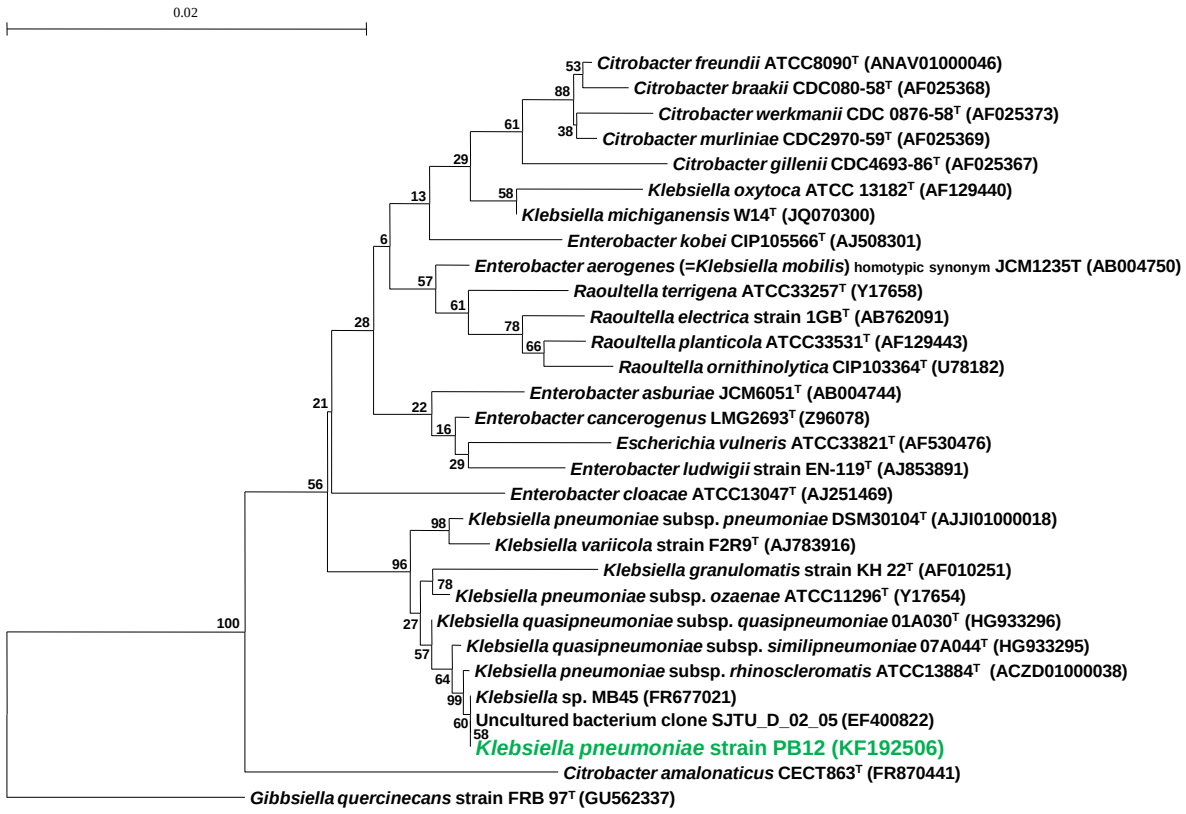

Fig. 1.2. 16S rRNA gene sequence based neighbor-joining tree, showing the position of *Klebsiella pneumoniae* PB12 (green color) among the members of genus *Klebsiella*. Bootstrap percentages are given at the branching nodes. *Gibbsiella quercinecans* strain FRB 97T (GU562337) was used as outgroup. EMBL/GenBank accession numbers are given in parentheses.

1.3.2. Demonstration of oligotrophic trait of PB12 and time course of EPS production

The cells of PB12 were able to grow in 0.001x LB broth as well as sterile river water without supplementation of any carbon or nitrogen source or growth factors. An

increment of nearly 13 times the initial cell number was noted in a span of 3 days in 0.001x LB (Fig. 1.3a). The ability of PB12 to survive without any reduction in viable cell number from the input cells explains the oligotrophic nature.

Yield of EPS in R2A varied with time and was maximal (1.3 g l^{-1}) at 48 h of incubation at 30 °C (Fig. 1.3b). The depletion in the amount of EPS was noticed after 48 h indicating probable utilization of the same as nutrient source for cell growth and viability.

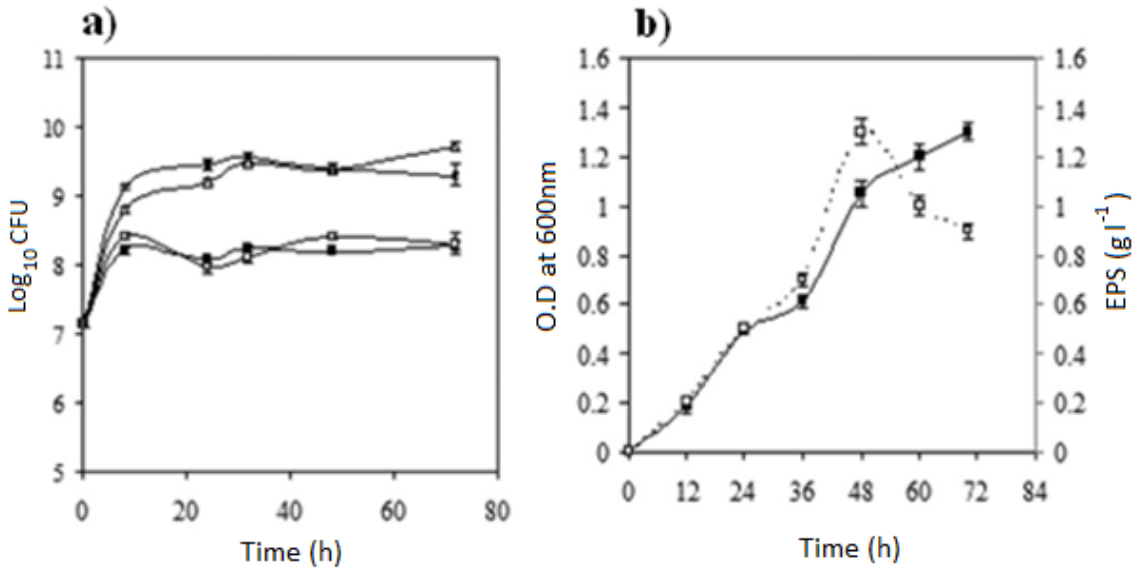

Fig. 1.3. a) Growth pattern (in terms of viability) of PB12 in LB (closed triangles), R2A (open triangles), river water (open squares) and 0.001x LB (closed squares) at 30 °C; **b)** Growth (closed squares; O.D at 600 nm) and EPS production (open squares; g l^{-1}) of *Klebsiella pneumoniae* PB12 in R2A (nutrient poor) broth at 30 °C, pH 7.2 ± 0.2. Data are the mean of triplicates ± S.E.

1.3.3. Effect of supplementation of carbon source in R2A medium on growth and EPS production

Growth and production of EPS in R2A was enhanced maximally by 62% and 38.4%, respectively, when supplemented with 1% glucose. When supplemented with 1% lactose, growth and production was enhanced by 43% and 30%, respectively. In sucrose and rhamnose supplemented R2A, the growth was negligibly affected but the EPS production was enhanced roughly by 18%. Growth was enhanced by 43% with only 8% increase in EPS production when grown in arabinose supplemented R2A medium (Fig. 1.4). Least alteration in growth or EPS production occurred in mannose supplemented R2A medium.

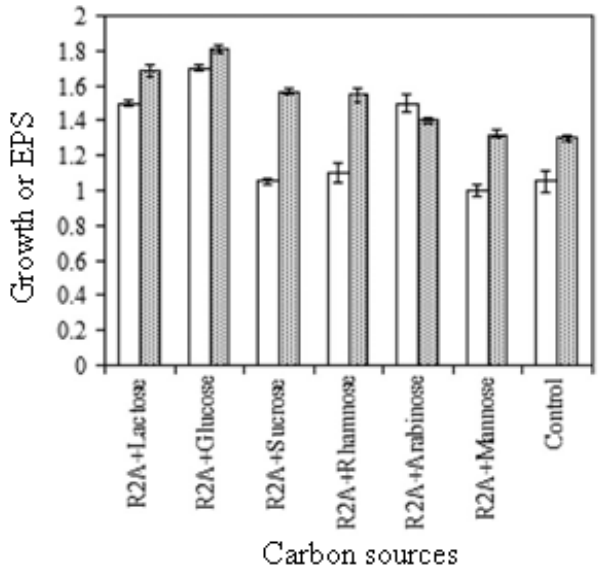

Fig. 1.4. Effect of various carbon source (1%) on growth (open columns) and EPS production (solid columns) at 30 °C. Data are the mean of triplicates ± S.E.

1.3.4. Effect of temperature and pH on EPS production

The highest productivity (1.3 g l^{-1}) of EPS was obtained at 30 ºC (Fig. 1.3b). Above 30 ºC, the productivity of EPS was reduced. Furthermore, maximum growth in terms of optical density was also noticed at 30 ºC, below and above this temperature, both growth and EPS production decreases. The high productivity of EPS (1.3 g l^{-1}) was observed at pH 7. The yield of EPS as well as growth decreased below and above pH 7.

1.4. Discussion

The results obtained from biochemical (Table 1.1) and physiological studies revealed that it belongs to genus *Klebsiella*. As evident from the phylogenetic tree (Fig. 1.2), the strain PB12 forms a clade along with the uncultured bacterial clone, with very high bootstrap value of confidence and it is located within the *Klebsiella pneumoniae* subsp. *Pneumoniae* cluster. The cluster contains four more subspecies of *Klebsiella pneumoniae*, *Klebsiella variicola* and *Klebsiella granulomatis*. Since, during RDP manalyses (CLASSIFIER), the conclusive report of CLASSIFIER tool suggested affiliation of strain PB12 to *Klebsiella* with 86%. In order to validate and confirm its taxonomic status a more extensive phylogenetic analyses of the strain PB12 with closest four genera (*Klebsiella*, *Enterobacter*, *Raoultella* and *Citrobacter*), within the family Enterobacteriaceae was undertaken.

As evident, different representative spp. of the two genera namely, *Citrobacter* and *Raoultella* distinctly occupied two different monophyletic clusters. Majority of the members of Enterobacter-*Escherichia* and *Klebsiella* were positioned in way that reflects monophyletic nature. The *Klebsiella michiganensis- K.oxytoca cluster* was positioned in

between two distinct monophyletic clusters constituted by *Citrobacter freundii- C. gillenii* and *Raoultella terrigena- R. Ornithinolytica*. This cluster constitutd by 2 *Klebsiella* spp. (i.e. *K. michiganensis- K. oxytoca*) looks away from basic monophyletic cluster constituted by other *Klebsiella* spp. This is similar to what has been reported by Drancourt et al (2001), where the genus *Klebsiella* has been suggested to be polyphyletic and heterogenous in nature.

The genus is composed of species that forms three different clusters and the strain PB12 falls within cluster I (that contains *K. granulomatis*, three sub spp of K. *pneumoniae*). Isolates identified as *K. pneumoniae* has been phylogenetically placed under three groups Kp-I, Kp-IIA, Kp-IIB and Kp-III (Brisse & Verhoef, 2001; Brisse et al., 2004; Fevre et al., 2005). No species under *K. granulomatis* is under axenic culture (Carter et al., 1999). Based on genetic and phenotypic characteristics, the names *Klebsiella quasipneumoniae* subsp. *quasipneumoniae* subsp. nov. and *K. quasipneumoniae* subsp. *similipneumoniae* subsp. nov. has been proposed very recently for strains of KpII-A and KpII-B, respectively (Brisse et al., 2014).

The strain PB12 showed gas production from lactose like the three sub spp. of *K. pneumoniae* and like K. *pneumoniae* sun sp. *pneumoniae*, it is positive for VP test and urease activity but negative for MR test (Li et al., 2004). Thus, based on phenotypic and phylogenetic analysis, the strain PB12 was identified as *Klebsiella pneumoniae*.

Fig. 1.3a shows the viability of PB12 in 0.001x LB, river water, R2A and LB broth. In our earlier reports, facultative oligotrophic strains, *Acinetobacter johnsonii* MB52 and *Klebsiella pneumoniae* MB45 showed an increase of 2.5 and 4.6 times the initial cell number when grown in 0.001x LB in the span of 8 and 2 days, respectively

(Kumar et al., 2010; Kumar et al., 2011). Fig. 1.3b shows reduction in EPS amount after 48 h which was probably due to utilization of the EPS by the bacterium. Similar utilization of EPS as carbon source was also observed by earlier authors (Gauri et al., 2009). Microorganisms are known to produce more EPS when grown in carbon enriched medium (high C:N ratios) (Souza & Sutherland, 1994). Nitrogen limitation is known to trigger increased EPS production by microorganisms (Fajon et al 1999). Similarly, increase in EPS yield was observed for *Pseudomonas* PB1 under minimal nitrogen and phosphate concentrations (Williams & Wimpenny, 1977). Although very little is known about the mechanism regulating the production of EPS in nutrient depleted conditions, a shift in the biosynthetic pathways might explain the observed changes. The production of the EPS during the growth of PB12 had certain distinct features. EPS production increased rapidly within 24 to 48 h of culture growth. The EPS production was maximal as the culture approached stationary phase. Bacteria produce EPS during their log-phase depending upon the growth conditions and age of the culture (Decho, 1990). *Klebsiella pnemoniae* PB12 in the present study showed decrease in approximately 31% of EPS during further incubation from 48 h to 72 h in the same batch culture was associated with two times increment in viable cell number. Results showed that supplementation of glucose in R2A support both growth and EPS production in PB12. Similar observation was noted where the supplementation of glucose in nitrogen-free Burk's medium was found to be the best for EPS production by *Azotobacter* sp. SSB81 (Gauri et al., 2009). In the case of *Chryseobacterium daeguense* W6, supplementation of mannose or maltose or glucose in low nutrient medium were favorable carbon source for both production of EPS and cell growth (Liu et al., 2010). EPS produced during different phases of growth have

specific properties and functions. For example, capsular form of EPS is generally produced during log phase that forms a tight envelope around the cell, promoting cell attachment to substratum (Costerton, 1984). Capsules may also provide better protection against predation and help bacteria survive in low pH (Decho & Lopez, 1993). Bacterial capsules also act as a good metal adsorbent (Brown & Lester, 1980) and may act as a buffer against metal toxicity. There are reports on EPS production by the genus *Klebsiella* (Cheng et al., 2004; Ramírez-Castillo & Uribelarrea, 2004). Thus the production of EPS in the exponential phase has ecological significance and may play an important role during the growth of specific bacteria.

CHAPTER 2

Chapter 2

Revealing Basic Physiology of *Klebsiella pneumoniae* Strain PB12

2.1. Introduction

Almost all natural aquatic and terrestrial environments are nutrient inadequate and, as a result, a major portion of the biosphere exists as oligotrophic (nutrient-depleted) habitats (Morita, 1997) The word "oligotroph" is a combination of the Greek adjective *oligos* meaning "few" and the adjective *trophikos* meaning "feeding". It is generally used to refer the environments (like deep oceanic sediments, caves, glacial and polar ice, deep subsurface soil, aquifers, ocean waters, and leached soils) which offer little to sustain life, organisms that survive in such environments, or the adaptations that support survival. In spite of the low-level of nutrients in oligotrophic waters, microbial numbers persist on the order of $0.5–5x10^5$ cells ml^{-1} (Whitman et al., 1998). Furthermore, of the three largest microbial habitats seawater, soil, and sediment/soil sub-surface the rates of cellular activity and turnover are highest in the open ocean (Whitman et al., 1998). In these oligotrophic environments, prokaryotes play a vital role in regulating the world's largest pool of organic carbon via accumulation, export, remineralization and transformation (Cole et al., 1988). Molecular investigations of microbial community have revealed a broad diversity of bacteria in oligotrophic environment, particularly members of the α- and γ-Proteobacteria, as well as members of the *Cytophaga–Flavobacterium–Bacteroides* group. The obscurity in isolating oligotrophs is well reported. The fundamental problem is that obligate oligotrophs are inherently sensitive to high nutrient concentation. As a result bacteria possessing the ability to adapt nutrient composition and generally grow on

media used in laboratory are mostly facultative oligotrophs. (Schut et al., 1997a). A number of aquatic facultative oligotrophs have been isolated including *Caulobacter*, *Hyphomicrobium* (Moaledj, 1978; Poindexter, 1981), *Cydoclastus oligotrophus* (Wang et al., 1996), and *S. alaskensis* (Schut et al., 1997b). Some of the factors which may restrict the ability of oligotrophs to adapt and its isolation include (1) intolerance to high concentrations of nutrients, (2) undesired growth substrates, (3) the lack of various growth factors or specific vitamins, (4) presence of inhibitory growth substrates or other additives, (5) inactivation by the close proximity to other cells (in colonies on agar plates), (6) susceptibility to the oxidative respiratory burst in the presence of fresh nutrients, and (7) the lethal effects of lytic phage.

In the oligotrophic ocean the limited availability of nutrients limits microbial growth which possesses a major impact on microbial physiology. Growth limitation relates largely to the availability of utilizable nutrients, such as carbon, nitrogen and phosphorus, however, the availability of trace metals, vitamins and a variety of physicochemical factors may also impact on the abundance of microorganisms. Although simple laboratory systems cannot confine the richness and complexity of natural ecosystems, such systems do offer a starting point for studying responses to controlled environmental changes and allow the rigorous experimental testing of hypothesis (Velicer & Lenski, 1999). The conventional and perhaps the most clear-cut method of microbial cultivation is the batch culture. Within this system at first all nutrients are in excess allowing the organism to grow at an optimal, unlimited rate. At a point where the concentration of one or more nutrients become limiting the exponential growth rate eventually ceases and the organism enters a starvation state.

The induction of stress resistance mechanisms is a defining characteristic of nonspore forming bacteria that are able to survive long periods of starvation. An ecologically relevant characteristics gained by microorganisms in aquatic environments is the ability to resist damaging effects of oxidative stress (e.g., hydrogen peroxide). This is possibly due to the common challenge to microorganisms by endogenous (due to ongoing metabolism) and exogenous oxidative stress in aquatic environment (Cooper & Zika, 1983). Reactive oxygen species (ROS) can cause damage to DNA, RNA, protein and lipids and as a consequence, cells have evolved a broad range of mechanisms to cope with this type of stress (reviewed in Storz and Imlay, 1999). Bacteria may require various oxidative stress induced proteins in order to defend the cellular machinery from endogenously derived oxidative stress (Dukan & Nystrom, 1999). In this context, defense against oxidative stress may also be a significant issue for slowly growing cells, since their capacity to replace damaged cellular components by new synthesis is limited by resource availability. To validate this, an attempt was made to check the survivability of PB12 in presence of a ROS producer, ZnO-PEI NPs (Chakraborti et al., 2014). Apart from ROS, Nitrous oxide (NO) has many of the properties of a prototypical signaling molecule. It is freely diffusible, transient, and highly reactive in biological systems. Some recent evidence suggests that NO and or its equivalents [S-nitrosothiols (SNO)] may also be involved in signaling in bacteria. Nitric-oxide synthases (NOSs) are widely distributed among prokaryotes and eukaryotes and have diverse functions in physiology. It was confirmed earlier that NOS in *B. subtilis* have the ability to synthesize NO from arginine (Adak et al., 2002), although it's physiological role remains obscure.

In contrast to our understanding of the physiological responses to starvation, little is known about the physiological changes that occur when nutrients are present, but at concentrations that result in sub maximal (being less than the maximum of which it is capable) rates of growth, such as those that are likely to occur in the ocean. Although starvation-induced cross protection is not observed, a marine oligotrophic ultramicrobacterium *Sphingomonas alaskensis* RB2256, maintains a high level of resistance to a variety of stress inducing agents (hydrogen peroxide, heat, ethanol and UV) regardless of whether it is growing or starved (Eguchi et al., 1996; Joux et al., 1999). For all the living organisms, cell size is a key characteristic. In bacteria, cell size plays, both directly and indirectly, an important role in fitness. For example, a bacteria susceptibility to predation by protists and host immune cells, such as neutrophils, depends on its cell size (Justice et al., 2008; Pernthaler, 2005). In addition, the cell size is relevant to mechanisms of antibiotic resistance and protection from bacterial phages (Miller et al., 2004; St-Pierre & Endy, 2008). It was noted earlier that there is a significant increase in antibiotic resistance to gentamicin in cells grown under osmotic stress (higher NaCl concentrations) (Crompton et al., 2014). The possible mechanism is mainly due to the down regulation of synthesis of cell-wall associated proteins under conditions of higher NaCl concentrations which could impede the passage of the antibiotic through the cell wall (McMahon et al., 2006; Frank & Patel, 2007). This increased resistance against antibiotics was often maintained after removal of the stress providing evidence of a stable phenotype and altered metabolism in response to the stress. Moreover, cell size is also closely related to cell proliferation via altering the surface area to volume ratio. Cell size influences the uptake of nutrients, the concentrations of cellular components and the

advancement of intracellular biochemical reactions (Young, 2006). Significantly, the initiation of chromosomal replication and the assembly of the division machinery also depend on cell size, resulting in homeostatic and recursive reproduction of an optimal cellular state (Donachie, 1968; Weart et al, 2007). These facts establish that the bacterial cell size is strongly coupled with its growth rate. During the last decade flow cytometry has been established as a major experimental technique in biology for enumeration of cells. Several reports on a wide variety of applications of this method to various parts of cell biology have been published. So far, however, the work has been limited almost exclusively to eukaryotic cells, while reports on prokaryotic cells have been very limited (Bailey et al., 1977). Previously, tedious physicochemical techniques (like dilution plating) have been used to unravel the growth kinetics of bacteria. Flow cytometry, however, seems ideally suited for the purpose provided sufficient sensitivity and appropriate staining procedures are fulfilled. In this chapter an attempt was made to explore the physiological trends choose by a facultative oligotrophic bacteria in order to reveal the strategy use to survive in nutrient deprived condition.

2.2. Materials and methods

2.2.1. Bacterial strain and growth

All experiments were done using the facultative oligotrophic strain *Klebsiella pneumoniae* PB12 (KF192506). Fresh inoculum was prepared by transferring a single colony of 24 h old culture of PB12 into 10 ml sterile LB (pH 7.0) in 100 ml Erlenmeyer flask. The inoculated medium was incubated at 30 °C for 4 h with agitation. The culture was harvested by centrifuging at 9587.5 x *g* for 5 min at 4 °C and washed twice with

sterile phosphate buffer saline (PBS) to remove traces of media if any. The washed pellet was finally suspended in 3 ml sterile PBS. Aliquots of approximately 10^4 cells were added to 10 ml of LB or diluted (0.01x or 10^{-2}) LB in 100 ml Erlenmeyer flask. The flask was kept at 30 °C (with shaking at 200 rpm) throughout the period of investigation. Survivability of PB12 cells in LB or diluted LB was assessed through dilution-plating of pure culture aliquots at different time intervals on fresh LB agar plates. Colony diameter of PB12 was determined along with the number of cells present on that particular colony was also enumerated using dilution-plating technique.

2.2.2. Scanning electron microscopic (SEM) studies

Overnight grown culture of PB12 cells (10^8 cells ml^{-1}) was washed and re-suspended in PBS as described previously (Chakraborti et al., 2014). Cells were fixed with 2% glutaraldehyde and dehydrated with series of ethanol treatments (10%, 30%, 50%, 70%, 90% and 100%) and examined by SEM (FEI Quanta-200 MK2) with an accelerating voltage of 20 kV. Multiple fields of visions were viewed at different magnifications.

2.2.3. Growth study using Flow cytometry or Fluorescence assisted cell sorting (FACS)

2.2.3.1. Instrumentation

Flow cytometry was performed with an FACS CALIBUR, Becton Dickinson, USA using CellQuest software. Sample excitation was done with an argon laser operating at 15 mW and 488 nm. Filter settings were 525 BP for FITC and 550 LP and 630 BP for

measurement of PI. Acquisition and data analysis were done with standard ELITE software, using the Immuno-4 program to determine the percentage of stained events.

2.2.3.2. Calibrations and discriminator

The flow cytometer was calibrated with Fluoresbrite plain microspheres (Polysciences, Inc., Warrington, PA), 0.72 µm in diameter, on forward scatter (FSC), side scatter (SSC), and FITC fluorescence. Fluorescence quantitation was done with fluorescein quantitation kits (Quantum 24 and Quantum 25, from Flow Cytometry Standards Corp., Research Triangle Park, NC). To determine the level of background noise, plain microspheres (Polysciences, Inc.), 0.79 µm in diameter, were used and were assumed to have no fluorescence. The mean fluorescence (logarithmic scale) was the fluorescence value corresponding to the calculated mean channel number (linear scale) of all events and was therefore not a true mean. Percentages of stained bacteria were determined with Immuno-4 software (Coulter). Sorting experiments were performed with gates on FSC >1,000 and on FSC <1,000 in combinations with gates on SSC or PI. Samples were injected through the instrument using the low pressure setting (12 pvrnin), which ensured the clear detection of individual bacterial cells. All media, buffers, and solutions were filtered through a 0.22-µm membrane filter (Nalgene Brand Products, Rochester, NY, USA) to remove microparticulates that would otherwise contribute to background noise during data acquisition. *K. pneumoniae PB12* cultured aerobically in LB broth (Difco, Detroit, Michigan, USA) at 30 °C overnight. A 1:100 dilution of this culture was made into fresh, sterile LB or 0.01x LB broths and incubated for another 8 h at 30 °C in a shaking waterbath (250 rpm) until the culture had entered early log-phase. Each sample was centrifuged at 8000 rpm for 5 min, the pellet re-suspended in 1 ml 0.1

M Tris-HC1 buffer, and then fixed by rapid injection into a 10 ml volume of ice-cold 70% ethanol. The fixed samples were kept at 4 °C until analysed. Following the fixation process, cells were prepared for flow cytometric analysis by using the following procedure. Cells were centrifuged and washed twice in 1 ml ice-cold 0.1 M Tris-HC1 buffer. FITC was added to give a final concentration of 20 mg l^{-1}. Cells were left to stain at room temperature for 15 min, then sedimented by centrifugation (as earlier), and resuspended in 1 ml 0.1 M Tris-HC1 buffer before flow cytometric analysis. Data was collected from 10,000 cells for each sample, at a flow rate of approximately 500 cells per second. All the photomultiplier amplifier gains were set in linear mode.

2.2.4. Determination of intracellular ROS

Measurements of intracellular ROS levels in PB12, grown in LB broth and 10^{-2} LB broth were made using 2', 7'-dichlorodihydrofluoroscein diacetate ($DCFH_2$-DA). Samples were incubated in the presence of 10 mM $DCFH_2$-DA in phosphate buffered saline (PBS) at 30 °C for 30 min then washed two times with PBS and centrifuged at 1200 rpm to remove the extracellular $DCFH_2$-DA. The trapped fluorescent dye (DCF) inside the cells used to evaluate and detect intracellular ROS. The fluorescence values at different conditions were monitored by excitation at 498 nm and emission 530 nm.

2.2.5. Determination of NO generation

NO generation was determined according to the method of Chakraborty et al. 2011. In brief, 100 µl of Griess reagent (containing 1 part of 1% sulfanilamide in 5% phosphoric acid, and 1 part of 0.1% of N-C-1napthyl ethylene diaminedihydrochloride) was added to 100 µl of sample, incubated at room temperature for 10 minutes, readings

were taken in a UV spectrophotometer at 550 nm and compared to a sodium nitrite standard curve (values ranging between 0.5 and 25 μM). The level of NO was expressed as μM/mg protein.

2.2.6. Determination of SOD activity

Cu,ZnSOD activity was assayed by the pyrogallol method (Marklund & Marklund 1974). The periplasmic fraction was obtained by a procedure described previously (Battistoni et al., 1996). The low expression level of Cu,ZnSOD and the presence of small amounts of cytoplasmic FeSOD and MnSOD in the periplasmic extracts prevent accurate measurements of Cu,ZnSOD. Therefore, to characterize our model we have determined the Cu, ZnSOD activity in periplasmic extracts before and after 15 min incubation with 2 mM diethyldithiocarbamate, a copper chelator which inactivates the Cu,ZnSOD enzyme without affecting the activity of MnSOD and FeSOD (Benov & Fridovich, 1994). Protein content was determined by the method of Lowry et al. β-Gal activity was measured by a previously described procedure (Sambrook et al., 1989). Cu,ZnSOD activity was determined by subtracting diethyldithiocarbamate resistant activity from the total SOD activity present in periplasmic extracts in the absence of such a copper-chelating agent. One unit is defined as the amount of Cu,ZnSOD necessary to achieve 50% inhibition of pyrogallol autoxidation.

2.2.7. Determination of catalase (CAT) activity

Catalase activity was measured in the cell lysate by the method decribed earlier (Luck, 1963). The final reaction volume of 3 ml contained 0.05 M Tris-buffer, 5 mM EDTA (pH 7.0), and 10 mM H_2O_2 (in 0.1 M potassium phosphate buffer, pH 7.0). About

50 µl aliquot of the lysates were added to the above mixture. The rate of change of absorbance per min at 240 nm was recorded. Catalase activity was calculated by using the molar extinction coefficient of 43.6 M^{-1} cm^{-1} for H_2O_2. The level of catalase was expressed in terms of mmol/min/mg protein.

2.2.8. Survivability of PB12 cells in presence of ZnO-PEI nanoparticles (ZnO-PEI NPs)

Fresh inoculum of *Klebsiella pneumoniae* PB12 was prepared by transferring a single colony of 24 h old culture into 10 ml sterile LB (pH 7) in 100 ml Erlenmeyer flask. The inoculated medium was incubated at 30 °C for 12 h with agitation (200 rpm). Survival experiments were performed by sub-culturing overnight grown culture in LB or 10^{-2} LB broths with agitation (200 rpm). After 8 h (for LB; nutrient rich medium) or 24 h (for 0.01x LB; nutrient-poor medium) of growth, cells were harvested by centrifuging at 10,000 × g for 10 min at 4 °C respectively. Pellets obtained were washed thrice with sterile phosphate buffer saline (PBS) to remove traces of media. Washed pellets obtained from LB or 0.01x LB was then re-suspended in PBS and the O.D was adjusted before any treatment with LD_{50} dosage (15 µg ml^{-1}) of ZnO-PEI NPs (Chakraborti et al., 2014) respectively for 30 min, serially diluted and plated on fresh LB agar plates. After overnight incubation at 30 °C, difference in percentage survival was then calculated from the cell count obtained before and after treatment with ZnO-PEI NPs.

2.2.9. Analysis of Raman Spectra of nanoparticles treated PB12 cells grown in diluted and undiluted Luria broth

A Renishaw RM1000 Raman spectrometer system (Gloucestershire, UK) equipped with equipped with a Leica DMLB microscope (Wetzlar, Germany) and a 785 nm near infrared diode laser source (maximum at 300 mW) was used in this study. Raman scattering signals were detected by a 578 x 385 pixels CCD array detector. Raman spectra were acquired from PB12 culture grown in LB (without ZnO-PEI NPs) or PB12 culture grown in 0.01x LB (without ZnO-PEI NPs) or PB12 culture grown in LB (treated with ZnO-PEI NPs) or PB12 culture grown in 0.01x LB (treated with ZnO-PEI NPs) using a 50x objective with a detection range from 700-1900 cm^{-1} in the extended mode. The measurement was conducted with a 10 s exposure time and c.10 mW laser power. Data analysis was performed using Delight version 3.2.1 (D-Squared Development Inc., LaGrande, OR, USA) software. Preprocessing algorithms such as smoothing and polynomial subtract were employed to analyse the data.

2.3. Results

2.3.1. Growth study

The growth of PB12 cells were observed in LB or diluted (0.01x) LB (without any supplementation) (Fig. 2.1a). The mean generation time of PB12 in LB or 0.01x LB was 25 min or 36 min respectively. The ability of PB12 to survive (without reduction in viable cell number since inoculation) and grow in a low nutrient medium establishes the oligotrophic nature of the strain. This means that, even at 10 times diluted LB, the nutrient concentration was high enough to support the growth of these cells; in other

words, the cells can carry out reproduction along with the macromolecular synthesis with whatever in their milieu over a given time period even at 10 times diluted LB. Colony diameter of PB12 grown on LB agar after 24 h was found to be 1.5 mm (Fig. 2.1b), whereas, colony diameter of PB12 on 0.01x LB after 24 h of incubation was 0.5 mm (Fig. 2.1c). After assessing the number of cells presents in this colony it was noted that colonies obtained on LB agar (d=1.5 mm) there are 1.8 x 10^8 cells present. Interestingly, 5.4 x 10^8 number of cells was obtained from the colony grown on diluted LB agar plates.

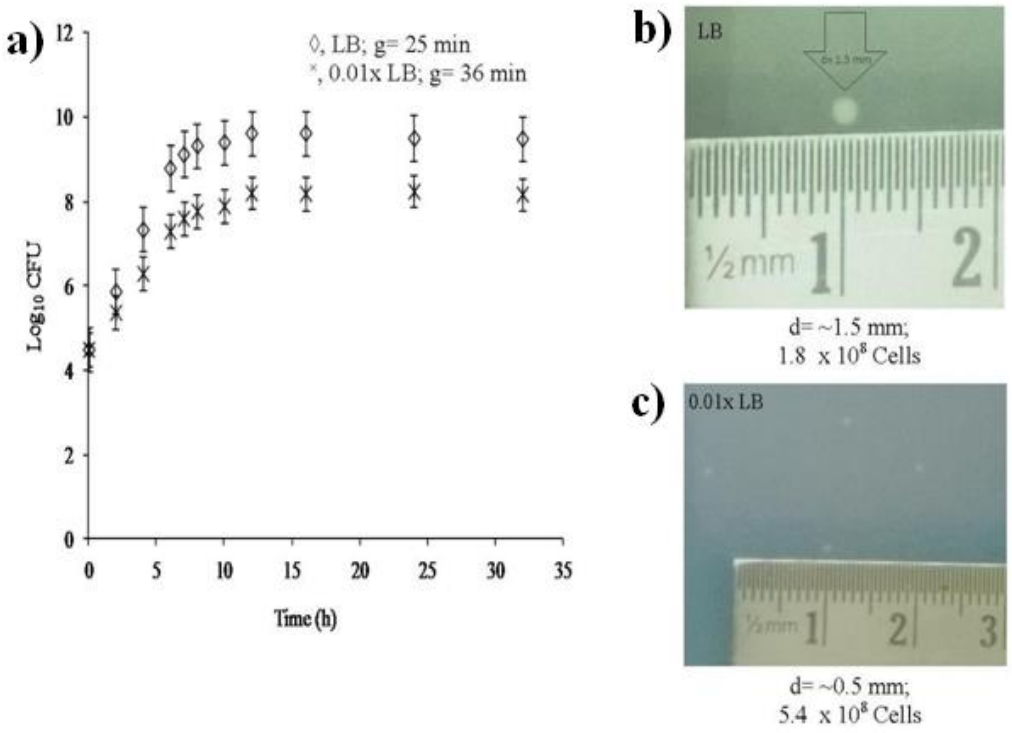

Fig.2.1. a) Viability and growth curve of *K. pneumoniae* PB12 in LB broth, ◊ (g= 25 min) and in 0.01x LB broth, × (g= 36 min); **b)** *K. pneumoniae* PB12 bacterial obtained on LB agar plate after 24 h of incubation (d= ~1.5 mm; CFU= 1.8 x 10^8 cells); **c)** *K. pneumoniae* PB12 bacterial obtained on 0.01x LB agar plate after 24 h of incubation (d=

~0.5 mm; CFU= 5.4 x 10^8 cells). The data represent the mean ± standard deviation of three independent experiments (n = 3).

2.3.2. SEM and FACS study

Scanning electron micrograph of PB12 cells grown on LB or 0.01x LB was found to be 1.55 ± 0.15 µm or 0.787 ± 0.18 µm respectively (Fig 2.2a & b). In an earlier studies, flow cytometry was successfully used to detect and quantify cell shape differences between the rod-shaped cells of *E. coli*: CS109 and the seriously deformed cells of *E. coli*: CS315-1K, a mutant lacking PBPs 4, 5, and 7 (Meberg et al., 2004). When PB12 cells grown in LB was compared with the cells grown in 0.01x LB in the absence of added fluorophore, the two populations could be distinguished from one another by examining the distribution of forward scattered light (Fig. 2.2c & d). The application of flow cytometry to the study of bacterial responses to antibiotics was done earlier (Gant et al., 1993). PB12 cells population grown in LB was skewed to the right on the *x* axis (forward- scattered light), indicating that the cells were possibly larger (Fig. 2.2c) than PB12 cells grown in 0.01x LB (which as skewed to the left on the *x* axis) (Fig. 2.2d).

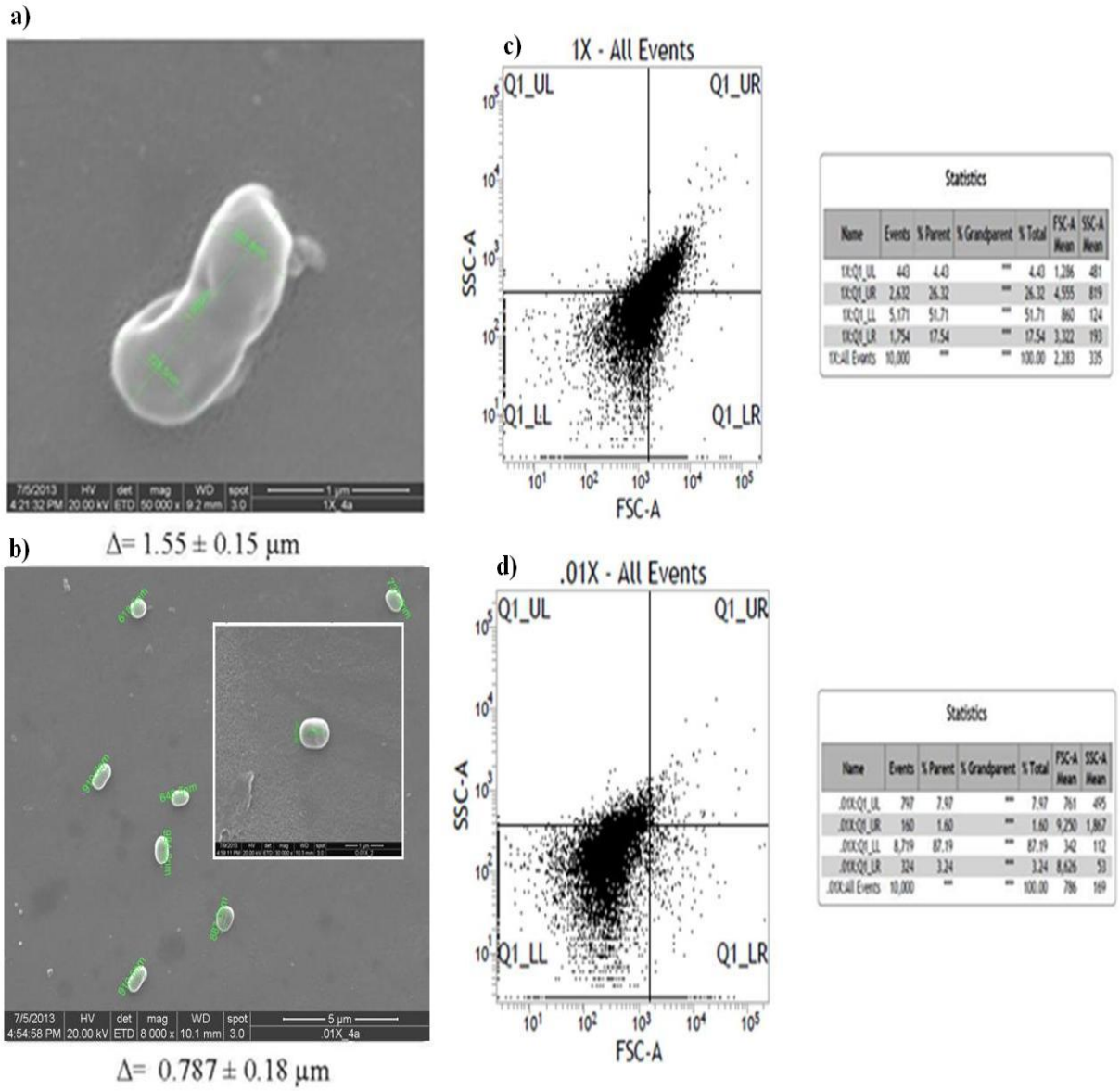

Fig.2.2. SEM micrograph of PB12 cell: **a)** grown in LB; **b)** grown in 0.01x LB; scatter plot of FSC vs SSC to visualize the distribution of PB12 cells based upon size; **c)** PB12 cells grown in LB; **d)** PB12 cells grown in 0.01x LB. The data represent the mean ± standard deviation of three independent experiments (n = 3).

2.3.3. Determination of intracellular ROS

Oxidative stress can cause several types of damage to the bacterial cell, including metabolic pathway disruptions and bacteriostatic and bactericidal effects (Berlett & Stadtman, 1997; Fridovich, 1998). Using an oxidant-sensing fluorescent probe 2', 7'-dichlorodihydrofluorescein diacetate ($DCFH_2$-DA) intracellular ROS can be measured. $DCFH_2$-DA, a nonpolar dye, converted into the polar derivative $DCFH_2$ (nonfluorescent) by means of cellular esterase. After getting oxidized by intracellular ROS and other peroxides it switched to highly fluorescent DCF. Scheme 1 represents the basic principal of $DCFH_2$-DA dye. Fig. 2.3a and Fig. 2.3b indicates the intracellular ROS production in PB12 cells grown in LB and 0.01x LB respectively. Results showed that intracellular ROS production is more in LB grown cells compare to 0.01x LB grown cells. Oxygen derivatives like superoxide (O_2^-), hydrogen peroxide (H_2O_2), and the hydroxyl radical (OH) are usually generated as toxic by-products of aerobic metabolism in a cascade of monovalent reductions from molecular oxygen (Shimizu, 2014). Although these are not so reactive *per se*, O_2^- and H_2O_2 cause severe cell damage. H_2O_2 along with Fe^{2+} *via* the Fenton reaction produces OH, which reacts with any macromolecule such as protein, membrane constituents, and DNA (Greenberg et al., 1990; Liochev & Fridovich, 1994)

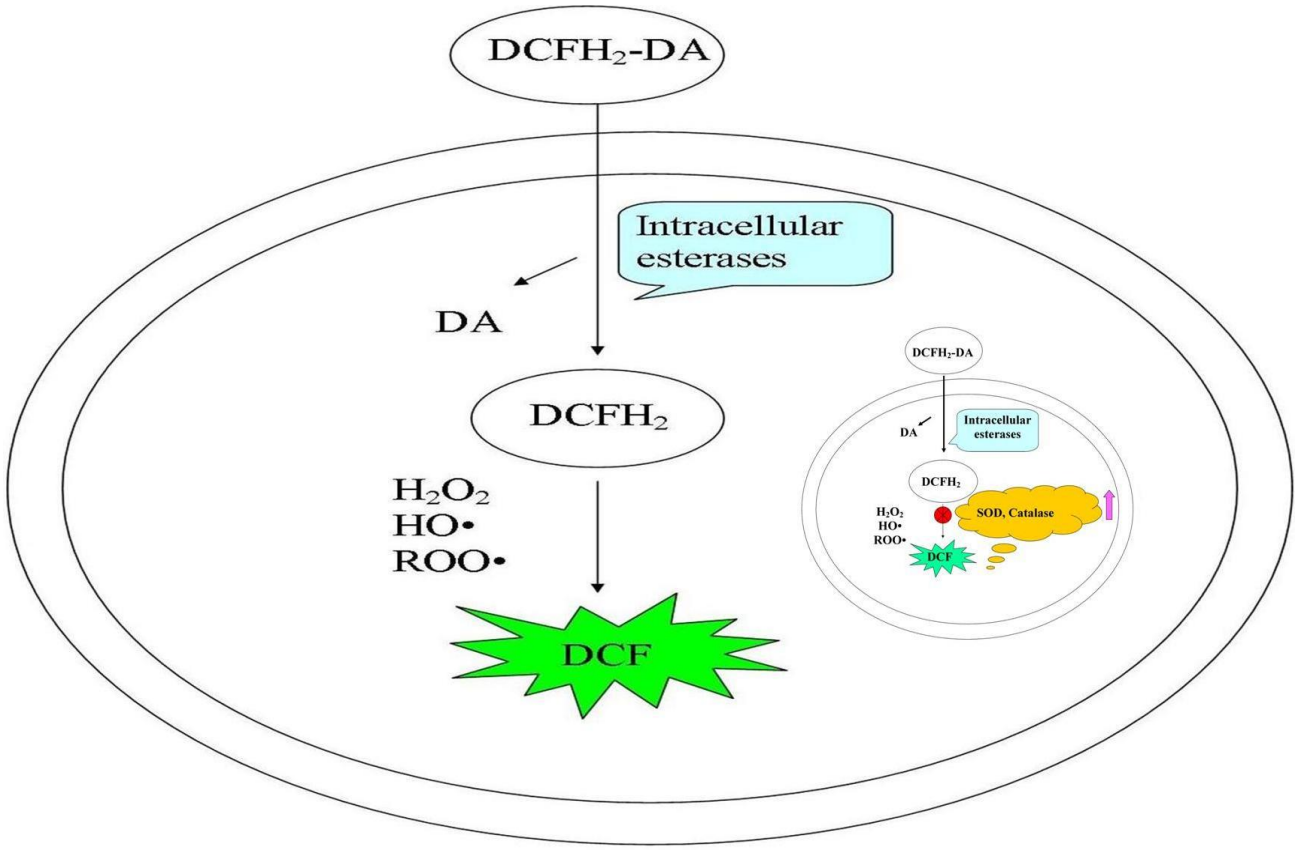

Scheme 2.1. The principal of the $DCFH_2$-DA dye. High intracellular level of SOD or Catalase enzyme prevents oxidation of $DCFH_2$ and the formation of fluorescent DCF product (figure inset).

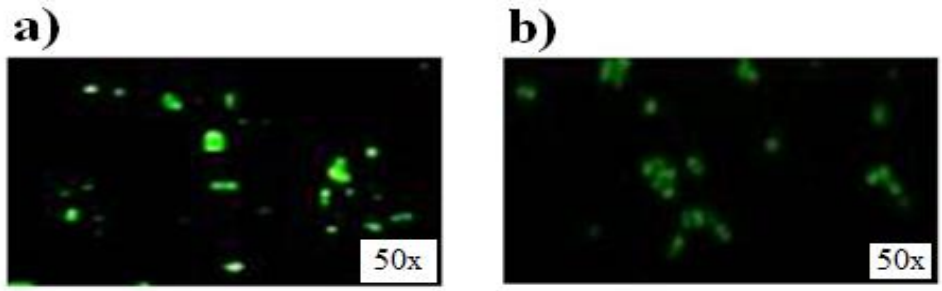

Fig. 2.3. Fluorescence micrographs of PB12 cells: **a)** grown in LB; **b)** grown in 0.01x LB.

2.3.4. Determination of NO generation

The bioactive gas nitric oxide (NO) has multiple biological functions in a very broad range of organisms. It is well-known that NO exerts both pro-oxidant and antioxidant effects, depending on the ambient redox status, the presence of other reactants, and the nature of the reaction (Wilson et al., 2008). It was noted that the PB12 cells grown in LB exhibited higher NO production than the cells grown in 0.01x LB (Fig. 2.4.).

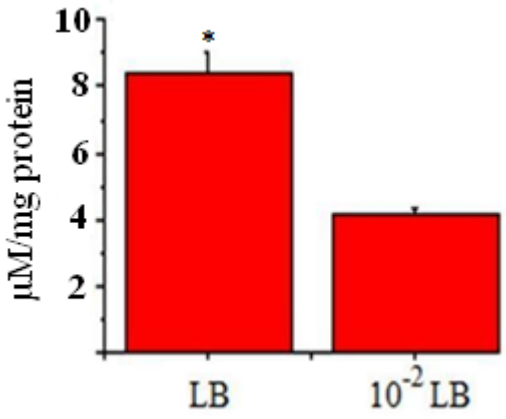

Fig. 2.4. Variations of NO production in *Klebsiella pneumoniae* PB12 cells grown in either LB or 0.01x LB (10^{-2}) broth.

2.3.5. Determination of Cu,ZnSOD and CAT activity

It now seems clear that starvation adaptation is important for cells to initiate long-term survival via developing resistance to oxidative stress. Clearly, oxidative stress is a condition likely to be professed by many bacteria, for example, in the form of reactive oxygen species. As SOD functions to detoxify superoxide, we sought to determine the

Cu,ZnSOD activity in *Klebsiella pneumoniae* PB12 grown in LB and 0.01x LB. Our present result focused in Fig. 2.5a, where Cu,ZnSOD activity has increased significantly ($P< 0.05$) in 0.01x LB grown PB 12 cells compared to LB grown PB 12 cells.

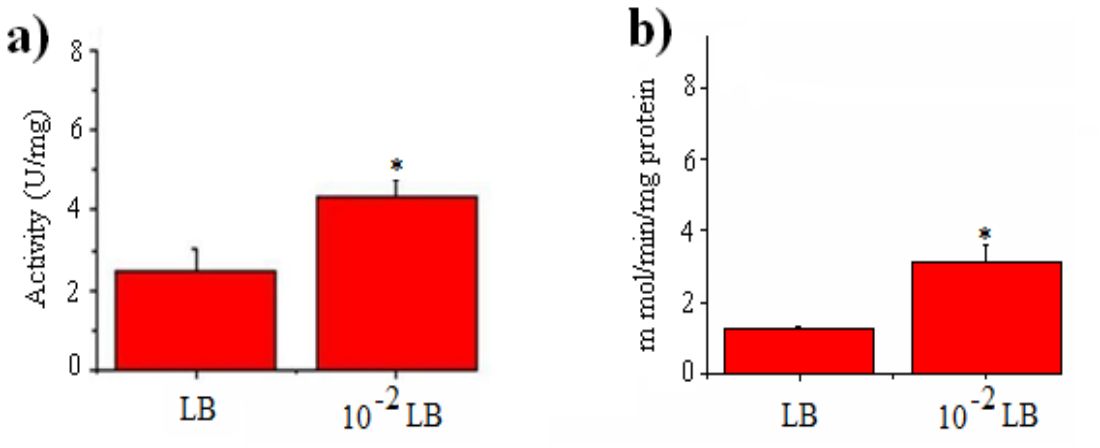

Fig. 2.5. a) Variations of Cu,ZnSOD activity in *Klebsiella pneumoniae* PB12 cells grown in LB or 0.01x (10^{-2}) LB; **b)** Variations of catalase activity *Klebsiella pneumoniae* PB12 cells grown in LB or 0.01x (10^{-2}) LB.

The superoxide radical is also generated by autoxidation of intracellular compounds. Its spontaneous dismutation in water, which yields H_2O_2 and also $^{-}O_2$, proceeds at a very high rate, yet in the cell the dismutation is additionally catalyzed by SOD. Superoxide free radicals are neutralized by the action of superoxide dismutase, generating hydrogen peroxide, which in turn is broken down by catalase. Here, catalase level has been found to be higher in 0.01x LB grown PB12 cells than LB grown cells (Fig. 2.5b). This rapid removal of O_2^- is very important for the cell because superoxide can give rise to very reactive ROS, such as H_2O_2, HO• or singlet oxygen; the peroxynitrite anion ($ONOO^-$) is formed when O_2^- reacts with NO. Despite its low

reactivity, O_2^- has been shown to inhibit antioxidant enzymes, such as catalase (Halliwell & Gutteridge 1986).

2.3.6. Survivability of PB12 cells in presence of ZnO-PEI nanoparticles (ZnO-PEI NPs) and its interpretation using Raman spectra

In one of the reports, it was established that ZnO-PEI NPs possess the potential to generate extracellular ROS and which is related to its antibacterial activity (Chakraborti et al., 2014). In this study, ZnO-PEI NPs was used as a model ROS generator to study its effect on PB12 cells grown in LB or 0.01x LB. Results showed that LD_{50} dosage of ZnO-PEI NPs cause only 35% reduction in bacterial growth of 0.01x LB grown cells whereas, approximately 50% reduction in bacterial growth was noted when LB grown cells were treated with same dosage of NPs ($p < 0.05$) (Fig. 2.6a). Moreover, Raman spectroscopy was used to derive more insight. Results showed that subtle differences were observed in the spectra of LB grown cells compared to 0.01x LB grown cells treated with same concentration of ZnO-PEI NPs (Fig. 2.6b). *Klebsiella pneumoniae* PB12 spectra showed distinctive absorption bands between 600 and 1800 cm^{-1}, that includes peak for proteins, lipids, carbohydrates and nucleic acids and these spectra are in good agreement with the previously published spectra (Chan et al., 2007). The main Raman peaks of PB12 cells showing bands around 853, 1005, 1252 and 1665 cm^{-1} were assigned to proteins; bands around 726, 783, 936, 1101, 1340 and 1577 cm^{-1} were assigned to nucleic acids; bands around 977 and 1453 cm^{-1} were assigned to lipids; and those around 1035 cm^{-1} was assigned to carbohydrates.

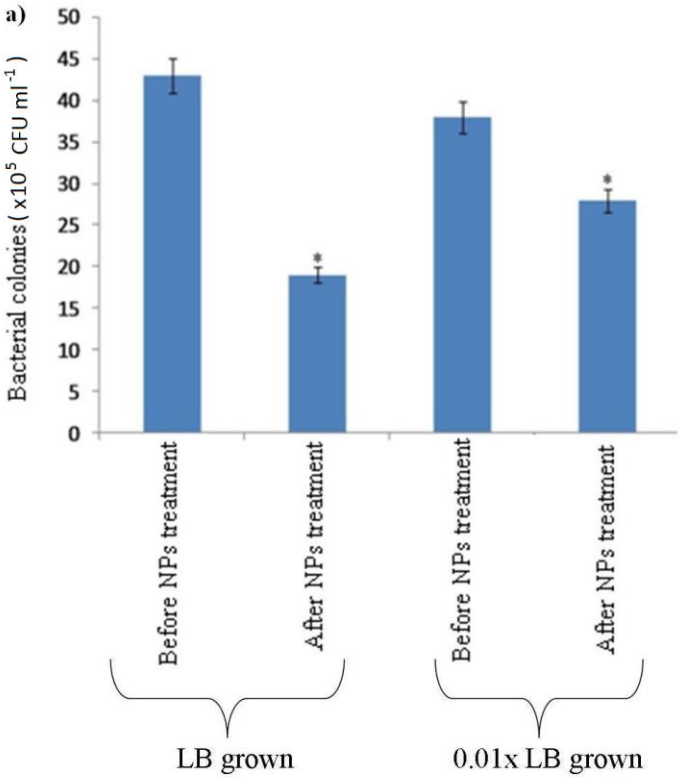
a)
Bacterial colonies (x10^5 CFU ml^{-1})
50
45
40
35
30
25
20
15
10
5
0
*
*
Before NPs treatment
After NPs treatment
Before NPs treatment
After NPs treatment
LB grown
0.01x LB grown

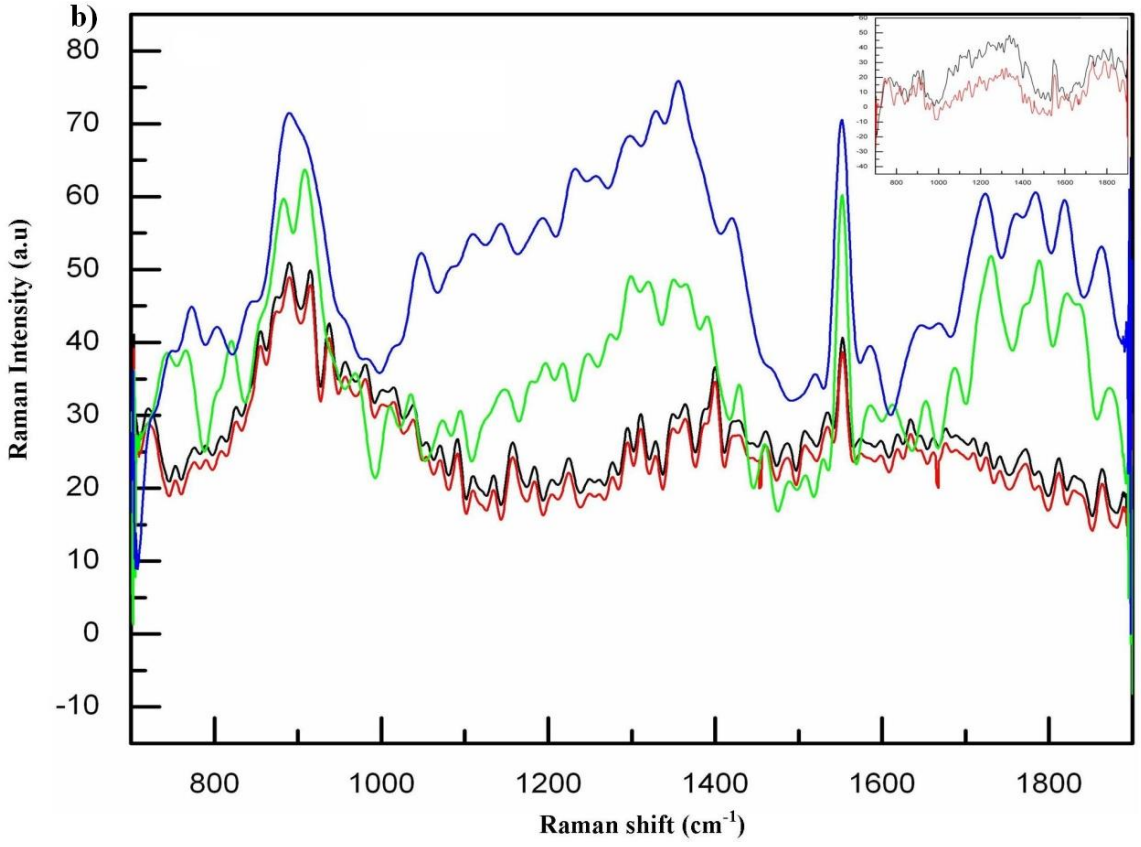
b)
Raman Intensity (a.u)
80
70
60
50
40
30
20
10
0
-10
800
1000
1200
1400
1600
1800
Raman shift (cm^{-1})

Fig.2.6. a) Histogram of number of bacterial colonies as function of NP treated and untreated PB12 cells grown in either LB or 0.01x LB broth; **b)** Raman spectra of PB12 cells grown in either presence or absence of ZnO-PEI suspension (red colour line, PB12 cells grown in 0.01x LB broth; black colour line, PB12 cells grown in LB; green colour line, ZnO-PEI NPs treated PB12 cells grown in 0.01x LB broth; ZnO-PEI NPs treated PB12 cells grown in LB broth). Measurements were taken from 700 to 1900 cm^{-1} at 10 s and c. 10 mW laser power.

2.4. Discussion

Bacterial stress can be caused by environmental modifications (physical/nutritional) that can have many consequences, such as retarded growth and cell death (Fridovich, 1998). Living organism always struggle to survive in response to variety of environmental perturbations. For this, living organisms sense environmental changes by detecting extracellular signals such as the concentrations of nutrients such as carbon, nitrogen, phosphate, sulfur, ion sources, or physical growth factors like pH, temperature, oxygen availability or stresses induced by oxygen, osmolarity, or solvent. These signals ultimately feed into the transcriptional regulatory systems, which affect the physiological and morphological changes to cope effectively for their survival (Seshasayee et al., 2006). Bacterial cells possess complex but efficient mechanisms to respond to the change in culture environment. This is mainly achieved by the so-called global regulators, where they generally act at transcriptional level. A two-component signal transduction system is considered to be the important means of detecting extracellular signals and transducing the signals into cytosol for metabolic regulation. These involve a phospho-relay from a transmembrane histidine protein kinase sensor to the target response regulator. In the case

of *E. coli*, 29 transcription factors (TFs) show such regulation with 28 histidine protein kinase (Kanehisa et al., 2006), where the genes encoding the two components are usually located within the same operon, enabling their coordinated expression. Coordinating growth with division is essential to ensure that cells are the appropriate size for a given environmental condition or developmental fate. This is true not only for multicellular plants and animals, but also for single-celled organisms that need to adapt quickly to rapid changes in environmental conditions. Like their eukaryotic counterparts, in the absence of environmental or internal pressure to increase size, exponentially growing bacteria cultured under a constant set of parameters exhibit little size variation between cells. Similar type of size variation was noted in PB12 cells when it allows growing in nutrient-poor condition. It is essential to note that cell size and shape are, not surprisingly, sensitive to changes in the morphogenesis of the bacterial cell wall because it was noted earlier that bacteria without such cell walls also have complicated morphologies (Miyata & Ogaki, 2006). It was found that bacterial morphology is determined by the coordinated operation of at least two mechanisms: one responsible for cell elongation and the other for division. By means of an actin homologue elongation is driven (e.g., MreB or its relatives) whereas, cell division is driven by the tubulin homologue, FtsZ. FtsZ assembles as a ring at the middle of the cell to localize and initiate cell division (Buddelmeijer & Beckwith, 2002), while MreB is required for cells to grow as rods instead of spheres and coordinates its activities with the FtsZ ring (Vats et al., 2009).

Bacteria in natural environments are relentlessly challenged by the need to familiarize it under varied nutrient availability and stress conditions. In response to such

changes, *Eschericia coli* (Jenkins et al. 1988), *Salmonella spp.* (Foster & Spector 1995), *Pseudomonas spp*. (Jørgensen et al. 1994), and *Vibrio spp.* (Östling et al. 1993) have been shown to elicit classical intracellular reorganization programmes. Naturally, these programmes are operative to make possible the development of cells for long-term survival as well as immediate recovery and consequently by a series of physiological and genetic alteration (Östling et al. 1993). In the present study, it was however attempted to understand how *Klebsiella pneumoniae* PB12 becomes accustomed to stasis, whether induced by lack of nutrients or as provoked by stress conditions. It was observed that Cu,ZnSOD production was higher in 0.01x LB grown PB12 cells compare to PB12 cells grown in LB broth. Literature reveals that periplasmic Cu,Zn-cofactored superoxide dismutase (SodC) protects Gram-negative bacteria from exogenous oxidative damage. Recently, a Cu,Zn-SOD has been found in *Escherichia coli* (Benov & Fridovich, 1994). The factors that may have contributed for the considerably increase in SodC is the selection of conditions under which bacteria are to be cultured. In fact it was found that the level of Cu,Zn-SOD activity was high when organisms are allowed to grown in 0.01x LB rather than in LB. In agreement with this observation, production of the *E. coli* putative Cu,Zn-SOD is strongly induced during aerobic growth (Benov & Fridovich, 1994). Moreover, Kroll et al. found that Cu,Zn-SOD activity can be considerably increased when organisms are grown in shaking liquid media rather than on nutrient agar plates. It was reported earlier that ZnO-PEI NPs possess the potential to generate ROS (Chakraborti et al., 2014). Viability assay in terms of decrease in CFU/ml was done in the presence of ZnO-PEI NPs. It was noted that 0.01x LB grown PB12 cells are more resistant towards NP challenge. This could be explained by the fact that 0.01x LB grown

PB12 cells showed high level of Cu,Zn-SOD and catalase activity compared to its other counterpart grown in undiluted LB. Moreover, the effect of NPs was also demonstrated using Raman spectroscopy which further supports our claim. It was reported earlier that *B. subtilis* utilizes endogenous and exogenous NO for rapid protection from oxidative damage (Gusarov & Nudler, 2005). It was well known that NO suppresses the Fenton reaction by transiently inhibiting cysteine reduction. Our hypothesis is: because the production of catalase and Cu,Zn-SOD is less in LB grown PB12 cells compare to 0.01x LB grown cells, the possible role of NO is to activate catalase vis-a-vis to detoxify excess H_2O_2. Similar type of explanation was also reported earlier (Gusarov & Nudler, 2005). These physiological studies conducted in this chapter may enlighten the survival strategy of a model facultative oligotrophic bacterium, PB12.

CHAPTER 3

Chapter 3

Determination of Structure and Immunological Function of the Exopolysaccharide Synthesized by *Klebsiella pneumoniae* PB12

3.1. Introduction

Klebsiella pneumoniae, a Gram-negative opportunistic pathogen causes hospital-acquired urinary tract infections, respiratory tract infections, and septicaemias (Podschun & Ullmann, 1998). A common feature shown by *K. pneumoniae* strains is its ability to form biofilm which provides shelter and homoeostasis to the cell population under its cover. Biofilm comprised of extracellular polymeric substance (EPSs) which has the potential to prevent the influx of certain antimicrobial agents (Gilbert et al., 1997). EPSs possess metal binding property and can seize toxic metal ions to protect bacterial cells (Wolfaardt et al., 1999). EPS also renders a major virulence factor contributing towards expression of diseases (NIH, 2002). The chemical composition of EPSs differs widely depending on the microorganism. EPSs are generally composed of glycoprotein, polysaccharide, protein, cellulose, lipid, glycolipid and nucleic acid (Branda et al., 2005). The major structural component of EPSs is polysaccharide which is either neutral or polyanionic in nature. The anionic nature is due to the presence of uronic acids which is thought to improve the binding ability of bivalent cations and enhance the mechanical strength of the EPSs (Davey & O'Toole, 2000). Bacterial exopolysaccharides have also shown biological activities like anti-tumor and immunomodulatory properties that significantly varied with the degree of branching, molecular mass, conformation and

chemical modification (Sen et al., 2014). Some species of the genus *Klebsiella* were reported earlier to produce exopolysaccharides in culture medium. Fucogel, a polysaccharide produced by *Klebsiella pneumoniae* I-1507 was found to compose of galactose, 4-*O*-acetyl-galacturonic acid and fucose (Guetta et al., 2003). In a separate study, Rättö et al. (2001) isolated galacturonic acid containing heteropolysaccharide from two *K. Pneumoniae* strains. Bales et al. (2013) characterized another EPSs isolated from *K. pneumoniae* which was found to comprise of 1.3 % glucose, 49.4 % mannose, and 5.0% GlcA. In general, polysaccharides activate macrophages, T-helper, NK, and other effector cells and thereby activate various chemokines, cytokines (IL-2, IL-6, IL-10, TNF-α, and IL-12) and interferon (IFN-γ) resulting stimulation of host's immune system (Yu et al., 2014). Earlier study has shown that the capsular polysaccharide of pyrogenic liver abscess (PLA) *K. pneumoniae* induces secretion of tumor necrosis factor-α (TNF-α) and interleukin-6 (IL-6) by macrophages through Toll-like receptor 4 (TLR4) (Yang et al., 2011). In another study Hsieh et al. established the role of virulence of O1 antigen obtained from PLA-associated *K. pneumoniae* (Hsieh et al., 2012). It was proposed by earlier authors that EPS of *K. pneumoniae* have infection-enhancing capabilities by hindering the acid phosphatase release from the lysosomal fraction of peritoneal macrophages (Straus et al., 1985). It was shown earlier that trace amount of *K. pneumoniae* extracellular capsular polysaccharide inhibited macrophage maturation and function (Yokochi et al. 1977). The details of the structural characterization of the exopolysaccharide isolated from *Klebsiella pneumoniae* PB12 along with the investigations of biological activities are reported in this chapter.

3.1.1. Parameters effecting EPS production

3.1.1.1. Nutrient concentration

The concentration of nutrient has a significant effect on EPS production and composition. Medium containing excess of glucose has been shown to increase the production of EPS (Flemming & Wingender, 2001). Earlier report showed that a variety of nitrogen sources including ammonium, nitrate, nitrite, and amino acids can be utilized by bacteria for EPS synthesis (Sutherland, 1990a; Amarger, 2001). Among these, ammonium salts and amino acids are the most common ones (Sutherland, 1990a). Depending upon the nitrogen substrate utilized, the yield of EPS varied (Datta & Basu, 1999). Low nitrogen content in the growth medium also influences the EPS production (Sleytr, 1997). Under nitrogen limited condition in the medium, 60% of the glucose was converted into exopolysaccharides in some species of *Aureobasidium*, *Sinorhizobium*, *Escherichia* and *Pseudomonas* (Lee et al., 1999; Sutherland, 2001). Whereas, increase in nitrogen content (ammonium salts) in the medium provokes microbes like *Pseudomonas* sp. and *Rhodococcus* sp. to produce extracellular protein (Sanin et al., 2003).

3.1.1.2. Growth phase

The production of EPS varies with growth phase in different genera. In few strains of *Pseudomonas aeruginosa* and *Staphylococcus epidermidis*, the production of EPS has been observed during late logarithmic and early stationary phase of growth (Sutherland, 2001). In many bacterial species, growth and EPS production occur concurrently (Datta & Basu, 1999). In some species maximum EPS production occurs in

the exponential phase (Bramhachari & Dubey, 2006), while in others, EPS production is maximized in the stationary phase (Datta & Basu, 1999).

3.1.1.3. pH and temperature of the cultivation medium

The pH of the culture medium has an intense effect on the EPS production. Studies have shown that the extremes of pH of the medium (pH 2.0-3.0 or pH 10) resulted in inhibition of microbial growth as well as the biosynthesis of extracellular polymers (Stredansky & Conti, 1999). In *Antrodia camphorate*, the pH of the medium was found to have stimulatory effect on EPS production. Shu and lung (2004) reported that the maximum EPS production in *Antrodia camphorates* occured at pH 5.0. They also proposed that the pH profiles of the culture medium also influence molecular mass of the EPS compounds. The effect of the cultivation temperature on the EPS biosynthesis has been investigated by many authors. In general, the optimal cultivation temperature for the production of the majority of EPS molecules was projected between 26 and 31 °C (Lory, 1992). However, in certain cases low temperature was found to be more favorable for EPS production as reported in *Listeria*. It was observed earlier that in *Listeria monocytogenes* cells, a cultivation temperature of 10 °C induces the production of extracellular cold shock protein (Briandet et al., 1999).

3.1.2. Various methods for extraction and characterization of EPS

3.1.2.1. Extraction of EPS

It is important to adopt a method where no or minimal cell lysis or disruption or alteration of the EPS occurs while extracting it from the bulk of extracellular biopolymeric substances. Several physical, chemical or combined methods have been proposed to extract EPS from cells from different sources (e.g. biofilm, sludge and cell suspension) such as the high-speed centrifugation, heating, ultrasonication. Physical extraction includes centrifugation, ultrasonication and heating. Whereas, common chemical extraction includes uses of NaOH, ethylenediamine tetraacetic acid (EDTA) and cation exchange resin.

3.1.2.2. Characterization of EPS

3.1.2.2.1. Colorimetric analyses

It is known that the EPS is often associated with other complex extracellular polymeric like substances Colorimetric analyses can be made to quantify these components contaminated with EPS. The carbohydrate content is usually measured by the phenol–sulfuric acid method (York et al., 1985). The protein content can be quantified by using the method described previously (Bradford, 1976). The uronic acid content of the EPS can be measured by using carbazole-sulfuric acid reaction (Chaplin & Kennedy, 1986). For quantification of nucleic acid content of the EPS, various methods have been used such as DAPI fluorescence method (Frolund et al., 1996), diphenylamine method (Liu & Fang, 2002), or the UV absorbance method (Boonaert et al., 2001).

3.1.2.2.2. A) Chemical methods

3.1.2.2.2.1. Estimation of total carbohydrate

Total carbohydrate content of polysaccharide was estimated using phenol–sulfuric acid method (York et al., 1985). A 1000 μg solution of sample was prepared by 5 mg sample in 5 ml distilled water and two other concentrations, 100 μg and 80 μg from that solution were prepared. Standard glucose solution of different concentrations (20 μg, 40 μg, 80 μg, 100 μg and 200 μg) were prepared. Then, 1 ml of each standard glucose solution was taken into five test tubes. 1 ml of each solution of sample was pipette out into two test tubes while 1 ml water taken into a test tube served the blank test. After that 1 ml of 5% phenol solution and then followed by 5 ml of concentrated sulfuric acid (H_2SO_4) were added into each test tube. All the tubes were shaken very well and kept for 15 min at ambient temperature. Finally, absorptions of each solution were recorded at 490 nm in Shimadzu UV-visible spectrophotometer, model 1601. Concentrations of standard solution were plotted against absorption in a graph to obtain standard curve. From absorption values of the sample solution, exact carbohydrate percentage of the sample was estimated with the aid of the standard curve.

3.1.2.2.2.2. Monosaccharide composition

The monosaccharide composition with their absolute configurations is needed to determine the complete structure of polysaccharide. The polysaccharide was hydrolyzed with trifluroacetic acid (TFA) [CF_3COOH] (2M) to obtain monosaccharide constituents. Sugar composition was identified by chromatographic studies with the hydrolyzed

product. Solution of strong acids such as sulfuric, hydrochloric or TFA can be used in acid hydrolysis. In the present work, TFA had been used to degrade polysaccharide (glycosidic linkages) due to its volatility. Then monosaccharides were converted into alditols by $NaBH_4$ reduction followed by acetylation to increase the volatility. The derivatives were identified from retention times compared to standards by GLC. The overall reaction scheme has been presented below (Scheme 3.1).

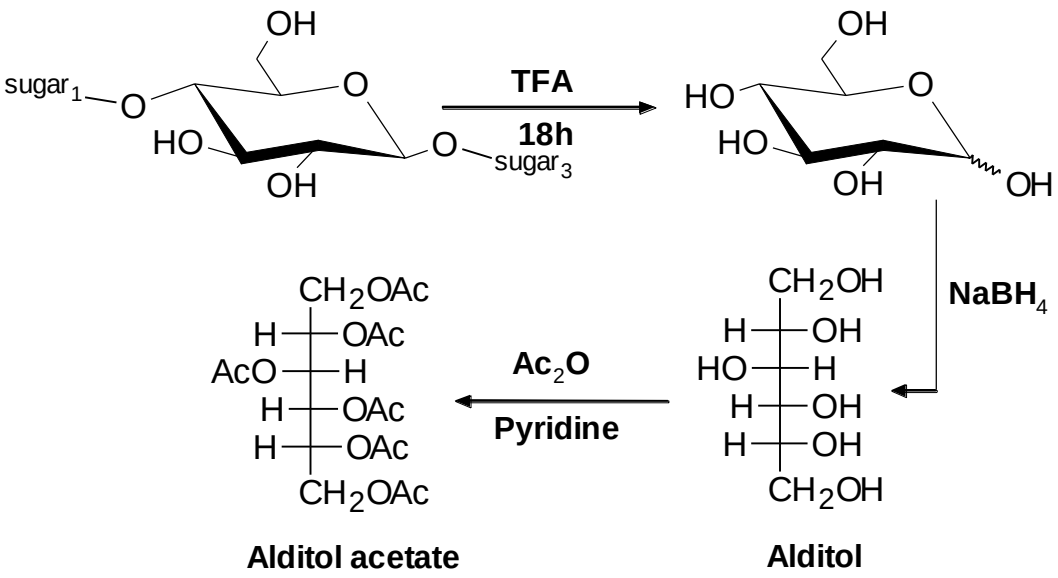

Scheme 3.1.

Uronic acids (its derivatives) are resistant to normal acid catalyzed hydrolysis due to the inductive effect of the carboxyl group (BeMiller JN, 1967). So in the present case (reaction strategy shown below; Scheme 3.2) carboxyl-methyl reduced polysaccharide (Maness et al., 1990) on hydrolysis followed by GLC examination of the corresponding alditol acetates provided the identification of the sugar residues.

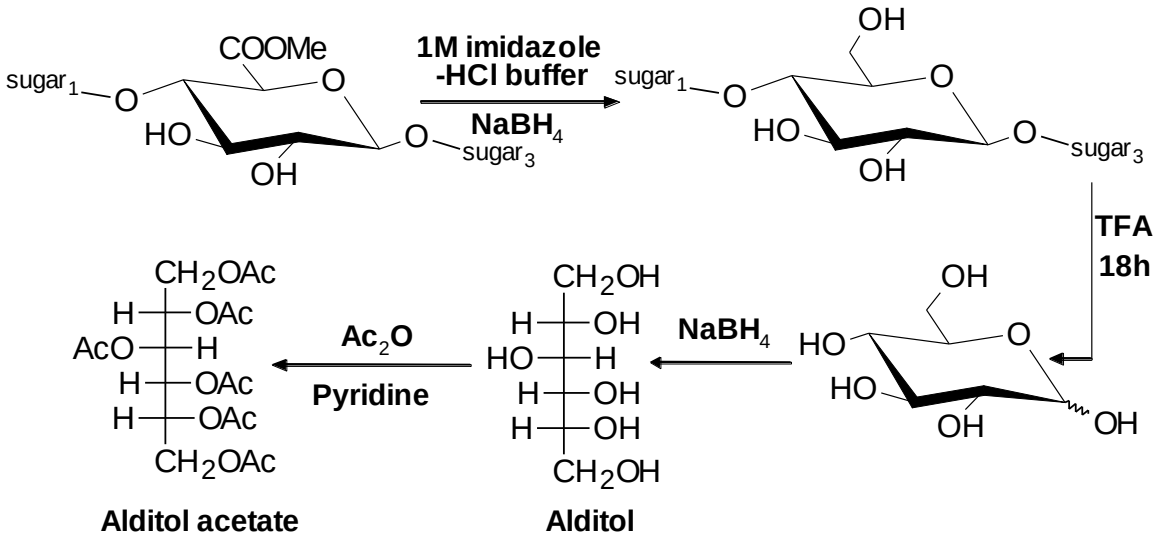

Scheme 3.2.

Sugars have either D or L configuration. To determine their absolute configurations, monosaccharides were subjected to acid catalyzed reaction with optically active 2-butanol or 2-octanol. The glycosides obtained were then trimethylsilylated or acetylated and analyzed by GLC. The diastereomers obtained from the D and L isomers had different GLC retention times and can be distinguished with the help of authentic standards (Gerwig et al., 1978).

3.1.2.2.2.3. Preparation of alditol acetates

The polysaccharide was hydrolyzed with TFA. The mixture of sugars in water was reduced by treating with sodium borohydride at room temperature for 4 hours. Excess $NaBH_4$ was destroyed by acidification with acetic acid and the free boric acid was removed as methyl borate by co-distillation with MeOH. The alditols were dried and then

acetylated by heating with (Ac_2O)-pyridine (1:1) mixture at 100ºC for 1 hour. The material was taken up in $CHCl_3$ for injecting into GLC (Bjorndal et al., 1967).

3.1.2.2.2.4. Determination of absolute configuration of monosaccharide

The absolute configurations of sugar residues were determined by the method based on Gerwig et.al. (1978). After trifluoro acetic acid hydrolysis, the polysaccharide (1.5 mg) was treated with (+)-2-butanol (in 250 µl of 0.625 M HCl) and Per-*O*-TMS-derivatives were prepared with N,O-bis (trimethylsilyl) trifluoro acetamide (BSTFA). The products were analyzed by GLC using a capillary column (SPB-1, 30 m x 0.26 mm) with a temperature program (3 ºC min^{-1}) from 150-210 ºC. The (+)-2-butyl 2,3,4,6-tetra–*O*-TMS-glycosides obtained were identified by comparison with those prepared from the D and L enantiomers of the monosaccharides.

3.1.2.2.2.5. Linkage analysis

Methylation analysis is a well-known chemical method for determination of the linkage position of sugar residues present in polysaccharide. Although this information can be obtained non-destructively by nuclear magnetic resonance (NMR) spectroscopy, methylation analysis is still a powerful method in carbohydrate structural analysis (Ciucanu & Kerek, 1984) alone or in combination with NMR spectroscopy.

The derivetization of polysaccharide for methylation analysis involves conversion of all free hydroxyl groups into methoxy group. Then acid hydrolysis breaks only the interglycosidic linkages leaving the methyl ether bonds intact. The hydrolyzed monomers

are then reduced, followed by acetylation to produce volatile partially methylated alditol acetates (PMAA).

The substitution pattern of the *O*-acetyl group of the PMAA indicates the linkage patterns of the corresponding sugars in the polysaccharide. PMAA (Sweet et al., 1975) are separated and identified through GLC. On a specific column the retention times of PMAAs is highly reproducible. Relative retention times (generally with respect to 1,5-di-O-acetyl-2,3,4,6-tetra-O-methyl-D-glucitol) are used in the literature. The comparison with literature values should only be made with the same column run under the same condition. When methyl esters of galacturonic acid are present as a monomer unit in polysaccharide, carboxy methyl reduced polysaccharide (Maness et al., 1990) is used for methylation. The methylated $LiAlH_4$ reduced polysaccharide (Abdel-Akher & Smith, 1950) is also used.

3.1.2.2.2.6. Methylation analysis: Ciucanu and Kerek method

In the present thesis the polysaccharides were methylated according to the methods described by Ciucanu & Kerek (1984). The polysaccharide (3-5 mg) was kept overnight on phosphorous pentoxide (P_2O_5) in a vacuum decicator and dissolved in 0.5 ml of distilled DMSO. Solid finely grounded NaOH dust was added and stirring for 30 min. Then 0.5-1 ml CH_3I was added and stirred for 1-1.5 h. The methylated material was isolated by partition between $CHCl_3$ and H_2O (5:2, v/v). The $CHCl_3$ solution of methylated product was dried on water bath to yield solid product. The methylated sugar was then hydrolyzed with formic acid (HCOOH) for 1 h and the excess acid was removed by co-distillation with water (Scheme 3.3). The hydrolyzed methylated products

were acetylated by Ac_2O-pyridine (1:1) mixture at 100 ºC for 1 h. The alditol acetates of methylated sugars were identified by GLC (using column A and column B) and GLC-MS (using HP-5 fused silica capillary column).

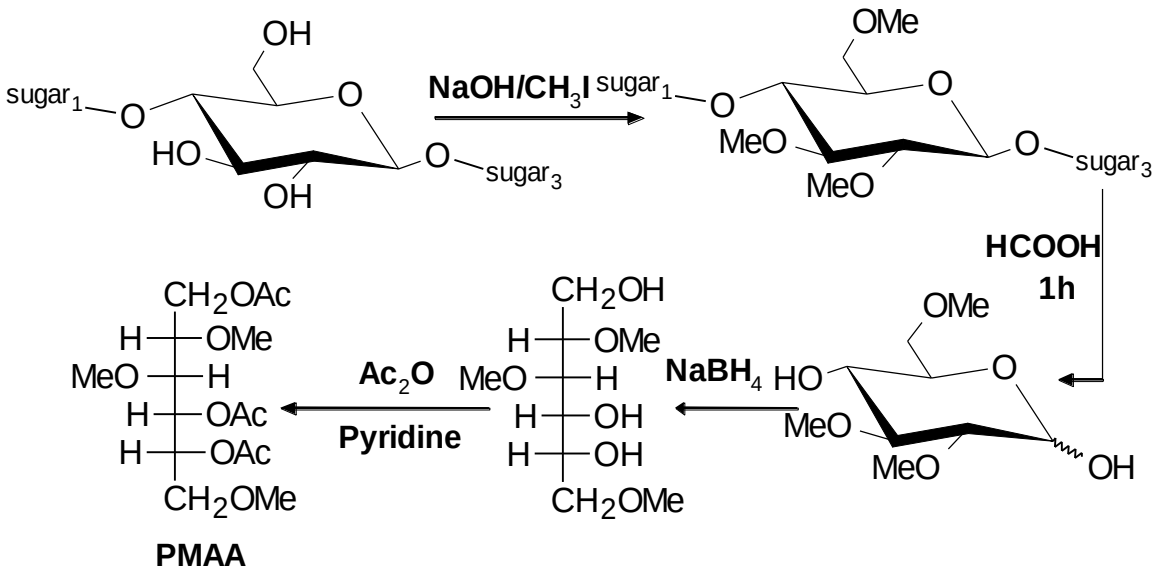

Scheme 3.3.

3.1.2.2.2.7. Periodate oxidation

Polysaccharides are susceptible towards the reaction with oxidizing agents such as periodic acid or its salts due to the presence of free hydroxyl groups. Non-terminal units e.g. (1→2) and (1→4)-linked hexopyranose units consume one equivalent of periodate per mole yielding dialdehydes. Whereas, (1→3)-linked hexopyranose unit or branched at C-2 or C-4 positions will not be affected by this reaction due to absence of adjacent–OH groups. The products of the periodate oxidation reaction are methylated, followed by reduction and conversion to alditol acetates. PMAA are then identified by GLC and GLC-MS. The partially methylated alditol acetates corresponding to hexopyranose

moieties that contain (1→3)-linkage or branched at C-2 or C-4 positions will survive in the native polysaccharide after this reaction. So the periodate oxidation study further supports the linkages of sugar units as determined by methylation experiments.

In the present chapter polysaccharide was treated with sodium metaperiodate and mixture was kept 48 h in the dark at 4ºC. The excess periodate was destroyed by ethylene glycol and the solution was dialyzed against distilled water and dried. A portion of the dried product was reduced with $NaBH_4$ and neutralized with AcOH. The resulting material was obtained by co-distillation with MeOH. Then the product was hydrolyzed by 2M TFA for 18 h at 100 ºC and the alditol acetates were prepared as usual. Another portion was methylated by the method of Ciucanu & Kerek (1984) and the alditol acetate of this methylated product was prepared for GLC and GLC-MS analysis.

In case of polysaccharide containing methyl ester of galacturonic acid, then periodate-oxidized, $LiAlH_4$-reduced polysaccharide was mixed with 0.5 M CF_3COOH and allowed to stand for 48 h at room temperature. The acid was removed and the hydrolyzed material was analyzed by GLC after conversion to alditol acetates.

3.1.2.2.2.8. Smith degradation

Oligosaccharides (OS) are more easily characterized than polysaccharide (PS) with the help of NMR spectroscopy. Smith degradation is another method to degrade PS to OS or modified PS. This method is utilized to simplify the identification of the repeating unit by selective removal of some of the residue. The oxidation yields a product in which vicinal hydroxyl groups have been oxidized to aldehydes by cleavage of carbon-

carbon bonds. $NaIO_4$ does not affect residues with out any vicinal hydroxyl groups. The reduction of aldehyde yields a polyalcohol. On mild acidic hydrolysis, these yield OS or modified PS that contains sugar residues and fragments have modified sugar residue.

3.1.2.2.3. B) Analytical methods

3.1.2.2.3.1. Gas liquid chromatography

Chromatography is a non-destructive method for resolving a mixture of components into individual components through equilibrium distribution between two phases. Gas-liquid chromatography consists of a mobile gas phase and a stationary liquid phase that is coated on to either a solid matrix (e.g. diatomaceous earth) or the wall of a capillary tube. Stationary phase has a sufficiently low vapour pressure at the column temperature. So that it can be considered as non-volatile. The sample mixture in gaseous form is run through the column with a carrier gas (e.g. N_2). Separation can be achieved by the differences in the distribution ratios of the components of the sample between the mobile (gaseous) and stationary (liquid) phases causing them to move through the column at different rates and with different retention times. After elution, the components can be detected by a suitable detector.

For GLC (Bjorndal et al., 1967) separation, sample must be volatile. As monosaccharides are not volatile, there must be derivetized into their alditol acetates. The essential part of the derivetization procedure (Southgate, 1976) is the reduction of neutral sugars to alditol and subsequent acetylation. The alditol acetates are dissolved in suitable solvents such as chloroform or methylene chloride and injected into a GLC column.

In this work two types of columns: 3% ECNSSM (a nitrile-silicon polyester copolymer) and 1% OV-225 (a silicon polymer containing methyl, phenyl and nitrile groups) have been used. For detection the flame ionization detector was used. The detector responds to all organic compounds except formic acid, the response being greatest for hydrocarbons.

3.1.2.2.3.2. Gas liquid chromatography-Mass spectrometry

Mass spectrometry coupled with gas chromatography has been reported to be a very useful tool in biological and chemical studies. GLC-MS (Bjorndal et al., 1967) analysis of carbohydrate has advantages because it is very sensitive and a small amount of sample is required. In GLC-MS, volatile molecules are identified by their GLC-retention times and by their mass spectra. GLC-MS is used to analyze the monosaccharide composition obtained from different degradation methods e.g. the alditol acetates, the partially methylated alditol acetates (PMAA). The electron impact fragmentation pattern of the mass spectra of PMAA is well documented for all linkage patterns of all known sugars.

3.1.2.2.3.3. Nuclear Magnetic Resonance (NMR) Spectroscopy

Nuclear Magnetic Resonance (NMR) is the most powerful and non-destructive technique for identification of monosaccharide composition, elucidation of α or β anomeric configurations, linkage patterns and sequence of sugar units in the repeating unit of the polysaccharide. Different types of 1D (^{1}H, ^{13}C) and 2D (COSY, DQF-COSY,

TOCSY, NOESY, ROESY, HMQC and HMBC) NMR techniques are adapted to characterize the structure of a polysaccharide.

3.1.2.2.3.4. One-dimensitional NMR

Two types of 1D NMR spectroscopy in common use today are ^{1}H (proton NMR) and ^{13}C (carbon-13 NMR). The sample was kept over P_2O_5 in vacuum to remove water and deuterium exchanged by lyophilization with D_2O. The signal for residual HOD was suppressed. The protons of polysaccharide show chemical shifts in the range of 1.0-6.0 ppm. The anomeric proton region is found in the range of 4.4-5.5 ppm. The remaining rings protons resonate in the range of 3.0-4.2 ppm. Signal of acetyl methyl proton appears at 2.0-2.2 ppm. Normally, the α-anomer resonates downfield compared to the β-anomer in D-pyranoses. From coupling constant $^{3}J_{H1,H2}$, the anomeric configuration of a glucopyranosyl residue can be determined. If $^{3}J_{H1,H2}$ is nearly 3-4 Hz, the anomeric configuration of this residue is α. On the other hand, the configuration will be β if that value is nearly 7-10 Hz. $J_{H1,H2}$ values are not always sufficient to determine the anomeric configuration of the sugars. If the glycosyl residue has the manno configuration, the distinction between the α and β anomer is very difficult as the coupling constant values for α ($J_{H1,H2}$ ~ 1.8 Hz.) and β ($J_{H1,H2}$ ~ 1.5 Hz.) are too close.

The one bond ^{13}C-^{1}H couplings constant are useful for the determination of anomeric configuration of sugar residues (Bock et al., 1982) For D sugars 1JC1,H1 ~ 170 Hz indicates an α-anomeric configuration whereas 1JC1,H1 ~160 Hz indicates a β-anomeric configuration (Bock & Pedersen, 1974) which is reversed for the L sugars.

In the ^{13}C NMR spectra, anomeric carbon signals lie in the region 90-110 ppm whereas non-anomeric carbons in 60-90 ppm. The α-anomeric carbon signals appear generally in the range of 95-103 ppm whereas most of the β-anomeric carbons appear in the region of 101-105 ppm. In case of methoxy sugar, the methyl carbons appear in the region 55-61 ppm. Acetyl methyl carbon appears in the region 18-22 ppm. Signals for carbonyl carbons are generally observed in the range of 165-185 ppm. Unsubstituted ring carbons usually have the chemical shifts between 65 ppm and 75 ppm (Agarwal, 1992). If there is any linkage at any carbon, the signal for that carbon will suffer a downfield shift by 4-10 ppm and the carbon next to that one will appear in a little upfield region (by 0.7-4.7 ppm) (Agarwal, 1992).

3.1.2.2.3.5. Two-dimensional NMR

A conventional ^{1}H NMR spectrum has a frequency axis and an intensity axis; Two-dimensional (2D)- NMR spectra have two frequency axes and one intensity axis. 2D-NMR can be applied to analyze complex spectra, which are difficult to predict by conventional methods (Kalsi, 2004). In present work different 2D-NMR experiments such as DQF-COSY (Double quantum filtered correlation spectroscopy), TOCSY (Total correlation spectroscopy), NOESY (Nuclear overhauser enhancement spectroscopy), ROESY (Rotating frame overhauser enhancement spectroscopy), HMQC (Heteronuclear multiple quantum coherence) and HMBC (Heteromultiple bond coherence spectroscopy) have been used.

COSY (Correlation spectroscopy) identifies pairs of protons, which are coupled to each other. COSY or DQF-COSY gives information about the protons of an individual

sugar residue through a three-bond coupling. It is a ^{1}H homonuclear shift correlation spectrum that provides information on spin coupling networks with in a residue through the observation of the cross peaks off diagonal.

A TOCSY spectrum correlates protons that are in the same spin system and gives both short range and long-range correlations. It is useful in the identification of individual monosaccharide residue.

The NOESY spectrum provides information on through space rather than through bond couplings. NOE connectivities are often observed between the anomeric protons of a particular sugar residue to protons of another sugar residue that is glycosidically linked to the former. NOESY experiments give information on linkages and sequence of sugar residues in a polysaccharide.

ROESY is used to determine signals arisen from protons, which are close in space but not closely connected by chemical bonds. A ROESY spectrum yields through space correlations via the Rotational nuclear overhauser effect (ROE). ROESY is especially useful for cases where NOESY signals are weak because they are near the transition between negative and positive. ROESY cross peaks are always negative. The ROESY experiment also yields cross peaks arisen from chemical exchange.

In a heteronuclear spectrum like HMQC NMR spectrum, all signals in the spectra represent a direct correlation between a carbon and a proton.

An HMBC experiment gives long range coupling between proton and carbon (two or three bonds) with high sensitivity. HMBC experiments establish multiple-bond

correlation through the glycosidic bonds and this together with NOESY experiments gives necessary information on linkages and sequence of sugar residues in a polysaccharide.

3.1.2.2.4.. Physical methods

3.1.2.2.4.1. SEM and Energy dispersive X-ray study (*EDS)*

SEM is commonly used for studying the surface morphology of cells and other biomaterials. The technique makes use of a primary beam of electrons that interact with the specimen of interest, in a vacuum environment, resulting in different types of electrons being emitted. The secondary electrons ejected from the specimen surface are collected and displayed to provide a high-resolution micrograph. SEM sample preparation involves fixation (if proteins, cells, or tissue are present), followed by drying, attachment to a metallic stub, and then coating with a metal prior to data collection. In addition to imaging the surface morphology of polymeric biomaterials, the SEM can be combined with other analytical methods such as EDS to determine elemental distribution and composition (Sodhi, 1996). Viewing 3D images of microscopic areas only solves half the problem in an analysis. It is sometime necessary to identify the different elements associated with a specimen. This can be done by using the "built-in" spectrometer called an EDS. EDS utilizes X-rays that are emitted from the specimen when bombarded by the electron beam to identify the elemental composition of the specimen. When the sample is bombarded by the electron beam of the SEM, electrons are ejected from the atoms on the specimen's surface. A resulting electron vacancy is filled by an electron from a higher shell, and an X-ray is emitted to balance the energy difference between the two electrons.

The EDS X-ray detector measures the number of emitted X-rays versus their energy. The energy of the X-ray is characteristic of the element from which the X-ray was emitted. A spectrum of the energy versus relative counts of the detected X-rays is obtained and evaluated for qualitative and quantitative determinations of the elements present in the specimen.

3.1.2.2.4.2. Thermogravimetric analysis (TGA)

Thermogravimetric analysis or thermal gravimetric analysis (TGA) is a type of testing performed on samples that measures the weight loss of a material as a function of temperature in a controlled atmosphere (Gooch, 2010). TGA is commonly employed in research and testing to determine the characteristics such as degradation temperature and moisture content of polymer materials including EPS (Mishra et al., 2011). Analysis is carried out by increasing the temperature of the sample gradually and plotting weight (%) against temperature. Measurements are used primarily to determine the composition of polymers and to predict their thermal stability at temperatures up to 1000 °C.

3.1.2.2.4.3. Differential Scanning Calorimetry (DSC)

Differential Scanning Calorimetry measures the dissimilarity in heat flow between a sample and a reference as the material is heated or cooled. DSC instrument convert temperature differences into a measurement of the energy per unit mass related with the phase change that caused the temperature differences to arise. Any alteration in a material that involves a change in the heat content of the material can be detected and measured by DSC. These measurements provide quantitative and qualitative information

about physical and chemical changes that involve endothermic or exothermic processes, or differences in heat capacity. A primary use of DSC in polymer analysis is the detection and quantification of the crystalline melting process. Since the crystalline state in a polymer is influenced by inherent properties such as molecular weight distribution and the subsequent environmental treatment, this property is of considerable importance. Many polymers are unable to crystallize under normal condition and even semi-crystalline polymers contain a significant amount of material that remains in the amorphous state. Without crystals there can be no melting point; however the amorphous regions do undergo an important phase change known as the glass transition. The glass transition is defined as the beginning of conjugated main chain motion, a phenomenon where extended sections of individual chains become capable of independent motion. In amorphous polymers the glass transition indicates the softening of polymer. DSC detects the glass transition as a step change in the heat capacity of the polymer. Degradation is a catastrophic event and involves irreversible modification that can reduce the performance of a material. In semi-crystalline materials degradation can be detected by DSC as decrease in the melting and re-crystallization temperatures as well as the energy of these reactions.

3.1.2.2.4.4. Fourier transform infrared spectroscopy (FT-IR)

Infrared spectroscopy is a technique that measures the bond vibration frequencies in a molecule and can provide unique insights about the functional group within a molecule (Smith, 2011). The technique is relatively simple, reproducible, nondestructive, and only small amounts of material (micrograms to nanograms) with a minimum sample

preparation are required. FT-IR peaks are in many cases found associated with the vibration of a particular chemical bond (or a single functional group) in the molecule (Hofman et al., 2006). Due to the ability of infrared spectroscopy to identify the types and number of different chemical functional groups like hydroxyl, carboxyl, amino etc. present at a surface in a nondestructive manner, it has been widely used in the field of chemistry and biology. Many investigators have used FT-IR technique for the determination of functional groups in EPS (Yadav et al., 2012).

It is well documented that polysaccharides activate macrophages, T-helper, NK, and other effector cells and thereby activate the various cytokines (IL-2, IL-6, IL-10, and IL-12), interferon (IFN- γ), and chemokines which ultimately stimulate host's immune system. It has been observed that the molecular mass, degree of branching, conformation and chemical modification of polysaccharides significantly affect their anti-tumor and immunomodulatory activities (Bohn & BeMiller, 1995).

In this part of the work structural elucidation and immunogenic properties of the purified *K. pneumoniae* PB12 EPS has been presented following each of the analytical methodologies described in the preceding paragraphs.

3.2. Materials and methods

3.2.1. Functional group analysis

The functional group of EPS was determined by Fourier transform infrared (FT-IR) spectroscopy. Pellets of 2 mg of purified EPS were prepared with KBr followed by pressing the mixture into a 16 mm diameter mold. The infrared spectrum was recorded on

Perkin Elmer spectrum GX FT-IR system (PerkineElmer, USA) with resolution of 4 cm^{-1} in 4000-400 cm^{-1} region as described previously (Yadav et al., 2012).

3.2.2. Purification and chemical analysis of the polysaccharide fraction of Klebsiella pneumonaie EPS

Protein fraction of EPS was removed by adding trichloroacetic acid (30%) followed by centrifugation and residue was discarded. Two volumes of 95% ethanol was added to the supernatant and centrifuged at 9587.5 x *g* for 30 min to obtain 300 mg of protein-free crude polysaccharide (Zhang et al., 2002). This crude polysaccharide (25 mg) was passed through Sepharose 6B gel permeation column (90×2.1 cm) using water as the eluent with a flow rate of 0.3 ml min^{-1} as described in the earlier report (Davey & O'Toole, 2000). A total of 95 test tubes were collected using Redifrac fraction collector and monitored spectrophotometrically (Shimadzu UV-vis spectrophotometer, model-1601) at 490 nm using phenol-sulfuric acid method (York et al., 1986). Single fraction of purified polysaccharide (test tubes, 24-40) named KNPS was obtained.

3.2.3. General methods

The average molecular weight of KNPS was determined by gel chromatography using standard dextrans T-200, T-70 and T-40 as reported earlier (Sen et al., 2014). KNPS (2 mg) was hydrolyzed with 2 M CF_3COOH (2 ml) in a round-bottomed flask at 100 ºC for 18 h in a boiling water bath and the sugar composition analysis was carried out adopting the methods as described earlier (Sen et al., 2014). Gas Chromatography (GC) analysis of the alditol acetates was carried out by a gas-liquid chromatography, Hewlett-

Packard model 5730 A, with flame ionization detector and glass columns (1.8 m x 6 mm) packed with 3% ECNSS-M (A) on Gas Chrom Q (100-120 mesh) and 1% OV-225 (B) on Gas Chrom Q (100-120 mesh). All GC analyses were performed at 170 ºC. The absolute configuration of the monosaccharide was determined by the method of Gerwig et al. (1978). KNPS (3.5 mg) was methylated using the procedure reported earlier (Ciucanu & Kerek, 1984) and the partially methylated alditol acetates were analyzed by GC-MS. GC-MS analysis was performed on Shimadzu GC-MS Model QP-2010 Plus automatic system, using ZB-5MS capillary column (30 m x 0.25 mm). The program was isothermal at 150 ºC; hold time 5 min, with a temperature gradient of 2 ºC min^{-1} up to a final temperature of 200 ºC. NMR experiments were carried out by a Bruker Avance DPX-500 instrument at 30 °C as reported earlier (Sen et al., 2014).

3.2.4. Smith degradation study

KNPS (30 mg) was added to 7.5 ml 0.1 M sodium metaperiodate solution and the mixture was kept for 48 h in the dark at 4 °C. The excess periodate was destroyed by adding ethylene glycol (5.0 ml) and the solution was dialyzed against distilled water for 2 h. The volume of the dialyzed material was concentrated to 2–3 ml. This material was reduced with $NaBH_4$, 12 h, neutralized with 50% AcOH, and dialyzed with distilled water and finally freeze dried (14.0 mg). The periodate-oxidized, reduced material was subjected to mild hydrolysis by the addition of 0.5 M CF_3COOH for 15 h at 25 °C to destroy the residues of oxidized sugars attached to the polysaccharide backbone. The excess acid was removed by repeated freeze drying. The material was further purified by

passing through a Sephadex G-25 column, kept over P_2O_5 in vacuum for several days and finally used for ^{13}C NMR studies.

3.2.5. Biological activities

3.2.5.1. Isolation of lymphocytes from peripheral blood mononuclear cells (PBMCs)

Blood samples (total 30 blood samples, 6 samples for each group) were freshly collected satisfying the Helsinki protocol from all groups of individuals. From the heparinized blood samples the lymphocytes were isolated according to the method described earlier (Chattopadhyay et al., 2013). Blood was diluted in PBS (pH 7.0), layered carefully on the density gradient (histopaque 1077) in a ratio of 1:2, centrifuged at 1400 rpm for 20 min. The white milky layer of mononuclear cells were carefully removed and cultured in RPMI 1640 medium for 2 h under 5% CO_2 and 95% humidified atmosphere at 37 °C (Chattopadhyay et al., 2013). Non adherent layer of the cultured cells were collected and washed twice with PBS and centrifuged at 2000 rpm for 10 min to obtain lymphocytes. As described previously, the depletion of macrophages and B cells in PBMC were done by passing it through a nylon wool column (Saxena et al., 1980). After washing the column for two times with the medium, the non-adherent $CD4^+$ T cells and $CD8^+$ T cells were stained with Phycoerythrin (PE) and Fluorescein isothiocyanate (FITC) conjugated antibody as described earlier (Garcia et al., 2007). Samples were then analyzed using flow cytometer (FACS CALIBUR, Becton Dickinson, USA) using CellQuest software.

3.2.5.2. Sulforhodamine B assay (SRB)

The isolated human lymphocytes were seeded into 96 well tissue culture plates having 180 µl of complete media and were incubated for 48 h. KNPS was added to the cells at varied concentrations (25, 50, 100 and 200 µg $m1^{-1}$) and incubated for 24 h at 37 °C in a humidified incubator (NBS) containing 5% CO_2. The toxicity of KNPS on human lymphocytes were determined using SRB assay following the protocol described earlier (Vichai & Kirtikara, 2006).

3.2.5.3. Preparation of cell lysate

The cell suspension was centrifuged at 1500 rpm for 5 min, after treatment schedule. The supernatants were collected and stored at -20 °C. The cell pellets were re-suspended in ice cold PBS and subjected to four cycles of freeze-thaw cycles followed by sonication for 20 s (Ultrasonic Processor, Tekmar, Cincinnati, OH, USA). Lysates were centrifuged at 9587.5 x *g* for 20 min at 4 °C to remove cellular debris. Protein content of lysate was measured as described earlier using bovine serum albumin as standard (Lowry et al., 1951).

3.2.5.4. Determination of reduced glutathione (GSH), oxidized glutathione level (GSSG) and lipid peroxidation

The estimation of reduced glutathione in the cell lysate was done by the method described previously (Maity et al., 2014). The oxidized glutathione level was measured after derivatization of GSH with 2-vinylpyridine according to the method reported earlier

(Mahapatra et al., 2009). Lipid peroxidation was estimated using the method of Ohkawa et al. (1979) in the cell lysate.

3.2.6. Statistical analysis

The data were expressed as the mean ± the standard error of the mean (n = 6). Comparisons between the means of control and treated groups were made by one-way Anova analysis of variance (using a statistical package; Origin 6.1, Origin Lab, Northampton, MA, USA) with multiple-comparison tests, with $p<0.05$ as the limit of significance. The correlation analysis was performed using Statistica software version 8.0.

3.3. Results

3.3.1. Functional group determination, purification of polysaccharide fraction and chemical analysis of exopolysaccharide produced by K. pneumoniae PB12

FT-IR analysis showed the presence of hydroxyl (3384 cm^{-1}), weak C-H band at 2930 cm^{-1}, carboxyl (1616 cm^{-1} and 1408 cm^{-1}) and methoxyl (1077 cm^{-1}) groups (Fig. 3.1a). The isolation and purification steps are summarized in the flow diagram (Fig. 3.1b).

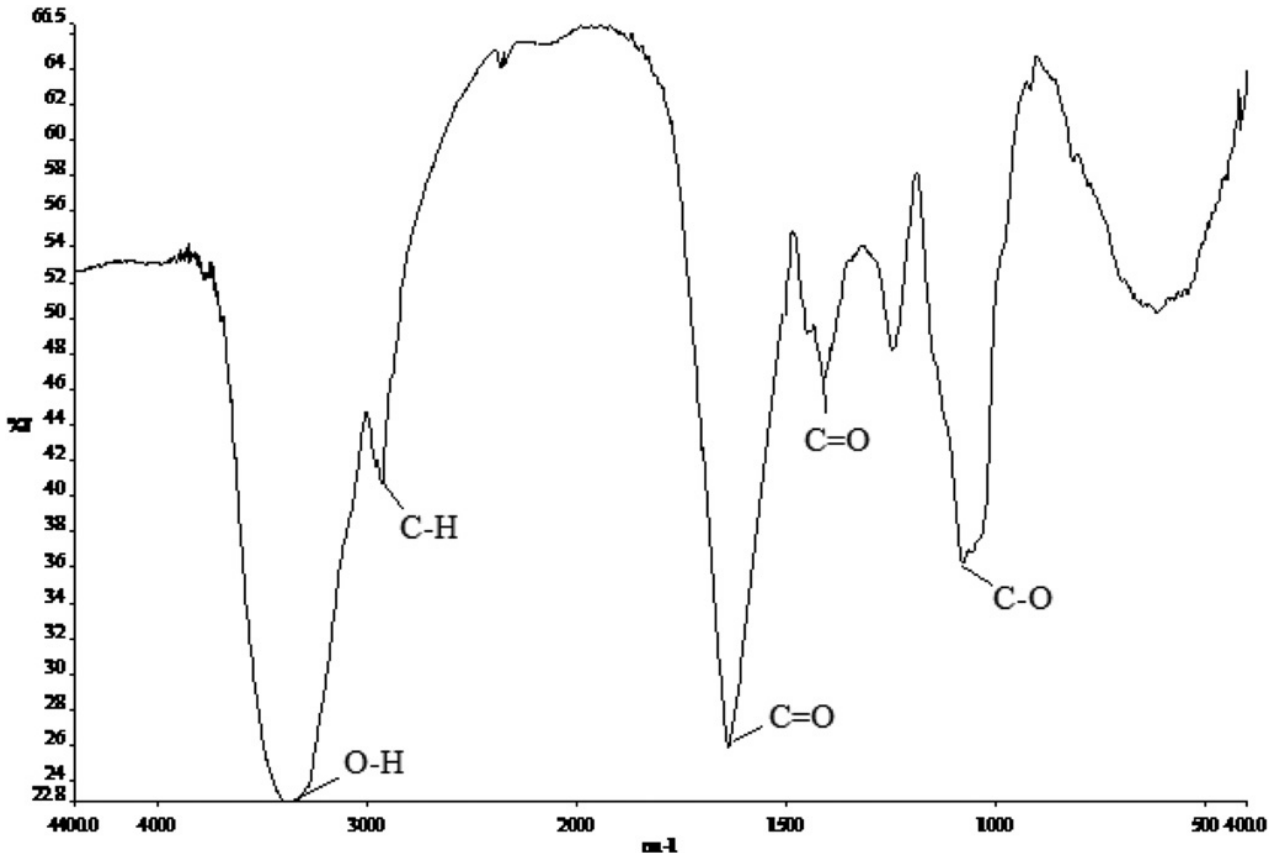

Fig. 3.1. a) FT-IR spectra of purified EPS.

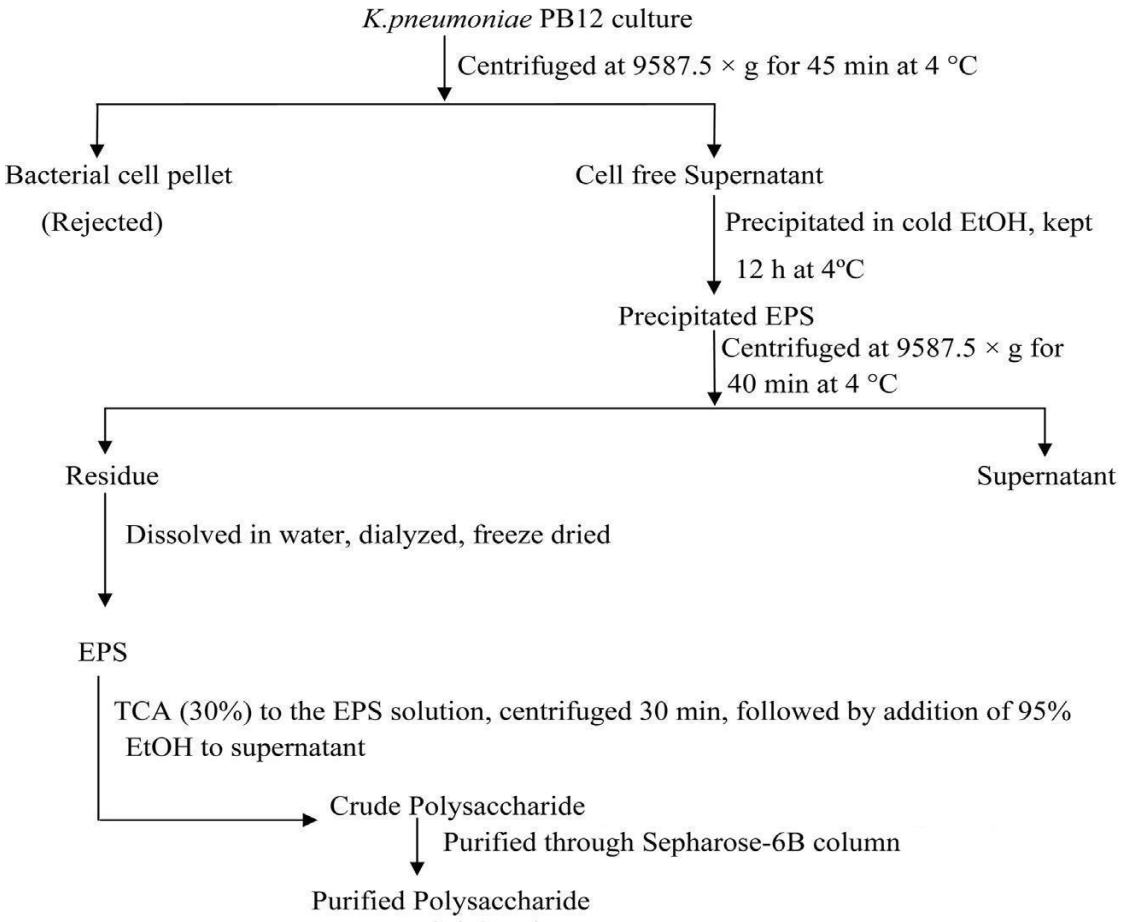

Fig. 3.1. b) Flow diagram of isolation and purification of the exopolysaccharide, KNPS produced by *K. pneumoniae* PB12.

A single fraction (Fig 3.2) of purified polysaccharide (KNPS) was obtained after fractionation of water soluble crude polysaccharide through Sepharose 6B column.

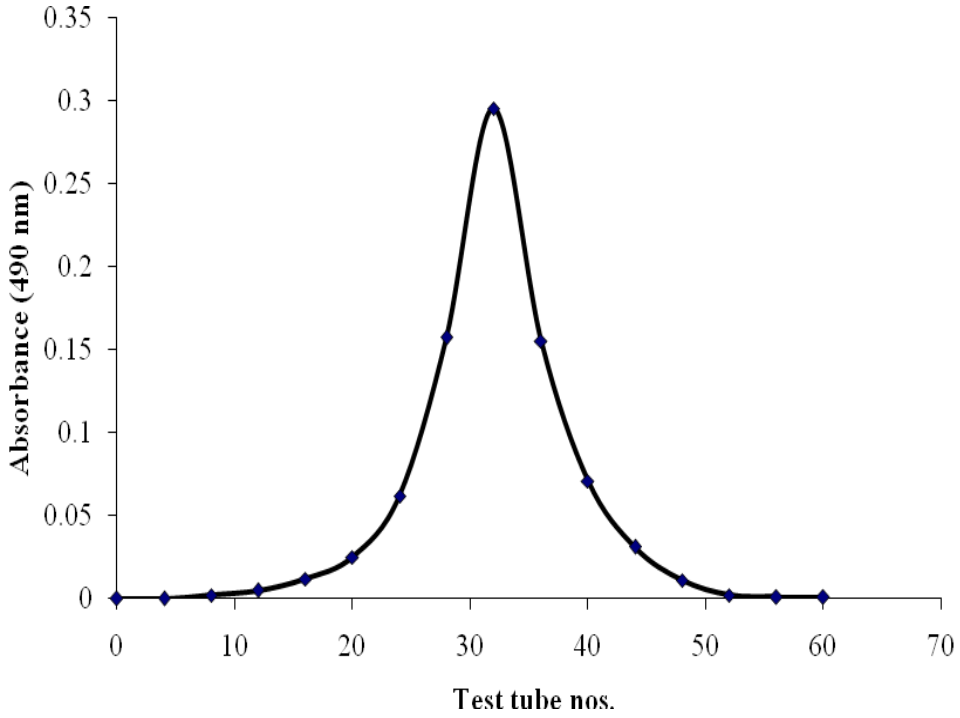

Fig. 3.2. Gel permeation chromatogram of crude exopolysaccharide isolated from the culture medium of *K. pneumoniae* PB12 using Sepharose 6B column.

The fraction was collected and freeze dried. KNPS was composed of arabinose, galactose, 3-*O*-methyl-galctose and glucose in a molar ratio of nearly 4:3:1:1. Determination of absolute configuration of the monosaccharides showed that galactose, 3-*O*-methyl-galctose and glucose were present in D and arabinose in L configuration. The GC–MS analysis of partially methylated alditol acetates revealed the presence of 3,5-linked-arabinofuranosyl, 2,6-linked-galactopyranosyl, 6-linked-galactopyranosyl, 6-linked-glucopyranosyl, 2-linked-galactopyranosyl, 5-linked-arabinofuranosyl, 3-linked-arbinopyranosyl, terminal galactopyranosyl and arabinofuranosyl residues in a relative proportion of approximately 1:1:1:1:1:1:1:1:1.

3.3.2. Structural analysis of KNPS

The ^{1}H NMR spectrum (500 MHz, Fig. 3.3) of KNPS recorded in D_2O at 30 ºC showed the presence of eight signals in the anomeric region at δ 5.20 (**A**), 5.17 (**B**), 5.16 (**C** and **D**), 5.10 (**E**), 5.05 (**F**), 5.02 (**G**), 4.46 (**H**), and 4.42 (**I**) as evidenced from HSQC couplings.

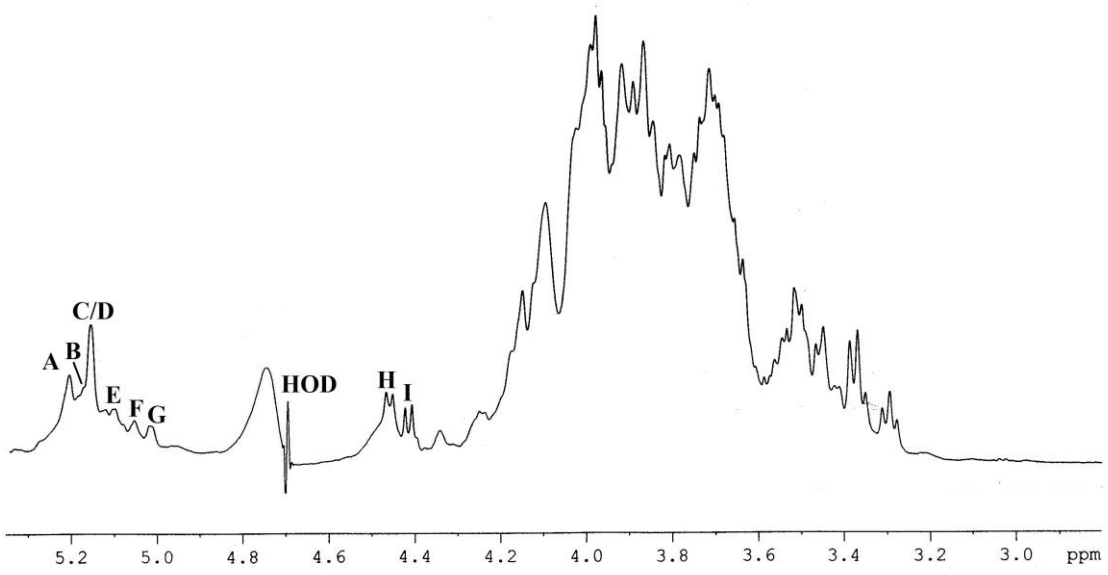

Fig. 3.3. ^{1}H NMR spectrum (500 MHz, D_2O, 30 ºC) of exopolysaccharide, KNPS produced by *K. pneumoniae* PB12. Acetone was taken as the internal standard, fixing the methyl proton signal at δ 2.225.

In ^{13}C NMR spectrum (125 MHz; Fig. 3.4) at the same temperature, eight signals were observed in the anomeric region at δ 109.4, 106.8, 103.3, 102.7, 102.2, 101.5, 99.5, and 97.7.

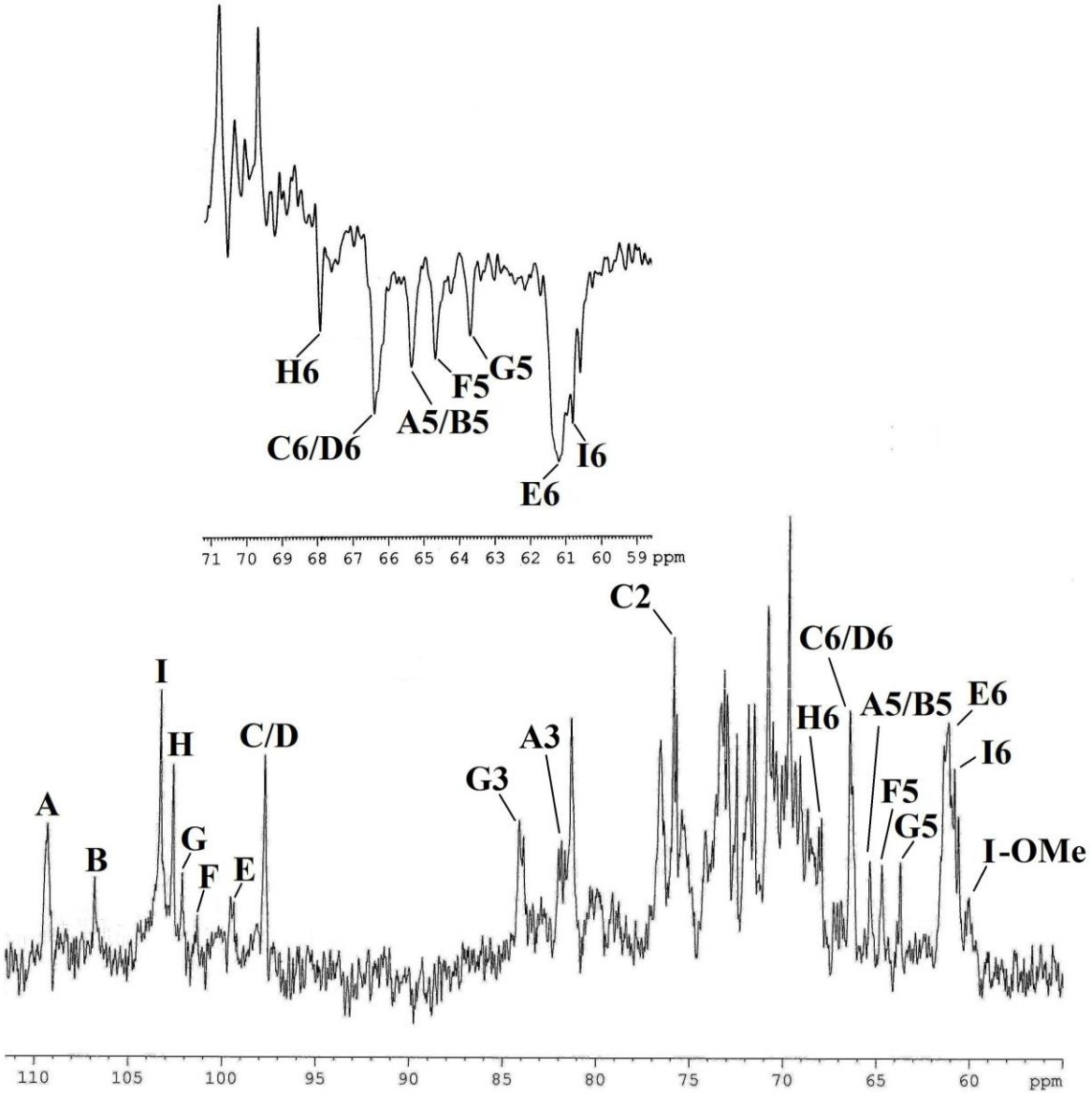

Fig. 3.4. ^{13}C NMR spectrum (125 MHz, D_2O, 30 ºC) of exopolysaccharide, KNPS produced by *K. pneumoniae* PB12, acetone was taken as the internal standard, fixing the methyl carbon signal at δ 31.05. Inset shows part of DEPT-135 spectrum (D_2O, 30 ºC) of exopolysaccharide, KNPS.

These eight anomeric carbon signals were correlated to the anomeric proton signals of residue (**A**), (**B**), (**I**), (**H**), (**G**), (**F**), (**E**), (**C** and **D**), respectively as assigned from the HSQC spectrum (Fig. 3.5a, Table 3.1).

The proton and carbon chemical shifts were assigned from DQF-COSY, TOCSY, and HSQC [Fig. 3.5a & 3.5 b] experiments. The proton coupling constants were measured from DQF-COSY experiment.

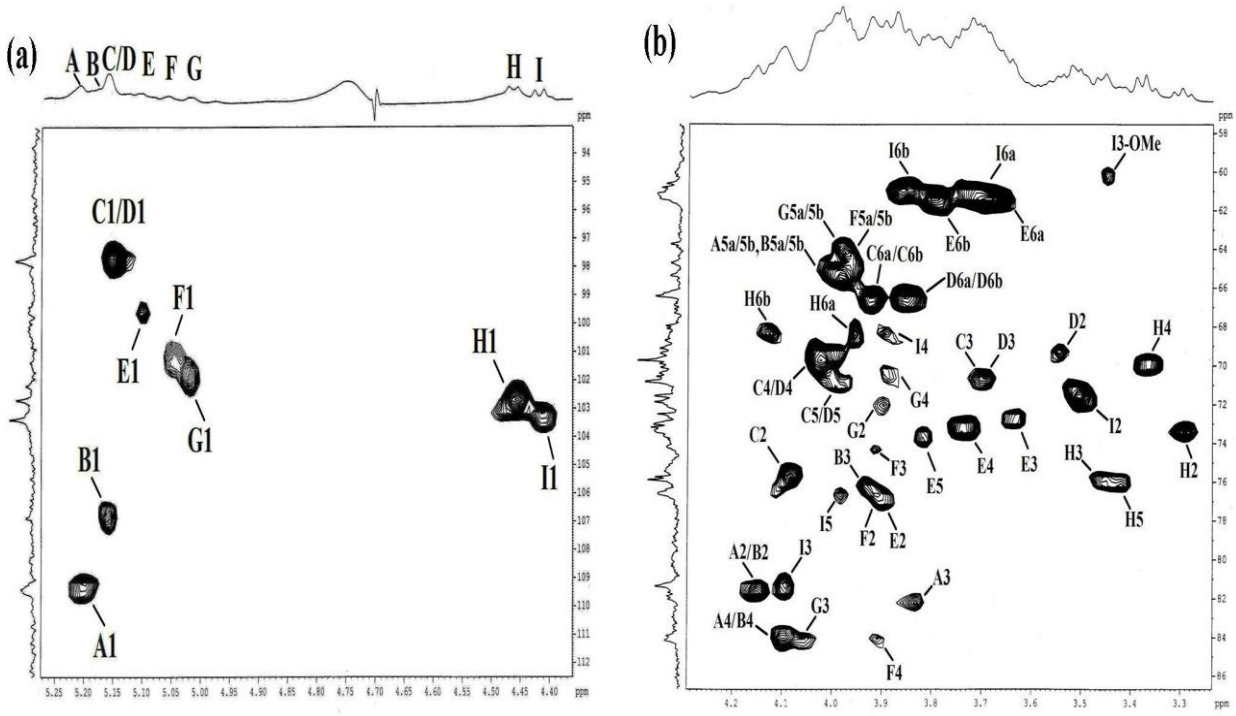

Fig. 3.5. The HSQC spectrum of **a**) anomeric part and **b**) other than anomeric part of the exopolysaccharide, KNPS produced by *K. pneumoniae* PB12. The annotation **A**1 refers to **A**H1/**A**C1 cross peak, **B**1 refers to **B**H1/**B**C1 cross peak and so on.

Table 3.1

The ^{1}H NMR[a] and ^{13}C NMR[b] chemical shifts of the exopolysaccharide, KNPS produced by *K. pneumoniae* PB12 in D_2O at 30 ºC.

Glycosyl residue	H-1/C-1	H-2/C-2	H-3/C-3	H-4/C-4	H-5a, H-5b/C-5	H-6a, H-6b/C-6	*O*Me
→3,5)-α-L-Ara*f*-(1→ **A**	5.20 109.4	4.15 81.5	3.85 81.8	4.09 84.0	3.98[c], 3.98[d] 65.4		
→5)-α-L-Ara*f*-(1→ **B**	5.17 106.8	4.15 81.4	3.92 76.6	4.09 84.0	3.98[c], 3.98[d] 65.4		
→2,6)-α-D-Gal*p*-(1→ **C**	5.16 97.7	4.09 75.9	3.70 70.8	4.02 69.7	3.99 70.8	3.92[c], 3.92[d] 66.4	3.45 59.9
→6)-α-D-Gal*p*-(1→ **D**	5.16 97.7	3.55 69.3	3.70 70.8	4.02 69.7	3.99 70.8	3.84[c], 3.84[d] 66.4	
→2)-α-D-Gal*p*-(1→ **E**	5.10 99.5	3.92 76.6	3.63 72.5	3.74 72.6	3.81 73.4	3.69[c], 3.78[d] 61.1	
β-L-Ara*f*-(1→ **F**	5.05 101.5	3.92 76.6	3.91 74.1	3.90 84.1	3.97[c], 3.97[d] 64.7		
→3)-β-L-Ara*p*-(1→ **G**	5.02 102.2	3.89 71.9	4.09 84.1	3.88 70.8	3.98[c], 3.98[d] 63.7		
→6)-β-D-Glc*p*-(1→ **H**	4.46 102.7	3.30 73.2	4.46 75.7	3.38 69.8	3.42 75.9	3.95[c], 4.13[d] 67.9	
3-*O*-Me-β-D-Gal*p*-(1→ **I**	4.42 103.3	3.50 70.8	4.09 81.4	3.89 68.0	3.98 76.6	3.70[c], 3.87[d] 60.8	

[a] Values of the ^{1}H chemical shifts were recorded with respect to the HOD signal fixed at δ 4.70 at 30 °C.

[b] Values of the ^{13}C chemical shifts were recorded with reference to acetone as the internal standard and fixed at δ 31.05 at 30 °C.

[c,d] Interchangeable.

The residues **A** and **B** were assigned as (1→3,5)-α-L-Ara*f* and (1→5)-α-L-Ara*f* residues respectively. The α-configuration of both **A** and **B** residues were assigned from the chemical shift values of anomeric carbon and proton (δ 109.4/5.20 and δ 106.8/5.17) respectively. The downfield shift of C-3 (δ 81.8) and C-5 (δ 65.4) with respect to the standard methyl glycosides (Rinaudo & Vincendon, 1982; Agarwal, 1992; Mandal et al., 2011) indicated that the residue **A** was (1→3,5)-linked-α-L-arabinofuranose. The downfield shift of C-5 (δ 65.4) with respect to the standard methyl glycosides indicated that the residue **B** was (1→5)-linked α-L-arabinofuranosyl moiety. The linkage at C-5 of the both residues **A** and **B** were further confirmed from DEPT-135 spectrum (Fig. 3.4 inset). Hence, these observation confirmed that the residue **A** was (1→3,5)-α-L-Ara*f* and the residue **B** was (1→5)-α-L-Ara*f*.

The anomeric proton chemical shifts (δ 5.16 for **C** and **D,** δ 5.10 for **E**) and carbon chemical shifts (δ 97.7 for **C** and **D,** δ 99.5 for **E**) confirmed that the residues were α-D-galactopyranosyl residues. In case of residue **C**, the carbon chemical shifts of C-2 (δ 75.9) and C-6 (δ 66.4) appeared at downfield with respect to the standard values of methyl glycosides (Rinaudo & Vincendon, 1982; Agarwal, 1992) which suggests that residue **C** was linked at C-2 and C-6. The linkage at C-6 of the residue **C** was further confirmed from DEPT-135 spectrum (Fig. 3.4 inset). Hence, **C** was confirmed as (1,2→6)-linked α-D-galactopyranosyl residue. Residue **D** had an anomeric carbon signal at δ 97.7. The downfield shift of C-6 (δ 66.4) of residue **D** with respect to standard methyl glycosides indicated that it was linked at C-6. The linkage at C-6 was further supported by DEPT-135 spectrum (Fig. 3.4 inset). Therefore, **D** was confirmed as (1→6)-

linked α-D-galactopyranosyl residue. The downfield shift of C-2 (δ 76.6) with respect to standard values of methyl glycosides (Rinaudo & Vincendon, 1982; Agarwal, 1992) indicated that residue **E** was a (1→2)-linked α-D-galactopyranosyl.

Residue **F** was assigned as non reducing end β-L-Ara*f*. The anomeric proton chemical shift for residue **F** at δ 5.05 and carbon chemical shift of δ 101.5 indicated that it was a β-linked anomer (Agarwal, 1992; Das et al., 2013).

The residue **G** was assigned as (1→3)-β-L-Ara*p*. The anomeric proton (δ 5.02) and carbon (δ 102.2) chemical shift values indicated that **G** was a β-linked anomer. The downfield shift of C-3 at δ 84.1 indicated that it was (1→3)-β-L-Ara*p* (Chandra et al., 2009).

Anomeric proton chemical shift (δ 4.46), anomeric carbon chemical shift (δ 102.7), and the coupling constant value $J_{H\text{-}1,H\text{-}2}$ (~8.0 Hz) confirmed that **H** was β-D-glucopyranosyl residue. The downfield shifts of C-6 (δ 67.9) with respect to standard values of methyl glycosides indicated that residue **H** was linked at this position. The linking at C-6 of the residue **H** was further confirmed by DEPT-135 spectrum (inset, Fig. 3D). Thus, **H** was confirmed as (1→6)-β-D-glucopyranosyl residue.

β-configuration of residue **I** was assigned from $J_{H\text{-}1,H\text{-}2}$ coupling constant (~8.5 Hz) from its anomeric proton (δ 4.42) and carbon (δ 103.3) signals. All the proton and carbon chemical signals except C-3 matched nearly to the standard values of methyl glycosides (Rinaudo & Vincendon, 1982; Agarwal, 1992). The ^{13}C chemical shift of C-3 is about ~δ 10.0 higher than the standard value (Agarwal, 1992; Popper et al., 2001) which is consistent with the presence of -*O*Me group at C-3. This was further confirmed by the presence of cross coupling between the methoxy proton (δ 3.45) and the C-3 (δ

81.4) of residue **I** in the HMBC experiment (Figure not shown). Thus, **I** was confirmed as terminal 3-*O*-methyl-β-D-galactopyranosyl residue.

The sequence of glycosyl residues (**A** to **I**) were determined from ROESY (Table 3.2, Fig. 3.6) experiment.

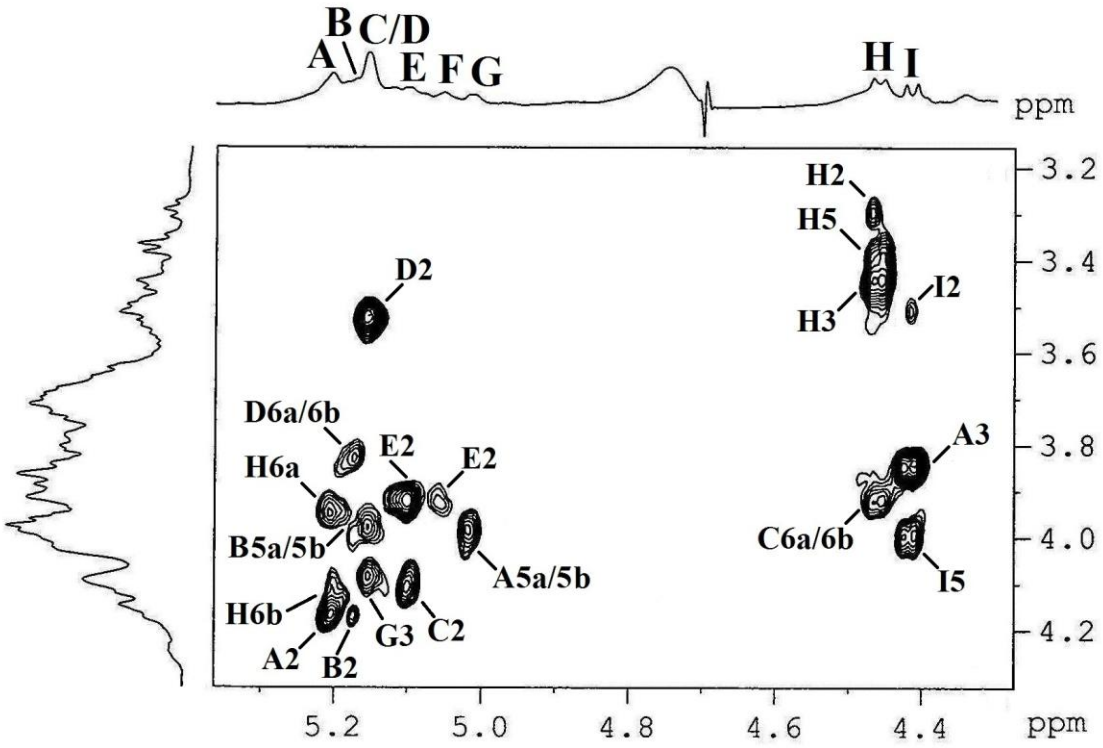

Fig. 3.6. Part of ROESY spectrum of exopolysaccharide, KNPS produced by *K. pneumoniae* PB12. The ROESY mixing time was 300 ms.

Table 3.2

ROESY data of exopolysaccharide, KNPS produced by *K. pneumoniae* PB12 in D_2O at 30 ºC.

Glycosyl residue	Anomeric proton	ROE contact protons	
	δ	δ	Residue, atom
→3,5)-α-L-Ara*f*-(1→ **A**	5.20	3.95	**H** H-6a
		4.13	**H** H-6b
		4.15	**A** H-2
→5)-α-L-Ara*f*-(1→ **B**	5.17	3.84	**D** H-6a/b
		4.15	**B** H-2
→2,6)-α-D-Gal*p*-(1→ **C**	5.16	3.98	**B** H-5a/b
		4.09	**G** H-3
→6)-α-D-Gal*p*-(1→ **D**	5.16	3.55	**D** H-2
		4.09	**C** H-2
→2)-α-D-Gal*p*-(1→ **E**	5.10	3.92	**E** H-2
		3.92	**E** H-2
β-L-Ara*f*-(1→ **F**	5.05	3.98	**A** H-5a/b
		3.92	**C** H-6a/b
→3)-β-L-Ara*p*-(1→ **G**	5.02	3.30	**H** H-2
		3.46	**H** H-3
→6)-β-D-Glc*p*-(1→ **H**	4.46	3.42	**H** H-5
		3.85	**A** H-3
3-*O*-Me-β-D-Gal*p*-(1→ **I**	4.42	3.98	**I** H-5
		3.50	**I** H-2

In ROESY experiment, the inter-residual contacts **A**H-1/**H**H-6a, 6b; **B**H-1/**D**H-6a, 6b; **C**H-1/**B**H-5a, 5b; **D**H-1/**G**H-3; **E**H-1/**C**H-2; **F**H-1/**E**H-2; **G**H-1/**A**H-5a, 5b; **H**H-1/**C**H-6a, 6b; and **I**H-1/**A**H-3 along with other intra-residual contacts were also observed (Fig. 3.6). The above ROESY connectivities established the following sequences: **A** (1→6) **H; B** (1→6) **D; C** (1→5) **B**; **D** (1→3) **G; E** (1→2) **C; F** (1→2) **E**; **G** (1→5) **A**; **H** (1→6) **C**; and **I** (1→3) **A**. Hence, the structure of repeating unit present in KNPS was proposed as:

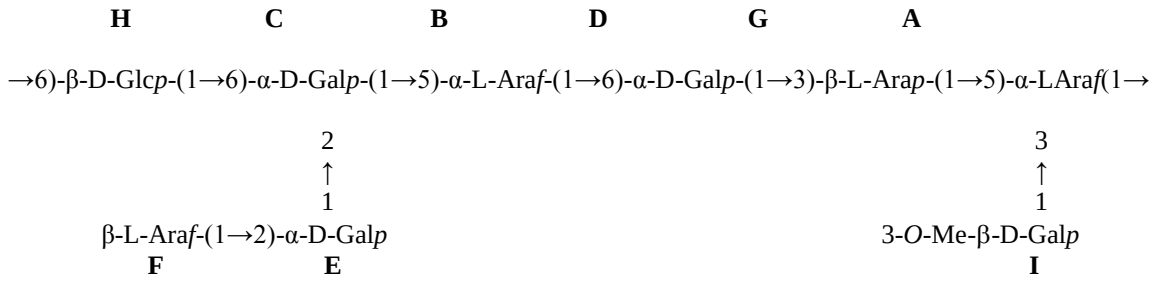

3.3.3. Smith degradation study

Smith degradation was carried out with KNPS and the product was analyzed by ^{13}C NMR (Table 3.3, Fig. 3.7) to confirm the sequence of the sugar residues present in the repeating unit.

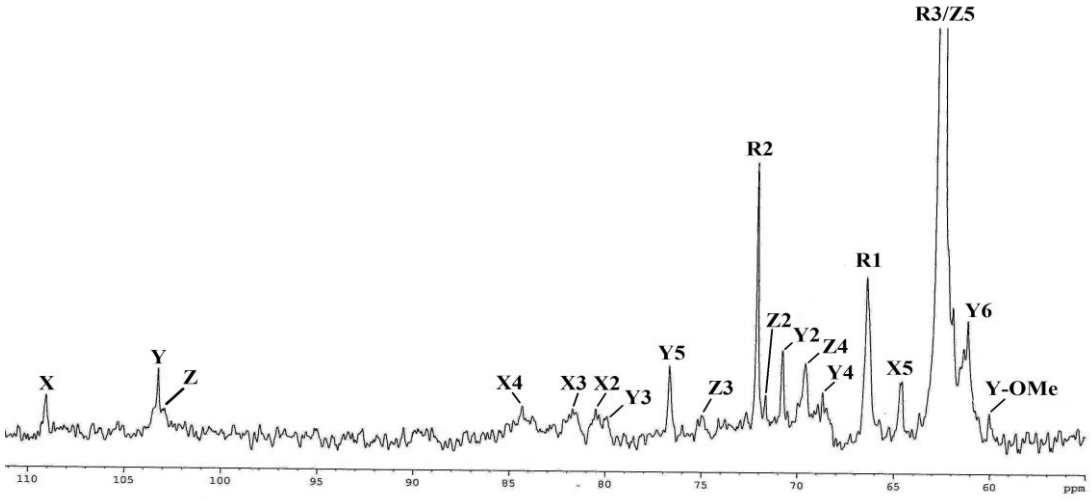

Fig. 3.7. ^{13}C NMR spectrum (125 MHz, D_2O, 30 ºC) of glycerol containing trisaccharide residue obtained from Smith-degradation of KNPS produced by *K. pneumoniae* PB12.

Table 3.3.

The ^{13}C NMR[n] chemical shifts of trisaccharide unit obtained after Smith-degradation of exopolysaccharide, KNPS produced by *K. pneumoniae* PB12 in D_2O at 30 ºC.

Sugar residue	C-1	C-2	C-3	C-4	C-5	C-6	*O*Me
→3,5)-α-L-Ara*f*-(1→ **X**	109.2	80.2	81.5	84.0	64.6	-	
3-*O*-Me-β-D-Gal*p*-(1→ **Y**	103.2	70.8	79.8	68.8	76.7	61.2	60.0
β-L-Ara*p*-(1→ **Z**	102.9	71.8	74.9	69.6	63.0	-	
1 2 3 (CH$_2$OH) CH(OH) CH$_2$O→ **R**	66.4	72.1	62.6	-	-	-	

[n] Values of the ^{13}C chemical shifts were recorded with reference to acetone, fixing the methyl carbon signal at δ 31.05.

A trisaccharide containing glycerol moiety was obtained as a product of Smith degradation of KNPS. The ^{13}C NMR spectrum of Smith-degraded KNPS showed three anomeric signals at δ 109.2, 103.3 and 102.9 corresponding to the anomeric carbon of →3,5)-α-L-Ara*f*-(1→ residue (**X**), 3-*O*-Me-β-D-Gal*p*-(1→ residue (**Y**) and β-L-Ara*p*-(1→ moiety (**Z**), respectively. The carbon signal at δ 64.6 and δ 81.5 clearly indicated the presence of linking at C-5 and C-3 of →3,5)-α-L-Ara*f*-(1→ residue (**X**). The residue (**A**) of KNPS being (1→3,5)-linked remains unaffected during oxidation and assigned as residue (**X**) in the degraded product. The →3)-β-L-Ara*p*-(1→ residue (**G**) was converted to nonreducing end β-L-Ara*p*-(1→ (**Z**) during Smith degradation. The glycerol moiety (**R**) was generated from the (1→6)-β-D-Glc*p* moiety (**H**) which was linked glycosidically with the residue (**C**) in KNPS and remains attached to the →3,5)-α-L-Ara*f*-(1→ moiety (**X**) in the Smith degraded product. The residue 3-*O*-Me-β-D-Gal*p*-(1→, (**I**) remains unaffected during Smith degradation and assisgned as residue (**Y**) in the degraded product. The remaining residues **B**, **C**, **D**, **E**, **F** of KNPS were completely destroyed during oxidation. Hence, the structure of glycerol containing trisaccharide unit obtained from exopolysaccharide, KNPS after Smith degradation was established as:

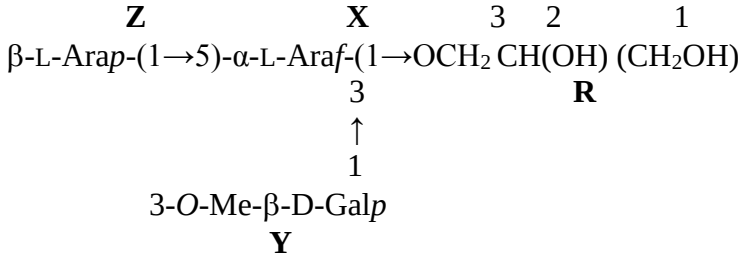

Therefore, Smith degradation results further confirmed the repeating unit present in the exopolysaccharide, KNPS produced by *K. pneumoniae* PB12.

3.3.4. Biological activities

The phenotypic characteristics of lymphocytes were confirmed by FACS analysis. The dot plot results showed that, 48% lymphocyte cells were $CD4^+$ and 23% $CD8^+$ [Fig. 3.8a]. The viability of the human lymphocytes was studied using SRB assay with varied concentrations of KNPS (ranging from 25-200 µg ml^{-1}) [Fig. 3.8b]. SRB, a bright pink aminoxanthene dye binds under mild acidic conditions to basic amino acid residues and dissociates under basic conditions. In order to understand the glutathione level, an important antioxidant in cellular system, both the reduced and oxidized form of glutathione were measured. It was observed that there was decrease in reduced glutathione (GSH) level at the dosage of 200 µg $m1^{-1}$ of KNPS whereas the same dosage of KNPS showed a mild increment of oxidized glutathione level (GSSG) ($p< 0.05$) [Fig. 3.8c]. Thus, it can be said that there is some relation between the redox ratios (GSH/GSSG) in cellular system with the concentration of KNPS used. Lipid peroxidation is one of the essential determinants to assess the cellular damage due to ROS. Several toxic by-products especially malondialdehyde (MDA) is released due to lipid peroxidation (Wood et al., 2003). Hence, the concentration of malondialdehyde (MDA) was measured to check the involvement of ROS in the alteration of redox status [Fig. 3.8d]. To further validate our observations, intracellular ROS was measured using a oxidant-sensing fluorescent probe 2',7'-dichlorodihydrofluorescein diacetate ($DCFH_2$-DA). $DCFH_2$-DA, a nonpolar dye, converted into the polar derivative DCFH (nonfluorescent) by means of cellular esterase. After getting oxidized by intracellular ROS and other peroxides it switched to highly fluorescent DCF. Fig. 3.8e, showed that

fluorescence intensity of DCF increase with the increment of KNPS dosage (varied between 25-200 µg $m1^{-1}$) and it becomes maximum at 200 µg $m1^{-1}$ (Fig.3.9.).

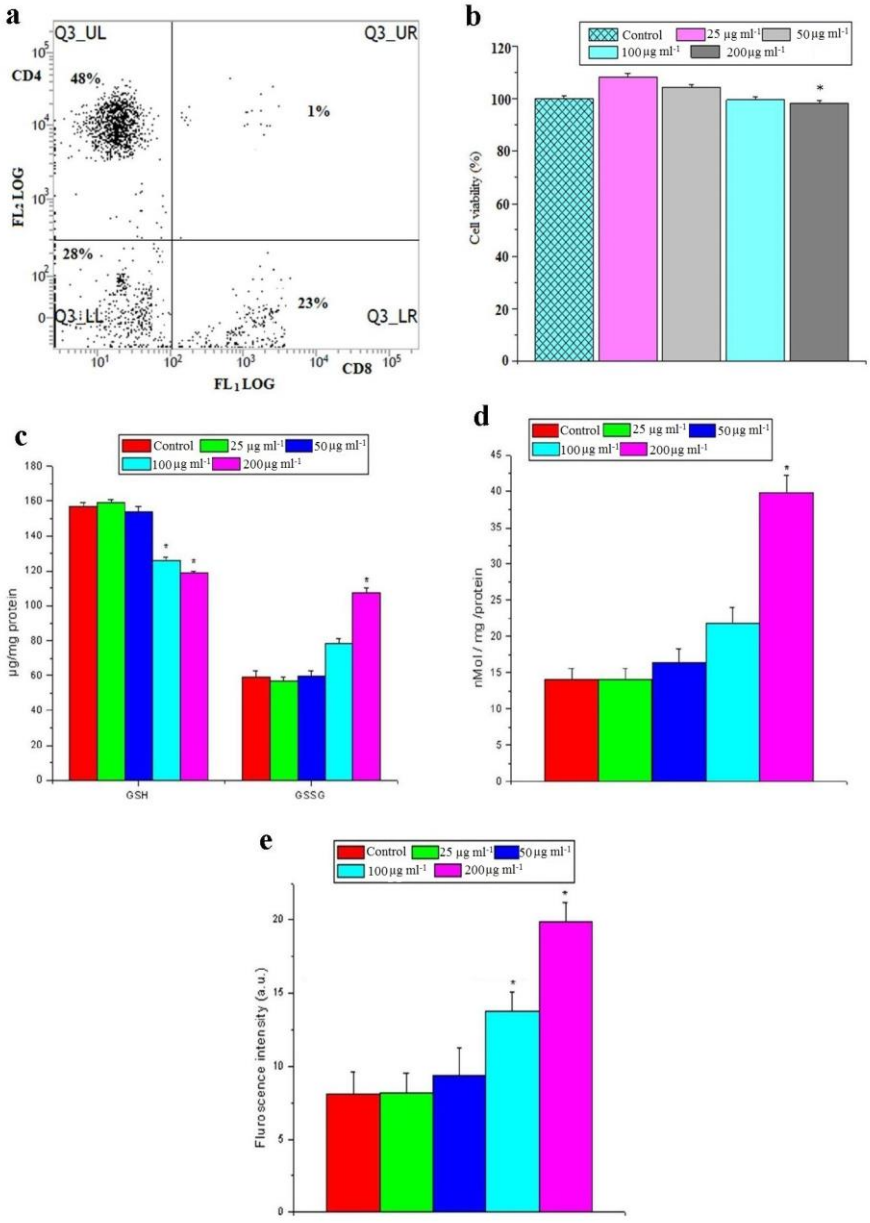

Fig. 3.8. a) Dot plot of lymphocytes stained with anti-CD4 or anti-CD8 antibodies. b) Cytotoxicity of KNPS against human lymphocytes. c) Concentration of reduced glutathione (GSH) and oxidized glutathione (GSSG) of normal human lymphocytes when

treated with KNPS. d) Lipid peroxidation study in terms of MDA release in KNPS treated human lymphocytes. e) Measurement of intracellular ROS in lymphocytes, using a oxidant-sensing fluorescent probe 2',7'-dichlorodihydrofluorescein diacetate (DCFH-DA), treated with varied concentration of KNPS. (n = 6, values are expressed as mean ± SEM. * Indicates the significant difference as compared to control group).

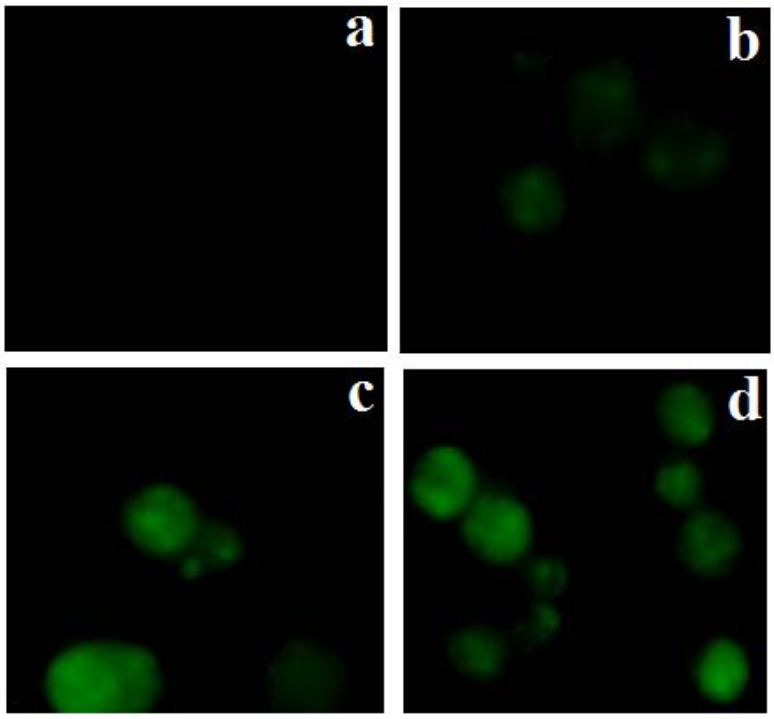

Fig. 3.9. Fluorescence micrographs of human lymphocytes treated with different concentrations of KNPS. a) Control, b) 50 µg $m1^{-1}$, c) 100 µg $m1^{-1}$ and d) 200 µg $m1^{-1}$.

3.4. Discussion

The average molecular weight of KNPS was estimated ~1.8×10^5 Da. Results obtained from biological studies showed that 200 µg $m1^{-1}$ dosage of KNPS exhibited toxicity ($p< 0.05$) (Fig. 3.9). Previous report established the potent role of *K. pneumoniae* CPS in initiation of cytotoxicity during the infection of lung epithelial cells (Cano et al., 2009). The increasing GSSG level may be due to the generation of free singlet species inside the cells. When the dose of the KNPS was increased from 25 to 200 µg $m1^{-1}$, the redox ratio decreased significantly ($p < 0.05$) to 1.11 compared to their respective control (redox ratio 2.66) indicating that 200 µg $m1^{-1}$ of KNPS was toxic. The significantly ($p< 0.05$) enhanced production of MDA was noted at 200 µg $m1^{-1}$ of KNPS dosage, which confirms the potential of KNPS to alter the intracellular redox status via ROS production. Similar type of enhanced ROS generation was reported in macrophage cell lines by the polysaccharide, PSG-1 (Yu et al., 2014). These results showed that KNPS treatment enhanced the generation of intracellular reactive oxygen species (ROS). It was reported earlier that the CPS of *K. pneumoniae* induce ROS production in macrophages (Yang et al., 2011). Hence, this study may help to put on more insights into the mechanisms of septic shock and KNPS-induced immunosuppression and autoimmunity.

CHAPTER 4

Chapter 4

Exploring Biotechnological Prospect of Exopolysaccharide Produced by *K. pneumoniae* PB12: Flocculation Studies

4.1. Introduction

Flocculants have been widely used in a variety of industrial processes, such as wastewater treatment, food and fermentation industries, drinking water purification, and industrial downstream processes (Shih et al., 2001). They are typically used to accelerate or improve the settling of suspended solids in various types of wastewater. Water pollution is one of the major problems these days and researchers are trying to solve this problem. Flocculants used in water treatment can be classified into three main groups: (i) inorganic flocculants such as alum, ferric flocculants or polyaluminum chloride; (ii) synthetic organic flocculants like polyacrylamide derivatives or polyethylene imine; and (iii) naturally occurring flocculants like sodium alginate or microbial flocculants. Some inorganic and synthetic organic flocculants are carcinogenic and neurotoxic. Polyferric sulfate flocculant can be costly and the resultant excess iron may cause unpleasant taste, odor, color etc. Although synthetic flocculants are used because of their cost effectiveness, they are not biodegradable and are some of their degraded monomers such as acrylamide are neurotoxic and even show strong carcinogen (Yokoi et al., 1995). Bioflocculants are generally non-toxic and biodegradable. Most of the reported bioflocculants are principally comprised of exopolysaccharide (EPS). Several microorganisms in nature are genetically pre-disposed to produce EPS having flocculating properties. Microbial biopolymers having flocculating activities are basically EPS containing glycoprotein,

polysaccharide, protein, cellulose, lipid, glycolipid and nucleic acid (Czaczyk & Myszka, 2007). Flocculants produced by a haloalkalophilic *Bacillus* sp. I-471 (Kumar et al., 2004), *Bacillus subtilis* DYU1 (Wu & Ye, 2007) and *Vagococcus* sp. W31 (Gao et al, 2006) are polysaccharides. *Nocardia amarae* YK-1 (Takeda et al., 1992), *Bacillus licheniformis* (Shih et al., 2001) and *Rhodococcus erythropolis S-1*(Kurane et al., 1986) all produces protein flocculant, while *Arcuadendron* sp. TS-4 (Lee et al., 1995) and *Arathrobacter* sp. (Wang et al., 1995) produce glycoprotein bioflocculant. The bioflocculants can be applied in various processes, such as removal of microorganisms in the fermentation industry and different industrial waste treatment of textile, cosmetic, paper, leather, pharmaceutical, and food industries (Deng et al., 2005).

4.1.1. Mechanism of biofloccuation

The biopolymers have the property to anchor and bridge the adjacent cells and hence they are thought to be responsible for the bioflocculation process. There are three theories which explain the mechanisms of bioflocculation: DLVO theory (or double layer theory), alginate theory, and divalent cation bridging (DCB) theory.

4.1.1.1. The DLVO theory

The DLVO theory (named after Derjaguin, Landau, Verwery and Overbeek) is a classical colloidal theory which explains that the charged particles have a double layer of counter-ions. The first layer (also known as Stern layer) is composed of a strongly associated counter-ion layer, and the second layer (known as diffuse layer) is made of loosely associated counter-ions (Adamson, 1990). The concentration of ions in the diffuse layer decreases with distance from the particle surface until the

concentration of ions equals to that of the bulk solution and thus an electric potential develops around the particle. This double layer of ions surrounding the particle results in repulsion of adjacent particles and reduces aggregation (Fig 4.1). With increasing ionic concentration, repulsion between the particles gets decreased due to the compression of double layer and allows short range attractive forces (van der Waal forces) to promote aggregation (Sobeck & Higgins, 2002).

Negatively charged ions of the dispersion medium when adsorbed on the colloidal particles surface renders them negative electric charge.	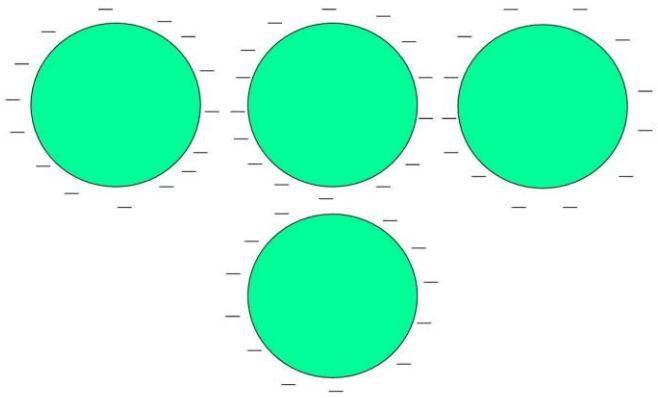
A negatively charged particle attracts the positive counter-ions from the surrounding medium, resulting in the formation of electrical double layer. The outer layer is diffused and	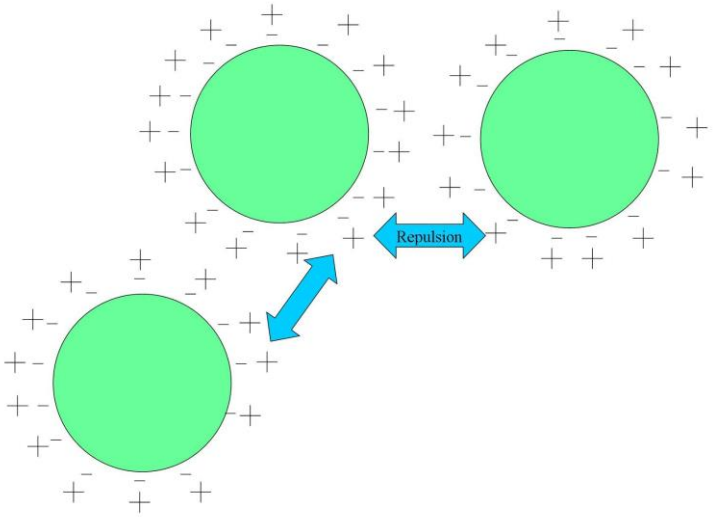

causes repulsion. Because of which colloidal particle remain suspended in the medium.	
At high ionic strength the electrical double layer shrinks, allowing the particle to get closer. At such a close distance, attractive forces such as weak van der Waal forces comes to play, resulting in aggregation and flocculation/ precipitation.	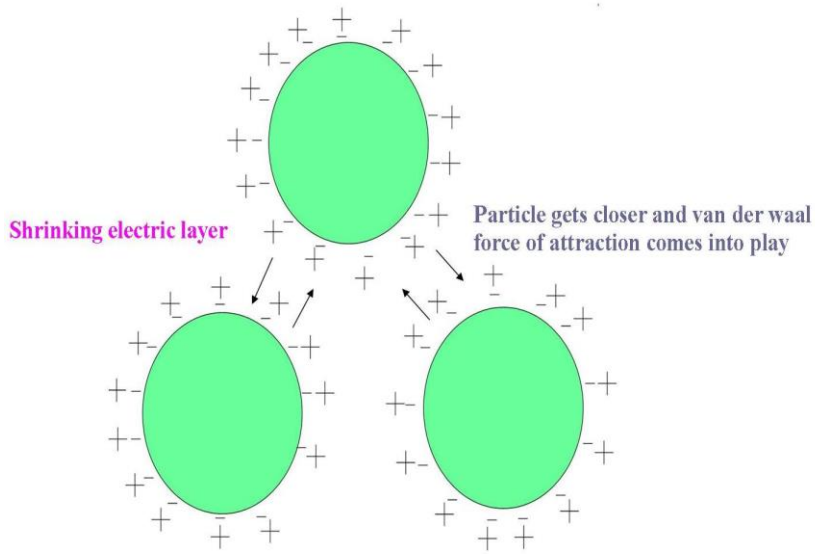

Fig. 4.1. The DLVO theory of bioflocculation.

4.1.1.2. The alginate theory

This theory was first proposed by Bruus et al. (1992) for describing the role of cations in bioflocculation. Alginate is a polysaccharide produced by bacteria and is made up of repeating mannuronic and gluronic acids. In presence of calcium ions this

polysaccharide forms gel. They concluded that the biopolymers have high affinity for Ca^{2+}, and this support their role in bioflocculation.

4.1.1.3. The DCB theory

The divalent cation bridging (DCB) theory was first proposed by McKinney (1952) and Tezuka (1969). According to this theory, divalent cations such as Ca^{2+} and Mg^{2+} play an important role in bioflocculation by forming bridges between the negatively charged functional groups within the EPS and this bridging helps to aggregate and stabilize the matrix of biopolymer and microbes and therefore promote bioflocculation.

4.1.2. Emulsification

Surfactants and emulsifiers are widely used in the pharmaceutical, cosmetic, detergents in various industrial sectors, petroleum and food industries (Makkar & Cameotra, 1998). Most of these compounds are synthetic and are not easily biodegradable and their manufacturing processes and by-products can be environmentally hazardous. Bio-emulsifiers are microbial products that have the property of reducing surface tension and various advantages over synthetic emulsifiers. As they are microbial origin, they are also biodegradable and hence their use can prevent toxicity problems and accumulation in natural ecosystems (Leahy & Colwell, 1990). Besides possessing biodegradable property, microbial emulsifiers are more effective over a wide range of pH, temperature and salinity (Banat et al., 2000). Microbial emulsifiers are composed of low-molecular-weight glycolipids, lipopeptides and high-molecular-weight lipid-containing polymers such as lipoproteins, lipopolyssacharide-protein complexes and polysaccharide-protein-fatty

acid complexes (Ron & Rosenberg, 2001). A large number of microbial species from different genera produces emulsifiers which are composed of polysaccharides, proteins, lipopolysaccharides, lipoproteins, or complex mixtures of these biopolymers Bio-emulsifiers containing a polysaccharide component attached to lipid and/or protein has been widely studied. The best-studied are the bioemulsans produced by different species of *Acinetobacter* (Kaplan & Rosenberg, 1982; Navon-Venezia et al., 1995). Among the bacterial emulsifiers, emulsan obtained from from *Acinetobacter calcoaceticus* known as RAG-1 is the only commercialized one (Rosenberg et al., 1998). RAG-1 emulsan is a complex of an anionic heteropolysaccharide and protein (Rosenberg et al., 2002). Bio-emulsifier has the property to emulsify wide variety of hydrocarbon and thus can be used for bioremediation of oil pollutant (Calvo et al., 2009).

4.1.3. Metal Chelating property

During the last two decades, extensive attention has been paid on the use of microorganisms for environmental restoration. It is well known that several microbial biomasses are able to bind and accumulate heavy metals from solution through the process of biosorption (Baldrian & Gabriel, 2003). These relatively simple and inexpensive technologies try to exploit the cationic and anionic functional groups present on the surface of the cell which form a stable, non-toxic complex with the metal ion. Several studies have been undertaken to disclose the type of these different functional groups. Their result revealed the participation of carboxyl, sulfhydryl, hydroxyl sulfonate, phosphonate, amine, and amide groups in metal binding (Maier et al., 2009). In *Pseudomonas fluorescens*, the carboxyl groups in the cell envelop has been found to be associated with binding to Ni, Cu and Zn (Falla & Block, 1993).

EPSs produced by different microorganisms are of particular importance to the bioremediation process because of their involvement in the flocculation and binding of metal ions from solutions (Salehizadeh & Shojaosadati, 2003). The binding of cations to bacterial EPSs generally occurs through electrostatic interaction with negatively charged functional groups such as uronic acids, phosphoryl groups and carboxylic groups. In addition protein component of EPSs also plays a major role in complexation of metal ions (Mejare & Bulow, 2001). Proteins rich in acidic amino acids, including aspartic and glutamic acid, also provide anionic properties to the EPSs.

The application of EPSs for biosorption seems to be more economical, effective and safe alternative to chemical methods such as precipitation, coagulation, ion exchange, electrochemical and membrane processes. As the EPSs is a non-living sorbent, its potential application in the treatment process has been widely acknowledged (Gavrilescu, 2004). In this chapter the potential biotechnological application of the EPS has been explored.

4.2. Materials and methods

4.2.1. Flocculating rate measurement

Activated carbon was suspended in distilled water at a concentration of 5 g l-1 at pH 7 and used as a stock solution for the subsequent assays. After the pH of the suspension was adjusted, 0.1 ml of culture supernatant was added and stirred for 2 min. The solutions were allowed to settle for 5 min at room temperature and the optical density (OD) of the clarifying upper phase solution was measured at 550 nm with a UV-vis spectrophotometer. A control tube in which the culture supernatant was

replaced with distilled water was also included and measured under the same conditions. The flocculating rate was determined according to following equation:

$$[B-A]/B \times 100\% \quad (1)$$

Where A and B are optical densities at 550 nm of the sample and control, respectively. Mean % flocculating rate of three independent experiments was considered.

4.2.2. Emulsifying activity measurement

Toluene, n-hexadecane, olive oil, and kerosene oil were used to study the emulsifying activity of the purified EPS according to the procedure described earlier (Ashtaputre & Shah, 1995). To 3 ml aqueous solution of EPS (1 mg ml^{-1}), 3 ml of hydrocarbon or oil was added and agitated vigorously for 2 min on vortex. The emulsion and aqueous layers were measured after 24 h and emulsification index (E24) was calculated by the following formula (Cooper & Goldenberg, 1987):

$$E24 = \text{volume of the emulsion layer/total volume} \times 100 \quad (2)$$

4.2.3. Effect of dosage, temperature, pH and metal cations on the flocculating rate

The effects of EPS and $CaCl_2$ dosage, temperature, pH and metal ions on flocculating rate were examined. The dosage of EPS and $CaCl_2$ were varied from 1-30 mg l^{-1} and 0-100 mM, respectively. The pH of the activated carbon suspensions was adjusted using HCl and NaOH in the pH range of 1-11. The temperature of activated carbon suspension was changed in water bath in the range of 10-100 °C. The effects of various metal cations (monovalent: NaCl, KCl; divalent: $MgCl_2.6H_2O$, $MnCl_2.6H_2O$, $CoCl_2.6H_2O$, $NiCl_2.6H2O$, $ZnSO_4.7H_2O$, $CuSO_4.5H2O$, $CdCl_2.H_2O$;

and trivalent: $FeCl_3.6H_2O$ in the range of 0-100 mM concentration) on flocculation of activated carbon suspension were also studied.

4.3. Results

4.3.1. Emulsifying activity measurement

The EPS showed characteristic emulsifying activity with toluene (66.6%), n-hexadecane (65%), olive oil (63.3%) and kerosene (50%).

4.3.2. Effect of dosage, pH, temperature and metal ions on the flocculating rate

Effect of higher or lower dosage of both $CaCl_2$ and EPS on flocculating rate was studied in order to determine optimal dosage. The flocculating rate of 98% was achieved with EPS dosage of 17 mg l^{-1} and 4 mM $CaCl_2$ at pH 7. Higher or lower dosage of EPS and $CaCl_2$ caused poor flocculation (Fig. 4.2a & b).

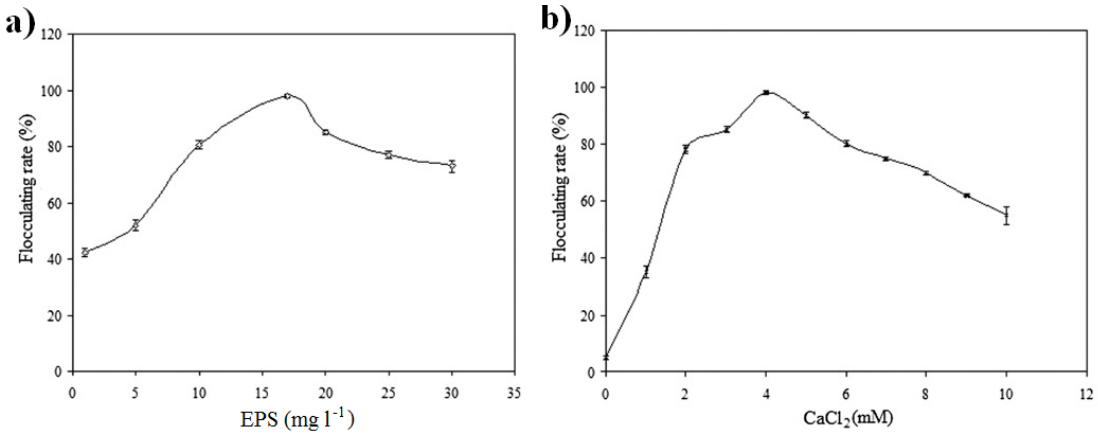

Fig. 4.2. a) Effect of EPS dosage on flocculating rate. **b)** Effect of CaCl2 concentration or dosage on flocculating rate.

In the pH range of 3-10, flocculating rates were above 80% showing maximum (98%) at pH 7 in presence of 4 mM $CaCl_2$ (Fig. 4.3).

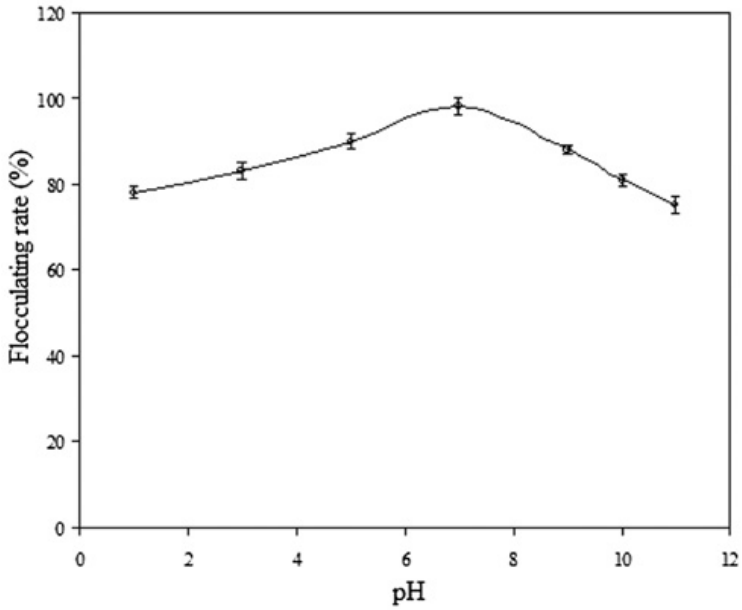

Fig. 4.3. Effect of pH on flocculating rate in presence of 4 mM $CaCl_2$.

Effects of various cations other than Ca^{2+} on the flocculating rate of the EPS were studied (Fig. 4.4) and compared with the flocculating rate in presence of $CaCl_2$ (control).

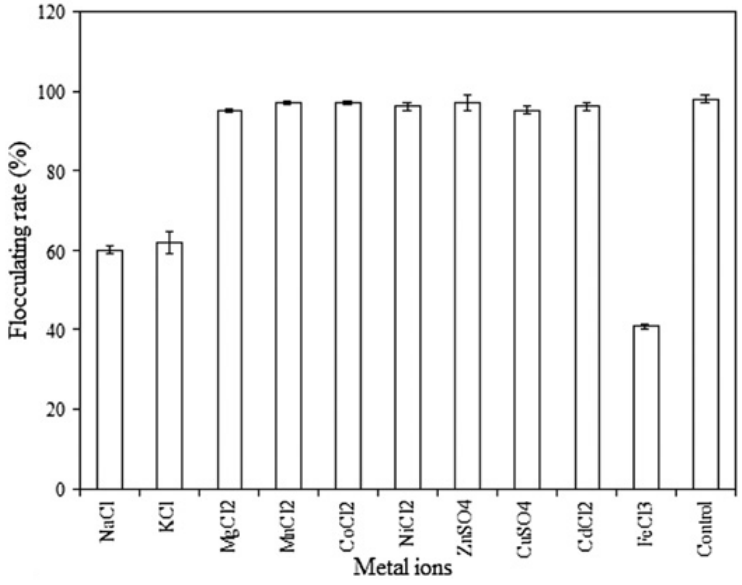

Fig. 4.4. Effect of various metal cations on flocculating rate

The optimal concentration of Mg^{2+} or Mn^{2+} or Co^{2+} or Ni^{2+} or Zn^{2+} or Cu^{2+} or Cd^{2+} was found to be 4 mM (same as that Ca^{2+}) whereas, the optimal concentration of Fe^{3+} was 1 mM and for monovalent cations, Na^{+} and K^{+}, the optimum dosage was 10 mM. The choice of using $CaCl_2$ over $FeCl_3$ in flocculation studies was due to the ease of handling the Ca^{2+} induced large and compact floc in contrast to the gelatinous floc produced by Fe^{3+}.

Effect of temperature on flocculating rate was also studied. The flocculating rate remained above 90% in the temperature range of 10-50 °C. Maximum flocculation of 98% was observed in both 10 °C and 20 °C (Fig. 4.5).

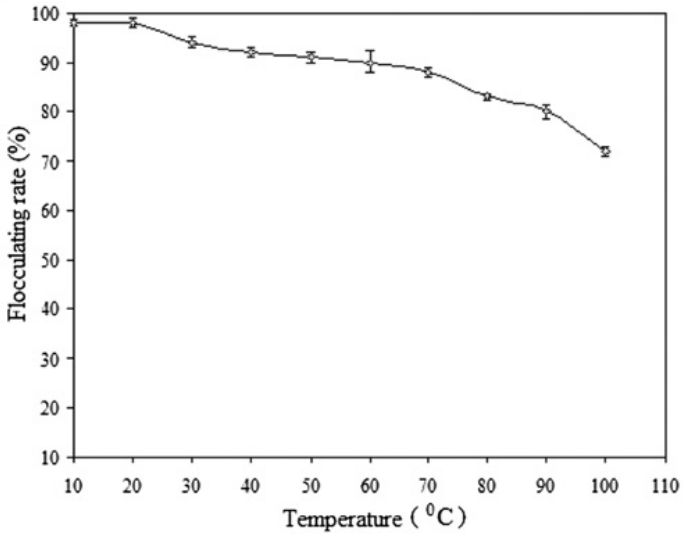

Fig. 4.5. Effect of temperature on flocculating rate

4.4. Discussion

Emulsifying activities of the EPS obtained from *K. pneumoniae* PB12 against hydrophobic compounds like n-hexadecane, toluene and olive oil were well comparable with emulsification index for the EPS produced by gram-negative bacteria *Pseudomonas oleovorans* (Freitas et al., 2009). Presently there is growing demand for biodegradable and renewable flocculants instead of chemical flocculants. In this study, flocculating property of EPS obtained from *K. Pneumoniae* PB12 was studied. The flocculating activity was determined by activated carbon assay. Flocculation of activated carbon was more than 98% with 17 mg l^{-1} of EPS dosage (Fig. 4.2a & Fig. 4.6).

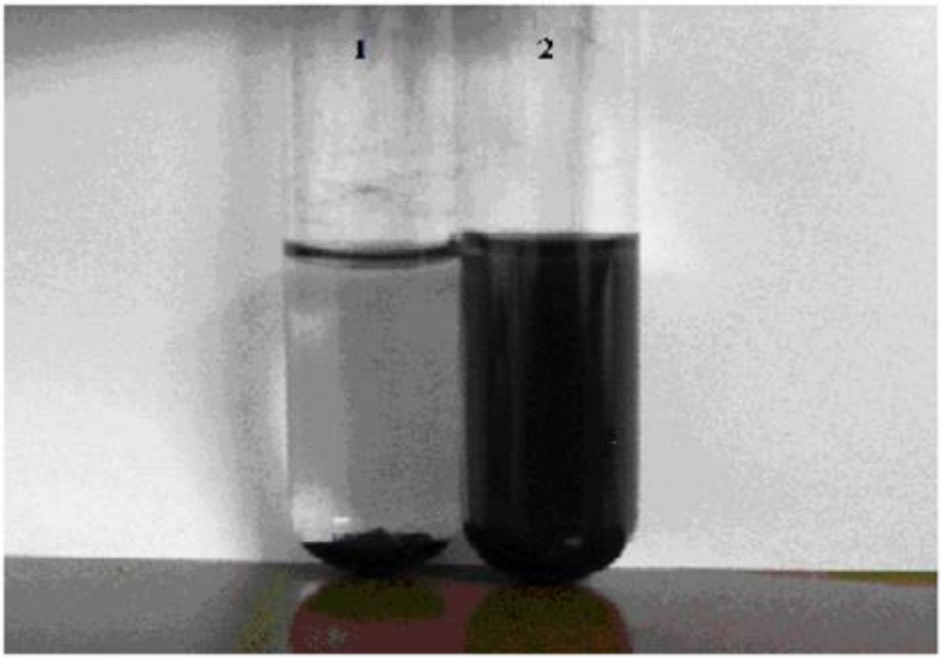

Fig. 4.6. Photograph showing flocculation of activated carbon in 5 min; sample 1: with EPS; sample 2: without EPS.

However, higher or lower dosages of EPS showed reduction in flocculating rate(s). When the dosage of EPS was inadequate, the effective bridging phenomenon gets hindered causing reduction in flocculation. The relationship between EPS dosage and flocculating rate was similar to the results described by earlier authors (Suh et al., 1997; Zheng et al., 2008). An EPS produced by a micro-alga, *Gyrodinium impudicum* KG03 required 7mM $CaCl_2$ for maximum flocculation (61%) of activated carbon (Yim et al., 2007). Results showed that at lower EPS dosage ineffective bridging caused poor flocculation; on the other side, over addition of negatively charged EPS caused incomplete dispersion of excess EPS leading to poor stability (Suh et al., 1997). The relationship between EPS dosage and flocculating rate was similar to the results described by earlier authors (Suh et al., 1997; Zheng et al., 2008). In alkaline condition, the flocculating rate decreases, suggesting that increase in OH^- concentration causes increment of negative charge density on activated carbon particles and consequently the neutralizing effect of $CaCl_2$ gets inhibited resulting in dispersion of suspended particles. In the absence of Ca^{2+} ion no effective flocculation was observed at pH 7 which dictates the requirements of $CaCl_2$ for effective flocculation by forming Ca^{2+} mediated complexes of the EPS and activated carbon (Kurane et al., 1986). The presence of C=O group as revealed in FT-IR may play an important role in flocculation and can serve as binding sites for divalent cations. Results showed that the flocculating rates determined with divalent cations Mn^{2+}, Co^{2+}, Ca^{2+}, Zn^{2+}, Cd^{2+}, Cu^{2+}, and Ni^{2+} were better than other tested cations. The flocculating rate in presence of Fe^{3+} was 53% lesser than that of Ca^{2+} induced flocculation. This may be because of its effect on changing the surface charge of activated carbon particle and coverage the EPS adsorb-sites. The competition of the positively charged particles and less adsorb sites reduce the flocculation efficiency

(Gong et al., 2008; Zheng et al., 2008). Such reduction in flocculation was also noted when excess of $CaCl_2$ was added; may be because of the similar phenomenon (Fig. 4.1B). Monovalent cations like K^+ and Na^+ are less effective for flocculation due to weaker electrostatic force of attraction between monovalent cations and EPS (Li et al., 2008). EPS produced by *C. daeguense* W6 in nutrient poor medium have shown flocculating rates above 90% in the temperature range of 0-45 °C with maximum of 97% at 15 °C (Liu et al., 2010). Maximum flocculation of 98% was observed by PB12 EPS in both 10 °C and 20 °C. When temperature was increased to 100 °C, a decrease of approximately 26% from the maximum flocculation rate was observed; such decrease (26%) at 100 °C from the maximum value was observed with EPS produced by *Bacillus mojavensis* 32A (Elkady et al., 2011). Decrease in flocculating rate at higher temperature (above 60 °C) could be explained by simultaneously rise in kinetic energy of activated carbon particles due to heating effect. The EPS produced by the oligotrophic bacterium PB12 could be an effective replacement of a commercial polymer with regard to flocculation. The high flocculation rate of PB12-EPS over a wide range of temperature (10 °C-50 °C) and pH (3-10) possess a promise for application in water treatment and other biotechnological applications including metal processing industries.

The optimal dosages for flocculation of activated carbon suspension were 17 mg l^{-1} EPS and 4 mM $CaCl_2$. EPS showed flocculating rate of above 80% over a wide range of pH (pH 3-10) whereas, more than 90% rate was noted in the temperature range (10-50 °C) tested in presence of $CaCl_2$. Moreover, EPS showed characteristic emulsifying activity with toluene (66.6%), n-hexadecane (65%), olive oil (63.3%) and kerosene (50%). Results showed that EPS was found suitable to be applied in alkaline, neutral,

and acidic conditions. Both the emulsifying and flocculating properties of the EPS were comparable with those of other commercially available flocculants and emulsifying agents. Thus, it is anticipated that EPS obtained from *K. pneumoniae* PB12 would be an attractive candidate for future use in environmental bioremediation processes like enhanced oil recovery.

GENERAL DISCUSSION AND SUMMARY

Bacteria are social when famished. They are slippery and mucous when they are social. Bacteria are attractive model of current research, as methodologies behind social organization have started getting revealed. Determining the costs and benefits of any bacterial behavior in a particular setting of an ecosystem enables one to understand the evolution of that behavior. In natural conditions, however, there is no scope for an experimenter to provide a readily available food source; but in laboratory we can create condition of famine or feast. When bacteria were forced to starve, natural instincts of finding each other could be demonstrated. Once the bacteria clumped together, they take part in a collective effort to find the nutrients they need. After they aggregate, the bacteria actually change their physiology to form a protective, adhesive gel-like biofilm. The spatial relationships between cells in micro-meter scale spectacularly gets altered when environmental circumstances of biofilm growth is changed that determines the quanta of benefits received by the bacteria out of the secretion of extra-cellular polymeric substances (EPS). Consequentially, in varied growth conditions a single behavior can yield reverse effect on competition. For example, certain mutants of *Vibrio cholera,* that produce EPS constitutively, outcompete cells which fails to secrete EPS within biofilms grown on solid surfaces. In real world situation, secretion of EPS is an important determinant of survival or in other words, EPS production is a competitive behavior. In the lungs of people with cystic fibrosis, mutant strains of *Pseudomonas aeruginosa*, that produce EPS constitutively, overpopulates and cause fatal lung infections.

Social life of bacteria when living in scarcity (oligotrophic conditions)

Oligotrophic environments usually deficient in exogenous supply of nutrients and are defined by a low nutrient flux, <1 mg carbon per litre per day (Schut et al., 1993) as well as by low absolute concentrations of nutrients (Morita, 1997). The aquatic environment is the

largest habitat on Earth, accounting for >90% of the biosphere by volume and harbouring microorganisms responsible for ~50% of total global primary production. Despite of highest cellular production rate of any ecosystem on the planet, aquatic environments has vast oligotrophic (e.g., nutrient-limited open ocean water) situation.

Numerous reports have shown that most marine bacteria adapt to oligotrophic environments and prefer lower nutrient conditions (<10 mg C 1^{-1}) to higher nutrient conditions (Carlucci & Shimp 1976, Akagi et al. 1977, Ishida et al. 1986). An oligotrophic bacterium growing slowly in nutrient-poor condition may have a life strategy in which dispersal is promoted to optimize cell access to substrates. In the latter scenario colony formation is possibly not adaptive. While aquatic ecologists have had an interest in oligotrophic bacteria (Yokoi et al., 1995; Tago and Aida 1977; Nguyen and Schiller 1989; Costerton et al., 1981), these organisms are still relatively unknown to many microbiologists, especially clinical microbiologists. Growth and continued existence of bacteria are often influenced by EPS produced by them.

Oligotrophic bacteria can tentatively be divided into 2 groups: obligate oligotrophs and facultative oligotrophs (Ishida et al. 1980, 1986). Facultative oligotrophs can grow in a relatively wide range of nutrient concentration, hence; can be used as model organisms to understand the various strategy used by oligotrophs for their survibility under nutrient deprived condition. In this thesis, an attempt was made to understand the physiology of a model facultative oligotrophic bacterium *K. pneimoniae* PB12. Since sustenance of bacteria is often influenced by EPS, structural investigation of the exopolysaccharide produced by *K. pneimoniae* PB12 was explored in details. In addition to the emphasis on the EPS structure, immunological and biotechnological prospects were also revealed.

Chapter 1 dealt with screening and characterization of the test strain. On the basis of the phenotypic and phylogenetic analyses, the strain PB12 was identified as *Klebsiella*

pneumoniae. It was observed that PB12 cells were able to grow in 0.001x LB broth as well as sterile river water without supplementation of any carbon or nitrogen source or growth factors. An increment of nearly 13 times the initial cell number was noted in a span of 3 days in 0.001x LB. In our earlier reports, facultative oligotrophic strains, *Acinetobacter johnsonii* MB52 and *Klebsiella pneumoniae* MB45 showed an increase of 2.5 and 4.6 times the initial cell number when grown in 0.001x LB in the span of 8 and 2 days, respectively (Kumar et al., 2010; Kumar et al., 2011). The ability of PB12 to survive without any reduction in viable cell number from the input cells establishes its oligotrophic nature. After the strain characterization, protocol for EPS extraction from the culture broth was optimized. It was noted that centrifugation along with alcoholic precipitation was found to be convenient and satisfactory method compared to other extraction methods reported in the literature (Comte et al., 2006; Peterson, 1979; Underwood & Paterson, 1995). This method is also the most common and widely used method for EPS extraction (Underwood et al., 1995). Yield of EPS in R2A varied with time and was maximal (1.3 g l^{-1}) at 48 h of incubation at 30 °C. Above 30 ºC, the productivity of EPS was reduced. Furthermore, maximum growth in terms of optical density was also noticed at 30 ºC, below and above this temperature, both growth and EPS production decreases. Moreover, the effect of various carbon sources on EPS production was checked and it was obtain that both the growth and production of EPS in R2A was enhanced maximally when supplemented with 1% glucose. The high productivity of EPS (1.3 g l^{-1}) was observed at pH 7. The yield of EPS as well as growth decreased below and above pH 7. There is reduction in the amount of EPS after 48 h which was probably due to utilization of the EPS by the bacterium. Similar utilization of EPS as carbon source was also observed by earlier authors (Gauri et al., 2009). In the present study *Klebsiella pnemoniae* PB12 showed decrease in approximately 31% of EPS during further incubation from 48 h to 72 h in the same batch culture was associated with two times increment in viable cell number. This

established that EPS somehow help this particular bacterium to survive under nutrient deprived condition via providing as an alternative carbon source.

Chapter 2 dealt with basic physiology of the test strain, *K. pneumoniae* PB12. It was noted that the PB12 cells can carry out reproduction along with the macromolecular synthesis with whatever in their milieu even at 10 times diluted LB i.e., 0.01x LB. When allowed to grow on LB or 10 times diluted LB agar plates (0.01x LB agar) it was noted that colony diameter of PB12 grown on LB agar after 24 h was found to be 1.5 mm, whereas, colony diameter of PB12 on 0.01x LB after 24 h of incubation was 0.5 mm. Interestingly, after assessing the number of cells presents in this colony it was noted that colonies obtained on LB agar (d=1.5 mm) there are 1.8 x 10^8 cells present. Whereas, 5.4 x 10^8 (approximately 3 times more) numbers of cells was obtained from the colony grown on diluted LB agar plates. SEM and FACS analysis of the PB12 cells grown in either LB or 0.01x LB showed that cells grown in diluted LB have reduced their size in order to increase its surface area to volume ratio to cope nutrient scarcity. It was established earlier that nutrient availability is a primary determinant of cell size for single-celled organisms. In 1958, Schaechter, Maaløe, and Kjeldgaard determined that *Salmonella* cell size is coupled to growth rate, which is itself a function of nutrient availability. PB12 cells population grown in LB showed increment in FSC (forward- scattered light), indicating that the cells were possibly larger than PB12 cells grown in 0.01x LB. Earlier researcher used flow cytometry to detect and quantify cell shape differences between the rod-shaped cells of *E. coli*: CS109 and the seriously deformed cells of *E. coli*: CS315-1K, a mutant lacking PBPs 4, 5, and 7 (Meberg et al., 2004). Organisms that grow aerobically are regularly exposed to unavoidable by-products of aerobic respiration like reactive oxygen species (ROS) [e.g. peroxide, superoxide (SO)] (Storz & Imlay, 1999) ROS damages cellular macromolecules and thus elicit adaptive oxidative stress responses in bacteria intended to permit survival in the presence of this stressor. Using an oxidant-sensing

fluorescent probe 2', 7'-dichlorodihydrofluorescein diacetate ($DCFH_2$-DA) intracellular ROS can be measured (Barzegar & Moosavi-Movahedi, 2011). Results showed that both intracellular ROS and NO production is more in LB grown cells compare to 0.01x LB grown cells. Whereas, both Cu,ZnSOD and catalase activity was higher in 0.01x LB grown PB12 cells compared to LB grown PB12 cells. To validate this observation a model ROS generator, ZnO-PEI NPs were used to study its effect on PB12 cells grown in either LB or 0.01x LB. Results showed that LD_{50} dosage of ZnO-PEI NPs cause only 35% reduction in bacterial growth of 0.01x LB grown cells whereas, approximately 50% reduction in bacterial growth was noted when LB grown cells were treated with same dosage of NPs. After NPs exposure it was further analysed using Raman spectroscopy to get more insight.

Chapter 3 dealt with the structure and functional aspects of the purified EPS (KNPS). The KNPS was found to be an average molecular weight of $\sim 1.8 \times 10^5$ Da. Structural characterization of KNPS was carried out using sugar and methylation analysis, Smith degradation and 1D/2D NMR experiments. Sugar analysis showed that the KNPS composed of arabinose, galactose, 3-O-methyl-galctose and glucose in a molar ratio of nearly 4:3:1:1. The GC–MS analysis of partially methylated alditol acetates revealed the presence of 3,5-linked-arabinofuranosyl, 2,6-linked-galactopyranosyl, 6-linked-galactopyranosyl, 6-linked-glucopyranosyl, 2-linked-galactopyranosyl, 5-linked-arabinofuranosyl, 3-linked-arbinopyranosyl, terminal galactopyranosyl and arabinofuranosyl residues in a relative proportion of approximately 1:1:1:1:1:1:1:1:1. The ^{1}H NMR spectrum (500 MHz) of KNPS recorded in D_2O at 30 ºC showed the presence of eight signals in the anomeric region at δ 5.20 (**A**), 5.17 (**B**), 5.16 (**C** and **D**), 5.10 (**E**), 5.05 (**F**), 5.02 (**G**), 4.46 (**H**), and 4.42 (**I**) as evidenced from HSQC couplings. In ^{13}C NMR spectrum (125 MHz; Fig. 3d) at the same temperature, eight signals were observed in the anomeric region at δ 109.4, 106.8, 103.3, 102.7, 102.2, 101.5, 99.5, and 97.7. These eight anomeric carbon signals were correlated to

the anomeric proton signals of residue (**A**), (**B**), (**I**), (**H**), (**G**), (**F**), (**E**), (**C** and **D**), respectively as assigned from the HSQC spectrum. The residues **A** and **B** were assigned as (1→3,5)-α-L-Ara*f* and (1→5)-α-L-Ara*f* residues respectively. The α-configuration of both **A** and **B** residues were assigned from the chemical shift values of anomeric carbon and proton (δ 109.4/5.20 and δ 106.8/5.17) respectively. The downfield shift of C-3 (δ 81.8) and C-5 (δ 65.4) with respect to the standard methyl glycosides (Rinaudo & Vincendon, 1982; Agarwal, 1992; Mandal et al., 2011) indicated that the residue **A** was (1→3,5)-linked-α-L-arabinofuranose. The downfield shift of C-5 (δ 65.4) with respect to the standard methyl glycosides indicated that the residue **B** was (1→5)-linked α-L-arabinofuranosyl moiety. The linkage at C-5 of the both residues **A** and **B** were further confirmed from DEPT-135 spectrum. Hence, these observation confirmed that the residue **A** was (1→3,5)-α-L-Ara*f* and the residue **B** was (1→5)-α-L-Ara*f*. The proposed repeating unit of the KNPS has a backbone chain consisting of two(1→6)-galactopyranosyl residues, two (1→5)-arabinofuranosyl residues, one (1→6)-glucopyranosylresidue and one (1→3)-arabinopyranosyl residue, out of which one (1→6)-galactopyranosyl residue was branched at O-2 position with a (1→2)-linked-galactopyranosyl residue terminated with non reducing arabinofuranosyl residue and one (1→5)-arabinofuranosyl residue branched at O-3 position with nonreducing end 3-O-Me-galactopyranosyl residue. KNPS enhanced malondialdehyde (MDA), reactive oxygen species (ROS), and have the potential to alter the ratio of oxidized glutathione (GSSG) and reduced glutathione (GSH) levels in the cellular system.

Chapter 4 dealt with the biotechnological aspects of EPS. It was noted that the optimal dosages for flocculation of activated carbon suspension were 17 mg l^{-1} EPS and 4 mM $CaCl_2$. However, higher or lower EPS dosages cause reduction in flocculating rate(s). When the dosage of EPS was inadequate, the effective bridging phenomenon gets hindered causing reduction in flocculation. This relationship between EPS dosage and flocculating rate was

similar to earlier authors (Suh et al., 1997; Zheng et al., 2008). In the absence of Ca^{2+} ion no effective flocculation was observed at pH 7 which dictates the requirements of $CaCl_2$ for effective flocculation by forming Ca^{2+} mediated complexes of the EPS and activated carbon (Kurane et al., 1986). The presence of C=O group as revealed in FT-IR may play an important role in flocculation and can serve as binding sites for divalent cations. Results showed that the divalent cations like Mn^{2+}, Co^{2+}, Ca^{2+}, Zn^{2+}, Cd^{2+}, Cu^{2+}, and Ni^{2+} were better than other tested cations. The flocculating rate in presence of Fe^{3+} was 53% lesser than that of Ca^{2+} induced flocculation. Monovalent cations like K^+ and Na^+ are less effective for flocculation due to weaker electrostatic force of attraction between monovalent cations and EPS (Li et al., 2008). EPS produced by *C. daeguense* W6 in nutrient poor medium have shown flocculating rates above 90% in the temperature range of 0-45 °C with maximum of 97% at 15 °C (Liu et al., 2010). Maximum flocculation of 98% was observed by EPS produced by PB12 in both 10 °C and 20 °C. When temperature was increased to 100 °C, a decrease of approximately 26% from the maximum flocculation rate was observed; such decrease (26%) at 100 °C from the maximum value was observed with EPS produced by *Bacillus mojavensis* 32A (Elkady et al., 2011). Decrease in flocculating rate at higher temperature (above 60 °C) could be explained by simultaneously rise in kinetic energy of activated carbon particles due to heating effect. The EPS produced by the oligotrophic bacterium PB12 could be an effective replacement of a commercial polymer with regard to flocculation. The high flocculation rate of PB12-EPS over a wide range of temperature (10 °C-50 °C) and pH (3-10) possess a promise for application in water treatment and other biotechnological applications including metal processing industries. Moreover, the physiological and structural studies conducted in this thesis may help to put on more insights on the survival strategy of oligotrophic bacteria under nutrient deprived conditions along with the mechanisms of septic shock and KNPS-induced immunosuppression and autoimmunity.

Bibliography

Abdel-Akher M, Smith F (1950) Use of lithium aluminium hydride in the study of carbohydrates. Nature 166: 1037-1038.

Adak S, Aulak K, Stuehr D (2002) Direct Evidence for Nitric Oxide Production by a Nitric-oxide Synthase-like Protein from *Bacillus subtilis*. J Biol Chem 277: 16167-16171.

Adamson AW (1990) Physical chemistry of surfaces, 5th ed, New York, Wiley.

Agarwal PK (1992) NMR spectroscopy in the structural elucidation of oligosaccharides and glycosides. Phytochemistry 31: 3307-3330.

Akagi Y, Taga N, Simidu U (1977) Isolation and distribution of oligotrophic marine bacteria. Can J Microbiol 23: 981-987.

Altschul SF, Gish W, Miller W, Myers EW, Lipman DJ (1990) Basic local alignment search tool. J Mol Biol 215:403-410.

Amarger N (2001) Rhizobia in the field. Adv Agron 73: 109-168.

American Public Health Association: Standard methods for examination of water and waste water, 17th ed. American Public Health Association, Washington, DC (1989).

Andrews JH, Harris RF (1986) r- and K-selection and microbial ecology. Adv Microb Ecol 9: 99-147.

Arcon I, Piccolo O, Paganelli S, Baldi F (2012) XAS analysis of a nanostructured iron

polysaccharide produced anaerobically by a strain of *Klebsiella oxytoca*. Biometals 25: 875-881.

Ashtaputre AA, Shah AK (1995) Emulsifying property of a viscous exopolysaccharide from *Sphingomonas paucimobilis*. World J Microbiol Biotechnol 11: 219-222.

Azam F, Malfatti F (2007) Microbial structuring of marine ecosystems. Nat Rev Microbiol 5: 782–791.

Bailey JE, Fazel-Madjlessi J. McQuitty DN, Lee LY, Allred JC, Oro JA (1977) Characterization of bacterial growth by means of flow microfluorometry. Science 198: 1175-1176.

Baldi F, Marchetto D, Battistel D, Daniele S, Faleri C, De Castro C, Lanzetta R (2009) Iron-binding characterization and polysaccharide production by *Klebsiella oxytoca* strain isolated from mine acid drainage. J Appl Microbiol 107: 1241-1250.

Baldrian P, Gabriel J (2003) Adsorption of heavy metals to microbial biomass. In: Sasek V and Glaser J (eds.), The Utilisation of bioremediation to reduce soil contamination: Problems and Solutions. Kluwer Academic Publishers, the Netherlands, pp. 115-125.

Bales PM, Renke EM. May SL, Shen Y, Nelson DC (2013) Purification and Characterization of Biofilm-Associated EPS Exopolysaccharides from ESKAPE Organisms and Other Pathogens. *PLoS ONE* 8: e67950.

Banat IM, Makkar IM, Cameotra SS (2000) Potential commercial applications of microbial surfactants. Appl Microbiol Biotechnol 53: 495-508.

Barzegar A, Moosavi-Movahedi AA (2011) Intracellular ROS Protection Efficiency and Free Radical-Scavenging Activity of Curcumin. PLoS ONE 6: e26012.

Battistoni A, Folcarelli S, Gabbianelli R, Capo C, Rotilio G (1996) The Cu,Zn superoxide dismutase from *Escherichia coli* retains monomeric structure at high protein concentration. Evidence for altered subunit interaction in all the bacteriocupreins. Biochem J 320: 713-716.

BeMiller JN (1967) Acid-catalyzed hydrolysis of glycosides. Adv Carbohydr Chem Biochem 22: 25-108.

Benov LT, Fridovich IJ (1994) Escherichia coli expresses a copper- and zinc-containing superoxide dismutase. Biol Chem 269: 25310-25314.

Berlett BS, Stadtman ER (1997) Protein oxidation in aging, disease and oxidative stress. J Biol Chem 272: 20313-20316.

Beveridge TJ, Graham LL (1991) Surface layers of bacteria. Microbiol Mol Biol Rev 55: 684-705.

Bjorndal H, Lindbergh B, Svensson S (1967) Gas-liquid chromatography of partially methylated alditols as their acetates. Acta Chem Scand 21: 1801-1804.

Bock K, Pedersen C (1974) A study of ^{13}CH coupling constants in hexopyranoses. J Chem Soc Perkin Trans 2: 293-297.

Bock K, Thøgersen H (1982) Nuclear Magnetic Resonance Spectroscopy in the Study of Mono- and Oligosaccharides. Ann Rep NMR Spectrosc 13: 1-57.

Bohn JA, BeMiller JN (1995) (1→3)-β-D-Glucans as biological response modifiers: A review of structure–functional activity relationships. Carbohyd Polym 28: 3–14.

Boonaert CJP, Dufrene YF, Derclaye SR, Rouxhet PG **(**2001) Adhesion of *Lactococcus lactis* to model substrata: direct study of the interface. Colloids Surf B: Biointerfaces 22: 171-182.

Bradford MM (1976) A rapid and sensitive method for the quantification of microgram quantities of protein utilizing the principle of protein-dye biding. Anal Biochem 72: 248-254.

Bramhachari PV, Dubey SK (2006) Isolation and characterization of exopolysaccharide produced by *Vibrio harveyi* strain VB23. Lett Appl Microbiol 43: 571-577.

Branda SS, Chu F, Kearns DB, Losick R, Kolter R (2006) A major protein component of the *Bacillus subtilis* biofilm matrix. Mol Microbiol 59: 1229-1238.

Branda SS, Vik A, Friedman L, Kolter R (2005) Biofilms: the matrix revisited. Trends Microbiol 13: 20-26.

Briandet R, Leriche V, Carpenter B, Bellonfontaine MN **(**1999). Effects of the growth procedure on the surface hydrophobicity of *Listeria monocytogenes* cells and their adhesion to stainless steel. J Food Prot 9: 994-998.

Brisse S, Passet V, Grimont PA (2014) Description of *Klebsiella quasipneumoniae* sp. nov., isolated from human infections, with two subspecies, *Klebsiella quasipneumoniae* subsp. *quasipneumoniae* subsp. nov. and *Klebsiella quasipneumoniae* subsp. *similipneumoniae* subsp. nov., and demonstration that *Klebsiella singaporensis* is a junior heterotypic synonym of *Klebsiella variicola*. Int J Syst Bacteriol 64: 3146-3152.

Brisse S, van Himbergen T, Kusters K, Verhoef J (2004) Development of a rapid identification method for *Klebsiella pneumoniae* phylogenetic groups and analysis of 420 clinical isolates. Clin Microbiol Infect 10: 942-945.

Brisse S, Verhoef J (2001) Phylogenetic diversity of *Klebsiella pneumoniae* and *Klebsiella oxytoca* clinical isolates revealed by randomly amplified polymorphic DNA, gyrA and parC genes sequencing and automated ribotyping. Int J Syst Evol Microbiol 51: 915-924.

Brown MJ, Lester JN (1980) Comparison of bacterial extracellular polymer extraction methods. Appl Environ Microbiol 40:179-185.

Bruus JH, Nielsen PH, Keiding K (1992) On the stability of activated sludge flocs with implications to dewatering. Water Res 26: 1597-1604.

Buddelmeijer N, Beckwith J (2002) Assembly of cell division proteins at the *E. coli* cell center. Curr Opin Microbiol 5: 553-557.

Button DK, Robertson BR (2000) Effect of nutrient kinetics and cytoarchitecture on bacterioplankter size. Limnol Oceanogr 45: 499-505.

Calleja GB (1984) Microbial Aggregation. Boca Raton, FL: CRC Press.

Calvo C, Manzanera M, Silva-Castro GA, Uad I, González-López J (2009) Application of bioemulsifiers in soil oil bioremediation processes. Future prospects Sci Total Environ 407: 3634-3640.

Campbell L, Nolla HA, Vaulot D (1994) Photosynthetic picoplankton community structure in the subtropical North Pacific Ocean. Limnol Oceanogr 34: 954-961.

Cano V, Moranta D, Llobet-Brossa E, Bengoechea JA, Garmendia J (2009) *Klebsiella pneumoniae* triggers a cytotoxic effect on airway epithelial cells. BMC Microbiol 9: 56.

Carlucci AF, Shimp SL (1976) Distribution, isolation, and culturable characteristics of low-nutrient marine bacteria. University of California Institute of Marine Resources, IMR report No. 76-7, pp. 827-875.

Carter JS, Bowden FJ, Bastian I, Myers GM, Sriprakash KS, Kemp DJ (1999) Phylogenetic evidence for reclassification of Calymmatobacterium granulomatis as *Klebsiella granulomatis* comb. nov. Int J Syst Bacteriol 49: 1695-1700.

Cegelski L, Pinkner JS, Hammer ND, Cusumano CK, Hung CS, Chorell E, Aberg V, Walker JN, Seed PC, Almqvist F, Chapman MR, Hultgren SJ (2009) Small-molecule inhibitors target *Escherichia coli* amyloid biogenesis and biofilm formation. Nat Chem Biol 5: 913-919.

Cerca N, Jefferson KK, Oliveira R, Pier GB, Azeredo J (2006) Comparative antibody-mediated phagocytosis of *Staphylococcus epidermidis* cells grown in a biofilm or in the planktonic state. Infect Immun 74: 4849-4855.

Chakraborty R, Kumar A, Bhowal SS, Mandal AK, Tiwary BK, Mukherjee S (2013) Diverse Gene Cassettes in Class 1 Integrons of Facultative Oligotrophic Bacteria of River Mahananda, West Bengal, India. PLoS ONE 8: e71753.

Chakraborti S, Mandal AK, Sarwar S, Singh P, Chakraborty R, Chakraborti P (2014) Bactericidal Effect of Polyethyleneimine Capped ZnO Nanoparticles on Multiple

Antibiotic Resistant Bacteria harboring Genes of High Pathogenicity Island. Colloid Surface B 121: 44-53.

Chakraborty SP, KarMahapatra SK, Sahu SK, Chattopadhyay S, Pramanik P, Roy S (2011) "Nitric oxide mediated *Staphylococcus aureus* pathogenesis and protective role of nanoconjugated vancomycin. Asian Pac J Trop Biomed 1: 102-109.

Chandra K, Ghosh K, Ojha AK, Islam SS (2009) Carbohyd Res 344: 2188-2194.

Characklis WG, Escher AR (1988) Microfouling in initial events. In: Thompson MF, Sarojini R, Nagabushanam R (ed.) Marine biodeterioration: advanced techniques applicable to the Indian Ocean. Oxford and IBH Publ, New Delhi, pp. 249-260

Chan JW, Winhold H, Corzett MH, Ulloa JM, Cosman M, Balhorn R, Huser T (2007) Monitoring dynamic protein expression in living *E. coli*. Bacterial cells by laser tweezers Raman spectroscopy. Cytometry Part A, pp. 468-474.

Chaplin MF, Kennedy JF (1986) Carbohydrate analysis: a practical approach. IRL Press, Washington DC.

Chattopadhyay S, Das SK, Ghosh T, Das S, Tripathy S, Mandal D, Das D, Pramanik P, Roy S (2013) Anticancer and immunostimulatory role of encapsulated tumor antigen containing cobalt oxide nanoparticles. J Biol Inorg Chem 18: 957‑973.

Cheng KK, Liu DH, Sun Y, Liu WB (2004) 1,3-Propanediol production by *Klebsiella pneumoniae* under different aeration strategies. Biotechnol Lett 26: 911-915.

Chien AC, Hill NS, Levin PA (2012) Cell size control in bacteria. Curr Biol 22: 340-349.

Cho BC, Azam F (1988) Major role of bacteria in biogeochemical fluxes in the oceans

interior. Nature 322: 441-443.

Chun J, Lee JH, Jung Y, Kim M, Kim S, Kim BK, Lim YW (2007) EzTaxon: a web-based tool for the identification of prokaryotes based on 16S ribosomal RNA gene sequences. Int J Syst Evol Microbiol 57: 2259-2261.

Ciucanu I, Kerek F (1984) A simple and rapid method for the permethylation of carbohydrates. Carbohyd Res 131: 209‑217.

Cole JJ, Findlay S, Pace ML (1988) Bacterial production in fresh and saltwater ecosystems: A cross-system overview. Mar Ecol Prog Ser 43: 1-10.

Cole JR, Wang Q, Fish JA, Chai B, McGarrell DM, Sun Y (2014) Ribosomal database project: data and tools for high throughput rRNA analysis. Nucleic Acids Res 42: 633-642.

Comte S, Guibaud G, Baudu M (2006) Relations between extraction protocols for activated sludge extracellular polymeric substances (EPS) and EPS complexation properties: part I. Comparison of the efficiency of eight EPS extraction methods. Enzyme Microb Technol 38: 237-245.

Corpe WA (1980) Microbial surface components involved in adsorption onto surfaces. In: Bitton G, Marshall KC (ed.) Adsorption of microorganisms to surfaces. John Wiley & Sons, Wiley Intersci Publ, New York, pp. 105-143.

Costerton JW (1984) Mechanisms of microbial adhesion to surfaces. Direct ultrastructural examination of adherent bacterial populations in natural and pathogenic ecosystems. In: Klug MJ, Reddy CA (ed.) Current Perspectives in

Microbial Ecology. Proc 3rd Int Symp Microbial Ecol, Michigan State University. pp. 115–123.

Costerton JW, Geesey GG, Cheng KJ (1978) How bacteria stick? Sci Am 238:86-95.

Costerton JW, Irvin RT, Cheng KJ (1981) The bacterial glycocalyx in nature and disease. Annu Rev Microbiol 35: 299-324.

Cooper DG, Goldenberg BG (1987) Surface active agents from two *Bacillus* species. Appl Environ Microbiol 53: 224-229.

Cooper WJ, Zika RG (1983) Photochemical Formation of Hydrogen Peroxide in Surface and Ground Waters Exposed to Sunlight. Science 220: 711-712.

Crompton MJ, Dunstan RH, Macdonald MM, Gottfries J, von Eiff C, Roberts TK (2014) Small Changes in Environmental Parameters Lead to Alterations in Antibiotic Resistance, Cell Morphology and Membrane Fatty Acid Composition in Staphylococcus lugdunensis. PLoS ONE 9: e92296.

Czaczyk K, Myszka K (2007) Biosynthesis of extracellular polymeric substances (EPS) and its role in microbial biofilm formation. Pol J Environm Stud 16: 799-806.

Das D, Maiti S, Maiti TK, Islam SS (2013) Carbohyd Polym 92: 1243-1248.

Datta C, Basu PS (1999) Production of extracellular polysaccharides by a *Rhizobium* species from root nodules of *Cajanus cajan*. Acta Biotechnol 19: 59-68.

Davey ME, O'Toole GO (2000) Microbial biofilms: from ecology to molecular genetics. Microbiol Mol Biol R 64: 847-867.

Decho AW (1990) Microbial exopolymer secretions in ocean environments: their role(s) in food webs and marine processes. Oceanogr Mar Biol Annu Rev 28: 73-153.

Decho AW (2000) Microbial biofilms in intertidal systems: an overview. Cont Shelf Res 20: 1257-1273.

Decho AW, Lopez GR (1993) Exopolymer microenvironments of microbial flora: multiple and interactive effects on trophic relationships. Limnol Oceanogr 38: 1633-1645.

Deming JW (1986) Ecological strategies of barophilic bacteria in the deep ocean. Microbiol Sci 3: 205-211.

Deng S, Yu G, Ting YP (2005) Production of a bioflocculant by *Aspergillus parasiticus* and its application in dye removal. Colloids Surf B Biointerfaces 44: 179-186.

De Philippis R, Sili C, Tassinato G, Vincenzini M & Materassi R (1991) Effects of growth conditions on exopolysaccharide production by *Cynospira capsulata*. Bioresource Technol 38: 101-104.

Dlamini AM, Peiris PS, Bavor JH, Kailasapathy K (2007) Characterization of the exopolysaccharide produced by a whey utilizing strain of Klebsiella oxytoca. Afr J Biotechnol 6: 2603-2611.

Donachie WD (1968) Relationship between cell size and time of initiation of DNA replication. Nature 219: 1077-1079.

Drancourt M, Bollet C, Carta A, Rousselier P (2001) Phylogenetic analyses of Klebsiella species delineate *Klebsiella* and *Raoultella* gen. nov., with description of *Raoultella ornithinolytica* comb. nov., *Raoultella terrigena* comb. nov. and *Raoultella planticola* comb. nov. Int J Syst Evol Microbiol 51: 925-932.

Ducklow HW, Mitchell R (1979) Composition of mucus released by coral reef coelenterates. Limnol Oceanogr 24: 706-714.

Dukan S, Nystrom T (1999) Oxidative stress defense and deterioration of growth-arrested *Escherichia coli* cells. J Biol Chem 274: 26027-26032.

Eguchi M, Nishikawa T, Macdonald K, Cavicchioli R, Gottschal JC, Kjelleberg S (1996) Responses to stress and nutrient availability by the marine ultramicrobacterium *Sphingomonas* sp. strain RB2256. Appl Environ Microbiol 62: 1287-1294.

Eilers H, Pernthaler J, Glockner FO, Amann R (2000) Culturability and *In situ* abundance of pelagic bacteria from the North Sea. Appl Environ Microbiol 66: 3044-3051.

Elkady MF, Farag S, Zaki S, Abu-Elreesh G, Abd-El-Haleem D (2011) *Bacillus mojavensis* strain 32A, a bioflocculant-producing bacterium isolated from an Egyptian salt production pond. Bioresour Technol 102: 8143-8151.

Falla J, Block JC (1993) Binding of Cd^{2+}, Ni^{2+}, Cu^{2+} and Zn^{2+} by isolated envelopes of *Pseudomonas fluorescens*. FEMS Microbiol Lett 108: 347-352.

Favero MS, Carson LA, Bond WW, Petersen NJ (1971) *Pseudomonas aeruginosa*: growth in distilled water from hospitals. Science 173: 836-838.

Ferguson RL, Buckley EN, Palumbo AV (1984) Response of marine bacterioplankton to differential filtration and confinement. Appl Environ Microbiol 47: 49-55.

Fevre C, Passet V, Weill FX, Grimont PA, Brisse S (2005) Variants of the *Klebsiella pneumoniae* OKP chromosomal beta-lactamase are divided into two main groups, OKP-A and OKPB. Antimicrob Agents Chemother 49: 5149-5152.

Flemming HC, Wingender J (2001) Relevance of microbial extracellular polymeric substances (EPSs)-Part I: Structural and ecological aspects. Water Sci Technol 43: 1-8.

Flemming HC, Wingender J (2010) The biofilm matrix. Nat Rev Microbiol 8: 623-633.

Fletcher M (1980) Adherence of marine microorganisms to smooth surfaces. In: Beachey EH (ed.) Bacterial Adherence. London: Chapman & Hall, pp. 347-373.

Forner L, Larsen T, Kilian M, Holmstrup P (2006) Incidence of bacteremia after chewing, tooth brushing and scaling in individuals with periodontal inflammation. J Clin Periodontol 33: 401-407.

Foster JW, Spector MP (1995) How *Salmonella* survive against the odds. Annu Rev Microbiol 49: 145-174.

Foxman B (2010) The epidemiology of urinary tract infection. Nat Rev Urol 7: 653-660.

Frank KL, Patel R (2007) Poly-N-Acetylglucosamine Is Not a Major Component of the Extracellular Matrix in Biofilms Formed by icaADBC-Positive *Staphylococcus lugdunensis* Isolates. Infect Immun 75: 4728-4742.

Freitas F, Alves VD, Pais J, Costa N, Oliveira C, Mafra L, Hilliou L, Oliveira R, Reis MA (2009) Characterization of an extracellular polysaccharide produced by a *Pseudomonas* strain grown on glycerol. Bioresour Technol 100: 859-865.

Freitas F, Alves VD, Reis MA (2011) Advances in bacterial exopolysaccharides: From production to biotechnological applications. Trends Biotechnol 29: 388-398.

Fridovich I (1998) The trail to superoxide dismutase. Protein Sci 7: 2688-2690.

Frolund B, Palmgren R, Keiding K, Nielsen PH **(**1996) Extraction of extracellular polymers from activated sludge using a cation exchange resin. Water Res 30: 1749-1758.

Fry JC (1990) Oligotrophs. In: Edwards C (ed.) Microbiology of extreme environments. *Open University Press*. Milton Keynes, pp. 93-116.

Fuhrman J (1981) Influence of method on the apparent size distribution of Bacterioplankton cells: Epifluoresence microscopy compared to scanning electron microscopy. Mar Ecol Prog Ser 5: 103-106.

Gallo G, Baldi F, Renzone G, Gallo M, Cordaro A, Scaloni A, Puglia AM. 2012. Adaptative biochemical pathways and regulatory networks in *Klebsiella oxytoca* BAS-10 producing a biotechnologically relevant exopolysaccharide during Fe(III)-citrate fermentation. Microb Cell Fact 11: 152.

Gant VA, Warnes G, Phillips I, Savidge GF (1993) The application of flow cytometry to the study of bacterial responses to antibiotics. J Med Microbiol 39: 147-154.

Gao J, Bao HY, Xin MX, Liu YX, Li Q, Zhang YF **(**2006) Characterization of a bioflocculant from a newly isolated *Vagococcus* sp. W31. J Zhejiang Univ Sci B 7: 186-192.

Garcia G, Humbert M, Capel F, Rimaniol AC, Escourrou P, Emilie D, Godot V (2007) Chemokine receptor expression on allergen-specific T cells in asthma and allergic bronchopulmonary aspergillosis. Allergy 62: 170-177.

Gauri SS, Mandal SM, Mondal KC, Dey S, Pati BR (2009) Enhanced production and partial characterization of an extracellular polysaccharide from newly isolated *Azotobacter* sp. SSB81. Bioresour Technol 100: 4240-4243.

Gavrilescu M (2004) Removal of heavy metals from the environment by biosorption. Eng Life Sci 4: 219-232.

Gerhardt P, Murray RGE, Costilow RN, Nester EW, Wood WA, Krieg NR, Phillips GB (1981) Manual of Methods for General Bacteriology. American Society for Microbiology, Washington D.C., WA, USA.

Gerwig GJ, Kamerling JP, Vliegenthart JFG (1978) Determination of the D and L configuration of neutral monosaccharides by high-resolution capillary g.l.c. Carbohyd Res 62: 349‑357.

Gilbert P, Das J, Foley I (1997) Biofilm susceptibility to antimicrobials. Adv Den Res 11: 160-167.

Giovannoni SJ, M. Rappé (2000) Evolution, diversity, and molecular ecology of marine prokaryotes. *In* D. L. Kirchman (ed.), Microbial ecology of the oceans. Wiley-Liss Inc., New York, pp. 47-84.

Gloaguen V, Morvan H, Hoffmann L (1995) Released and capsular polysaccharides of Oscillatoriaceae (Cyanophyceae, Cyanobacteria). Alg Studies 78: 53-69.

Gooch JW (2010) Encyclopedic Dictionary of Polymers, Volume 1,2nd Ed., New York; London, Springer, pp. 135.

Gong WX, Wang SG, Sun XF, Liu, XW, Yue QY, Gao BY (2008) Bioflocculant production by culture of *Serratia ficaria* and its application in wastewater treatment, Bioresour Technol 99: 4668-4674.

Govan JR, Deretic V (1996) Microbial pathogenesis in cystic fibrosis: Mucoid *Pseudomonas aeruginosa* and *Burkholderia cepacia*. Microbiol Rev 60: 539-574.

Greenberg JT, Monach P, Chou JH, Josephy PD, Demple B (1990) Positive control of a global antioxidant defense regulon activated by superoxide-generating agents in *Escherichia coli*. Proc Natl Acad Sci USA 87: 6181-6185.

Guetta O, Mazeau K, Auzely R, Milas M, Rinaudo M (2003) Structure and Properties of a Bacterial Polysaccharide Named Fucogel. Biomacromolecules 4: 1362-1371.

Gusarov I, Nudler E (2005) NO-mediated cytoprotection: instant adaptation to oxidative stress in bacteria. Proc Natl Acad Sci USA 102: 13855-13860.

Halliwell B, Gutteridge JM (1986) Oxygen free radicals and iron in relation to biology and medicine: some problems and concepts. Arch Biochem Biophys 246: 501-514.

Hattori T (1984) Physiology of soil oligotrophic bacteria. Microbiol Sci 1: 102-104.

Heissenberger A, Herndl GJ (1994) Formation of high molecular weight material by free-living marine bacteria. Mar Ecol Prog Ser 111: 129-135.

Hirsch P, Bernhard M, Cohen SS, Ensign JC, Jannasch HW, Koch AL, Marshall KC, Poindexter JS, Rittenberg SC, Smith DC, Veldkamp H (1979) Presented at the

Strategies of Microbial Life in Extreme Environments, Berlin.

Hoagland KD, Rosowski JR, Gretz MR, Roemer SC (1993) Diatom extracellular polymeric substances: Function, fine structure, chemistry and physiology. J Phycol 29: 537-566.

Horowitz A, Krichevsky MI, Atlas RM (1983) Characteristics and diversity of subarctic marine oligotrophic, stenoheterotrophic, and euryheterotrophic bacterial populations. Can J Microbiol 29: 527-535.

Hofman M, Pasieczna S, Wachowski L, Ryczkowski J **(**2006). Speciation of functional groups formed on the surface of carbonaceous materials modified by NO. J Phys IV France. 137: 287-290.

Hsieh PF, Lin TL, Yang FL, Wu MC, Pan YJ, Wu SH, Wang JT (2012) Lipopolysaccharide O1 antigen contributes to the virulence in *Klebsiella pneumoniae* causing pyogenic liver abscess. PLoS ONE 7: e33155.

Ishida Y, Eguchi M, Kadota H (1986) Existence of obligately oligotrophic bacteria as a dominant population in the South China Sea and the West Pacific Ocean. Mar Ecol Prog Ser 30: 197-203.

Ishida Y, Fukami K, Eguchi M, Yoshinaga I (1989) Strategies for growth of oligotrophic bacteria in the pelagic environment. In: Hattori T, Ishida **Y.** Maruyama Y. Morita RY, Uchida A (ed.) Recent advances in microbial ecology. Jap Scien Soc Press, Tokyo. pp. 89-93.

Ishida Y, Imai I, Miyagaki T, Kadota H (1982) Growth and uptake kinetics of a facultatively oligotrophic bacterium at low nutrient concentrations. Microb Ecol 8: 23-32.

Ishida Y, Kadota H (1981) Growth patterns and substrate requirements of naturally occurring obligate oligotrophs. Microb Ecol 7: 123-130.

Ishida Y, Shibahara K, Uchida H, Kadota H (1980) Distribution of obligately oligotrophic bacteria in Lake Biwa. Bull Jap Soc scient Fish 46: 1151-1158.

Jaeggi NE, Schmidt-Lorenz W (1990) Bacterial regrowth in drinking water. Bacterial flora in fresh and stagnant water in drinking water purification and in the drinking water distribution system. Zentralbl Hyg Umweltmed 190: 217-235.

Jenkins DE, Schultz JE, Matin A (1988) Starvation-induced cross protection against heat or H_2O_2 challenge in *Escherichia coli*. J Bacteriol 170: 3910-3914.

Jiang P, Li J, Han F, Duan G, Lu X, Gu Y, Yu W (2011) Antibiofilm activity of an exopolysaccharide from marine bacterium *Vibrio* sp. QY101. PLoS One. 6:e18514.

Jørgensen F, Nybroe O, Knøchel S (1994) Effects of starvation and osmotic stress on viability and heat resistance of *Pseudomonas fluorescens* AH9 77: 340-347.

Joux F, Jeffrey WH, Lebaron P, Mitchell DL (1999) Marine bacterial isolates display diverse responses to UV-B radiation. Appl Environ Microbiol 65: 3820-3827.

Justice SS, Hunstad DA, Cegelski L, Hultgren SJ (2008) Morphological plasticity as a bacterial survival strategy. Nat Rev Microbiol 6: 162-168.

Kalsi PS (2004) Spectroscopy of Organic compounds, New Age International Publishers, New Delhi, 6th Edition.

Kanehisa M, Goto S, Hattori M, Aoki-Kinoshita KF, Itoh M, Kawashima S, Katayama T, Araki M, Hirakawa M (2006) From genomics to chemical genomics: New developments in KEGG. Nucleic Acids Res 34: 354-357.

Kaplan N, Rosenberg E (1982) Exopolysaccharide distribution and bioemulsifier production in *Acinetobacter calcoaceticus* BD4 and BD413. Appl Environ Microbiol 44: 1335-1341.

Kimura M (1980) A simple method for estimating evolutionary rates of base substitutions through comparative studies of nucleotide sequences. J Mol Evol 16: 111-120.

Kroll JS, Langford PR, Wilks KE, Keil AD (1995) Bacterial Cu,Zn-superoxide dismutase, phylogenetically distinct from the eukaryotic enzyme, are not so rare after all! Microbiology 141: 2271-2279.

Kumar A, Chakraborti S, Joshi P, Chakrabarti P, Chakraborty R (2011) A multiple antibiotic and serum resistant oligotrophic strain, *Klebsiella pneumoniae* MB45 having novel dfrA30, is sensitive to ZnO QDs. Ann Clin Microbiol Antimicrob 10: 19.

Kumar A, Mukherjee S, Chakraborty R (2010) Characterization of a novel trimethoprim resistance gene, dfrA28, in class 1 integron of an oligotrophic *Acinetobacter johnsonii* strain, MB52, isolated from River Mahananda, India. Microb Drug Resist 16: 29-37.

Kumar CG, Joo HS, Kavali R, Choi JW, Chang CS (2004) Characterization of an extracellular biopolymer flocculant from a haloalkalophilic *Bacillus* isolate. World J Microbiol Biotechnol 20: 837-843.

Kuramitsu HK, Wang BY (2011) The whole is greater than the sum of its parts: Dental plaque bacterial interactions can affect the virulence properties of cariogenic *Streptococcus* mutans. Am J Dent 24: 153-154.

Kurane R, Hatamochi K, Kiyohara T, Hirao M, Taniguchi Y (1994) Production of a bioflocculant by *Rhodococcus erythropolis* S-1 grown on alcohols. Biosci Biotechnol Biochem 58: 428-429.

Kurane R, Toeda K, Takeda K, Suzuki T (1986) Culture Conditions for Production of Microbial Flocculant by *Rhodococcus erythropolis*. Agric Biol Chem 50: 2309-2313.

Kuznetsov SI, Dubinia GA. Lapteva NA (1979) Biology of oligotrophic bacteria. Annu Rev Microbiol 33: 377-387.

Lango Z **(**1988) Ring-forming, oligotrophic Microcyclus organisms in the water and mud of Lake Balaton. Acta Microbiol 35: 277-282.

Leahy JG, Colwell RR (1990) Microbial degradation of hydrocarbons in the environment Microbiol Rev 54: 305-315.

Lee JW, Yeomans WG, Allen AL, Deng F, Gross RA, Kaplan DL (1999) Biosynthesis of novel exopolymers by *Aureobasidium pullulans*. Appl Environ Microbiol 65: 5265-5271.

Lee SH, Lee SO, Jang KL, Lee TH (1995) Microbial flocculant from *Arcuadendron* sp. TS-49. Biotechnol Lett 17: 95–100.

Liochev SI, Fridovich I (1994) The role of O_2^- in the production of HO.: In *vitro* and *in vivo*. Free Radic Biol Med 16: 29-33.

Liu H, Fang HHP (2002) Extraction of extracellular polymeric substances (EPS) of sludges. J Biotechnol 95: 249-256.

Liu W, Wang K, Li B, Yuan H, Yang J (2010) Production and characterization of an intracellular bioflocculant by *Chryseobacterium daeguense* W6 cultured in low nutrition medium. Bioresour Technol 101: 1044-1048.

Li WW, Zhou WZ, Zhang YZ, Wang J, Zhu XB (2008) Flocculation behavior and mechanism of an exopolysaccharide from the deep-sea psychrophilic bacterium *Pseudoalteromonas* sp. SM9913. Bioresour Technol 99: 6893-6899.

Li X, Zhang D, Chen F, Ma J, Dong Y, Zhang L (2004) *Klebsiella singaporensis* sp. nov., a novel isomaltulose-producing bacterium. Int J Syst Evol Microbiol 54: 2131-2136.

Lory S (1992) Determinants of extracellular protein secretion in Gram-negative bacteria. J Bacteriol 174: 3423-3428.

Lowry OH, Rosebrough NJ, Farr AL, Randall RJ (1951) Protein measurement with the Folin phenol reagent. J Biol Chem 193: 265-275.

Luck H. Catalase (1963). In: Bergmeyer HW, editor. Methods of Enzymatic Analysis. Section 3. New York, NY, USA: Academic Press, pp. 885–894.

Mahapatra SK, Chakraborty SP, Majumdar S, Bag BG, Roy S (2009) Eugenol protects nicotine-induced superoxide mediated oxidative damage in murine peritoneal macrophages in vitro. Eur J Pharmacol, 623: 132–140.

Makkar RS, Cameotra SS (1998) Production of biosurfactant at mesophilic and thermophilic conditions by a strain of *Bacillus subtillis*. J Ind Microbiol Biotechnol 20: 48-52.

Mallory LM, Austin B, Colwell RR (1977) Numerical taxonomy and ecology of oligotrophic bacteria isolated from the estuarine environments. Can J Microbiol 23: 733-750.

Maier RM, Pepper IL, Gerba CP (2009) Remediation of organic and metal pollutants. Environ Microbial 2nd Ed., Academic press, pp. 430.

Maity P, Nandi AK, Sen IK, Pattanayak M, Chattopadhyay S, Dash SK, Roy S, Acharya K, Islam SS (2014) Heteroglycan of an edible mushroom *Entoloma lividoalbum*: Structural characterization and study of its protective role for human lymphocytes Carbohyd Polym 114: 157-164.

Mandal S, Patra S, Dey B, Bhunia SK, Maity KK, Islam SS (2011) Structural analysis of an arabinan isolated from alkaline extract of the endosperm of seeds of *Caesalpinia bonduc* (Nata Karanja) Carbohyd Polym 84: 471-476.

Maness NO, Ryan JD, Mort AJ (1990) Determination of the degree of methyl esterification of pectins in small samples by selective reduction of esterified galacturonic acid to galactose. Anal Biochem 185: 346-352.

Marklund S, Marklund G (1974) Involvement of the superoxide anion radical in the autoxidation of pyrogallol and a convenient assay for superoxide dismutase. Eur J Biochem 47: 469-474.

Matear RJ, Hirst AC (1999) Climate change feedback on the future oceanic CO_2 uptake. Tellus 51: 722-733.

McMahon MAS, Xu J, Moore JE, Blair IS, McDowell DA (2006) Environmental Stress and Antibiotic Resistance in Food-Related Pathogens. Appl Environ Microbiol 73: 211-217.

McKinney RE (1952) A fundamental approach to the activated sludge process. Sweage Ind Wastes 24: 280-287.

Meberg BM, Paulson AL, Priyadarshini R, Young KD (2004) Endopeptidase penicillin-binding proteins 4 and 7 play auxiliary roles in determining uniform morphology of *Escherichia coli.* J. Bacteriol 186: 8326-8336.

Mejare M, Bulow L (2001) Metal-binding proteins and peptides in bioremediation and phytoremediation of heavy metals. Trend Biotechnol 19: 67-73.

Miller C, Thomsen LE, Gaggero C, Mosseri R, Ingmer H, Cohen SN (2004) SOS response induction by beta-lactams and bacterial defense against antibiotic lethality. Science 305: 1629-1631.

Mishra A, Kavita K, B Jha (2011) Characterization of extracellular polymeric substance produced by micro-algae *Dunaliella salina*. Carbohyd Polym 82: 852-857.

Miyata M, Ogaki H (2006) Cytoskeleton of mollicutes. J Mol Microbiol Biotechnol 11: 256-64.

Moaledj K (1978) Qualitative analysis of an oligocarbophilic aquatic microflora in the Pluβsee. Arch Hydrobiol 82: 98-113.

Monds RD, O'Toole GA (2009) The developmental model of microbial biofilms: Ten years of a paradigm up for review. Trends Microbiol 17: 73-87.

Mopper K, Lindroth P (1982) Diel and depth variations in dissolved free amino acids and ammonium in the Baltic Sea determined by shipboard HPLC analysis. Limnol Oceanogr 27: 336-347.

Morita RY (1997) Bacteria in Oligotrophic Environments, Starvation-Survival Lifestyle. Chapman & Hall, New York.

Munster U (1993) Concentrations and fluxes of organic carbon substrates in the aquatic environment. Ant Leeuwenhoek 63: 243-274.

National Institutes of Health (2002) Research on Microbial Biofilms (PA-03-047). National Institutes of Health.

Navon-Venezia S, Zosim Z, Gottlieb A, Legmann R, Carmeli S, Ron EZ, Rosenberg E (1995) Alasan, a new bioemulsifier from *Acinetobacter radioresistens*. Appl Environ Microbiol 61: 3240-3244.

Ohkawa H, Ohishi N, Yagi K (1979) Assay for lipid peroxides in animal tissues by thiobarbituric acid reaction. Anal Biochem 95: 351-358.

O'Melia CR (1972) Coagulation and flocculation. In Physicochemical Processes for Water Quality Control. Ed. W J Weber jr. Wiley Interscience, New York, pp. 61-109.

Ostling J, Holmquist L, Fllrdh K, Svenblad B, Jouper-Jaan A, Kjelleberg S (1993) Starvation and recovery of *Vibrio*. In Starvation in Bacteria, Edited by S. Kjelleberg. New York: Plenum Press, pp. 103-127.

O'Toole G, Kaplan HB, Kolter R (2000) Biofilm formation as microbial development. Annu Rev Microbiol 54: 49-79.

Ouverney CC, Fuhrman JA (1999) Combined Microautoradiography-16S rRNA probe technique for determination of radioisotope uptake by specific microbial cell types *in situ*. Appl Environ Microbiol 65: 1746-1752.

Pahm MA, Alexander M (1993) Selecting inocula for the biodegradation of organic compounds at low concentrations. Microb Ecol 25: 275-286.

Partensky F, Hess WR, Vaulot D (1999) *Prochlorococcus*, amarine photosynthetic prokaryote of global significance. Microbiol Mol Biol Rev 63: 106-127.

Pernthaler J (2005) Predation on prokaryotes in the water column and its ecological implications Nat Rev Microbiol 3: 537-546.

Peterson GL (1979) Review of folin phenol quantitation method of lowry, Rosenborough, Farr and Randall. Anal Biochem 100: 201-220.

Podschun R, Ullmann U (1998) *Klebsiella* spp. as Nosocomial Pathogens: Epidemiology, Taxonomy, Typing Methods, and Pathogenicity Factors. Clin Microbiol Rev 11: 589-603.

Poindexter JS (1979) Presented at the Strategies of Microbial Life in Extreme Environments, Berlin.

Poindexter JS (1981) Oligotrophy Fast and famine existence. Adv Microb Ecol 5: 63-89.

Popper ZA, Sadler IH, Fry SC (2001**)** 3-*O*-Methyl-D-galactose residues in lycophyte primary cell walls. Phytochemistry 57: 711-719.

Qin Z, Ou Y, Yang L, Zhu Y, Tolker-Nielsen T, Molin S, Qu D (2007) Role of autolysin-mediated DNA release in biofilm formation of *Staphylococcus epidermidis*. Microbiology 153: 2083-2092.

Ramírez-Castillo ML, Uribelarrea JL (2004) Improved process for exopolysaccharide production by Klebsiella pneumoniae sp. pneumoniae by a fed-batch strategy. Biotechnol Lett 26: 1301-1306.

Rashid T, Ebringer A (2007) "Ankylosing spondylitis is linked to *Klebsiella*-the evidence". Clin Rheumatol 26: 858-864.

Rättö M, Mustranta A, Siika-aho M (2001) Strains degrading polysaccharides produced by bacteria from paper machines. Appl Microbiol Biotechnol 57: 182-185.

Rendueles O, Kaplan J.B, Ghigo JM (2012) Antibiofilm polysaccharides. Environ Microbiol 15: 334-346.

Rinaudo M, Vincendon M (1982) ^{13}C NMR structural investigation of scleroglucan. Carbohyd Polym 2: 135-144.

Ron EZ, Rosenberg E (2001) Natural roles of biosurfactants. Environ Microbiol 3: 229-236.

Rosenberg E, Ron EZ (1998) Surface active polymers from the genus *Acinetobacter*. In: Kaplan DL (ed.), Biopolymers from Renewable Resources. Springer-Verlag. Berlin, pp. 281-291.

Rosenberg E, Zuckerberg A, Rubinovitz C, Gutnick DL (2002) Emulsifier of *Arthrobacter* RAG-1: isolation and emulsifying properties. Appl Environ Microbiol 37: 402-408.

Ryan KJ, Ray CG (ed.) (2004) Sherris Medical Microbiology (4th ed.). McGraw Hill. ISBN 0-8385-8529-9.

Ryder C, Byrd M, Wozniak DJ (2007) Role of polysaccharides in *Pseudomonas aeruginosa* biofilm development. Curr Opin Microbiol 10: 644-648.

Salehizadeh H, Shojaosadati SA (2003) Removal of metal ions from aqueous solution by polysaccharide produced from *Bacillus firmus*. Water Res 37: 4231-4235.

Sambrook J, Fritsch EF, Maniatis T (1989) Molecular cloning: a laboratory manual. 2nd ed. Cold Spring Harbor, N.Y: Cold Spring Harbor Laboratory Press.

Sanin SL, Sanin FD, Bryers JD (2003) Effect of starvation on the adhesive properties of xenobiotic degrading bacteria. Process Biochem. 38: 909-914.

Sauer K, Cullen MC, Rickard AH, Zeef LA, Davies DG, Gilbert P (2004) Characterization of nutrient-induced dispersion in *Pseudomonas aeruginosa* PAO1 biofilm. J Bacteriol 186: 7312-7326.

Saxena QB, Mezey E, Adler WH (1980) Regulation of natural killer activity in vivo. II. The effect of alcohol consumption on human peripheral blood natural killer activity. Int J Cancer 26: 413-417.

Schaechter M, Maaløe O, Kjeldgaard NO (1958) Dependency on medium and temperature of cell size and chemical composition during balanced grown of *Salmonella* typhimurium. J Gen Microbiol 19: 592-606.

Schut F, DeVries E, Gottschal JC, Robertson BR, Harder W, Prins RA, Button DK (1993) Isolation of typical marine bacteria by dilution culture: growth, maintenance, and characteristics of isolates under laboratory conditions. Appl Environ Microbiol 59: 2150-2160.

Schut F, Gottschal JC, Prins RA (1997b) Isolation and characterisation of the marine ultramicrobacterium *Sphingomonas* sp strain RB2256. FEMS Microbiol Rev 20: 363-369.

Schut F, Prins RA, Gottschal JC (1997a) Oligotrophy and pelagic marine bacteria: facts and fiction. Aquat Microb Ecol 12: 177-202.

Semenov AM (1991) Physiological bases of oligotrophy of microorganisms and the concept of microbial community. Microb Ecol 22: 239-247.

Sen IK, Mandal AK, Chakraborty R, Behera B, Yadav KK, Maiti TK, Islam SS (2014) Structural and immunological studies of an exopolysaccharide from *Acinetobacter junii* BB1A. Carbohyd Polym 101: 188-195.

Seshasayee AS, Bertone P, Fraser GM, Luscombe NM (2006) Transcriptional regulatory networks in bacteria: From input signals to output responses. Curr Opin Microbiol 9: 511-519.

Shimizu K (2014) Regulation Systems of Bacteria such as *Escherichia coli* in Response to Nutrient Limitation and Environmental Stresses. Metabolites 4: 1-35.

Shih IL, Van YT, Yeh LC, Lin HG, Chang YN (2001) Production of a biopolymer flocculant from *Bacillus licheniformis* and its flocculating properties. Bioresour Technol 78: 267-272.

Shu CH, Lung MY **(**2004) Effect of ph on the production and molecular weight distribution of exopolysacharide by *Antrodia camphorate* in batch cultures. Process Biochem. 39: 931-937.

Sleytr UB (1997) Basic and applied S-layer research: an overview. FEMS Microbiol Rev 20: 5-12.

Smith BC (2011) Fundamentals of Fourier Transform Infrared Spectroscopy, Taylor and Francis–CRC Press, 2nd ed., pp 211.

Sobeck DC, Higgins MJ (2002) Examination of three theories for mechanisms of cation-induced bioflocculation. Water Res 36: 527-538.

Sodhi RNS **(**1996) Application of surface analytical and modification techniques to biomaterial research. J Electron Spectrosc Relat Phenom 81: 269-284.

Southgate DAT (1976) Determination of Food Carbohydrates, Essex, England, Applied Science Publishers Ltd, pp. 75-84.

Souza AM, Sutherland IW (1994) Exopolysaccharide and storage polymer production in *Enterobacter aerogenes* type 8 strains. J Appl Bacteriol 76: 463-468.

Stoderegger KE, Herndl GJ (1999) Production of exopolymer particles by marine bacterioplankton under contrasting turbulent conditions. Mar Ecol Prog Ser 189: 9-16.

Storz G, Imlay JA (1999) Oxidative stress. Curr Opin Microbiol 2: 188-94.

St-Pierre F, Endy D (2008) Determination of cell fate selection during phage lambda infection. Proc Natl Acad Sci USA 10: 20705-20710.

Straus DC, Atkisson DL, Garner CW (1985) Importance of a lipopolysaccharide-containing extracellular toxic complex in infections produced by *Klebsiella pneumoniae*. Infect Immun 50: 787-795.

Stredansky M, Conti E (1999) Xanthan production by solid state fermentation. Process Biochem. 34: 581-587St-Pierre F, Endy D (2008) Determination of cell fate selection during phage lambda infection. Proc Natl Acad Sci USA 105: 20705-20710.

Strehl B., Holtzendorff J, Partensky F, Hess WR (1999) A small and compact genome in the marine cyanobacterium *Prochlorococcus marinus* CCMP 1375: lack of an intron in the gene for tRNA (Leu) (UAA) and a single copy of the rRNA operon. FEMS Microbiol Lett 181: 261-266.

Suh HH, Kwon GS, Lee CH, Kim HS, Oh HM, Yoon BD (1997) Characterization of bioflocculant produced by *Bacillus* sp. DP-152. J Ferment Bioeng 84: 108-112.

Sutherland IW (1990a) Biotechnology of Microbial Exopolysaccharides; Cambridge University Press: New York, NY, USA.

Sutherland IW **(**1990b) Physiology and industrial production. In: Sutherland, I.W. (ed.), Biotechnology of microbial exopolysaccharides. Cambridge University Press, Cambridge, England, pp. 70-88.

Sutherland IW (2001) Microbial polysaccharides from gram-negative bacteria. Int Dairy J 11: 663-674.

Sutherland IW (2005) Polysaccharides from microorganisms, plants and animals. Biopolymers Online. doi: 10.1002/3527600035.bpo15001. Online ISBN: 9783527600038.

Sutherland IW, Vandamme EJ, De Baets S, Steinbüchel A (ed.) (2002) Polysaccharides from Prokaryotes. In Biopolymers: Polysaccharides I; Wiley-VCH: Weinheim, Germany, pp. 1-19.

Sweet DP, Shapiro R, Albersheim P (1975) Quantitative analysis by various GLC response-factor theories for partially methylated and partially ethylated alditol acetates. Carbohyd Res 40: 217–225.

Tada Y, Ihmori M, Yamaguchi Y (1995) Oligotrophic bacteria isolated from clinical materials. J Clin Microbiol 33: 493.

Takeda M, Koizumi J, Matsuoka H, Hikuma M (1992) Factors affecting the activity of a protein bioflocculant produced by *Nocardia amarae*. J Ferment Bioeng 47: 408-409.

Takeda M, Nakano F, Nagase T, Iohara K, Koizumi J (1998) Isolation and chemical composition of the sheath of *Sphaerotilus natans*. Biosci Biotechnol Biochem 62: 1138-1143.

Tezuka Y (1969) Cation dependent flocculation in a *Flavobacterium* species predominant in activated sludge. Appl Micrbiol 17: 222-226.

Thompson JD, Gibson TJ, Plewniak F, Jeanmougin F, Higgins DG (1997) The CLUSTAL_X Windows interface: flexible strategies for multiple sequence alignment aided by quality analysis tool. Nucleic Acids Res 25: 4876-4882.

Underwood GJC, Smith, DJ (1998). In situ measurements of exopolymer production by intertidal epipelic diatom-dominated biofilms in the Humber estuary. In: Black KS, Paterson DM, Cramp A (ed.) Sedimentary Processes in the Intertidal Zone. Geological Society, London, pp. 125-134.

Underwood GJC, Paterson, DM, Parkes RJ (1995) The measurement of microbialcarbohydrate exopolymers from intertidal sediments. Limnol Oceanogr 40: 1243-1253.

Van de Peer Y, Wachter De R (1997) Construction of evolutionary distance trees with TREECON for Windows: accounting for variation in nucleotide substitution rate among sites. Comput Appl Biosci 13: 227-230.

Van Gemerden H, Kuenen GJ (1984) Strategies for growth and evolution of microorganisms in oligotrophic habitats. In: Hobbie JEleB, Williams PJ (ed.) Heterotrophic activity in the sea. Plenum Press, New York, pp. 25-44.

Vats P, Yu J, Rothfield L (2009) The dynamic nature of the bacterial cytoskeleton. Cell Mol Life Sci 66: 3353-3362.

Velicer GJ, Lenski RE (1999) Evolutionary trade-offs under conditions of resource abundance and scarcity: experiments with bacteria. Ecology 80: 1168-1179.

Venditti M, Biavasco F, Varaldo PE, Macchiarelli A, De Biase L, Marino B, Serra P (1993) Catheter-related endocarditis due to glycopeptide-resistant *Enterococcus faecalis* in a transplanted heart. Clin Infect Dis 17: 524-525.

Vichai V, Kirtikara K (2006) Sulforhodamine B colorimetric assay for cytotoxicity screening. Nat Protoc 1: 1112-1116.

Vuong C, Voyich JM, Fischer ER, Braughton KR, Whitney AR, DeLeo FR, Otto M (2004) Polysaccharide intercellular adhesin (PIA) protects *Staphylococcus epidermidis* against major components of the human innate immune system. Cell Microbiol 6: 269-275.

Walters MC 3rd, Roe F, Bugnicourt A, Franklin MJ, Stewart PS (2003) Contributions of antibiotic penetration, oxygen limitation, and low metabolic activity to tolerance of *Pseudomonas aeruginosa* biofilms to ciprofloxacin and tobramycin. Antimicrob Agents Chemother 47: 317-323.

Wang Y, Lau PCK, Button DK (1996) A marine oligobacterium harboring genes known to be part of aromatic hydrocarbon degradation pathways of soil Pseudomonads. Appl Environ Microbiol 62: 2169-2173.

Wang Z, Wang KX, Xie YM, Yao YL (1995) Bioflocculant-producing microorganisms. Acta Microbiol Sin 35: 121-129.

Weart RB, Lee AH, Chien AC, Haeusser DP, Hill NS, Levin PA (2007) A metabolic sensor governing cell size in bacteria. Cell 130: 335-347.

Whiteley M, Bangera MG, Bumgarner RE, Parsek MR, Teitzel GM, Lory S, Greenberg EP. (2001) Gene expression in *Pseudomonas aeruginosa* biofilms. Nature 413: 860-864.

Whitman WB, Coleman DC, Wiebe WJ (1998) Prokaryotes: The unseen majority. Proc Natl Acad Sci USA 95: 6578-6583.

Williams AG, Wimpenny JWT (1977) Exopolysaccharide production by *Pseudomonas* NCIB 11264 grown in batch culture. J Gen Microbiol 102: 13-21.

Wilson ID, Neill SJ, Hancock, JT (2008) Nitric oxide synthesis and signalling in plants. Plant Cell Environ 31: 622-631.

Wingender J, Neu TR, Flemming HC (1999) Microbial Extracellular Polymeric Substances: Characterization, Structures and Function. Springer-Verlag, Berlin Heidelberg, Chapter 3.

Wolfaardt G, Lawrence JR, Korber DR (1999) Function of EPS. In: Wingender, J., Neu, T.R., Flemmin, H.C. (eds), Microbial Extracellular Polymeric Substances. Springer, Berlin, Germany, pp. 171-200.

Wood LG, Gibson PG, Garg ML (2003) Biomarkers of lipid peroxidation, airway inflammation and asthma. Eur Respir J 21: 177-186.

Wu JY, Ye HF (2007) Characterization and flocculating properties of an extracellular biopolymer produced from a *Bacillus subtilis* DYU1 isolate. Proc Biochem 42: 1114-1123.

Yadav KK, Mandal AK, Sen IK, Chakraborti S, Islam SS, Chakraborty R (2012) Flocculating property of extracellular polymeric substances produced by a biofilm forming bacterium *Acinetobacter junii* BB1A. Appl Biochem Biotechnol 168: 1621-1634.

Yanagita T, Ichlkawa T, Tsuji T, Kamata Y, Ito K, Sasaki M (1978) Two trophic groups of bacteria, oligotrophs and eutrophs: their distribution in fresh and sea water areas in the central northern Japan. J Gen Appl Microbiol 24: 59-88.

Yang FL, Yang YL, Liao PC, Chou JC, Tsai KC, Yang AS, Sheu F, Lin TL, Hsieh PF, Wang JT, Hua KF, Wu SH (2011) J Biol Chem 286: 21041-21051.

Yim JH, Kim SJ, Ahn SH, Lee HK (2007) Characterization of a novel bioflocculant, p-KG03, from a marine dinoflagellate, *Gyrodinium impudicum* KG03. Bioresour Technol. 98: 361-367.

Yokochi T, Nakashima I, Kato N (1977) Effect of Capsular Polysaccharide of *Klebsiella pneumoniae* on the Differentiation and Functional Capacity of Macrophages Cultured *In Vitro*. Microbiol Immunol 21: 601-610.

Yokoi H, Natsuda O, Hirose J, Hayashi S, Takasaka Y (1995) Characteristics of a biopolymer flocculant produced by *Bacillus subtilis*. J Ferment Bioeng 79: 378-380.

York WS, Darvill AK, Mcneil M, Stevenson TT, Albersheim P (1985) Isolation and characterization of plant cell walls and cell wall components. Methods Enzymol 118: 33-40.

Young KD (2006) The selective value of bacterial shape. Microbiol Mol Biol Rev 70: 660-703.

Yu Q, Nie SP, Wang JQ, Yin PF, Huang DF, Li WJ, Xie MY (2014) Toll-like receptor 4-mediated ROS signaling pathway involved in *Ganoderma atrum* polysaccharide-induced tumor necrosis factor-α secretion during macrophage activation. Food ChemToxicol 66: 14-22.

Zhang J, Liu Z, Wang S, Jiang P (2002) Characterization of a bioflocculant produced by the marine *Myxobacterium nannocystis* sp. NU-2. Appl Microbiol Biotechnol 59: 517-522.

PUBLICATIONS

❖ PUBLICATIONS

➢ RESEARCH ARTICLES:

1. **Mandal AK,** Sen IK, Maity P, Chattopadhyay S, Chakraborty R, Roy S, Islam SS (2015). Structural elucidation and biological studies of a novel exopolysaccaride from *Klebsiella pneumoniae* PB12. **International Journal of Biological Macromolecules (I.F. 3.1; Elsevier).**

2. **Mandal AK,** Yadav KK, Sen IK, Kumar A, Chakraborti S, Islam SS, Chakraborty R (2013). Partial characterization and flocculating behavior of an exopolysaccharide produced in nutrient-poor medium by a facultative oligotroph *Klebsiella* sp. PB12. **Journal of Bioscience and Bioengineering** (**I.F. 1.89; Elsevier**).

3. Chakraborti S, **Mandal AK,** Sarwar S, Singh P, Chakraborty R, Chakraborti P (2014) Bactericidal Effect of Polyethyleneimine Capped ZnO Nanoparticles on Multiple Antibiotic Resistant Bacteria harboring Genes of High Pathogenicity Island. **Colloids and Surfaces B: Biointerfaces** (**I.F. 4.5; Elsevier**). [**S. Chakraborti and A K Mandal were contributed equally].**

➢ BOOK CHAPTER:

1. Chakraborty R, **Mandal AK** (2015) Hunting Food Together is a Social Behavior. Do Bacteria Become Social in Scarcity and Selfish in Abundance? Biodiversity and Sustainability: Opportunities and Challenges. ISBN: 999-9-9999-9999-9.

International Journal of Biological Macromolecules 79 (2015) 413–422

Contents lists available at ScienceDirect

International Journal of Biological Macromolecules

journal homepage: www.elsevier.com/locate/ijbiomac

Structural elucidation and biological studies of a novel exopolysaccaride from *Klebsiella pneumoniae* PB12

Amit K. Mandal[a,b,1], Ipsita K. Sen[c,1], Prasenjit Maity[c], Sourav Chattopadhyay[d], Ranadhir Chakraborty[b], Somenath Roy[d], Syed S. Islam[c,*]

[a] Department of Microbiology, Vidyasagar University, Midnapore, West Bengal, India
[b] Omics Laboratory, Department of Biotechnology, University of North Bengal, Siliguri, West Bengal, India
[c] Department of Chemistry and Chemical Technology, Vidyasagar University, Midnapore, West Bengal, India
[d] Immunology and Microbiology Laboratory, Department of Human Physiology with Community Health, Vidyasagar University, Midnapore, West Bengal, India

ARTICLE INFO

Article history:
Received 20 February 2015
Received in revised form 27 April 2015
Accepted 30 April 2015
Available online 18 May 2015

Keywords:
Klebsiella pneumoniae PB12
Exopolysaccharide
NMR

ABSTRACT

An exopolysaccharide (KNPS) of an average molecular weight ~1.8×10^5 Da was isolated from the culture medium of *Klebsiella pneumoniae* PB12. Structural characterization of KNPS was carried out using sugar and methylation analysis, Smith degradation and 1D/2D NMR experiments. Sugar analysis showed that the KNPS composed of arabinose, galactose, 3-*O*-methyl-galctose and glucose in a molar ratio of nearly 4:3:1:1. The proposed repeating unit of the KNPS has a backbone chain consisting of two (1 → 6)-galactopyranosyl residues, two (1 → 5)-arabinofuranosyl residues, one (1 → 6)-glucopyranosyl residue and one (1 → 3)-arabinopyranosyl residue, out of which one (1 → 6)-galactopyranosyl residue was branched at *O*-2 position with a (1 → 2)-linked-galactopyranosyl residue terminated with non reducing arabinofuranosyl residue and one (1 → 5)-arabinofuranosyl residue branched at *O*-3 position with non reducing end 3-*O*-Me-galactopyranosyl residue. KNPS was found non-toxic toward human lymphocyte up to the dosage of 100 μg/ml. KNPS enhanced malondialdehyde (MDA), reactive oxygen species (ROS), and have the potential to alter the ratio of oxidized glutathione (GSSG) and reduced glutathione (GSH) levels in the cellular system.

1. Introduction

Klebsiella pneumoniae, a Gram-negative opportunistic pathogen causes hospital-acquired urinary tract infections, respiratory tract infections, and septicemias [1]. A common feature shown by *K. pneumoniae* strains is its ability to form biofilm. Biofilm provides shelter and homoeostasis to the cell population under its cover. It is chiefly composed of extracellular polymeric substance (EPS) which has the potential to prevent the influx of certain antimicrobial agents [2]. EPS possesses metal binding property and can seize toxic metal ions to protect bacterial cells [3]. EPS also renders a major virulence factor contributing toward expression of diseases [4]. The chemical composition of EPS differs widely depending on the microorganism. EPS are generally composed of glycoprotein, polysaccharide, protein, cellulose, lipid, glycolipid and nucleic acid [5–7]. The major structural component of EPS is polysaccharide which is either neutral or polyanionic in nature. The anionic nature is due to the presence of uronic acids which is thought to improve the binding ability of bivalent cations and enhance the mechanical strength of the EPS [8]. Bacterial exopolysaccharides have also shown biological activities like anti-tumor and immunomodulatory properties that significantly varied with the degree of branching, molecular mass, conformation and chemical modification [9–11]. Some species of the genus *Klebsiella* were reported earlier to produce exopolysaccharides in culture medium. Fucogel, a polysaccharide produced by *K. pneumoniae* I-1507 was found to compose of galactose, 4-*O*-acetyl-galacturonic acid and fucose [12]. In a separate study, Rättö et al. isolated galacturonic acid containing heteropolysaccharide from two *K. Pneumoniae* strains [13]. Bales et al. characterized another EPS isolated from *K. pneumoniae* which was found to comprise of 1.3% glucose, 49.4% mannose, and 5.0% GlcA [14]. In general, polysaccharides activate macrophages, T-helper, NK, and other effector cells and thereby activate various chemokines, cytokines (IL-2, IL-6, IL-10, TNF-α, and IL-12) and interferon (IFN-γ) resulting stimulation of host's immune system [15]. Earlier study showed that the capsular polysaccharide of pyrogenic liver abscess (PLA) *K. pneumoniae* induces secretion of tumor

* Corresponding author. Tel.: +91 9932 629 971; fax: +91 3222 276 554.
E-mail address: sirajul_1999@yahoo.com (S.S. Islam).
[1] These authors contributed equally to this work.

http://dx.doi.org/10.1016/j.ijbiomac.2015.04.077
0141-8130/

necrosis factor-α (TNF-α) and interleukin-6 (IL-6) by macrophages through Toll-like receptor 4 (TLR4) [16]. In a separate study Hsieh et al. established the role of virulence of O1 antigen obtained from PLA-associated *K. pneumoniae* [17]. It was proposed that EPS of *K. pneumoniae* have infection-enhancing capabilities by hindering the acid phosphatase release from the lysosomal fraction of peritoneal macrophages [18]. Yokochi et al. showed that trace amount of *K. pneumoniae* extracellular capsular polysaccharide inhibited macrophage maturation and function [19].

K. pneumoniae PB12, a novel facultative oligotrophic bacterium isolated from river Mahananda, Northern West Bengal, Siliguri, India, produces exopolysaccharide. In the present study, a detailed structural characterization of the exopolysaccharide isolated from *K. pneumoniae* PB12 along with the study of its biological activities were investigated and reported herein.

2. Materials and methods

2.1. Organism

All experiments were carried out using the strain *K. pneumoniae* PB12 isolated from the river Mahananda, Northern West Bengal, Siliguri, India. Whole cell DNA of *K. pneumoniae* PB12, amplification of 16S rRNA gene sequence, purification of PCR product and cloning were done as described earlier [20]. PCR product was sequenced with primers 27F and 1492R using BDT v3.1 cycle sequencing kit on ABI 3730 × 1 genetic analyzer following the manufacturer's recommendations. 16S rRNA gene sequence was used to carry out BLAST with the database of National Centre for Biotechnology Information (NCBI, http://blast.ncbi.nlm.nih.gov/Blast.cgi).

2.2. Purification and chemical analysis of KNPS

K. pneumoniae PB12 produces extracellular polymeric substances (EPS) in Reasoner's 2A (R2A) broth (Himedia M1687). Isolation of EPS was done after incubating the test strain at 30 °C for 48 h followed by centrifugation of the culture broth, precipitation of supernatant in double volume of cold 95% ethanol followed by dialysis in a dialysis tubing cellulose membrane (D9652, Sigma-Aldrich, retaining M_W > 12,400 Da) against distilled water for 24 h. The dialyzed material was again centrifuged at 9587.5 × *g* for 40 min at 4 °C and the supernatant was freeze-dried to obtain crude EPS (400 mg). Protein fraction of EPS was removed by adding trichloroacetic acid (30%) followed by centrifugation and residue was discarded. Two volumes of 95% ethanol was added to the supernatant and centrifuged at 9587.5 × *g* for 30 min to obtain 300 mg of protein-free crude polysaccharide [21]. This crude polysaccharide (25 mg) was passed through Sepharose 6B gel permeation column (90 × 2.1 cm) using water as the eluent with a flow rate of 0.3 ml min^{-1} as described in the earlier report [8]. A total of 95 test tubes were collected using Redifrac fraction collector and monitored spectrophotometrically (Shimadzu UV–vis spectrophotometer, model-1601) at 490 nm using phenol-sulfuric acid method [22]. Single fraction of purified polysaccharide (test tubes, 24–40) named KNPS (18 mg) was obtained.

2.3. General methods

The average molecular weight of KNPS was determined by gel chromatography using standard dextrans T-200, T-70 and T-40 as reported earlier [23]. KNPS (2 mg) was hydrolyzed with 2 M CF_3COOH (2 ml) in a round-bottomed flask at 100 °C for 18 h in a boiling water bath and the sugar composition analysis was carried out adopting the methods as described earlier [24]. Gas Chromatography (GC) analysis of the alditol acetates was carried out by a gas–liquid chromatography, Hewlett–Packard model 5730 A, with flame ionization detector and glass columns (1.8 m × 6 mm) packed with 3% ECNSS-M (A) on Gas Chrom Q (100–120 mesh) and 1% OV-225 (B) on Gas Chrom Q (100–120 mesh). All GC analyses were performed at 170 °C. The absolute configuration of the monosaccharide was determined by the method of Gerwig et al. [25]. KNPS (3.5 mg) was methylated using the procedure reported earlier [26] and the partially methylated alditol acetates were analyzed by GC–MS. GC–MS analysis was performed on Shimadzu GC–MS Model QP-2010 Plus automatic system, using ZB-5MS capillary column (30 m × 0.25 mm). The program was isothermal at 150 °C; hold time 5 min, with a temperature gradient of 2 °C min^{-1} up to a final temperature of 200 °C. NMR experiments were carried out by a Bruker Avance DPX-500 instrument at 30 °C as reported earlier [24].

2.4. Smith degradation study

KNPS (30 mg) was added to 7.5 ml 0.1 M sodium metaperiodate solution and the mixture was kept for 48 h in the dark at 4 °C. The excess periodate was destroyed by adding ethylene glycol (5.0 ml) and the solution was dialyzed against distilled water for 2 h. The volume of the dialyzed material was concentrated to 2–3 ml. This material was reduced with $NaBH_4$, 12 h, neutralized with 50% AcOH, and dialyzed with distilled water and finally freeze dried (14.0 mg). The periodate-oxidized, reduced material was subjected to mild hydrolysis by the addition of 0.5 M CF_3COOH for 15 h at 25 °C to destroy the residues of oxidized sugars attached to the polysaccharide backbone. The excess acid was removed by repeated freeze drying. The material was further purified by passing through a Sephadex G-25 column, kept over P_2O_5 in vacuum for several days and finally used for ^{13}C NMR studies.

2.5. Biological activities

2.5.1. Isolation of lymphocytes from peripheral blood mononuclear cells (PBMCs)

Blood samples (total 30 blood samples, 6 samples for each group) were freshly collected satisfying the Helsinki protocol from all groups of individuals. From the heparinized blood samples the lymphocytes were isolated according to the method described earlier [27]. Blood was diluted in PBS (pH 7.0), layered carefully on the density gradient (histopaque 1077) in a ratio of 1:2, centrifuged at 1400 rpm for 20 min. The white milky layer of mononuclear cells were carefully removed and cultured in RPMI 1640 medium for 2 h under 5% CO_2 and 95% humidified atmosphere at 37 °C [27]. Non adherent layer of the cultured cells were collected and washed twice with PBS and centrifuged at 2000 rpm for 10 min to obtain lymphocytes. As described previously, the depletion of macrophages and B cells in PBMC were done by passing it through a nylon wool column [28]. After washing the column for two times with the medium, the non-adherent $CD4^+$ T cells and $CD8^+$ T cells were stained with Phycoerythrin (PE) and Fluorescein isothiocyanate (FITC) conjugated antibody as described earlier [29]. Samples were then analyzed using flow cytometer (FACS CALIBUR, Becton Dickinson, USA) using CellQuest software.

2.5.2. Sulforhodamine B assay (SRB)

The isolated human lymphocytes were seeded into 96 well tissue culture plates having 180 μl of complete media and were incubated for 48 h. KNPS was added to the cells at varied concentrations (25, 50, 100 and 200 μg/ml) and incubated for 24 h at 37 °C in a humidified incubator (NBS) containing 5% CO_2. The toxicity of KNPS on human lymphocytes were determined using SRB assay following the protocol described earlier [30].

2.5.3. Preparation of cell lysate

The cell suspension was centrifuged at 1500 rpm for 5 min, after treatment schedule. The supernatants were collected and stored at −20 °C. The cell pellets were re-suspended in ice cold PBS and subjected to four cycles of freeze–thaw cycles followed by sonication for 20 s (Ultrasonic Processor, Tekmar, Cincinnati, OH, USA). Lysates were centrifuged at 12,000 rpm for 20 min at 4 °C to remove cellular debris. Protein content of lysate was measured as described earlier using bovine serum albumin as standard [31].

2.5.4. Determination of reduced glutathione (GSH), oxidized glutathione level (GSSG) and lipid peroxidation

The estimation of reduced glutathione in the cell lysate was done by the method described previously [32]. The oxidized glutathione level was measured after derivatization of GSH with 2-vinylpyidine according to the method reported earlier [33]. Lipid peroxidation was estimated using the method of Ohkawa et al. [34] in the cell lysate.

2.5.5. Statistical analysis

The data were expressed as the mean ± the standard error of the mean ($n = 6$). Comparisons between the means of control and treated groups were made by one-way Anova analysis of variance (using a statistical package; Origin 6.1, Origin Lab, Northampton, MA, USA) with multiple-comparison tests, with $p < 0.05$ as the limit of significance. The correlation analysis was performed using Statistica software version 8.0.

3. Results and discussion

3.1. Organism

Nearly complete 16S rRNA gene sequence (1504 bp) was amplified, cloned and sequenced. BlastN search of the 16S rRNA gene sequence (accession no. KF192506) of the isolate PB12 shows 99% similarity with the 16S rRNA gene sequence of *K. pneumoniae* sub sp. *pneumoniae* strain ATCC 43816 KPPR1 (accession no. CP009208).

3.2. Purification and chemical analysis of KNPS

The isolation and purification steps are summarized with flow diagram in Fig. 1a. A single fraction (Fig. 1b) of purified polysaccharide (KNPS) was obtained after fractionation of water soluble crude polysaccharide through Sepharose 6B column. The fraction was collected and freeze dried. The average molecular weight of KNPS was estimated $\sim 1.8 \times 10^5$ Da. KNPS was composed of arabinose, galactose, 3-*O*-methyl-galctose and glucose in a molar ratio of nearly 4:3:1:1. Determination of absolute configuration of the monosaccharides showed that galactose, 3-*O*-methyl-galctose and glucose were present in D and arabinose in L configuration. The GC–MS analysis of partially methylated alditol acetates revealed the presence of 3,5-linked-arabinofuranosyl, 2,6-linked-galactopyranosyl, 6-linked-galactopyranosyl, 6-linked-glucopyranosyl, 2-linked-galactopyranosyl, 5-linked-arabinofuranosyl, 3-linked-arbinopyranosyl, terminal galactopyranosyl and arabinofuranosyl residues in a relative proportion of approximately 1:1:1:1:1:1:1:1:1.

3.3. Structural analysis of KNPS

The ^{1}H NMR spectrum (500 MHz, Fig. 2a) of KNPS recorded in D_2O at 30 °C showed the presence of eight signals in the anomeric region at δ 5.20 (**A**), 5.17 (**B**), 5.16 (**C** and **D**), 5.10 (**E**), 5.05 (**F**), 5.02 (**G**), 4.46 (**H**), and 4.42 (**I**) as evidenced from HSQC couplings. In ^{13}C NMR spectrum (125 MHz; Fig. 2b) at the same temperature, eight signals were observed in the anomeric region at δ 109.4, 106.8, 103.3, 102.7, 102.2, 101.5, 99.5, and 97.7. These eight anomeric carbon signals were correlated to the anomeric proton signals of residue (**A**), (**B**), (**I**), (**H**), (**G**), (**F**), (**E**), (**C** and **D**), respectively as assigned from the HSQC spectrum (Fig. 3a, Table 1a). The proton and carbon chemical shifts were assigned from DQF-COSY, TOCSY, and HSQC (Fig. 3a and b) experiments. The proton coupling constants were measured from DQF-COSY experiment.

The residues **A** and **B** were assigned as (1 → 3,5)-α-L-Ara*f* and (1 → 5)-α-L-Ara*f* residues, respectively. The α-configuration of both **A** and **B** residues were assigned from the chemical shift values of anomeric carbon and proton (δ 109.4/5.20 and δ 106.8/5.17), respectively. The downfield shift of C-3 (δ 81.8) and C-5 (δ 65.4) with respect to the standard methyl glycosides [35–37] indicated that the residue **A** was (1 → 3,5)-linked-α-L-arabinofuranose. The downfield shift of C-5 (δ 65.4) with respect to the standard methyl glycosides indicated that the residue **B** was (1 → 5)-linked α-L-arabinofuranosyl moiety. The linkage at C-5 of the both residues **A** and **B** were further confirmed from DEPT-135 spectrum (inset, Fig. 2b). Hence, these observation confirmed that the residue **A** was (1 → 3,5)-α-L-Ara*f* and the residue **B** was (1 → 5)-α-L-Ara*f*.

The anomeric proton chemical shifts (δ 5.16 for **C** and **D,** δ 5.10 for **E**) and carbon chemical shifts (δ 97.7 for **C** and **D,** δ 99.5 for **E**) confirmed that the residues were α-D-galactopyranosyl residues. In case of residue **C**, the carbon chemical shifts of C-2 (δ 75.9) and C-6 (δ 66.4) appeared at downfield with respect to the standard values of methyl glycosides [35,36] which suggests that residue **C** was linked at C-2 and C-6. The linkage at C-6 of the residue **C** was further confirmed from DEPT-135 spectrum (inset, Fig. 2b). Hence, **C** was confirmed as (1,2 → 6)-linked α-D-galactopyranosyl residue. Residue **D** had an anomeric carbon signal at δ 97.7. The downfield shift of C-6 (δ 66.4) of residue **D** with respect to standard methyl glycosides indicated that it was linked at C-6. The linkage at C-6 was further supported by DEPT-135 spectrum (inset, Fig. 2b). Therefore, **D** was confirmed as (1 → 6)-linked α-D-galactopyranosyl residue. The downfield shift of C-2 (δ 76.6) with respect to standard values of methyl glycosides [35,36] indicated that residue **E** was a (1 → 2)-linked α-D-galactopyranosyl.

Residue **F** was assigned as non reducing end β-L-Ara*f*. The anomeric proton chemical shift for residue **F** at δ 5.05 and carbon chemical shift of δ 101.5 indicated that it was a β-linked anomer [35,38].

The residue **G** was assigned as (1 → 3)-β-L-Ara*p*. The anomeric proton (δ 5.02) and carbon (δ 102.2) chemical shift values indicated that **G** was a β-linked anomer. The downfield shift of C-3 at δ 84.1 indicated that it was (1 → 3)-β-L-Ara*p* [39].

Anomeric proton chemical shift (δ 4.46), anomeric carbon chemical shift (δ 102.7), and the coupling constant value $J_{H\text{-}1,H\text{-}2}$ (~8.0 Hz) confirmed that **H** was β-D-glucopyranosyl residue. The downfield shifts of C-6 (δ 67.9) with respect to standard values of methyl glycosides indicated that residue **H** was linked at this position. The linking at C-6 of the residue **H** was further confirmed by DEPT-135 spectrum (inset, Fig. 2b). Thus, **H** was confirmed as (1 → 6)-β-D-glucopyranosyl residue.

β-Configuration of residue **I** was assigned from $J_{H\text{-}1,H\text{-}2}$ coupling constant (~8.5 Hz) from its anomeric proton (δ 4.42) and carbon (δ 103.3) signals. All the proton and carbon chemical signals except C-3 matched nearly to the standard values of methyl glycosides [35,36]. The ^{13}C chemical shift of C-3 is about ~δ 10.0 higher than the standard value [35,40] which is consistent with the presence of -*O*Me group at C-3. This was further confirmed by the presence of cross coupling between the methoxy proton (δ 3.45) and the C-3 (δ 81.4) of residue **I** in the HMBC experiment (Figure not shown). Thus, **I** was confirmed as terminal 3-*O*-methyl-β-D-galactopyranosyl residue.

The sequence of glycosyl residues (**A** to **I**) were determined from ROESY (Table 1b, Fig. 4) experiment. In ROESY experiment, the inter-residual contacts **A**H-1/**H**H-6a, 6b; **B**H-1/**D**H-6a,

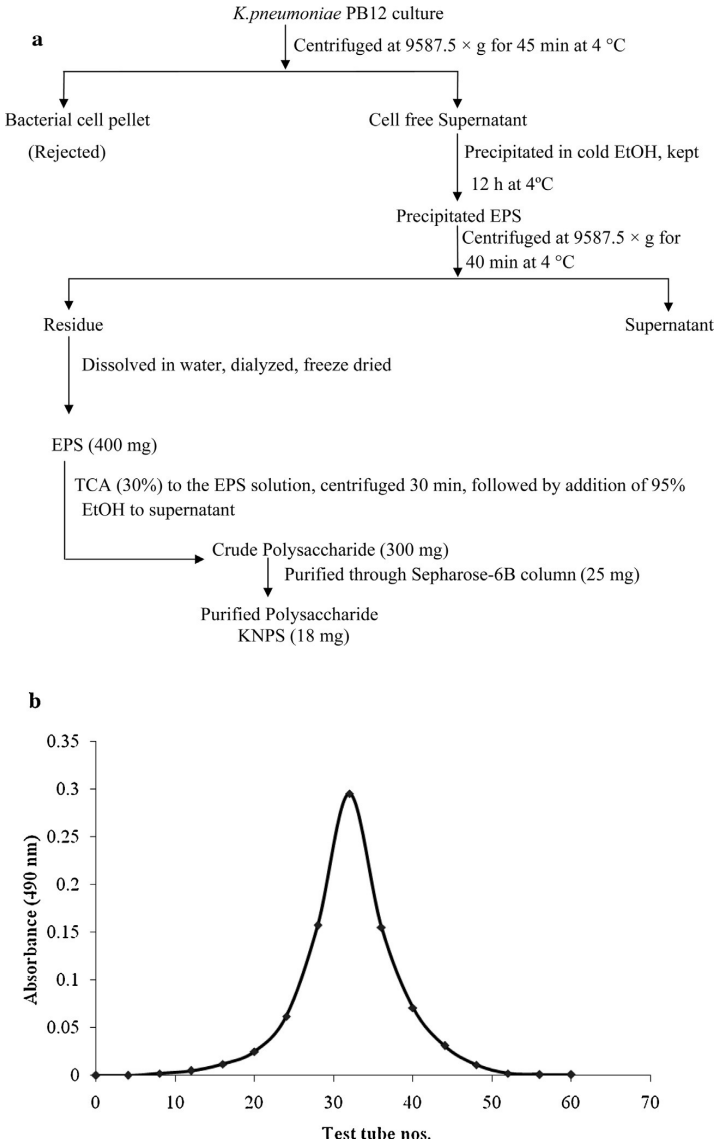

Fig. 1. (a) Flow diagram of isolation and purification of the exopolysaccharide, KNPS produced by *K. pneumoniae* PB12. (b) Gel permeation chromatogram of crude exopolysaccharide isolated from the culture medium of K. *pneumoniae* PB12 using Sepharose 6B column.

6b; **C**H-1/**B**H-5a, 5b; **D**H-1/**G**H-3; **E**H-1/**C**H-2; **F**H-1/**E**H-2; **G**H-1/**A**H-5a, 5b; **H**H-1/**C**H-6a, 6b; and **I**H-1/**A**H-3 along with other intra-residual contacts were also observed (Fig. 4). The above ROESY connectivities established the following sequences: **A** (1 → 6) **H**; **B** (1 → 6) **D;** **C** (1 → 5) **B**; **D** (1 → 3) **G**; **E** (1 → 2) **C;** **F** (1 → 2) **E**; **G** (1 → 5) **A**; **H** (1 → 6) **C**; and **I** (1 → 3) **A**. Hence, the structure of repeating unit present in KNPS was proposed as:

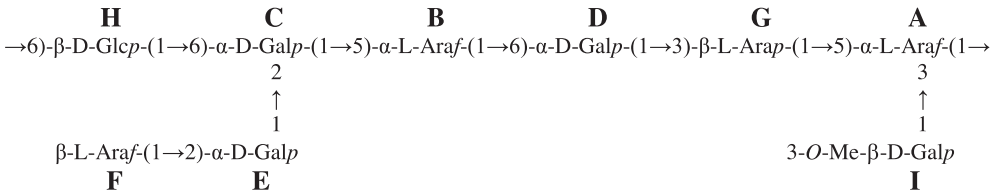

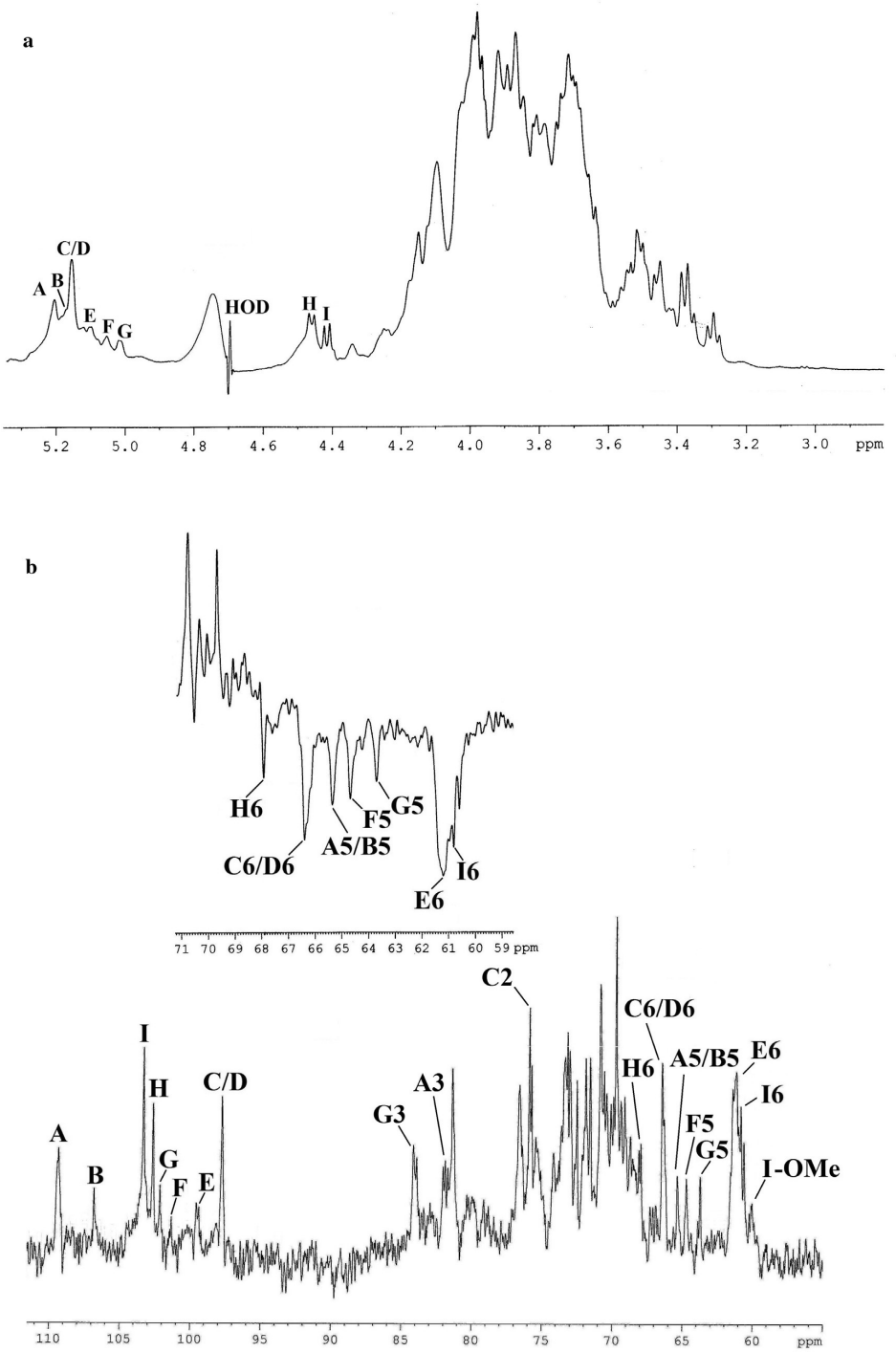

Fig. 2. (a) ^{1}H NMR spectrum (500 MHz, D_2O, 30 °C) of exopolysaccharide, KNPS produced by *K. pneumoniae* PB12. Acetone was taken as the internal standard, fixing the methyl proton signal at δ 2.225. (b) ^{13}C NMR spectrum (125 MHz, D_2O, 30 °C) of exopolysaccharide, KNPS produced by *K. pneumoniae* PB12, acetone was taken as the internal standard, fixing the methyl carbon signal at δ 31.05. Inset shows part of DEPT-135 spectrum (D2O, 30 °C) of exopolysaccharide, KNPS.

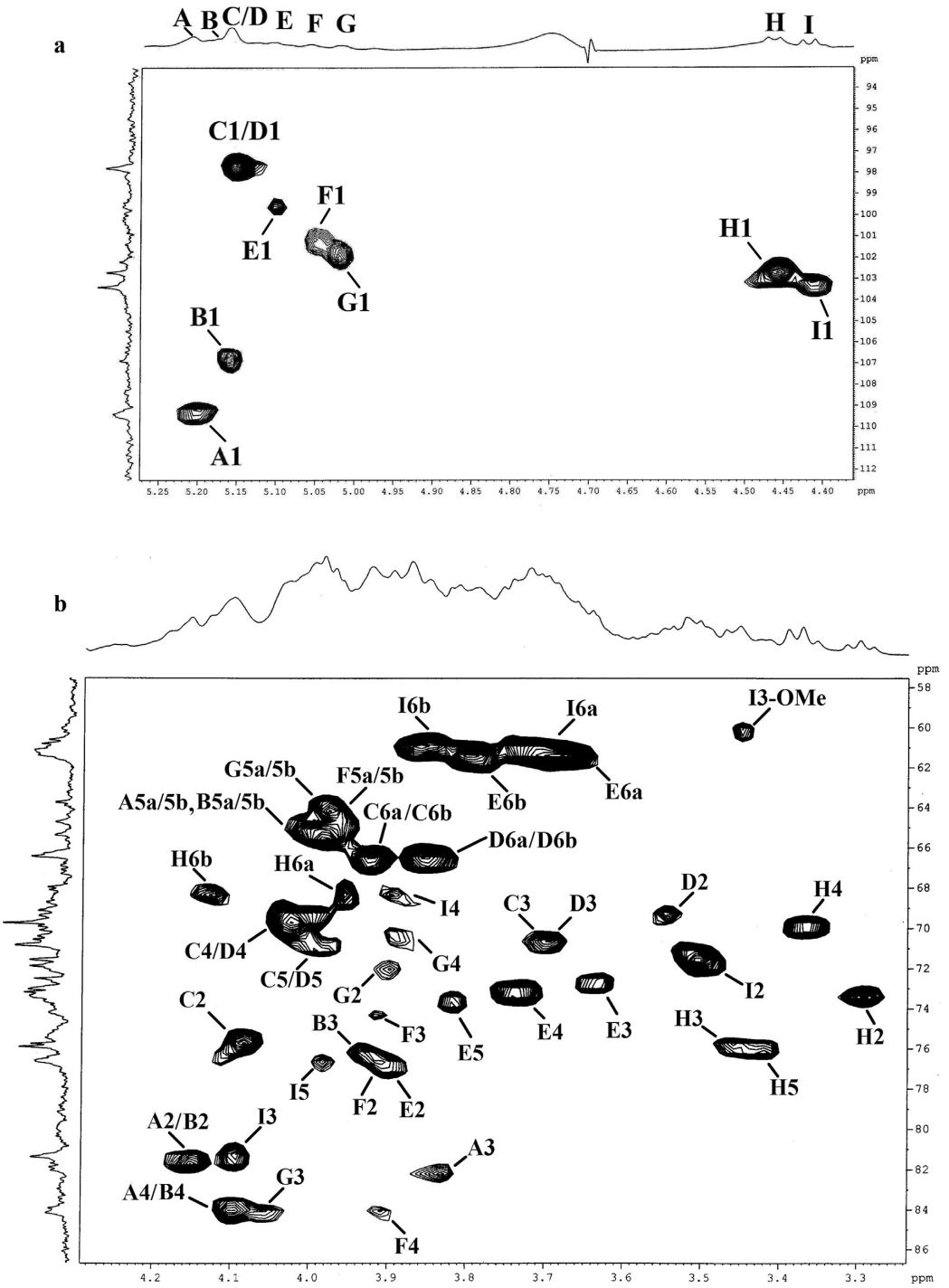

Fig. 3. The HSQC spectrum of (a) anomeric part and (b) other than anomeric part of the exopolysaccharide, KNPS produced by *K. pneumoniae* PB12. The annotation **A**1 refers to **A**H1/**A**C1 cross peak, **B**1 refers to **B**H1/**B**C1 cross peak and so on.

Table 1
(a) The ^{1}H NMR[a] and ^{13}C NMR[b] chemical shifts of the exopolysaccharide, KNPS produced by *K. pneumoniae* PB12 in D_2O at 30 °C. (b) ROESY data of exopolysaccharide, KNPS produced by *K. pneumoniae* PB12 in D_2O at 30 °C.

Glycosyl residue	H-1/C-1	H-2/C-2	H-3/C-3	H-4/C-4	H-5a, H-5b/C-5	H-6a, H-6b/C-6	*O*Me
→3,5)-α-L-Ara*f*-(1→	5.20	4.15	3.85	4.09	3.98[c], 3.98[d]		
A	109.4	81.5	81.8	84.0	65.4		
→5)-α-L-Ara*f*-(1→	5.17	4.15	3.92	4.09	3.98[c], 3.98[d]		
B	106.8	81.4	76.6	84.0	65.4		
→2,6)-α-D-Gal*p*-(1→	5.16	4.09	3.70	4.02	3.99	3.92[c], 3.92[d]	3.45
C	97.7	75.9	70.8	69.7	70.8	66.4	59.9
→6)-α-D-Gal*p*-(1→	5.16	3.55	3.70	4.02	3.99	3.84[c], 3.84[d]	
D	97.7	69.3	70.8	69.7	70.8	66.4	
→2)-α-D-Gal*p*-(1→	5.10	3.92	3.63	3.74	3.81	3.69[c], 3.78[d]	
E	99.5	76.6	72.5	72.6	73.4	61.1	
β-L-Ara*f*-(1→	5.05	3.92	3.91	3.90	3.97[c], 3.97[d]	3.95[c], 4.13[d]	
F	101.5	76.6	74.1	84.1	64.7	67.9	
→3)-β-L-Ara*p*-(1→	5.02	3.89	4.09	3.88	3.98[c], 3.98[d]	3.70[c], 3.87[d]	
G	102.2	71.9	84.1	70.8	63.7	60.8	
→6)-β-D-Glc*p*-(1→	4.46	3.30	4.46	3.38	3.42		
H	102.7	73.2	75.7	69.8	75.9		
3-*O*-Me-β-D-Gal*p*-(1→	4.42	3.50	4.09	3.89	3.98		
I	103.3	70.8	81.4	68.0	76.6		

Glycosyl residue	Anomeric proton	ROE contact protons	
	δ	*δ*	Residue, atom
→3,5)-α-L-Ara*f*-(1→	5.20	3.95	**H** H-6a
A		4.13	**H** H-6b
		4.15	**A** H-2
→5)-α-L-Ara*f*-(1→	5.17	3.84	**D** H-6a/b
B		4.15	**B** H-2
→2,6)-α-D-Gal*p*-(1→	5.16	3.98	**B** H-5a/b
C	5.16	4.09	**G** H-3
→6)-α-D-Gal*p*-(1→	5.10	3.55	**D** H-2
D	5.05	4.09	**C** H-2
→2)-α-D-Gal*p*-(1→	5.02	3.92	**E** H-2
E	4.46	3.92	**E** H-2
β-L-Ara*f*-(1→	4.42	3.98	**A** H-5a/b
F		3.92	**C** H-6a/b
→3)-β-L-Ara*p*-(1→		3.30	**H** H-2
G		3.46	**H** H-3
→6)-β-D-Glc*p*-(1→		3.42	**H** H-5
H		3.85	**A** H-3
3-*O*-Me-β-D-Gal*p*-(1→		3.98	**I** H-5
I		3.50	**I** H-2

[a] Values of the ^{1}H chemical shifts were recorded with respect to the HOD signal fixed at *δ* 4.70 at 30 °C.
[b] Values of the ^{13}C chemical shifts were recorded with reference to acetone as the internal standard and fixed at *δ* 31.05 at 30 °C.
[c,d] Interchangeable.

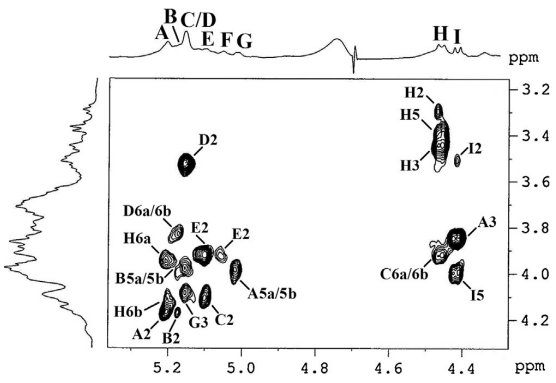

Fig. 4. Part of ROESY spectrum of exopolysaccharide, KNPS produced by *K. pneumoniae* PB12. The ROESY mixing time was 300 ms.

3.4. Smith degradation study

Smith degradation was carried out with KNPS and the product was analyzed by ^{13}C NMR (Table 2, Fig. 5) to confirm the sequence of the sugar residues present in the repeating unit. A trisaccharide containing glycerol moiety was obtained as a product of Smith degradation of KNPS. The ^{13}C NMR spectrum of Smith-degraded KNPS showed three anomeric signals at *δ* 109.2, 103.3 and 102.9 corresponding to the anomeric carbon of →3,5)-α-L-Ara*f*-(1→ residue (**X**), 3-*O*-Me-β-D-Gal*p*-(1→ residue (**Y**) and β-L-Ara*p*-(1→ moiety (**Z**), respectively. The carbon signal at *δ* 64.6 and *δ* 81.5 clearly indicated the presence of linking at C-5 and C-3 of →3,5)-α-L-Ara*f*-(1→ residue (**X**). The residue (**A**) of KNPS being (1→3,5)-linked remains unaffected during oxidation and assigned as residue (**X**) in the degraded product. The →3)-β-L-Ara*p*-(1→ residue (**G**) was converted to nonreducing end β-L-Ara*p*-(1→ (**Z**) during Smith degradation. The glycerol moiety (**R**) was generated from the (1→6)-β-D-Glc*p* moiety (**H**) which was linked glycosidically with the residue (**C**) in KNPS and remains attached to the →3,5)-α-L-Ara*f*-(1→ moiety (**X**) in the Smith degraded product. The residue 3-*O*-Me-β-D-Gal*p*-(1→, (**I**) remains unaffected

Table 2
The ^{13}C NMR[n] chemical shifts of trisaccharide unit obtained after Smith-degradation of exopolysaccharide, KNPS produced by *K. pneumoniae* PB12 in D_2O at 30 °C.

Sugar residue	C-1	C-2	C-3	C-4	C-5	C-6	OMe
→3,5)-α-L-Ara*f*-(1→ **X**	109.2	80.2	81.5	84.0	64.6	–	
3-*O*-Me-β-D-Gal*p*-(1→ **Y**	103.2	70.8	79.8	68.8	76.7	61.2	60.0
β-L-Ara*p*-(1→ **Z**	102.9	71.8	74.9	69.6	63.0	–	
1 2 3(CH_2OH) CH(OH) CH_2O→**R**	66.4	72.1	62.6	–	–	–	

[n] Values of the ^{13}C chemical shifts were recorded with reference to acetone, fixing the methyl carbon signal at δ 31.05.

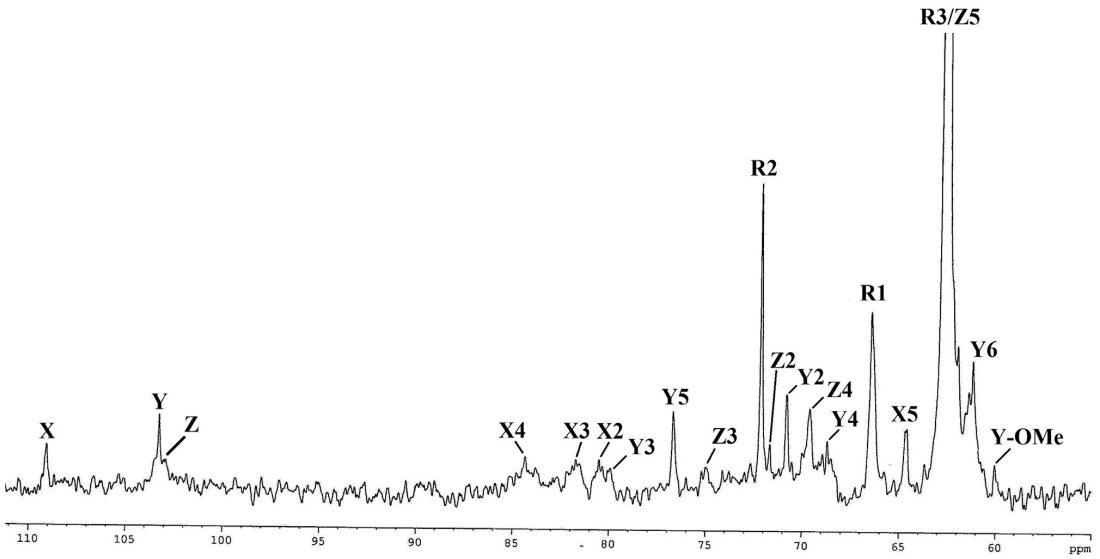

Fig. 5. ^{13}C NMR spectrum (125 MHz, D_2O, 30 °C) of glycerol containing trisaccharide residue obtained from Smith-degradation of KNPS produced by *K. pneumoniae* PB12.

during Smith degradation and assisgned as residue (**Y**) in the degraded product. The remaining residues **B**, **C**, **D**, **E**, **F** of KNPS were completely destroyed during oxidation. Hence, the structure of glycerol containing trisaccharide unit obtained from exopolysaccharide, KNPS after Smith degradation was established as:

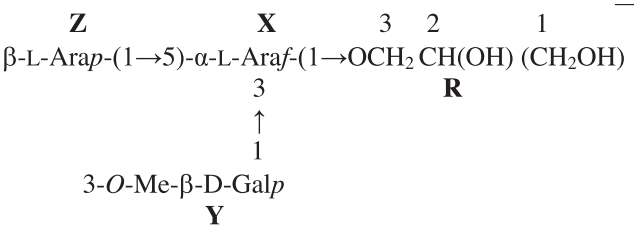

Therefore, Smith degradation results further confirmed the repeating unit present in the exopolysaccharide, KNPS produced by *K. pneumoniae* PB12.

3.5. Biological activities

The phenotypic characteristics of lymphocytes were confirmed by FACS analysis. The dot plot results showed that, 48% lymphocyte cells were $CD4^+$ and 23% $CD8^+$ (Fig. 6a). The viability of the human lymphocytes was studied using SRB assay with varied concentrations of KNPS (ranging from 25 μg/ml to 200 μg/ml). SRB, a bright pink aminoxanthene dye binds under mild acidic conditions to basic amino acid residues and dissociates under basic conditions. Results showed that 200 μg/ml dosage of KNPS exhibited toxicity ($p < 0.05$) (Fig. 6b). Previous report established the potent role of *K. pneumoniae* CPS in initiation of cytotoxicity during the infection of lung epithelial cells [41]. In order to understand the glutathione level, an important antioxidant in cellular system, both the reduced and oxidized form of glutathione were measured. It was observed that there was decrease in reduced glutathione (GSH) level at the dosage of 200 μg/ml of KNPS whereas the same dosage of KNPS showed a mild increment of oxidized glutathione level (GSSG) ($p < 0.05$) (Fig. 6c). Thus, it can be said that there is some relation between the redox ratios (GSH/GSSG) in cellular system with the concentration of KNPS. The increasing GSSG level may be due to the generation of free singlet species inside the cells. When the dose of the KNPS was increased from 25 to

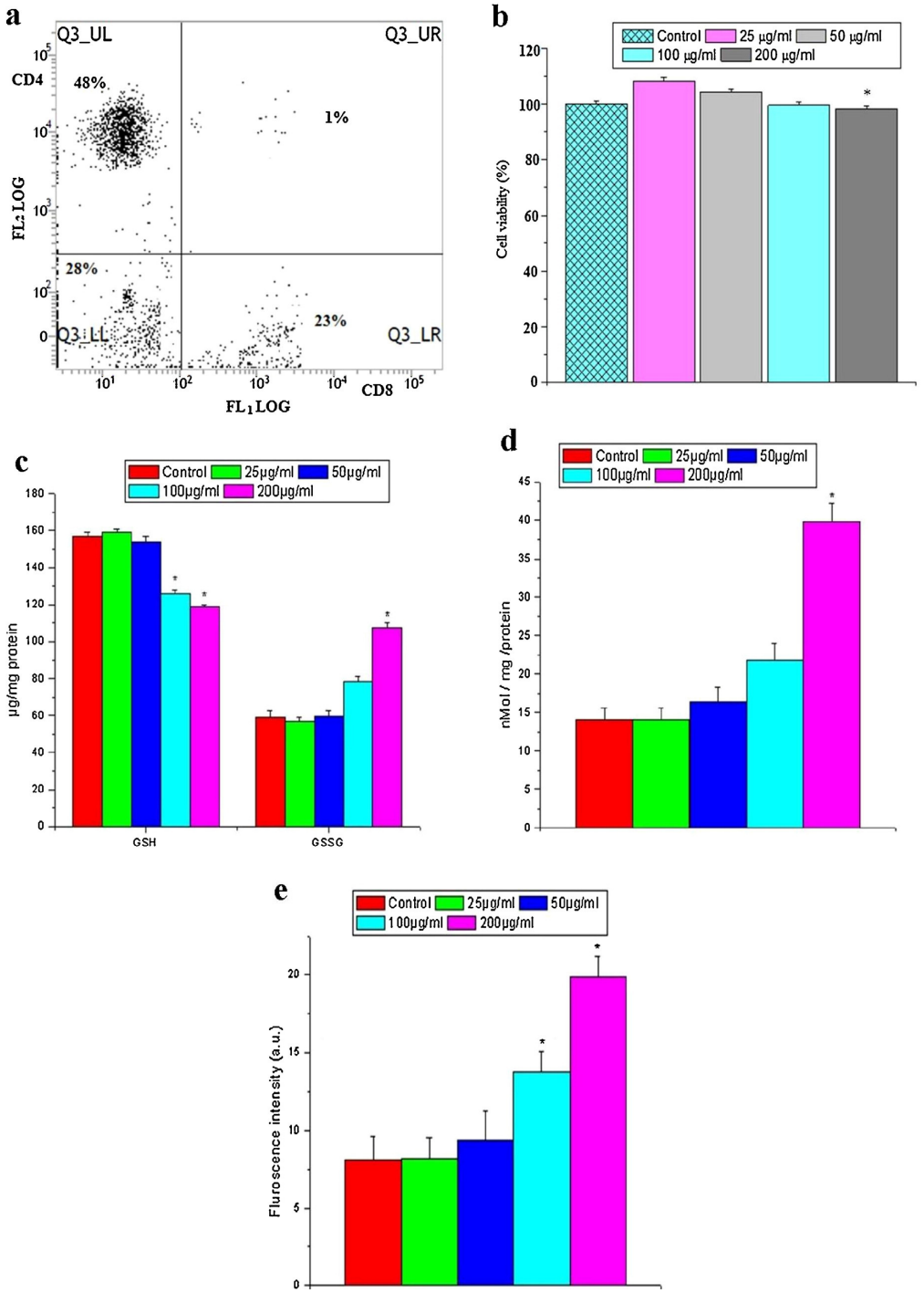

Fig. 6. (a) Dot plot of lymphocytes stained with anti-CD4 or anti-CD8 antibodies (b) Cytotoxicity of KNPS against human lymphocytes. (c) Concentration of reduced glutathione (GSH) and oxidized glutathione (GSSG) of normal human lymphocytes when treated with KNPS. (d) Lipid peroxidation study in terms of MDA release in KNPS treated human lymphocytes. (e) Measurement of intracellular ROS in lymphocytes, using a oxidant-sensing fluorescent probe 2′,7′-dichlorodihydrofluorescein diacetate (DCFH-DA), treated with varied concentration of KNPS. ($n = 6$, values are expressed as mean ± SEM. * Indicates the significant difference as compared to control group).

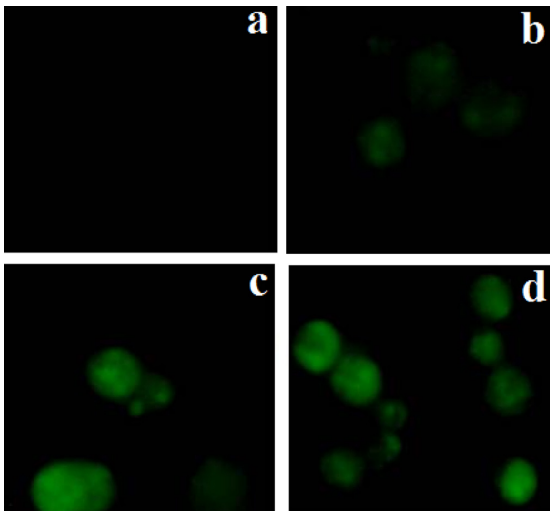

Fig. 7. Fluorescence micrographs of human lymphocytes treated with different concentrations of KNPS (a) control, (b) 50 μg/ml, (b) 100 μg/ml and (b) 200 μg/ml.

200 μg/ml, the redox ratio decreased significantly ($p < 0.05$) to 1.11 compared to their respective control (redox ratio 2.66) indicating that 200 μg/ml of KNPS was toxic. Lipid peroxidation is one of the essential determinants to assess the cellular damage due to ROS. Several toxic by-products especially malondialdehyde (MDA) is released due to lipid peroxidation [42]. Hence, the concentration of malondialdehyde (MDA) was measured to check the involvement of ROS in the alteration of redox status (Fig. 6d). The significantly ($p < 0.05$) enhanced production of MDA was noted at 200 μg/ml of KNPS dosage, which confirms the potential of KNPS to alter the intracellular redox status via ROS production. Similar type of enhanced ROS generation was reported in macrophage cell lines by the polysaccharide, PSG-1 [15]. To further validate our observations intracellular ROS was measured using a oxidant-sensing fluorescent probe 2′,7′-dichlorodihydrofluorescein diacetate (DCFH-DA). DCFH-DA, a nonpolar dye, converted into the polar derivative DCFH (nonfluorescent) by means of cellular esterase. After getting oxidized by intracellular ROS and other peroxides it switched to highly fluorescent DCF. Fig. 6e, showed that fluorescence intensity of DCF increase with the increment of KNPS dosage (varied between 25 and 200 μg/ml) and it becomes maximum at 200 μg/ml (Fig. 7). These results showed that KNPS treatment enhanced the generation of intracellular reactive oxygen species (ROS). It was reported earlier that the CPS of *K. pneumoniae* induce ROS production in macrophages [16]. Hence, this study may help to put on more insights into the mechanisms of septic shock and KNPS-induced immunosuppression and autoimmunity.

4. Conclusions

A novel exopolysaccharide, KNPS was isolated from the culture medium of biofilm forming bacterium *K. pneumoniae* PB12. On the basis of chemical analysis and NMR studies the structure of KNPS has been established. KNPS does not induce damage of human lymphocytes up to 100 μg/ml dosage as determined from SRB assay. KNPS enhanced MDA, ROS, and alter the ratio of GSSG and GSH levels in cellular system.

Acknowledgements

The authors are grateful to Dr. S. Roy, Director, IICB, Kolkata, for providing instrumental facilities. Mr. Barun Majumdar of Bose Institute, Kolkata, is acknowledged for preparing NMR spectra. I.K.S thanks CSIR, India for providing senior research fellowship (CSIR-09/599(042)/2011-EMR-I) and A.K.M thanks North Bengal University for providing Ph.D fellowship (NBUJRF/3726/R-2007). CSIR-OSDD, Government of India is acknowledged for sanctioning a project (Ref. No: OSDD/HCP001/11FYP/2011-12/131 dated 30/08/2011).

References

[1] R. Podschun, U. Ullmann, Clin. Microbiol. Rev. 11 (1998) 589–603.
[2] P. Gilbert, J. Das, I. Foley, Adv. Dent. Res. 11 (1997) 160–167.
[3] G. Wolfaardt, J.R. Lawrence, D.R. Korber, in: J. Wingender, T.R. Neu, H.C. Flemmin (Eds.), Microbial extracellular polymeric substances, Springer, Berlin, Germany, 1999, pp. 171–200.
[4] National Institutes of Health, Research on Microbial Biofilms (PA-03-047), National Institutes of Health, 2002.
[5] S.S. Branda, A. Vik, L. Friedman, R. Kolter, Trends Microbiol. 13 (2005) 20–26.
[6] K. Czaczyk, K. Myszka, Pol. J. Environ. Stud. 16 (2007) 799–806.
[7] I.W. Sutherland, Trends Microbiol. 9 (2001) 222–227.
[8] M.E. Davey, G.O. O'Toole, Microbiol. Mol. Biol. Rev. 64 (2000) 847–867.
[9] J.A. Bohn, J.N. BeMiller, Carbohydr. Polym. 28 (1995) 3–14.
[10] M. Okazaki, Y. Adachi, N. Ohno, T. Yadomae, Biol. Pharm. Bull. 18 (1995) 1320–1327.
[11] I.K. Sen, A.K. Mandal, R. Chakraborty, B. Behera, K.K. Yadav, T.K. Maiti, S.S. Islam, Carbohydr. Polym. 101 (2014) 188–195.
[12] O. Guetta, K. Mazeau, R. Auzely, M. Milas, M. Rinaudo, Biomacromolecules 4 (2003) 1362–1371.
[13] M. Ratto, A. Mustranta, M. Siika-aho, Appl. Microbiol. Biotechnol. 57 (2001) 182–185.
[14] P.M. Bales, E.M. Renke, S.L. May, Y. Shen, D.C. Nelson, PLoS ONE 8 (6) (2013) e67950.
[15] Q. Yu, S.P. Nie, J.Q. Wang, P.F. Yin, D.F. Huang, W.J. Li, M.Y. Xie, Food Chem. Toxicol. 66 (2014) 14–22.
[16] F.L. Yang, Y.L. Yang, P.C. Liao, J.C. Chou, K.C. Tsai, A.S. Yang, F. Sheu, T.L. Lin, P.F. Hsieh, J.T. Wang, K.F. Hua, S.H. Wu, J. Biol. Chem. 286 (2011) 21041–21051.
[17] P.F. Hsieh, T.L. Lin, F.L. Yang, M.C. Wu, Y.J. Pan, S.H. Wu, J.T. Wang, PLoS ONE 7 (3) (2012) e33155.
[18] D.C. Straus, D.L. Atkisson, C.W. Garner, Infect. Immun. 50 (1985) 787–795.
[19] T. Yokochi, I. Nakashima, N. Kato, Microbiol. Immunol. 21 (1977) 601–610.
[20] I.K. Sen, A.K. Mandal, S. Chakraborti, B. Dey, R. Chakraborty, S.S. Islam, Int. J. Biol. Macromol. 62 (2013) 439–449.
[21] J. Zhang, Z. Liu, S. Wang, P. Jiang, Appl. Microbiol. Biotechnol. 59 (2002) 517–522.
[22] W.S. York, A.G. Darvill, M. McNeil, T.T. Stevenson, P. Albersheim, Methods Enzymol. 118 (1986) 3–40.
[23] C. Hara, T. Kiho, Y. Tanaka, S. Ukai, Carbohydr. Res. 110 (1982) 77–87.
[24] I.K. Sen, P.K. Maji, B. Behera, T.K. Maiti, P. Mallick, S.R. Sikdar, S.S. Islam, Int. J. Biol. Macromol. 53 (2013) 127–132.
[25] G.J. Gerwig, J.P. Kamerling, J.F.G. Vliegenthart, Carbohydr. Res. 62 (1978) 349–357.
[26] I. Ciucanu, F. Kerek, Carbohydr. Res. 131 (1984) 209–217.
[27] S. Chattopadhyay, S.K. Das, T. Ghosh, S. Das, S. Tripathy, D. Mandal, D. Das, P. Pramanik, S. Roy, J. Biol. Inorg. Chem. 18 (2013) 957–973.
[28] Q.B. Saxena, E. Mezey, W.A. Adler, Int. J. Cancer 26 (1980) 413–417.
[29] G. Garcia, M. Humbert, F. Capel, A.C. Rimaniol, P. Escourrou, D. Emilie, V. Godot, Allergy 62 (2007) 170–177.
[30] V. Vichai, K. Kirtikara, Nat. Protoc. 1 (2006) 1112–1116.
[31] O.H. Lowry, N.J. Rosenbrough, A.L. Farr, R.J. Randall, J. Biol. Chem. 193 (1951) 255–275.
[32] P. Maity, A.K. Nandi, I.K. Sen, M. Pattanayak, S. Chattopadhyay, S.K. Dash, S. Roy, K. Acharya, S.S. Islam, Carbohydr. Polym. 114 (2014) 157–164.
[33] S.K. Mahapatra, S.P. Chakraborty, S. Majumdar, B.G. Bag, S. Roy, Eur. J. Pharmacol. 623 (2009) 132–140.
[34] H. Ohkawa, N. Ohishi, K. Yagi, Anal. Biochem. 95 (1979) 351–358.
[35] P.K. Agrawal, Phytochemistry 31 (1992) 3307–3330.
[36] M. Rinaudo, M. Vincendon, Carbohydr. Polym. 2 (1982) 135–144.
[37] S. Mandal, S. Patra, B. Dey, S.K. Bhunia, K.K. Maity, S.S. Islam, Carbohydr. Polym. 84 (2011) 471–476.
[38] D. Das, S. Maiti, T.K. Maiti, S.S. Islam, Carbohydr. Polym. 92 (2013) 1243–1248.
[39] K. Chandra, K. Ghosh, A.K. Ojha, S.S. Islam, Carbohydr. Res. 344 (2009) 2188–2194.
[40] Z.A. Popper, I.H. Sadler, S.C. Fry, Phytochemistry 57 (2001) 711–719.
[41] V. Cano, D. Moranta, E. Llobet-Brossa, J.A. Bengoechea, J. Garmendia, BMC Microbiol. 9 (2009) 56.
[42] L.G. Wood, P.G. Gibson, M.L. Garg, Eur. Respir. J. 21 (2003) 177–186.

Journal of Bioscience and Bioengineering
VOL. 115 No. 1, 76–81, 2013

ELSEVIER

www.elsevier.com/locate/jbiosc

Partial characterization and flocculating behavior of an exopolysaccharide produced in nutrient-poor medium by a facultative oligotroph *Klebsiella* sp. PB12

Amit Kumar Mandal,[1] Krishna Kant Yadav,[1] Ipsita Kumar Sen,[2] Arvind Kumar,[1] Soumyananda Chakraborti,[3] Syed Sirajul Islam,[2] and Ranadhir Chakraborty[1,*]

Department of Biotechnology, Omics Laboratory, University of North Bengal, Siliguri 734013, West Bengal, India,[1] Department of Chemistry and Chemical Technology, Vidyasagar University, Midnapore 721102, West Bengal, India,[2] and Department of Biochemistry, Bose Institute, Kolkata 700054, West Bengal, India[3]

Received 25 February 2012; accepted 7 August 2012
Available online 1 September 2012

A facultative oligotrophic strain from the water sample of River Mahananda, Siliguri India was selected for its property to produce exopolysaccharide (EPS) in nutrient-poor (oligotrophic) medium. Viability assay of the strain was performed in sterile liquid LB, R2A, river water and diluted (10^{-3}) LB at 30°C and pH 7 to understand oligotrophy. The selected strain was identified by 16S rRNA gene sequencing and designated as *Klebsiella* sp. PB12. Phylogenetic analysis showed its closest relationship with *Klebsiella variicola* ATCC BAA-830^T. Purification of EPS was performed by ethanol precipitation, dialysis and freeze-drying. Chemical analysis revealed that purified EPS was mainly composed of 72.32% (w/w) neutral sugar and 14.12% (w/w) uronic acids. Fourier transform infrared (FT-IR) spectroscopy indicated the presence of hydroxyl, carboxylic and methoxyl functional groups. The optimal dosages for flocculation of activated carbon suspension were 17 mg/l EPS and 4 mM $CaCl_2$. EPS showed flocculating rate of above 80% over a wide range of pH (pH 3–10) whereas, more than 90% rate was noted in the temperature range (10–50°C) tested in presence of $CaCl_2$. Moreover, EPS showed characteristic emulsifying activity with toluene (66.6%), *n*-hexadecane (65%), olive oil (63.3%) and kerosene (50%). The apparent molecular weight of the EPS was ~2 × 10^5 Da.

[**Key words:** Exopolysaccharide (EPS); *Klebsiella* sp. PB12; Oligotrophic bacteria; Fourier transform infrared (FT-IR); Flocculating rate]

Water pollution is one of the major problems these days and researchers are trying to solve this problem. Flocculants used in water treatment can be classified into three groups: (i) inorganic flocculants such as alum, ferric flocculants or polyaluminum chloride; (ii) synthetic organic flocculants like polyacrylamide derivatives or polyethylene imine; and (iii) naturally occurring flocculants like sodium alginate or microbial flocculants. Some inorganic and synthetic organic flocculants are carcinogenic and neurotoxic. Polyferric sulfate flocculant can be costly and the resultant excess iron may cause unpleasant taste, odor, color etc. Although synthetic flocculants are used because of their cost effectiveness, they are not biodegradable and are some of their degraded monomers such as acrylamide are neurotoxic and even show strong carcinogen (1). Bioflocculants are generally non-toxic and biodegradable. Most of the reported bioflocculants are principally comprised of exopolysaccharide (EPS).

Growth and survival of bacteria are often influenced by EPS produced by them. Literature reveals varied functional aspects of EPS, more commonly the formation of flocs, substrate attachment, resistance to heavy metals and antimicrobials, protection against environmental stresses, and localization of extracellular enzymes (2–6). Oligotrophic bacteria can survive in extremely nutrient-depleted environment. There are speculations that production of exopolymeric substances by bacteria growing under extremely nutrient-poor conditions (where these nutrients are available at levels below threshold concentrations) might aid in concentrating the nutrient for sustenance (7,8). Carbon sources generally used in culture media for bioflocculant production have direct impact on production cost of bioflocculants which limits the market potential of these biopolymers. Strains like *Bacillus* sp. F19 or *Proteus mirabilis* TJ1 when grown in high-nutrient media produced 1.47 or 1.33 g/l EPS (9,10). Therefore, strains which are able to produce EPS in nutrient poor condition would be an advantage from industrial point of view. Attempts are being done to search novel strains capable of producing EPS in low substrate containing medium (11,12).

In the present study, a facultative oligotrophic strain *Klebsiella* sp. PB12 isolated from River Mahananda in Siliguri, India, yielded 1.3 g/l of EPS in nutrient-poor medium. EPS was purified and the major components and functional groups were examined by chemical analysis and Fourier transform infrared (FT-IR), respectively. The optimal conditions for flocculation of activated carbon suspension were also ascertained.

MATERIALS AND METHODS

Screening and characterization of an exopolysaccharide-producing bacterium Composite water samples were collected using standard

* Corresponding author. Tel.: +91 0353 2776354; fax: +91 0353 2699001.
E-mail address: rcnbu2003@yahoo.com (R. Chakraborty).

1389-1723/$ – see front matter © 2012, The Society for Biotechnology, Japan. All rights reserved.
http://dx.doi.org/10.1016/j.jbiosc.2012.08.006

methodology (13) from a single sampling station on River Mahananda underneath the Mahananda Bridge, Siliguri, India. Serial dilutions of water samples were made in filtered (water passed through 0.2 μm filter, Millipore, Sydney, Australia) and autoclaved river water and plated on diluted (10^{-3} or 0.001×) Luria Bertani (LB) agar plates (HiMedia M575, India) (nutrient poor). After incubation at 30°C for 72 h, culturable oligotrophic bacterial colony-forming units (CFU) were obtained. Purification of single colonies was done by dilution streaking on 0.001× LB agar plates. Single colony cultures were maintained on R2A agar (HiMedia M1687) which is a standard environmental cultivation medium. Master plate made up of R2A agar was constructed with purified single colonies. Each master plate was replicated separately in triplicate on LB, 0.001× LB, and R2A agar plate. Colonies that had grown on 0.001× LB agars but not on LB agar were termed as obligate oligotrophs, whereas colonies that were able to grow on all the three different plates were termed as facultative oligotrophs (14). Pure colonies of each facultative oligotrophic isolates (capable of forming mucoid and ropy colonies in R2A) were then inoculated into 50 ml of screening medium (R2A) in 250 ml Erlenmeyer flask, incubated at 30°C in a rotary shaker at 160 rpm for 48 h. Flocculating properties of culture broth from different isolates were examined using two different suspensions (kaolin and activated carbon) following standard method (15,16). High concentration of Ca^{2+} (50 mM) was required for flocculation of kaolin suspension, whereas only 4 mM Ca^{2+} was required for flocculation of activated carbon.

Hence, one isolate, named PB12, with high flocculating rate for activated carbon suspension was selected as test strain for further study. Viability of the test strain in different media was also performed at 30°C to examine the nature of oligotrophic growth. Briefly, inoculum was prepared by transferring a single colony of 24 h old culture of PB12 into 10 ml sterile R2A (pH 7) in 100 ml Erlenmeyer flask. The inoculated medium was incubated at 30°C for 12 h with agitation (160 rpm). The culture was harvested by centrifuging at 10,000 ×*g* for 5 min at 4°C and washed twice with sterile saline (0.5% NaCl) water to remove traces of media. The washed pellet was finally suspended in 3 ml sterile saline water. Aliquot of 1.0 ml of concentrated (1×10^7 CFU/ml) cell suspension(s) was added to 25 ml of sterile LB or R2A or river water or 0.001× LB in 250 ml Erlenmeyer flask. The flasks were kept at 30°C (with shaking; 160 rpm) throughout the period of investigation. Survivability of PB12 cells in each tested medium was assessed through dilution-plating at different time intervals on fresh LB agar plates.

Whole cell DNA of PB12 cells, amplification of 16S rRNA gene sequence, purification of PCR product and cloning were done as described earlier (14). PCR product was sequenced with primers 27F and 1492R using BDT v3.1 cycle sequencing kit on ABI 3730x1 Genetic Analyzer following the manufacturer's recommendations. 16S rRNA gene sequence was used to carry out BLAST with the database of National Center for Biotechnology Information (NCBI, http://blast.ncbi.nlm.nih.gov/Blast.cgi). The 16S ribosomal gene sequences of all the known species were retrieved from GenBank and multiple alignment was performed with 16S rRNA gene sequence of *Klebsiella* sp. PB12 using CLUSTAL W (17). The resulted multiply aligned sequence was corrected and edited, and approximately 1290 bp long nucleotide stretch of all the *Klebsiella* sp. were selected for further analysis. Rest of the nucleotide sequence from both the ends was omitted due to alignment ambiguities. Sequence alignment, phylogenetic analysis were conducted in the software package MEGA4 (18).

Production and purification of EPS Time course of EPS production was performed in 500 ml flasks containing 100 ml of R2A (pH 7) with 160 rpm agitation at 30°C. Samples were taken every 12 h to measure growth (O.D. at 600 nm), and EPS yield. Purification of EPS was done after incubating the test strain for 48 h in 500 ml flask containing 100 ml R2A. Culture broth was centrifuged at 13,000 ×*g* at 4°C for 20 min to remove the cells. Two volumes of cold ethanol were added to the supernatant to precipitate the EPS. The resulting precipitate was collected by centrifugation at 12,000 ×*g* and 4°C for 20 min, redissolved in distilled water, dialyzed through dialysis tubing cellulose membrane (Sigma–Aldrich, retaining MW >12,400 Da) against deionized double distilled water for 24 h to remove low-molecular weight materials and freeze-dried to obtain purified EPS. To study the effect of various carbon sources on EPS production, R2A medium was supplemented singly with glucose, lactose, sucrose, mannose and arabinose (1% w/v). R2A medium without any supplementation was taken as control. Stock solutions of different carbon sources were filter-sterilized and aseptically added to the sterile medium before inoculation.

Characterization of EPS Neutral sugar and total sugar were determined by anthrone reaction and phenol–sulfuric acid reaction, respectively, using glucose as the standard solution. Uronic acids was determined by carbazole–sulfate reaction using glucuronic acid as standard; and amino sugar was determined by the Elson–Morgan reaction, using glucose amine as standard (19).

Purified EPS was analyzed for α-amino acids and aromatic amino acids by the Ninhydrin reaction and the Xanthoproteic reaction, respectively (20). Electric charge of EPS was determined by precipitation with cetylpyridinium chloride (CPC) (21). The major functional groups were detected using Fourier transform infrared (FT-IR) spectroscopy. Pellets of 2 mg of purified EPS were prepared with KBr followed by pressing the mixture into a 16 mm diameter mold. The infrared spectrum was recorded on Perkin Elmer spectrum GX FT-IR system (Perkin–Elmer, USA) with resolution of 4 cm^{-1} in 4000–400 cm^{-1} region (22). Other test includes solubility test of EPS in aqueous solutions (distilled water, 0.1 M HCl, 3.0 M HCl or NaOH and 0.5 M NaCl) and organic solvents (methanol, ethanol and acetone). EPS was passed through Sepharose 6B gel-permeation column (90 cm × 2.1 cm) using water as eluent with flow rate of 0.4 ml/min (23). A total of 95 test tubes (2 ml each) were collected using Redifrac fraction collector and monitored spectrophotometrically (Shimadzu UV–Vis spectrophotometer, model-1601) at 490 nm using phenol–sulfuric acid method (24). The average molecular weight of EPS was determined by gel-chromatographic technique. Standard dextrans T-200, T-70 and T-40 were passed through a Sepharose 6B column, and the elution volumes were plotted against the logarithms of their respective molecular weights. The elution volume of EPS was then plotted in the same graph, and molecular weight was determined.

Flocculating rate and emulsifying activity measurement Activated carbon was suspended in distilled water at a concentration of 5 g/l at pH 7 and used as a stock solution for the subsequent assays. After the pH of the suspension was adjusted, 0.1 ml of culture supernatant was added and stirred for 2 min. The solutions were allowed to settle for 5 min at room temperature and the optical density (OD) of the clarifying upper phase solution was measured at 550 nm with a UV–VIS spectrophotometer. A control tube in which the culture supernatant was replaced with distilled water was also included and measured under the same conditions. The flocculating rate was determined according to following equation:

$$[(B - A)/B] \times 100\% \quad (1)$$

where A and B are optical densities at 550 nm of the sample and control, respectively. Mean % flocculating rate of three independent experiments was considered.

Toluene, *n*-hexadecane, olive oil, and kerosene oil were used to study the emulsifying activity of the purified EPS according to the procedure described earlier (25). To 3 ml aqueous solution of EPS (1 mg/ml), 3 ml of hydrocarbon or oil was added and agitated vigorously for 2 min on vortex. The emulsion and aqueous layers were measured after 24 h and emulsification index (E24) was calculated by the following formula (26):

$$E_{24} = \text{volume of the emulsion layer/total volume} \times 100 \quad (2)$$

Effect of dosage, temperature, pH and metal cations on the flocculating rate The effects of EPS and $CaCl_2$ dosage, temperature, pH and metal ions on flocculating rate were examined. The dosage of EPS and $CaCl_2$ were varied from 1 to 30 mg/l and 0–100 mM, respectively. The pH of the activated carbon suspensions was adjusted using HCl and NaOH in the pH range of 1–11. The temperature of activated carbon suspension was changed in water bath in the range of 10–100°C. The effects of various metal cations (monovalent: NaCl, KCl; divalent: $MgCl_2 \cdot 6H_2O$, $MnCl_2 \cdot 6H_2O$, $CoCl_2 \cdot 6H_2O$, $NiCl_2 \cdot 6H_2O$, $ZnSO_4 \cdot 7H_2O$, $CuSO_4 \cdot 5H_2O$, $CdCl_2 \cdot H_2O$; and trivalent: $FeCl_3 \cdot 6H_2O$ in the range of 0–100 mM concentration) on flocculation of activated carbon suspension were also studied.

RESULTS AND DISCUSSION

Oligotrophic and phylogenetic characterization of the test strain, PB12 The strain PB12 showed highest flocculating rate (98%) amongst ten exopolysaccharide producing isolates. Hence, the test strain used in this study was PB12. It was straight rod 1–2 μm, gram-negative, non-motile, facultative anaerobic belonging to class γ-Proteobacteria of family Enterobacteriaceae. Colonies were circular, convex, translucent, mucoid, sticky and off-white in color with diameters of 2.0–3.0 mm after 3 days at 37°C on R2A agar. Fig. 1A shows the viability of PB12 in 0.001× LB, river water, R2A and LB broth. PB12 cells were able to grow in 0.001× LB broth as well as sterile river water without supplementation of any carbon or nitrogen source or growth factors. An increment of nearly 13 times the initial cell number was noted in a span of 3 days in 0.001× LB. In earlier reports, facultative oligotrophic strains, *Acinetobacter johnsonii* MB52 and *Klebsiella pneumoniae* MB45 showed an increase of 2.5 and 4.6 times the initial cell number when grown in 0.001× LB in the span of 8 and 2 days, respectively (14,27). The ability of *Klebsiella* sp. PB12 to survive without any reduction in viable cell number from the input cells explains the oligotrophic nature. The strain PB12 did not produce EPS in nutrient-rich (LB) medium while a nutrient-poor medium (R2A) supported the production. Yield of EPS in R2A varied with time and was maximal (1.3 g/l) at 48 h of incubation at 30°C (Fig. 1B). The depletion in the amount of EPS was noticed after 48 h indicating probable utilization of the same as nutrient source for cell growth and viability. Probable utilization of EPS as carbon source was also observed by earlier authors (28). A decrease in approximately 31% of EPS during

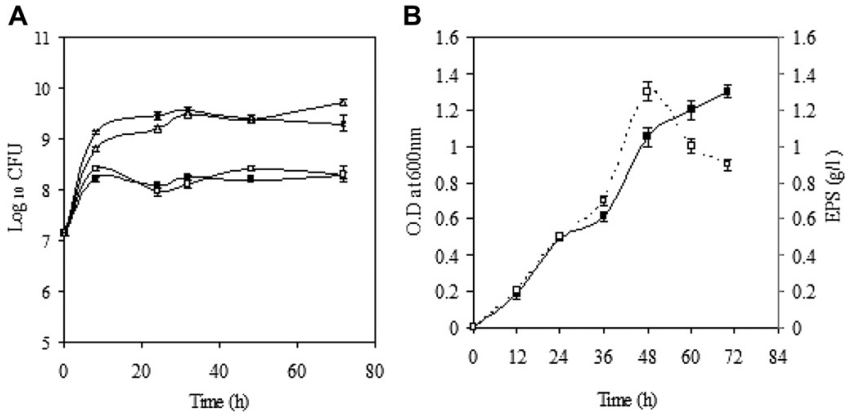

FIG. 1. (A) Viability of PB12 in sterile liquid LB (closed triangles), R2A (open triangles), river water (open squares) and 0.001× LB (closed squares) at 30°C. (B) Growth (closed squares; O.D at 600 nm) and EPS production (open squares; g l^{-1}) of *Klebsiella* sp. PB12 in R2A (nutrient poor) broth at 30°C, pH 7.2 ± 0.2. Data are the mean of triplicates ± S.E.

further incubation beyond 48 h (from 48 h to 72 h) in the same batch culture was associated with two times increment in viable cell number (Fig. 1A and B).

Nearly complete 16S rRNA gene sequence (1497 bp) was amplified, cloned and sequenced. BlastN search of the 16S rRNA gene sequence (accession no. HM989848) of the isolate PB12 shows maximum identity (99%) with the 16S rRNA gene sequence of *Klebsiella* sp. strain MB42 and uncultured *Klebsiella* sp. clone SL13 (GenBank accession nos. FR677020 and HQ264073, respectively). In the neighbor-joining tree (Fig. 2) strain PB12 formed deep branching with *Klebsiella variicola* ATCC BAA-830^T (99% 16S rRNA gene sequence similarity) within the cluster comprising *Klebsiella granulomatis* KH 22^T (AF010251), *Klebsiella alba* LMG 24441^T (EF154517), *K. pneumoniae* subsp. *pneumoniae* ATCC 13883^T (AF130981) and *Klebsiella singaporensis* LX3^T (AF250285). The same output was obtained in maximum-parsimony tree (data not shown).

Effect of supplementation of carbon source in R2A medium on growth and EPS production Growth and production of EPS in R2A was enhanced maximally by 62% and 38.4%, respectively, when supplemented with 1% glucose. When supplemented with 1% lactose, growth and production was enhanced by 43% and 30%, respectively. In sucrose and rhamnose supplemented R2A, the growth was negligibly affected but the EPS production was enhanced roughly by 18%. Growth was enhanced by 43% with only 8% increase in EPS production when grown in arabinose supplemented R2A medium (Fig. 3). Least alteration in growth or EPS production occurred in mannose supplemented R2A medium. Supplementation of glucose in nitrogen-free Burk's medium was found to be the best for EPS production by *Azotobacter* sp. SSB81 (28). In case of *Chryseobacterium daeguense* W6, supplementation of mannose or maltose or glucose in low nutrient medium were favorable carbon source for both production of EPS and cell growth (29).

Characterization of the purified EPS Purified EPS was mainly composed of 72.32% (w/w) neutral sugar, uronic acids 14.12% (w/w) (Table 1). The EPS was further classified according to its electric charge. The precipitation which occurs after addition of 10% CPC to the EPS solution indicated that it contain acidic groups in its structure due to the interaction with quaternary ammonium

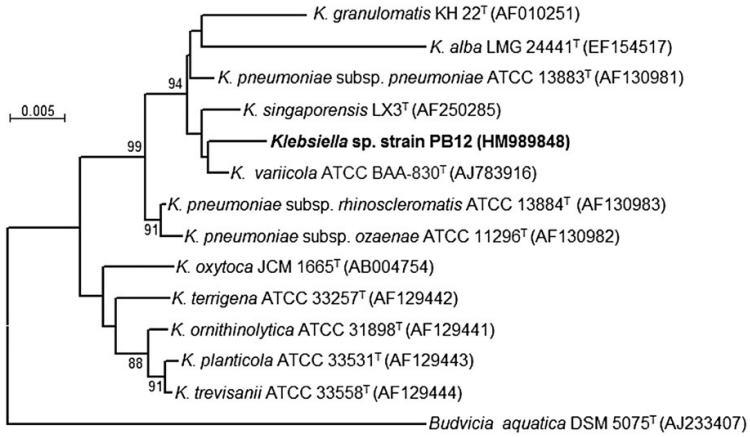

FIG. 2. 16S rRNA gene sequence based neighbor-joining tree, showing the position of *Klebsiella* sp. PB12 (bold face) among the members of genus *Klebsiella*. Bootstrap percentages (>80) are given at the branching nodes. *Budvicia aquatica* DSM 5075^T (AJ233407) was used as outgroup. EMBL/GenBank accession numbers are given in parentheses. Bar: 0.05% sequence divergence.

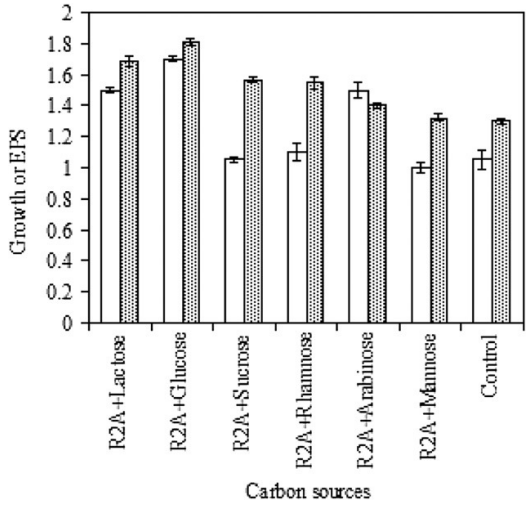

FIG. 3. Effect of carbon source (1%) on growth (open columns) and EPS production (grid columns) at 30°C. Data are the mean of triplicates ± S.E.

TABLE 1. Components of purified EPS obtained from *Klebsiella* sp. PB12.

Method	Item analyzed	% (w/w)
Qualitative test		
(a) Xanthoproteic reaction	Aromatic amino acids	Not detected
(b) Ninhydrin reaction	α-Amino acids	Not detected
Quantitative test		
(a) Anthrone reaction	Neutral sugar	72.32
(b) Phenol–sulfuric acid reaction	Total sugar	76.40
(c) Carbazole–sulfuric acid reaction	Uronic acids	14.12
(d) Elson–Morgan reaction	Amino sugar	Not detected

cation (QN^+) of CPC, resulting in the formation of cetylpyridinium chloride–polysaccharide complex. FT-IR analysis of the EPS showed the presence of hydroxyl (3384 cm^{-1}), weak C–H band at 2930 cm^{-1}, carboxyl (1616 cm^{-1} and 1408 cm^{-1}) and methoxyl (1077 cm^{-1}) groups (Fig. 4) (16,30,31). The presence of C=O group as revealed in FT-IR may play an important role in flocculation and can serve as binding sites for divalent cations.

The EPS obtained from *Klebsiella* sp. PB12 was soluble in all tested acidic (HCl) or basic (NaOH) solutions and in NaCl, but insoluble in tested organic solvents. A single fraction (test tubes nos. 24–32) was obtained after fractionating the EPS obtained from *Klebsiella* sp. PB12 through Sepharose 6B column. The molecular weight of the polysaccharide was estimated $\sim 2 \times 10^5$ Da from a calibration curve prepared with standard dextrans.

Emulsifying activity measurement The EPS showed characteristic emulsifying activity with toluene (66.6%), *n*-hexadecane (65%), olive oil (63.3%) and kerosene (50%). Emulsifying activities against hydrophobic compounds like *n*-hexadecane, toluene and olive oil were well comparable with emulsification index for the EPS produced by gram-negative bacteria *Pseudomonas oleovorans* (32).

Effect of dosage, pH, temperature and metal ions on the flocculating rate Effect of higher or lower dosage of both $CaCl_2$ and EPS on flocculating rate was studied in order to determine optimal dosage. The flocculating rate of 98% was achieved with EPS dosage of 17 mg/l and 4 mM $CaCl_2$ at pH 7. An EPS produced by a micro-alga, *Gyrodinium impudicum* KG03 required 7 mM $CaCl_2$ for maximum flocculation (61%) of activated carbon (33). Higher or lower dosage of EPS and $CaCl_2$ caused poor flocculation (Fig. 5A and B). Results showed that at lower EPS dosage ineffective bridging caused poor flocculation; on the other side, over-addition of negatively charged EPS caused incomplete dispersion of excess EPS leading to poor stability (16). The relationship between EPS dosage and flocculating rate was similar to the results described by earlier authors (9,16).

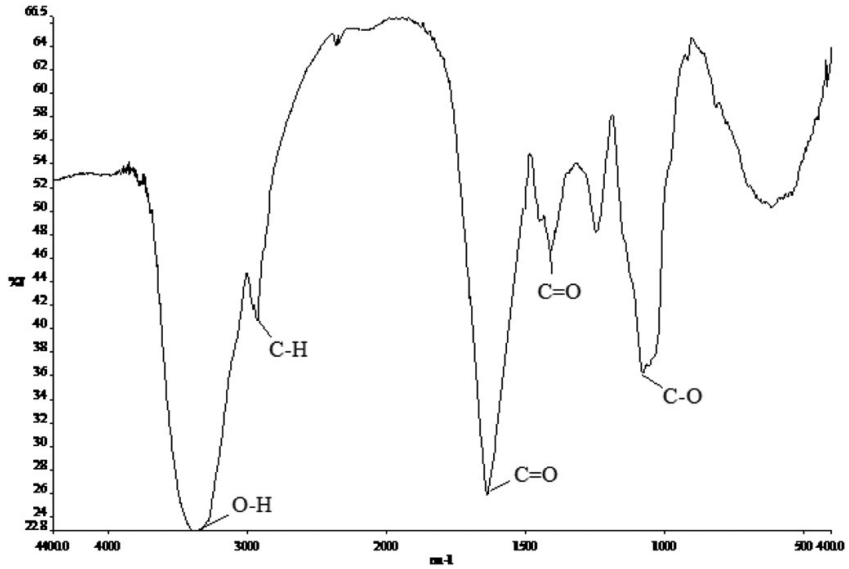

FIG. 4. FT-IR spectra of purified EPS.

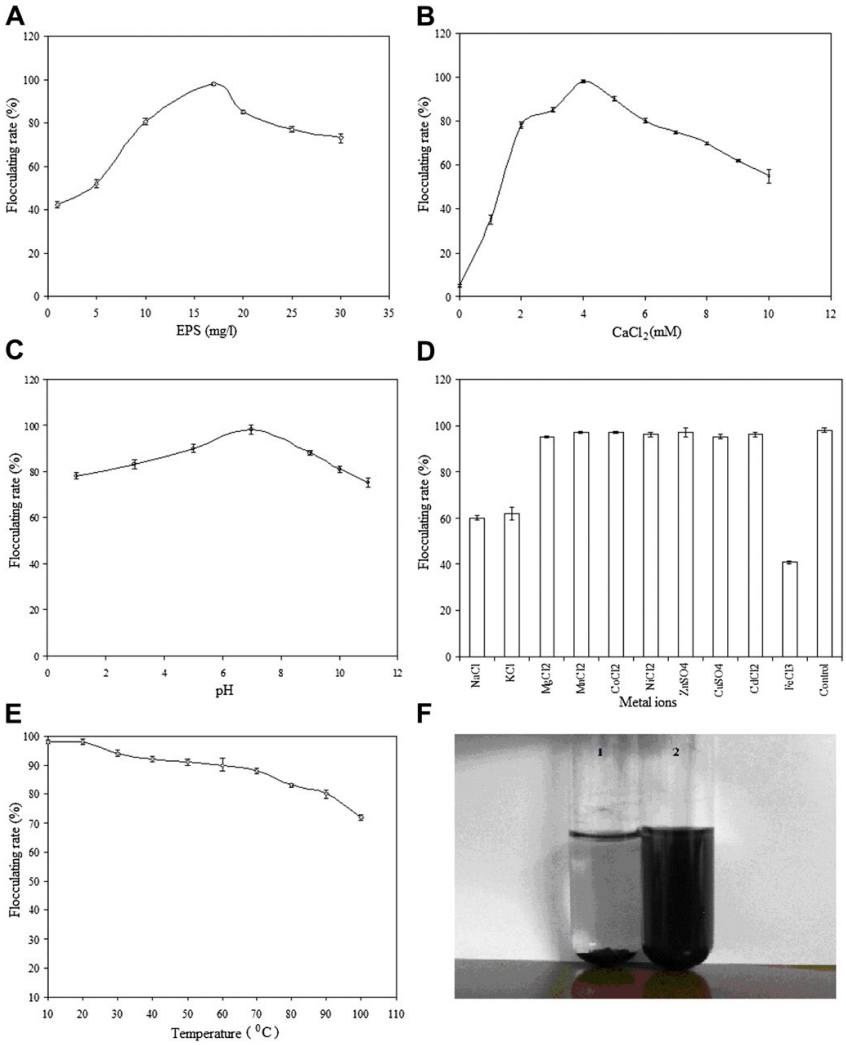

FIG. 5. (A) Effect of EPS dosage on flocculating rate. (B) Effect of $CaCl_2$ concentration or dosage on flocculating rate. (C) Effect of pH on flocculating rate in presence of 4 mM $CaCl_2$. (D) Effect of various metal cations on flocculating rate. (E) Effect of temperature on flocculating rate and (F) photograph showing flocculation of activated carbon in 5 min; sample 1: with EPS; sample 2: without EPS. Data are the mean of triplicates ± S.E.

In the pH range of 3–10, flocculating rates were above 80% showing maximum (98%) at pH 7 in presence of 4 mM $CaCl_2$ (Fig. 5C). In alkaline condition, the flocculating rate decreases, suggesting that increase in OH^- concentration causes increment of negative charge density on activated carbon particles and consequently the neutralizing effect of $CaCl_2$ gets inhibited resulting in dispersion of suspended particles. In the absence of Ca^{2+} ion no effective flocculation was observed at pH 7 which dictates the requirements of $CaCl_2$ for effective flocculation by forming Ca^{2+} mediated complexes of the EPS and activated carbon (34).

Effects of various cations other than Ca^{2+} on the flocculating rate of the EPS were studied (Fig. 5D) and compared with the flocculating rate in presence of $CaCl_2$ (control). The optimal concentration of Mg^{2+} or Mn^{2+} or Co^{2+} or Ni^{2+} or Zn^{2+}or Cu^{2+} or Cd^{2+} was found to be 4 mM (same as that Ca^{2+}) whereas, the optimal concentration of Fe^{3+} was 1 mM and for monovalent cations, Na^+ and K^+, the optimum dosage was 10 mM. The choice of using $CaCl_2$ over $FeCl_3$ in flocculation studies was due to the ease of handling the Ca^{2+} induced large and compact floc in contrast to the gelatinous floc produced by Fe^{3+}. Results showed that the flocculating rates determined with divalent cations Mn^{2+}, Co^{2+}, Ca^{2+}, Zn^{2+}, Cd^{2+}, Cu^{2+}, and Ni^{2+} were better than other tested cations. The flocculating rate in presence of Fe^{3+} was 53% lesser than that of Ca^{2+} induced flocculation. This may be because of its effect on changing the surface charge of activated carbon particle and coverage the EPS adsorb-sites. The competition of the positively charged particles and less adsorb sites reduce the flocculation efficiency (9,35). Such reduction in flocculation was also noted when excess of $CaCl_2$ was added; may be because of the similar phenomenon (Fig. 5B). Monovalent cations like K^+ and Na^+ are less effective for flocculation due to weaker electrostatic force of attraction between monovalent cations and EPS (36).

Effect of temperature on flocculating rate was studied. The flocculating rate remained above 90% in the temperature range of 10–50°C. Maximum flocculation of 98% was observed in both 10°C and 20°C (Fig. 5E). EPS produced by *C. daeguense* W6 in nutrient-poor medium have shown flocculating rates above 90% in the temperature range of 0–45°C with maximum of 97% at 15°C (29). When temperature was increased to 100°C, a decrease of approximately 26% from the maximum flocculation rate was observed; such decrease (26%) at 100°C from the maximum value was observed with EPS produced by *Bacillus mojavensis* 32A (37). Decrease in flocculating rate at higher temperature (above 60°C) could be explained by simultaneously rise in kinetic energy of activated carbon particles due to heating effect.

The EPS produced by the oligotrophic bacterium PB12 could be an effective replacement of a commercial polymer with regard to flocculation. The high flocculation rate of PB12-EPS over a wide range of temperature (10°C–50°C) and pH (3 to 10) possess a promise for application in water treatment and other biotechnological applications including metal processing industries.

ACKNOWLEDGMENTS

The consumables for research work were supported from a research grant (grant number BT/PR-164/BCE/08/448/2006) from (Department of Biotechnology DBT, India). Two of the authors, AKM and IKS, were provided with independent Ph.D fellowships (NBU-JRF/3726/R-2007) and (CSIR-09/599(042)/2011-EMR-I), respectively. One of the authors KKY was self supported for Ph.D. AK was supported by independent Ph.D studentship from DBT, Government of India (Award No. DBT-JRF/05-06/71/29.08.05). Authors are also thankful to Mr. B.K. Tiwary, Omics Laboratory, Department of Biotechnology, University of North Bengal.

References

1. **Yokoi, H., Natsuda, O., Hirose, J., Hayashi, S., and Takasaka, Y.:** Characteristics of a biopolymer flocculant produced by *Bacillus subtilis*, J. Ferment. Bioeng., **79**, 378–380 (1995).
2. **Tago, Y. and Aida, K.:** Exocellular mucopolysaccharide closely related to bacterial floc formation, Appl. Environ. Microbiol., **34**, 308–314 (1977).
3. **Nguyen, L. K. and Schiller, N. L.:** Identification of a slime exopolysaccharide depolymerase in mucoid strains of *Pseudomonas aeruginosa*, Curr. Microbiol., **18**, 323–329 (1989).
4. **Costerton, J. W., Irvin, R. T., and Cheng, K. J.:** The bacterial glycocalyx in nature and disease, Annu. Rev. Microbiol., **35**, 299–324 (1981).
5. **Rudd, T., Sterritt, R. M., and Lester, J. N.:** Mass balance of heavy metal uptake by encapsulated cultures of *Klebsiella aerogenes*, Microb. Ecol., **9**, 261–272 (1983).
6. **Decho, A. W.:** Microbial exopolymer secretions in ocean environments: their role(s) in food webs and marine processes, Oceanogr. Mar. Biol. Annu. Rev., **28**, 73–153 (1990).
7. **Jannasch, H. W.:** Growth of marine bacteria at limiting concentrations of organic carbon in seawater, Limnol. Oceanogr., **12**, 264–271 (1964).
8. **Pahm, M. A. and Alexander, M.:** Selecting inocula for the biodegradation of organic compounds at low concentrations, Microb. Ecol., **25**, 275–286 (1993).
9. **Zheng, Y., Ye, Z. L., Fang, X. L., Li, Y. H., and Cai, W. M.:** Production and characteristics of a bioflocculant produced by *Bacillus* sp. F19, Bioresour. Technol., **99**, 7686–7691 (2008).
10. **Xia, S. Q., Zhang, Z. Q., Wang, X. J., Yang, A. M., Chen, L., Zhao, J. F., Leonard, D., and Jaffrezic-Renault, N.:** Production and characterization of a bioflocculant by *Proteus mirabilis* TJ-1, Bioresour. Technol., **99**, 6520–6527 (2007).
11. **Yang, Y. N., Ren, N., Xue, J. M., Yang, J., and Rong, B. L.:** Mutation effect of MeV protons on bioflocculant bacteria *Bacillus cereus*, Nucl. Instrum. Methods B, **262**, 220–224 (2007).
12. **Wang, S. G., Gong, W. X., Liu, X. W., Lin, T., Yue, Q. Y., and Gao, B. Y.:** Production of a novel bioflocculant by culture of *Klebsiella mobilis* using dairy wastewater, Biochem. Eng. J., **36**, 81–86 (2007).
13. **American Public Health Association:** Standard methods for examination of water and waste water, 17th ed. American Public Health Association, Washington, DC (1989) .
14. **Kumar, A., Mukherjee, S., and Chakraborty, R.:** Characterization of a novel trimethoprim resistance gene, dfrA28, in class 1 integron of an oligotrophic *Acinetobacter johnsonii* strain, MB52, isolated from River Mahananda, India, Microb. Drug Resist., **16**, 29–37 (2010).
15. **Kurane, R., Hatamochi, K., Kiyohara, T., Hirao, M., and Taniguchi, Y.:** Production of a bioflocculant by *Rhodococcus erythropolis* S-1 grown on alcohols, Biosci. Biotechnol. Biochem., **58**, 428–429 (1994).
16. **Suh, H. H., Kwon, G. S., Lee, C. H., Kim, H. S., Oh, H. M., and Yoon, B. D.:** Characterization of bioflocculant produced by *Bacillus* sp. DP-152, J. Ferment. Bioeng., **84**, 108–112 (1997).
17. **Thompson, J. D., Higgins, D. G., and Gibson, T. J.:** CLUSTALW: improving the sensitivity of progressive multiple sequence alignment through sequence weighting, position-specific gap penalties and weight matrix choice, Nucleic Acids Res., **22**, 4673–4680 (1994).
18. **Tamura, K., Dudley, J., Nei, M., and Kumar, S.:** MEGA4: Molecular Evolutionary Genetics Analysis (MEGA) software version 4.0, Mol. Biol. Evol., **24**, 1596–1599 (2007).
19. **Chaplin, M. F. and Kennedy, J. F.:** Carbohydrate analysis: a practical approach. IRL Press, Washington DC (1986).
20. **Plummer, D. T.:** An introduction to practical biochemistry, 2nd ed. McGraw-Hill, London (1978).
21. **Scott, J. E.:** Fractionation by precipitation with quaternary ammonium salts. pp. 38–44, in: Whistler, R. L. (Ed.), Methods in carbohydrate chemistry. General polysaccharides, vol. V. Academic Press, New York (1965) .
22. **Wang, Y., Zhang, M., Ruan, D., Shashkov, A. S., Kilcoyne, M., and Savage, A. V.:** Chemical components and molecular mass of six polysaccharides isolated from the sclerotium of *Poria cocos*, Carbohydr. Res., **339**, 327–334 (2004).
23. **Nandan, C. K., Ramsankar, S., Bhanja, S. K., Mondal, S., and Islam, S. S.:** Structural characterization of a heteropolysaccharide isolated from the rhizomes of *Curcuma zedoaria* (Sati), Carbohydr. Polym., **86**, 1252–1259 (2011).
24. **York, W. S., Darvill, A. K., Mcneil, M., Stevenson, T. T., and Albersheim, P.:** Isolation and characterization of plant cell walls and cell wall components, Methods Enzymol., **118**, 33–40 (1985).
25. **Ashtaputre, A. A. and Shah, A. K.:** Emulsifying property of a viscous exopolysaccharide from *Sphingomonas paucimobilis*, World J. Microbiol. Biotechnol., **11**, 219–222 (1995).
26. **Cooper, D. G. and Goldenberg, B. G.:** Surface active agents from two *Bacillus* species, Appl. Environ. Microbiol., **53**, 224–229 (1987).
27. **Kumar, A., Chakraborti, S., Joshi, P., Chakrabarti, P., and Chakraborty, R.:** A multiple antibiotic and serum resistant oligotrophic strain, *Klebsiella pneumoniae* MB45 having novel dfrA30, is sensitive to ZnO QDs, Ann. Clin. Microbiol. Antimicrob., **10**, 19 (2011).
28. **Gauri, S. S., Mandal, S. M., Mondal, K. C., Dey, S., and Pati, B. R.:** Enhanced production and partial characterization of an extracellular polysaccharide from newly isolated *Azotobacter* sp. SSB81, Bioresour. Technol., **100**, 4240–4243 (2009).
29. **Liu, W., Wang, K., Li, B., Yuan, H., and Yang, J.:** Production and characterization of an intracellular bioflocculant by *Chryseobacterium daeguense* W6 cultured in low nutrition medium, Bioresour. Technol., **101**, 1044–1048 (2010).
30. **Brauer, G. M. and Kline, G. M.:** Chemical analysis, pp. 632–665, in: Mark, H. F., Gaylord, N. G. and Bikales, N. M. (Eds.), Encyclopedia of polymer science and technology, vol. 3. Wiley, New York (1995).
31. **Sawyer, D. T., Heineman, W. R., and Beebe, J. M.:** Chemistry experiments for instrumental methods. Wiley, New York (1984).
32. **Freitas, F., Alves, V. D., Pais, J., Costa, N., Oliveira, C., Mafra, L., Hilliou, L., Oliveira, R., and Reis, M. A.:** Characterization of an extracellular polysaccharide produced by a *Pseudomonas* strain grown on glycerol, Bioresour. Technol., **100**, 859–865 (2009).
33. **Yim, J. H., Kim, S. J., Ahn, S. H., and Lee, H. K.:** Characterization of a novel bioflocculant, p-KG03, from a marine dinoflagellate, *Gyrodinium impudicum* KG03, Bioresour. Technol., **98**, 361–367 (2007).
34. **Kurane, R., Takeda, K., and Suzuki, T.:** Screening for and characteristics of microbial flocculants, Agric. Biol. Chem., **50**, 2301–2307 (1986).
35. **Gong, W. X., Wang, S. G., Sun, X. F., Liu, X. W., Yue, Q. Y., and Gao, B. Y.:** Bioflocculant production by culture of *Serratia ficaria* and its application in wastewater treatment, Bioresour. Technol., **99**, 4668–4674 (2008).
36. **Li, W. W., Zhou, W. Z., Zhang, Y. Z., Wang, J., and Zhu, X. B.:** Flocculation behavior and mechanism of an exopolysaccharide from the deep-sea psychrophilic bacterium *Pseudoalteromonas* sp. SM9913, Bioresour. Technol., **99**, 6893–6899 (2008).
37. **Elkady, M. F., Farag, S., Zaki, S., Abu-Elreesh, G., and Abd-El-Haleem, D.:** *Bacillus mojavensis* strain 32A, a bioflocculant-producing bacterium isolated from an Egyptian salt production pond, Bioresour. Technol., **102**, 8143–8151 (2011).

Colloids and Surfaces B: Biointerfaces 121 (2014) 44–53

Contents lists available at ScienceDirect

Colloids and Surfaces B: Biointerfaces

journal homepage: www.elsevier.com/locate/colsurfb

Bactericidal effect of polyethyleneimine capped ZnO nanoparticles on multiple antibiotic resistant bacteria harboring genes of high-pathogenicity island

Soumyananda Chakraborti[a,1,3], Amit Kumar Mandal[b,2,3], Shamila Sarwar[a], Prashantee Singh[b], Ranadhir Chakraborty[b,*], Pinak Chakrabarti[a,*]

[a] Department of Biochemistry, Bose Institute, P1/12 CIT Scheme VIIM, Kolkata 700054, India
[b] Omics Laboratory, Department of Biotechnology, University of North Bengal, Siliguri 734013, West Bengal, India

ARTICLE INFO

Article history:
Received 14 November 2013
Received in revised form 13 March 2014
Accepted 25 March 2014
Available online 22 May 2014

Keywords:
PEI-capped ZnO nanoparticle
Antibacterial activity
Multiple-antibiotic-resistant bacteria
Reactive oxygen species
Synergistic effect of antibiotics

ABSTRACT

Zinc oxide nanoparticles (ZnO-NP) were synthesized by alcoholic route using zinc acetate as the precursor material and lithium hydroxide as hydrolyzing agent. Further ZnO–PEI NP (derivative of ZnO-NP) was made in aqueous medium using the capping agent polyethyleneimine (PEI). The nanoparticles were characterized by XRD measurements, TEM and other techniques; the weight % of coating shell in the polymer-capped particles was determined by TGA. ZnO–PEI NP is more soluble in water than the uncapped ZnO-NP, and forms a colloidal suspension in water. PEI-capped ZnO-NP exhibited better antibacterial activity when compared with that of uncapped ZnO-NP against a range of multiple-antibiotic-resistant (MAR) Gram-negative bacterial strains harboring genes of high-pathogenicity island. ZnO-NP effectively killed these microorganisms by generating reactive oxygen species (ROS) and damaging bacterial membrane. ZnO–PEI NP at LD_{50} dose in combination with tetracycline showed synergistic effect to inhibit tetracycline-resistant *Escherichia coli* MREC33 growth by 80%. These results open up a new vista in therapeutics to use antibiotics (which have otherwise been rendered useless against MAR bacteria) in combination with minimized dosage of nanoparticles for the more effective control of MAR pathogenic bacteria.

1. Introduction

The discovery of penicillin in 1928 by Sir Alexander Fleming has paved the way for the synthesis of new generation of antimicrobials. Presently antibiotics are manufactured at an estimated scale of about 100,000 t annually worldwide [1]. On the other hand, bacteria have the potential to develop resistance against antibiotics. The abilities of bacteria to utilize various strategies to resist antibiotics are genetically encoded. If a bacterium carries resistance genes to resist more than two antibiotics, it is generally referred to as a multiple-antibiotic-resistant (MAR) bacterium, informally termed a superbug or a super bacterium. Mechanisms by which bacteria avoid the lethality of antibiotics include modification of the antibiotics, not allowing these to enter the cells or by pumping these out at a rate higher than that of its entry, bringing out alterations in the primary site of antibiotic action, and by the production of an alternative target of the antibiotic. Hospital-acquired infections by opportunistic MAR bacteria spread rapidly from one person to another in ICU set-up, and are very difficult to get rid of [2,3]. In spite of the common antibiotic therapy, morbidity and mortality associated with these infections are soaring with time. Mobility of antibiotic-resistance genes (ARGs) in self transmissible plasmids and integrons in environmental strains were evident from earlier studies [4–7]. ARGs are capable of getting transferred to and replicate in a wide range of hosts to encode resistance to clinically relevant antibiotics. Resistance may also occur by the increased expression of genes that code for multidrug efflux pumps, extruding a wide range of drugs [8]. Besides antibiotic resistance, the

* Corresponding authors at: Department of Biochemistry, Bose Institute, P1/12 CIT Scheme VIIM, Kolkata 700054, India. Tel.: +91 3325693253 (PC); Omics Laboratory, Department of Biotechnology, University of North Bengal, Siliguri 734013, West Bengal, India (RC).
E-mail addresses: rcnbu2003@yahoo.com (R. Chakraborty), pinak@jcbose.ac.in, pinak.chak@yahoo.co.in (P. Chakrabarti).
[1] Present address: Department of Signalling Neurobiology and Cancer, Institute Curie, Bat 110, Centre University, 91405 Orsay Cedex, France.
[2] Present address: Department of Microbiology, Vidyasagar University, Midnapore 721102, West Bengal, India.
[3] Authors contributed equally.

http://dx.doi.org/10.1016/j.colsurfb.2014.03.044
0927-7765/

incidence of serum resistance in clinical isolates of pathogenic bacteria is an additional threat. There appears to be a strong correlation between serum resistance and the ability of a variety of Gram-negative bacteria to invade and survive in the human blood stream [9]. New strategies are therefore needed to identify and develop the next generation of drugs or agents to control bacterial infections.

Nanoparticles have been found to be effective against bacterial strains for a long time. Silver is the most utilized nanoparticle against pathogenic strains; however, its application is limited since it has severe toxic side effects. Several groups have established that silver nanoparticles are powerful weapons against the multiple-drug (including antibiotics)-resistant bacteria, such as *Pseudomonas aeruginosa*, ampicillin-resistant *Escherichia coli*, erythromycin-resistant *Streptococcus pyogenes*, methicillin-resistant *Staphylococcus aureus* and vancomycin-resistant *S. aureus* [10]. In addition to these, Namasivayam et al. have recently reported the efficacy of silver nanoparticles against the multidrug resistant *Klebsiella pneumoniae* [11]. Copper oxide (CuO), Titanium dioxide (TiO_2) and Iron oxide (Fe_2O_3) nanoparticles have also found promising applications against the MAR bacterial strains and *Saccharomyces cerevisiae* [12,13]. Although Ag is the most utilized antimicrobial nanoparticle [14], the use of ZnO as an alternative agent is escalating because of its biocompatibility and robustness [13]. Recent studies have shown that these nanoparticles have selective toxicity towards bacteria, but exhibit minimal effects on human cells [15]. It has been reported that ZnO nanoparticles (ZnO-NPs) possesses antibacterial activities against both Gram-positive and Gram-negative bacteria, including major food borne pathogens, such as *E. coli* O157:H7, *Salmonella*, *Listeria monocytogenes*, and *S. aureus* [16]. There are only a few reports demonstrating antibacterial activity of ZnO-NPs against MAR strains [13]. The first evidence of ZnO action against multidrug resistance *S. aureus* came from Jones et al. [17], who found that the killing ability of zinc oxide against multidrug resistance cells increased in the presence of some common antibiotics such as ciprofloxacillin. Although the combination therapy is found useful against multidrug resistance bacteria, the exact mechanism of nanoparticle action still remains ambiguous [18].

A number of studies have indicated that the primary cause of the antibacterial action might be from the disruption of cell membrane [19]. Another possibility could be the induction of extracellular and intracellular reactive oxygen species (ROS), including hydrogen peroxide (H_2O_2) [20]. It was also reported that ZnO can be activated by UV and visible light to generate increasing amounts of ROS, such as •OH, H_2O_2, and O_2^- [21]. Among these radicals, the negatively charged hydroxyl radicals and superoxide cannot penetrate inside the cell membrane and are likely to remain on the cell surface, whereas H_2O_2 can penetrate inside the bacterial cells [22]. Yet another possibility could be the release of toxic Zn^{2+} from the dissolution of NP [12,23].

There have been attempts to increase the dispersion of NPs in bio-compatible solvents by capping ZnO-NPs with polymeric agents, such as chitosan, polyvinyl alcohol (PVA) and polyethyleneimine (PEI) in order to enhance the bactericidal activity [19,24]. PEI was identified as a transfection agent and also for its efficiency to pervade Gram-negative bacterial membrane [25–27]. It was also found that the quaternary polyethyleneimine NP has enduring antibacterial activity against the cariogenic *Streptococcus mutans* [28]. PEI encapsulation also improves the colloidal dispersion and antimicrobial activity of silver NP [29]. However, despite these qualities, the toxicity of PEI always remains a matter of debate. Interestingly, a recent study has revealed that the careful selection of the size of the polymer (PEI) can greatly reduce the toxicity emanating from its cationic nature. It was shown that 10 kDa PEI was particularly efficient in the safe delivery of siRNA and DNA material with minimal or no cytotoxicity to pancreatic cancer cells [30]. Safe use of PEI-polymers or nano ZnO crystals in cell lines, such as FE1 was proposed after quantifying mutagenic activity or its ability to damage cellular DNA by ROS [31]. To improve the bactericidal effect and the stability of nanoparticle in biological fluid we used PEI capping over ZnO and targeted it against MAR bacteria. The rationale behind designing such nano-conjugate is to enhance the internalization rate of NP within the bacterial cells—it has already been established that PEI can specifically target lipopolysacharide present in the outer membrane of Gram-negative bacteria [32].

In this investigation, PEI-capped ZnO-NP was synthesized, characterized and targeted against several enteropathogenic MAR bacteria harboring genes of high-pathogenicity island (HPI). Membrane and DNA damaging potential of ZnO–PEI NP were also assessed using various spectroscopic and imaging techniques. Furthermore, the synergistic antibacterial effect of PEI-capped ZnO-NP at LD_{50} dosage in combination with tetracycline against the MAR bacterium *E. coli* MREC33 was also studied.

2. Materials and methods

2.1. Synthesis and characterization of PEI-capped ZnO nanoparticles

The acetate adsorbed ZnO-NP (i.e., ZnO-Ac NP) was synthesized by modifying the sol–gel route using zinc acetate dihydrate [$Zn(CH_3COO)_2{\cdot}2H_2O$] as the precursor—the details of the synthesis have already been described [33,34]. Unless otherwise specified ZnO-NP and ZnO–PEI NP were suspended in sterile de-ionized water and briefly sonicated before experiments by means of ultrasonic-homogenizer (LABSONIC©, Germany) to prevent any aggregation of nanoparticles.

2.2. Thermogravimetric analysis (TGA) of ZnO–PEI NP

The samples weight was about 2.5 mg and the measurement was carried out under nitrogen atmosphere. Thermogravimetric analysis (TGA) was carried out from room temperature to 700 °C with a heating rate of 10 °C/min using Pyris Diamond TG/DTA (Perkin Elmer, Boston, USA).

2.3. Selection of MAR isolates bearing high-pathogenicity island (HPI) genes

The methods for the isolation, determination of antibiotic resistance/susceptibility and 16S r-RNA gene analysis of the test strains are discussed in Supplementary material Section S1. Each of the MAR isolate was subjected to PCR assay for detection of *irp2* and *fyuA* genes of the core region of the high-pathogenicity island (HPI). (i) Primers for *irp2* gene were (FP), 5′-aaggattcgctgttaccggac-3′ and (RP), 5′-tcgtcgggcagcgtttcttct-3′, and (ii) for *fyuA* gene, 5′-ggcggcgtgcgcttctcgca-3′ and 5′-cgcagtaggcacgatgttgta-3′ [35,36]. The PCR reaction mixture for *fyuA* or *irp2* amplification in 25 μL contained 2.5 μL 10X PCR buffer, 200 μmol/L each dNTP, 1U Taq Pol, 25 pmol of each of both forward and reverse primers of the gene *fyuA* or 7.5 pmol of each of both forward and reverse primers of *irp2* gene, and 7.5 μL of template DNA (obtained from boiling lysis of overnight cultures of the isolates). PCR amplification was done using Bio-Rad DNA Engine, Peltier Thermal Cycler. The following cycling parameters were used: for *fyuA* amplification: 5 min initial denaturation at 95 °C and 30 cycles of denaturation at 95 °C for 1 min; annealing at 58 °C for 1 min and extension at 72 °C for 2 min followed by a final elongation step at 72 °C for 7 min; for *irp2* amplification: denaturing for 7 min at 94 °C, and 35 cycles of 1 min at 94 °C, 1 min at 63 °C and 1 min at 72 °C and a final elongation step for 7 min at 72 °C. Amplicons were observed after electrophoretic

separation in 1.5% agarose gel. Three test strains, YSI6A, HPM13 and MREC33, showing positive amplification of *irp2* and *fyuA* genes, were then selected for further study.′

2.4. Serum bactericidal assay and determination of the virulence factors by multiplex PCR assay

For determining the serum resistance of the three test strains, a simple rapid serum bactericidal assay was performed by the reported methods [37]. Multiplex-PCR assay for the determination of virulence factors was conducted by the method described below. Cells obtained from 100 μL of mid-log phase culture were suspended in 200 μL of sterile distilled water for boiling lysis followed by centrifugation at 10,000 rpm for 10 min to pellet the cell debris. 5 μL of the supernatant was used as the template for the PCR amplification in a total reaction volume of 25 μL. The isolates were subjected to multiplex PCR following published protocols [38]. The primer pairs for genes coding for heat stable toxin ST (*stIa*) and heat labile toxin LT (*elt*) of ETEC (enterotoxigenic *E. coli*) and (*uid*A) of β-glucouronidase were used in Assay no. 1 (n1). Assay no. 2 (n2) was specific for detection of *eae* (structural gene for intimin found in EPEC (enteropathogenic *E. coli*) and *bfp*A (structural gene for bundle-forming pilus) of EPEC, and assay no. 3 (n3) for detecting the presence of stx_1 and stx_2 of shiga-toxin producing EHEC (enterohemorghagic *E. coli*), and *ial* (invasion-associated locus of the invasion plasmid) found in EIEC (enteroinvasive *E. coli*)/*Shigella.* Primers of variant gene *st1b* coding for heat stable toxin of ETEC were included in a separate assay no. 4 (n4) together with *uid*A gene. For detecting the presence of two plasmid genes of EAEC (enteroaggregative *E. coli*), namely *aat* and *agg*R, assay no. 5 (n5) was performed. Amplicons and their sizes were determined by using 100 bp DNA ladder after electrophoretic separation in 2% agarose gel.

2.5. Growth kinetic studies of the test strains in presence of ZnO–PEI nanoparticles

Time dependent growth inhibition studies of the three test strains (MREC33, YSI6A and HPM13) in the presence of varied concentrations of ZnO–PEI nanoparticles were done. From the above growth data, the minimum inhibitory concentration (MIC) and LD_{50} concentration (where 50% bacterial growth was arrested) were calculated. One loopful of bacterial culture from overnight grown slant of each strain was inoculated into 100 mL of LB broth (Himedia, India). From each of the broth culture, 10 μL of mid-log cells were then inoculated in 100 mL of sterile LB broth supplemented with varied concentration of NP (ranging between 10 and 35 μg/mL) similar to an earlier study [39]. Controls, both positive (consisting of NP in LB broth without inoculums) and negative control (consisting of LB broth with bacterial inoculum without any NP) were also used. All the flasks were incubated at 37 °C in a rotary shaker (150 rpm). Growth was measured at different time intervals in terms of absorbance at 600 nm. All the experiments were carried out in triplicate and the mean value was reported. Difference in percentage of viable bacterial cells treated with uncapped ZnO-NP at concentrations equal to MIC obtained for ZnO–PEI NP was also enumerated. Of the three MAR bacteria, one strain, MREC33, resistant to more number of antibiotics in comparison to the other two, was chosen for further study.

2.6. Live/dead viability assay

E. coli MREC33 culture, grown to log phase in LB medium, was treated with NP. Following exposure, the impact on bacterial membrane integrity was assessed using a Live/Dead BacLight bacterial viability kit (Invitrogen) as per instruction provided by the manufacturer. To quantify the relative numbers of live and dead cells, the relative fluorescence intensities were measured using a fluorescence plate reader (excitation at 485 nm, emission at 525 and 625 nm).

2.7. Scanning electron microscopic (SEM) studies

SEM has been used as a tool to characterize surface features of the bacteria on NP treatment. Overnight grown culture of *E. coli* MREC33 (10^8 cells/mL) was washed and re-suspended in PBS, incubated with NP for 6 h at 37 °C. After incubation, cells were fixed with 2% glutaraldehyde and dehydrated with series of ethanol treatments and examined by SEM (FEI Quanta-200 MK2) with an accelerating voltage of 20 kV. Multiple fields of visions were viewed at different magnifications.

2.8. Bacteriolytic effect of ZnO–PEI nanoparticle

ZnO–PEI NP induced damage to *E. coli* MREC33 cells was investigated in the following way. Leakages of proteins, if any, from live MREC33 cells (exponentially growing cells) exposed to ZnO–PEI NP suspended in sterile phosphate-buffered-saline (PBS) were detected by comparing protein profile of similarly suspended cells without NPs (control) [40]. Cells harvested from mid-log phase culture was suspended in PBS and incubated with or without 35 μg/mL ZnO–PEI NP for 12 h at 37 °C. After incubation, cells were centrifuged (8,000 rpm, 4 °C for 10 min) to pellet down the cells. Both cell pellet and the supernatant were analyzed separately. The protein content in the supernatant(s) [abbreviated as SupC (for control) and SupT (for treated) throughout the text] was determined by using Bradford method [41]. On the other hand, each cell-pellet obtained was re-suspended in PBS and subjected to sonication (LABSONIC® M, Sartorius Stedim, Germany) to lyse the bacteria [42]. Lysate obtained after sonication [abbreviated as CelyC (cell lysate from cell pellet of control) and CelyT (cell lysate from cell pellet treated with NP) throughout the text] was collected by centrifugation, and the protein content was measured [41]. The collected protein samples were subjected to 12% SDS-PAGE. The gel was stained by Coomassie brilliant blue R-250 and observed for the protein profile and comparison was made between control and ZnO–PEI NP treated [41,42].

2.9. FTIR spectra of bacterial cells in presence of NP

Alteration in the bacterial cell surface after interaction with NP (35 μg/mL) was established using FTIR spectroscopy. Mid-log *E. coli* MREC33 cells after 6 h of incubation with or without NP were centrifuged for 10 min at 8,000 rpm. The pellets (both treated and untreated) were washed with sterile PBS and lyophilized. Freeze-dried pellets were then subjected to FTIR analysis in the 4000–500 cm^{-1} region under ambient conditions using KBr pellet techniques.

2.10. Determination of extracellular ROS by XTT

XTT [2,3-bis-(2-methoxy-4-nitro-5-sulfophenyl)-2*H*-tetrazolium-5-carboxanilide] assay was used to measure the extracellular reactive oxygen species (ROS) generated by ZnO-NP. In presence of superoxide radical, the dye XTT is reduced to form a colored adduct (XTT formazan) [43]. A fixed concentration of ZnO-NP or its capped analogue (15 μg/mL) was incubated in presence 10 μL XTT. After a fixed time of incubation the suspension was centrifuged and the supernatant was taken for spectroscopic measurement. The identical sets of experiments were also carried out in light and dark to see the difference in ROS generation under these two conditions.

2.11. Determination of intracellular ROS in bacterial cells

Intracellular ROS was measured using dichlorofluorescein diacetate (DCF-DA) [44]. *E. coli* MREC33 cells were grown up to an OD_{600} value of 0.5 in LB medium and then incubated with 30 μg/mL of DCF-DA for 30 min at 37 °C under shaking conditions. DCF-DA loaded cells were then treated with 15 μg/mL of ZnO–PEI NP for 30 min. Cell suspension was centrifuged to pellet the cells. The cell pellet was re-suspended in PBS, and fluorescence values were either measured at an excitation wavelength of 485 nm and emission wavelength of 528 nm using a spectrofluorimeter or visualized under a fluorescent microscope.

2.12. Effect of histidine on antibacterial effect of ZnO–PEI nanoparticles

As ZnO-NPs were reported to be ROS generators, ZnO–PEI NP was evaluated for its mechanism of antibacterial activity due to production of ROS. Growth studies of *E. coli* MREC33, in terms of OD (600 nm) values obtained at different time intervals, were performed in presence and absence of 5 mM histidine (as ROS scavenger) [45] supplemented with or without 15 μg/mL of ZnO–PEI NP.

2.13. Analysis of fragmentation of DNA treated with ZnO–PEI nanoparticles

Plasmid DNA (pMREC33) of *E. coli* MREC33 was incubated for 8 h at 37 °C with 35 μg/mL of ZnO–PEI NP. The DNA was then evaluated on 0.8% agarose gel using ethidium bromide as staining agent, and the DNA pattern generated was documented by a gel documentation system. To further validate our earlier data, NP treated MREC33 cells were stained with 4′,6-diamidino-2-phenylindole (DAPI) and finally subjected to flow cytometry (FACS CALIBUR, Becton Dickinson, USA) analysis to measure DNA fragmentation rate. Flow cytometry analysis was also carried out with control MREC33 cells (cells without any NP treatment).

2.14. Synergistic or additive bactericidal effect of ZnO–PEI nanoparticles with tetracycline

To study the additive or synergistic effect (if any), growth of *E. coli* MREC33 cells in presence of both ZnO–PEI NP (at LD_{50} dose) and tetracycline (20 μg/mL; at concentration which did not affect the growth) was compared with the growth in the presence of LD_{50} dose of ZnO–PEI NP alone (no tetracycline) or growth in the presence of 20 μg/mL tetracycline alone (no ZnO–PEI). *E. coli* MREC33 cells (equal quantity of inoculums) were grown in flasks containing 10 mL LB broth supplemented either singly with 20 μg/mL tetracycline or 15 μg/mL ZnO–PEI NP (LD_{50} concentration), or both ZnO–PEI NP (15 μg/mL) and tetracycline (20 μg/mL). A culture flask containing only inoculums and LB broth, devoid of tetracycline or ZnO-NP was taken as negative control. Growth was measured at different time intervals in terms of absorbance at 600 nm. All the experiments were carried out in triplicate and the mean value was reported.

2.15. Interaction of ZnO–PEI NP with BSA

The flasks containing liquid LB supplemented with or without 35 g/L concentration of BSA were inoculated with log-phase cells of *E. coli* MREC33 and incubated at 37 °C for 4 h to attain an approximate bacterial density of 10^8 CFU/mL. Aliquots of 4 h cultures (prior to addition of ZnO–PEI NP to the same growing culture) were withdrawn, serially diluted in saline water, plated on LB agar and incubated overnight at 37 °C to enumerate the viable cell number present in the culture before the addition of ZnO–PEI NP. To the above 4 h cultures, 35 μg/mL of ZnO–PEI NP was aseptically added to both the flasks with or without BSA and allowed to grow for 12 h at 37 °C. Aliquots from the resultant 16 h cultures were withdrawn, serially diluted and plated on LB agar to quantify the number of surviving (viable) cells. Taking the initial count of viable cells as 100%, the survivability or % killed was then calculated from the final count [46].

3. Results

3.1. Characterization of ZnO–PEI NP

The PEI content in ZnO–PEI NP was determined from the weight loss at 700 °C in N_2 atmosphere using thermogravimetric analysis (TGA), as performed to determine the content of grafted polymers on ZnO-NP [47]. The TGA curve in Fig. S1 reveals that thermal transition occurred in two temperature ranges, 50–120 and 250–450 °C. In the first zone the decrease of weight is 8.2% which may be due to desorption of water molecules. The second weight loss corresponds to the polymer. This illustrates that PEI was grafted on the surface of ZnO NP and the content was 29.5%. Other features characterizing the nanoparticles have already been published and compiled in Table S1.

3.2. Antibiotic resistance/susceptibility profile of the test strains

As per EUCAST (www.eucast.org) criteria for defining antibiotic resistance (*R*)/susceptibility (*S*), the test strains were resistant to multiple antibiotics. Strain YS16A was resistant to ampicillin ($R > 50$ mg/L) and cefepime ($S \leq /R > 1/4$ mg/L) tetracycline ($R > 20$ mg/L) and azithromycin ($R > 10$ mg/L); HPM13 was resistant to ampicillin($R > 50$ mg/L), azithromycin($R > 10$ mg/L), cefepime ($S \leq /R > 1/4$ mg/L), ciprofloxacin ($S \leq /R > 0.5/1$), levofloxacin ($S \leq /R > 1/2$), sulfamethoxazole ($R \geq 15$ mg/L), and tetracycline ($R \geq 20$ mg/L). MREC33 was resistant to ampicillin ($R > 50$ mg/L), azithromycin ($R > 10$ mg/L), cefepime ($S \leq /R > 1/4$ mg/L), cefotaxime ($S \leq /R > 1/4$), ciprofloxacin ($S \leq /R > 0.5/1$ mg/L), kanamycin ($R \geq 10$ mg/L), levofloxacin ($S \leq /R > 1/2$ mg/L), netilmicin ($S \leq /R > 2/4$ mg/L), sulfamethoxazole ($R \geq 15$ mg/L), streptomycin ($R \geq 2.5$ mg/L) and tetracycline ($R \geq 20$ mg/L). (Antibiotics kanamycin and streptomycin are not included in EUCAST table of clinical breakpoints).

3.3. PCR screening of MAR strains for detecting HPI specific genes, irp2 and fyuA

Amplicons were produced with primer pair(s) specific for *irp2* and *fyuA* gene(s) which corresponded to the reported sizes (~280 and ~209 bp for *irp2* and *fyuA* specific amplicon, respectively) in all the three test strains (Fig. S2). MREC33, HPM13 and YSI6A were also found to be serum resistant. The results of the multiplex PCR assays are summarized in Table S2. The assay revealed that YSI6A contains the least number of virulence genes. The assays corresponding to n1 and n4 showed that MREC33 and HPM13 displayed the presence of *uidA*. n2 assay showed the presence of *eae* only in YSI6A, and *bfpA* in MREC33. The n3 assay showed the presence of stx_2 in both YSI6A and MREC33 but not in HPM13. Isolate HPM13 showed the presence of *ial* and aagR in n4 and n5 assays, respectively, while YSI6A and MREC33 did not. None of the isolates showed the presence of five virulence genes *elt*, *stIa*, stx_1, *stlb* and *aat*.

3.4. Characterization of the test strains

On EMB agar plates *E. coli* strain MREC33 produced dark blue, black colonies with metallic green sheen, while *K. pneumoniae*

strain YSI6A produced brown, dark-centered and mucoid colonies. On Mac Conkey agar plates, HPM13 produced colorless colonies. HPM13 also produced red colonies on XLD agar plates, and displayed green and moist colonies on Hektoen enteric (HE) agar surface. HPM13 and MREC33 produced indole and were negative to Voges–Proskauer (VP) and a citrate utilization test, while YSI6A was unable to produce indole, was positive to VP and utilized citrate. BLAST search of the 16S rRNA gene sequence of YSI6A (Ac. no. JQ624587) showed the maximum identity (99%) with the 16S rRNA gene sequence of *K. pneumoniae* strain sctccT53 (Ac. no. HQ622344). 16S rRNA gene sequence of MREC33 (Ac. no. JQ904752) showed maximum identity with *E. coli* strain Y38 (Ac. no. JN578647), whereas HPM13 (Ac. no. JQ904751) showed the maximum identity (99%) with 16S rRNA gene sequence of *Shigella sonnei* strain AU65 (Ac. no. EF032687).

3.5. Growth kinetic studies of the test strains in presence of ZnO–PEI NP

To quantify the antibacterial activity of the synthesized ZnO–PEI NP against HPI specific genes bearing MAR test strains, the LD_{50} of ZnO–PEI NP was determined. LD_{50} values of ZnO–PEI NP for all the three tested strains were found to be 15 μg/mL. Growth was found to be completely arrested at 35 μg/mL of NP (Fig. 1a–c). This bactericidal activity of ZnO–PEI NP was compared with uncapped ZnO NP for all the three MAR strains and the data indicate that former possessed higher antimicrobial potential (Fig. 1d). Based on our observation that ZnO–PEI NP has superior antibacterial activity compared to ZnO-NP, we continued our further study with the former.

3.6. Live/dead viability assay

The viability of MAR bacterial cells in the presence of ZnO–PEI NP was quantified using Live/Dead BacLight Kit (Invitrogen). The kit consists of two stains, propidium iodide (PI) and SYTO9. Green fluorescing dye, SYTO9, due to their small size, is able to enter all cells irrespective of their nature and is used for assessing total cell count, whereas red fluorescing PI (much bulkier in size compared to SYTO9) can only enter into those cells which have compromised cytoplasmic membrane. The live cells with intact membrane (incubation for 30 min) only shows green fluorescence (from SYTO9), as PI remains in the medium. In duration of 1.5 h, in the compromised cells, PI entered the cell and got bound to DNA showing red fluorescence in addition to green fluorescence. Duration of 2.0 h incubation in the presence of ZnO–PEI NP has caused death of the cells due to massive perforation of the membrane. The leakage of SYTO9 from the dead cells resulted in considerable decrease of green fluorescence with concomitant dominance of red fluorescence (due to binding of PI to the nucleic acid) (Fig. 2) [48]. It was observed that the intensity of green fluorescence and red fluorescence (PI) of the analyzed cells changed as a function of time-period of incubation. The intensity of green fluorescence decreased at higher incubation time (2 h) indicating loss of membrane integrity.

3.7. Demonstration of morphological transition and bacterial cell damage on exposure to ZnO–PEI NP

Effects of ZnO–PEI NP on *E. coli* MREC33 cell morphology was examined by scanning electron microscopy. After 3 h exposure of cells to NP (35 μg/mL) in LB broth, rod-shaped *E. coli* cells underwent a dramatic change in structural morphology. SEM studies clearly show that on NP exposure bacterial cells were damaged heavily with disintegrated membrane (Fig. 3).

3.8. Bacteriolytic effect of ZnO–PEI nanoparticles

In order to reveal the lethal action of ZnO–PEI, leakage of cellular proteins due to lysis of membrane was checked. The supernatant of control cells, SupC, (MREC33 cells without any treatment with NP) showed 5% of the protein, whereas 32.42% of protein was noted in SupT (when bacterial cells were treated with 35 μg/mL of ZnO–PEI NP). CelyT contained 67.58% protein compared to 95% in case of CelyC. Increase in protein content of SupT and decrease in protein content of CelyT in NP-treated MREC33 cells clearly indicate the bacteriolytic property of ZnO–PEI NP. SDS-PAGE has also supported the results as indicated by a decrease in the intensity of protein bands in NP treated pellet when compared to that of control pellet (Fig. 4). These data further support the SEM results (Fig. 3) revealing the rupture of cell wall and cavity formation in MREC33.

3.9. Fourier transform infrared study

FTIR is a powerful analytical technique that has been utilized for a long time for microbiological analysis, including identification, studying effects of different antibiotic and cell-nanoparticle interaction [19,49]. FTIR was used here to investigate the effect of ZnO–PEI NP on *E. coli* MREC33, in particular (a) to study the effect of NP on the bacterial protein, and (b) to detect the changes/damages inflicted upon the cell wall on NP exposure.

In the FTIR spectrum of the untreated sample, twin peaks around 1635 cm^{-1} and 1530 cm^{-1} appeared which corresponded to the amide-I and the amide-II bands, respectively, of the protein. Amide-I band primarily represents the carbonyl stretching vibration ν(C=O) in the peptide, while amide II band was assigned to bending vibration of N—H and C—N in amide. On NP treatment we have observed slight shift in amide-I band peak position, which reflects the change in protein structure. The peak around 1070 cm^{-1} actually corresponds to sugar vibration on intact bacterial cell which further blue shifted to 1050 cm^{-1} in presence of NP (Fig. S3). The shift may have resulted from binding of the nanoparticle to the functional groups (LPS) present on the bacterial surface.

3.10. Extracellular ROS generation

Extracellular ROS measurement was performed using XTT assay. XTT is used for colorimetric determination of radical, where the generated radicals reduce the tetrazolium dye, 2,3-bis(2-methoxy-4-nitro-5-sulfophenyl)-2*H*-tetrazolium-5-carboxanilide (XTT) to the highly colored (yellow) XTT formazan. It was found that ZnO–PEI NP generated more amount of ROS compared to uncapped counterpart. It has been found that due to photo-activation of electrons, in the presence of light, the degree of ROS generation increased by several fold for ZnO–PEI NP (Fig. 5a).

3.11. Intracellular ROS generation

Intracellular ROS in the bacterial cells was calculated using dichlorofluorescein diacetate (DCF-DA). In the presence of ROS, the dye gets oxidized and produces intense green fluorescence. It was found that ZnO–PEI NP at a concentration of 35 μg/mL induced significant production of ROS inside the bacterial cell (Fig. 5b). To further validate the phenomenon of bacterial killing by ROS, bacteria were grown in the presence and absence of histidine. Histidine is a known for the ROS scavenging activity [45,39] and our result shows that in the presence of 5 mM histidine, the killing effect of ZnO–PEI was reduced significantly, thereby establishing the involvement of ROS in ZnO–PEI NP mediated killing of bacteria (Fig. 5c).

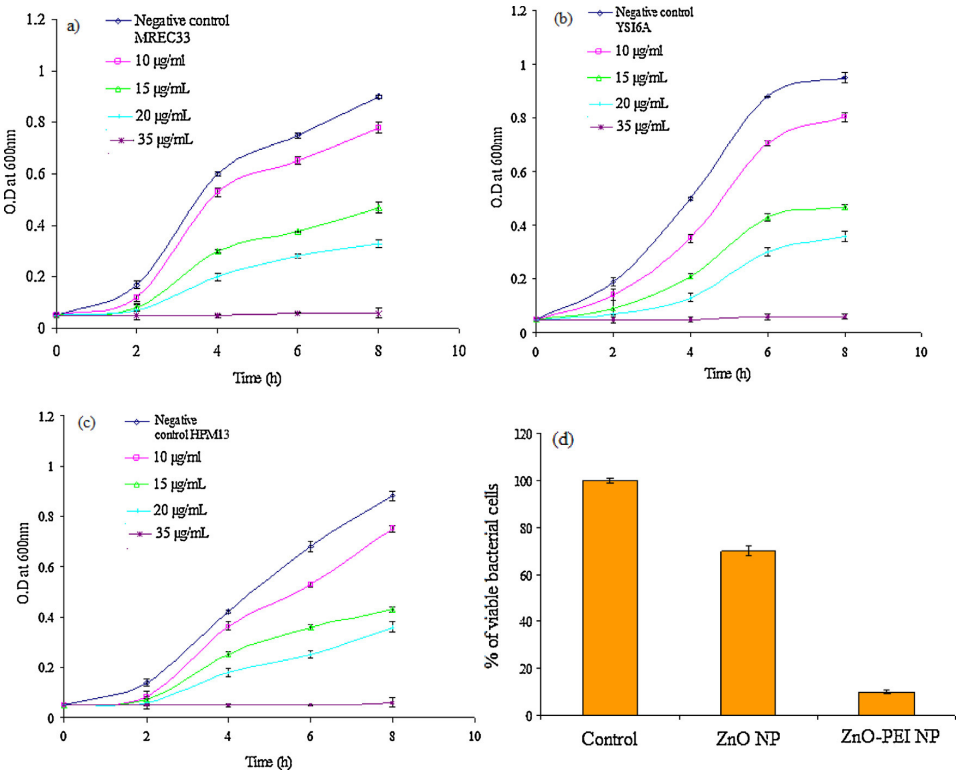

Fig. 1. Growth curves of MAR isolates in LB broth in presence of different concentrations of ZnO–PEI NP; (a) *E. coli* MREC33, (b) *Klebsiella* sp. YSI6A and (c) *Shigella* sp. HPM13. Different concentrations of NP were used: ◊, Negative control (0 μg/mL); □, 10 μg/mL; Δ, 15 μg/mL; +, 20 μg/mL; and *, 35 μg/mL; and (d) % of viable bacterial cells in presence of 35 μg/mL PEI capped ZnO NP or 35 μg/mL uncapped ZnO NP. The data represent the mean ± standard deviation of three independent experiments ($n = 3$).

3.12. DNA fragmentation analysis

The plasmid DNA (pMREC33) isolated from MREC33 DNA was not fragmented whereas the ZnO–PEI NP (35 μg/mL) treated DNA showed significant fragmentation (Fig. S4). Earlier Kumar et al. have shown nuclear fragmentation of *E. coli* in presence of nanoparticle using confocal fluorescence microscopy [50]. Usually ROS attack cellular DNA and produce chain breaks, modify sugar residues and

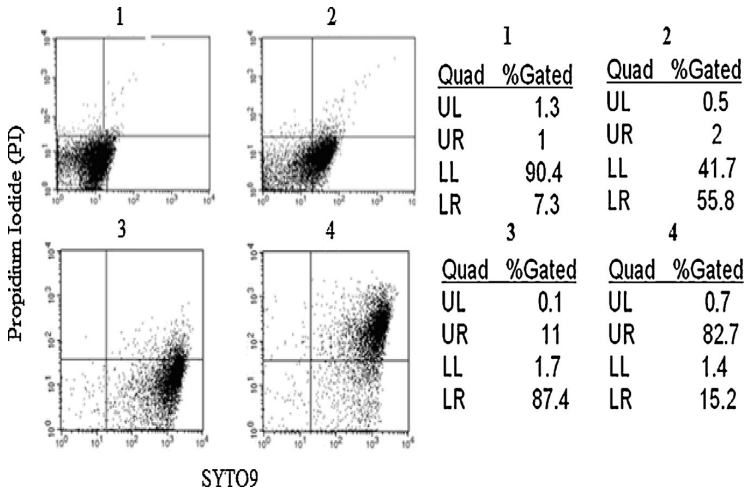

Fig. 2. Live/dead viability assay of ZnO–PEI NP treated *E. coli* MREC33 by flow cytometry. After NP exposure cell samples were stained with mixture of SYTO9 and PI [Live–Dead BacLight Kit (Invitrogen)] and analyzed on a cell sorter. (1) (=0.5 h); (2) (=1 h); (3) (=1.5 h) and (4) (=2 h) corresponds to incubation period. UL, UR, LL, LR in the figure stands for upper left, upper right, lower left and lower right.

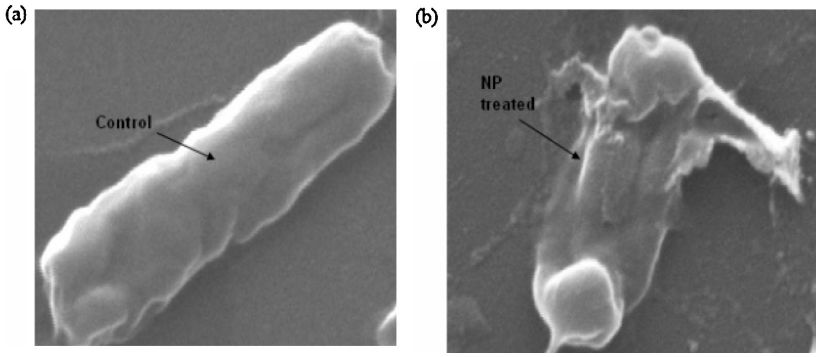

Fig. 3. SEM micrographs of (a) *E. coli* MREC33 cells without NP treatment (b) cells treated with ZnO–PEI NP (3 h of treatment).

nitrogen bases by oxidation, nitration, mutilation, or deamination reactions. Severe DNA fragmentation ultimately leads to cell death. In the present study we have found that bacterial DNA damage occurs within the first two hours of nanoparticle treatment (data not shown).

3.13. Synergistic or additive effect of ZnO–PEI NP with tetracycline

Interestingly, it has been found that when only antibiotic or nanoparticle was supplemented to bacterial medium, it caused moderate killing. In contrast when they are administered together, killing activity enhanced significantly which indicates synergistic action (Fig. 6). In our test cells (tetracycline-resistant), the entry of the drug was either inhibited or pumped out by efflux protein coded by the tetracycline-resistance gene. After treatment with NP, disruption of cell membrane may lead to the inactivation of efflux pump resulting in accumulation of tetracycline. Intracellular tetracycline may now bind to its target which it failed in cells not treated with NP. Seizure of protein synthesis coupled with membrane damage may have contributed to this synergism.

3.14. Effect of protein binding on nanoparticle mediated killing

A concentration of 35 μg/mL ZnO–PEI NP was used (where >95% inhibition was observed) to establish the effect of BSA on nanoparticles mediated killing of bacterium. On adding a fixed concentration of BSA to the medium containing ZnO–PEI NP, it was observed that the percent viability of bacteria was significantly enhanced. The data indicate that in presence of BSA the viability was approximately 28% in contrast to 2.4% in absence of BSA (Fig. 7). In our earlier publication we showed that ZnO is capable of binding BSA [51]. The result suggests that the binding of ZnO–PEI NP with BSA has reduced the effective concentration of NP in the medium and as a possible outcome we observe the enhancement in bacterial viability.

4. Discussion

Although many studies have reported the antibacterial activity of different NPs, the exact mechanism of toxicity due to nanoparticle is still uncertain. There are several questions that need to be answered before the commencement of any clinical application of nanoparticles. To address whether the size or surface chemistry of

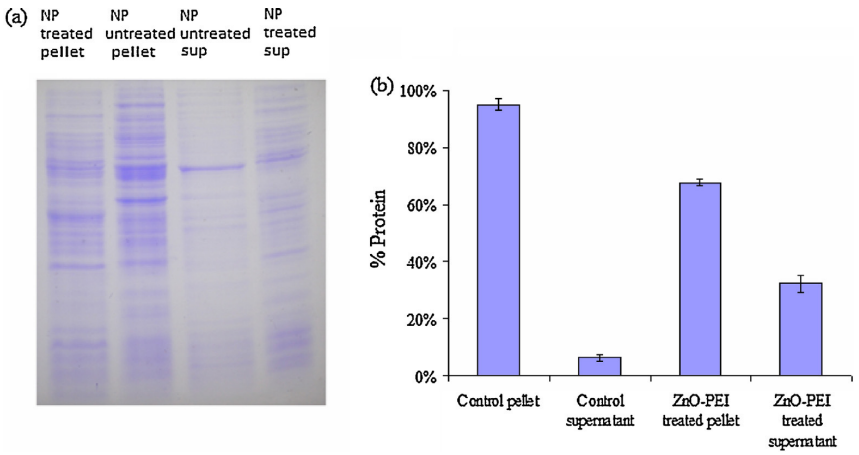

Fig. 4. (a) Demonstration of bacteriolytic effect of ZnO–PEI NP on *E. coli* MREC33 cells using SDS-PAGE. Lane 1: lysed pellet from ZnO–PEI NP treated cells (CelyT), lane 2: lysed pellet from untreated cells (CelyC), lane 3: supernatant from untreated cells (SupC) and lane 4: supernatant from ZnO–PEI NP treated cells (SupT). (b) Relative percent protein in the pellet and supernatant of control and ZnO–PEI NP treated *E. coli* MREC33 cells. The data represent the mean ± standard deviation of three independent experiments ($n = 3$).

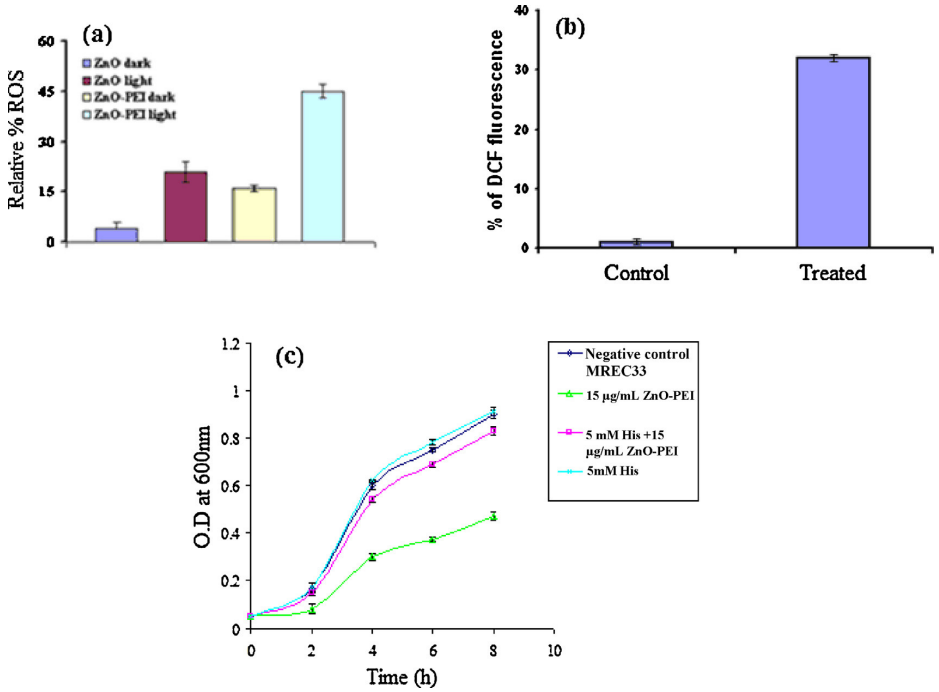

Fig. 5. (a) Extracellular ROS generation by ZnO-NP and ZnO–PEI NP in presence and absence of light, determined by XTT assay. (b) Intracellular ROS generation, determined by DCF-DA fluorescence. (c) The effect of histidine (5 mM) on growth curve of *E. coli* MREC33 in presence of ZnO–PEI NP (15 μg/mL). The data represent the mean ± standard deviation of three independent experiments ($n = 3$).

NP is directly related to the toxicity, some studies have found a relationship between the ability of NP to generate ions and cytotoxicity [12,15]. On the question of the surface functionalization of nanoparticle playing any significant role in antibacterial activity, the general belief is that the surface modification has good impact [52,53]. Some investigators have reported that the surface functionalization on ZnO-NPs has improved their antibacterial activity [19], which may be attributed to enhanced ROS production by nanoparticles due to the surface modification. On the question if the nanoparticles have any direct interaction with bacterial cell surface it has been suggested that the disruption of bacterial outer membrane in the presence of NP is the reason for its toxicity [54]. However, the exact mechanism of the disruption has not been ascertained. There could be several possibilities, such as the chemical damage to membrane biomolecules, robbing of lipid molecules through adsorption

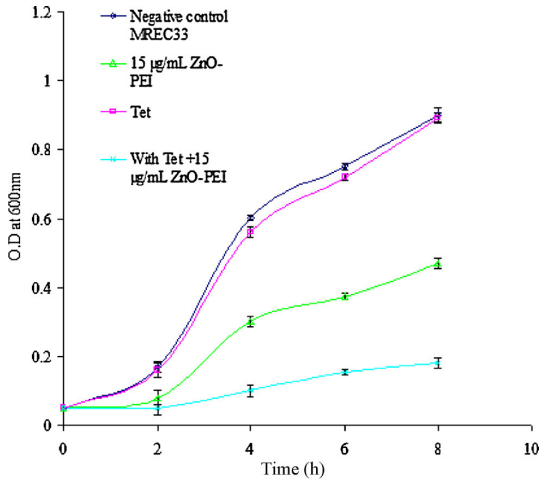

Fig. 6. Growth curve of *E. coli* MREC33 in liquid LB medium (◊, Negative control; □, with 20 μg/mL tetracycline; Δ, 15 μg/mL ZnO–PEI NP; and ×, with both 15 μg/mL ZnO–PEI NP and 20 μg/mL tetracycline). The data represent the mean ± standard deviation of three independent experiments ($n = 3$).

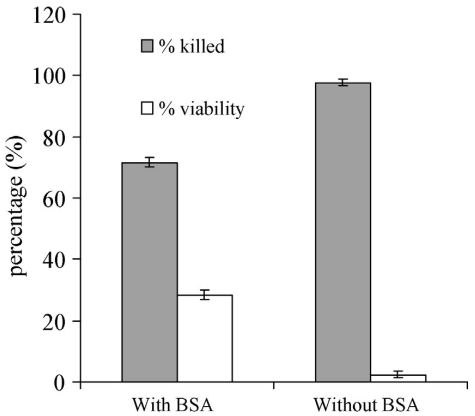

Fig. 7. Counterproductive effect of BSA (35 mg/mL) on ZnO–PEI NP mediated killing. Solid column represents % killed and the open column represents % of viability of *E. coli* MREC33 cells. The data represent the mean ± standard deviation of three independent experiments ($n = 3$).

of NP, or membrane gelation/fluidization after NP attachment. The effect of NP on outer membrane proteins is yet to be addressed systematically.

Our results indicate the involvement of direct interaction of PEI-capped NP with membrane, which causes disruption and disorganization of bacterial membrane and leakage of cytosolic content (Figs. 3–5). We further monitored an enhancement in internalization of nanoparticles, which may result from the possible loss of membrane integrity. Internalization of ZnO–PEI in bacterial and mammalian cells was also compared in our earlier study, which showed the internalization to be much higher in the case of bacteria [55], and this could be attributed to the presence of PEI at the surface of ZnO. Preferential interaction of ZnO–PEI NP with bacterial cells over the mammalian cells could be explained because of the presence of lipopolysacchides (LPS) in the outer leaflet of the bilayer; as LPS contains more charge per unit of surface area than any phospholipid, this renders the cell surface of the Gram-negative bacteria highly negatively charged [56,57]. Neutralization of LPS charges by cations must be incomplete because divalent and monovalent cations should diffuse faster across the high negative electrostatic potential layer as explained by Guoy–Chapman–Stern. Thus, the interaction of large polycation (ZnO–PEI NP in our case) with such a surface will first involve a localized neutralization on a surface layer, including charge displacement or localized exclusion of cations, leading to the integration of such polycation into the outer surface and causing permeabilization of the outer membrane [58]. Hence, high negative zeta potential (in mV) of bacterial cell membrane ($-47.8\,mV \pm 0.7$) compared to mammalian cell like human RBCs (-15.7 mV) could be the possible reason why internalization of PEI capped ZnO-NP was more in bacteria compared to mammalian cells [55,59,60]. Our data have also revealed that NP binding to bacterial surface is fast, as we have found NP internalization in bacteria within a couple of hours of treatment (data not shown). We found an extensive membrane distortion and the formation of pores due to bacteria-nanoparticle interaction (Fig. 3). Once these pores are formed in the bacterial membrane, the amount of antibiotic getting access to bacterial cytosol may be enhanced and the organism would become more susceptible to antibiotics. The observation of the synergistic effect (Fig. 6) has provided support to the mechanism. The increased antibacterial activity observed in the present study hints upon polyethyleneimine capping which has caused the enhanced production of the reactive oxygen species (ROS) from the NP (Fig. 5). ROS, such as hydrogen peroxide (H_2O_2), superoxide anion (O_2^-), hydroxyl radical (•OH) and organic hydroperoxides (OHPs) are toxic to the cells as they damage cellular constituents such as DNA, lipids and proteins. The role of ROS in bacterial killing has been the subject of intense debate, and a general consensus seems to be obscure. In this investigation, we have convincingly established that the observed cell/DNA damage is an outcome of ROS mediated oxidative stress. Further, we have shown that in the presence of histidine (a known ROS quencher), the antimicrobial effect of ZnO–PEI NP is reduced several folds, which further confirms the role of ROS in bacterial killing (Fig. 5c).

5. Conclusions

The present study demonstrated the importance of PEI coating in enhancing the antimicrobial activity of ZnO NPs. PEI functionalized ZnO NP was found to be excellent bactericidal agent against MAR bacteria bearing HPI genes. We have also demonstrated the ROS mediated membrane damage resulting in intracellular protein leakage and degradation of DNA. Finally, synergistic antibacterial effect was noted with LD_{50} concentration when used in combination with tetracycline.

Acknowledgments

We are grateful to Dr. Santi M. Mandal (Central Research Facility, Indian Institute of Technology, Kharagpur) for carrying out the TGA analysis. The research work was supported by a major research grant (grant number BT/PR-164/BCE/08/448/2006) from the Department of Biotechnology (DBT), India. PC is a recipient of the JC Bose National Fellowship from the Department of Science and Technology (DST). AKM gratefully acknowledges North Bengal University, India for research fellowship (NBU-JRF/3726/R-2007); SS is a Council of Scientific and Industrial Research (CSIR) research fellow.

Appendix A. Supplementary data

Supplementary material related to this article can be found, in the online version, at http://dx.doi.org/10.1016/j.colsurfb.2014.03.044.

References

[1] H. Nikaido, Annu. Rev. Biochem. 78 (2009) 119.
[2] O. Oncül, O. Keskin, H.V. Acar, Y. Küçükardali, R. Evrenkaya, E.M. Atasoyu, C. Top, S. Nalbant, S. Ozkan, G. Emekdaş, S. Cavuşlu, M.H. Us, A. Pahsa, M. Gökben, J. Hosp. Infect. 51 (2002) 47.
[3] B. Spellberg, R. Guidos, D. Gilbert, J. Bradley, H.W. Boucher, W.M. Scheld, J.G. Bartlett, J. Edwards Jr., Clin. Infect. Dis. 46 (2008) 155.
[4] P.M. Bennett, Br. J. Pharmacol. 153 (2008) 347.
[5] S. Mukherjee, R. Chakraborty, Acta Microbiol. Immunol. Hung. 54 (2007) 379.
[6] S. Mukherjee, R. Chakraborty, Res. Microbiol. 157 (2006) 220.
[7] A. Kumar, S. Mukherjee, R. Chakraborty, Microb. Drug Resist. 16 (2010) 29.
[8] K. Poole, J. Antimicrob. Chemother. 56 (2005) 20.
[9] K.S. Sharma, T. Fatma, S.S. Thukral, J. Microbiol. Methods 39 (1999) 45.
[10] S.L. Percival, P.G. Bowler, J. Dolman, Int. Wound J. 4 (2007) 186.
[11] S.K.R. Namasivayam, S. Ganesh, B. Avimanyu, Int. J. Med. Res. 1 (2011) 131.
[12] K. Kasemets, A. Ivask, H.C. Dubourguier, A. Kahru, Toxicol. In Vitro 23 (2009) 1116.
[13] P.J.P. Espitia, N.F.F. Soares, J.S.R. Coimbra, N.J. De Andrade, R.S. Cruz, E.A.A. Medeiros, Food Bioprocess Technol. 5 (2012) 1447.
[14] M.K. Rai, S.D. Deshmukh, A.P. Ingle, A.K. Gade, J. Appl. Microbiol 112 (2012 841).
[15] K.M. Reddy, K. Feris, J. Bell, D.G. Wingett, C. Hanley, A. Punnoose, Appl. Phys. Lett. 90 (2007) 213902.
[16] T. Jin, D. Sun, J.Y. Su, H. Zhang, H.J. Sue, J. Food Sci. 74 (2009) 46.
[17] N. Jones, B. Ray, K.T. Ranjit, A.C. Manna, FEMS Microbiol. Lett. 279 (2008) 71.
[18] M. Banoee, S. Seif, Z.E. Nazari, P. Jafari-Fesharaki, H.R. Shahverdi, A. Moballegh, K.M. Moghaddam, A.R. Shahverdi, J. Biomed. Mat. Res. B 93 (2010) 557.
[19] P. Bhadra, M.K. Mitra, G.C. Das, R. Dey, S. Mukherjee, Mater. Sci. Eng. C 31 (2011) 929.
[20] T. Ohira, O. Yamamoto, Y. Iida, Z. Nakagawa, J. Mater. Sci. 19 (2008) 1407.
[21] K. Ghule, A.V. Ghule, B.J. Chen, Y.C. Ling, Green Chem. 8 (2006) 1034.
[22] R. Jalal, E.K. Goharshadi, M. Abareshi, M. Moosavi, A. Yousefi, P. Nancarrow, Mater. Chem. Phys. 121 (2010) 198.
[23] M. Li, S. Pokhrel, X. Jin, L. Madler, R. Damoiseaux, E.M. Hoek, Environ. Sci. Technol. 45 (2011) 755.
[24] D.S. Vicentini, A. Smania Jr., M.C.M. Laranjeira, Mater. Sci. Eng. C 30 (2010) 503.
[25] O. Boussif, M.A. Zanta, J.P. Behr, Gene Ther. 3 (1996) 1074.
[26] N. Beyth, Y. Houri-Haddad, L. Baraness-Hadar, I. Yudovin-Farber, A.J. Domb, E.I. Weiss, Biomaterial 29 (2008) 4157.
[27] N. Beyth, I. Yudovin-Farber, M. Perez-Davidi, A.J. Domb, E.I. Weiss, Proc. Nat. Acad. Sci. U.S.A. 107 (2010) 22038.
[28] N. Beyth, R. Pilo, E.I. Weiss, J. Nanomater. 1155 (2012).
[29] H.J. Lee, S.G. Lee, E.J. Oh, H.Y. Chung, S.I. Han, E.J. Kim, S.Y. Seo, H.D. Ghim, J.H. Yeum, J.H. Choi, Colloids Surf., B: Biointerfaces 88 (2011) 505.
[30] T. Xia, M. Kovochich, M. Liong, H. Meng, S. Kabehie, S. George, J.I. Zink, A.E. Nel, ACS Nano 3 (2009) 3273.
[31] A. Beyerle, A.S. Long, P.A. White, T. Kissel, T. Stoeger, Mol. Pharm. 8 (2011) 976.
[32] I.M. Helander, H.L. Alakomi, K. Latva-Kala, P. Koski, Microbiology 143 (1997) 3193.
[33] P. Joshi, S. Chakraborti, P. Chakrabarti, D. Haranath, V. Shanker, Z.A. Ansari, S.P. Singh, V. Guptas, J. Nanosci. Nanotechnol. 9 (2009) 6427.
[34] P. Joshi, Z.A. Ansari, S.P. Singh, V. Shanker, Adv. Sci. Lett. 2 (2009) 360.
[35] S. Schubert, A. Rakin, H. Karch, E. Carniel, J. Heesemann, Infect Immun. 66 (1998) 480.
[36] S. Bach, A. de Almeida, E. Carniel, FEMS Microbiol. Lett. 183 (2000) 289.
[37] K.S. Sharma, T.S. Fatma, S. Thukral, J. Microbiol. Methods 39 (1999) 45.
[38] S.J. Moyo, S.Y. Maselle, M.I. Matee, N. Langeland, H. Mylvaganam, BMC Infect. Dis. 7 (2007) 92.
[39] R.K. Dutta, B.P. Nenavathu, M.K. Gangishetty, A.V.R. Reddy, Colloids Surf., B: Biointerfaces 94 (2012) 143.
[40] B.M. Srikanta, M.A.H. Nayaka, S.M. Dharmesh, Biochimie 93 (2011) 678.

[41] M.M. Bradford, Anal. Biochem. 72 (1976) 248.
[42] J.W. Liou, M.H. Gu, Y.K. Chen, W.Y. Chen, Y.C. Chen, Y.H. Tseng, Y.J. Hung, H.H. Chang, PLoS One 6 (5) (2012) e19982.
[43] M.W. Sutherland, B.A. Learmonth, Free Radical Res. 27 (1997) 283.
[44] D.Y. Lyon, L. Brunet, G.W. Hinkal, M.R. Wiesner, P.J. Alvarez, Nano Lett. 8 (2008) 1539.
[45] A. Lipovsky, Y. Nitzan, A. Gedanken, R. Lubart, Nanotechnology 22 (2011) 105101.
[46] S. Schmidt, K. Röck, M. Sahre, O. Burkhardt, M. Brunner, M.T. Lobmeyer, H. Derendorf, Antimicrob. Agents Chemother. 52 (2008) 3994.
[47] E. Tang, G. Cheng, X. Ma, X. Pang, Q. Zhao, Appl. Surf. Sci. 252 (2006) 5227.
[48] M. Berney, F. Hammes, F. Bosshard, H.U. Weilenmann, T. Egli, Appl. Environ. Microbiol. 73 (2007) 3283.
[49] W. Jiang, A. Saxena, B. Song, B.B. Ward, T.J. Beveridge, S.C.B. Myneni, Langmuir 20 (2004) 11433.
[50] A. Kumar, A.K. Pandey, S.S. Singh, R. Shanker, A. Dhawan, Free Radical Biol. Med. 51 (2011) 1872.
[51] S. Chakraborti, P. Joshi, D. Chakravarty, V. Shanker, Z.A. Ansari, S.P. Singh, P. Chakrabarti, Langmuir 28 (2012) 11142.
[52] G. Applerot, A. Lipovsky, R. Dror, N. Perkas, Y. Nitzan, R. Lubart, A. Gedanken, Adv. Funct. Mater. 19 (2006) 842.
[53] R. Brayner, R. Ferrari-Iliou, N. Brivois, S. Djediat, M.F. Benedetti, F. Fiévet, Nano Lett. 6 (2006) 866.
[54] P.K. Stoimenov, R.L. Klinger, G.L. Marchin, K.J. Klabunde, Langmuir 18 (2002) 6679.
[55] S. Chakraborti, S. Bhattacharya, R. Chowdhury, P. Chakrabarti, PLoS One 8 (2013) [7076e].
[56] B. Lugtenberg, L.V. Alphen, Biochim. Biophys. Acta 737 (1983) 51.
[57] T.J. Beveridge, J. Bacteriol. 181 (1999) 4725.
[58] R.E.W. Hancock, D.N. Karunaratne, C. Bernegger-Egli, in: J.M. Ghuysen, R. Hakenbeck (Eds.), Bacterial cell wall, Elsevier Science B.V., 1994, Chapter 12.
[59] K.A. Soni, A.K. Balasubramanian, A. Beskok, S.D. Pillai, Curr. Microbiol. 56 (2008) 93.
[60] F. Tokumasu, G.R. Ostera, C. Amaratunga, R.M. Fairhurst, Exp. Parasitol. 131 (2012) 245.